UNIVERSITY OF MODENA AND REGGIO EMILIA

PhD in

"Agri-Food Sciences, Technologies and Biotechnologies"

DOCTORATE SCHOOL IN LIFE SCIENCE:

XXXVI CYCLE

STUDY AND EVALUATION OF STRATEGIES TO REDUCE/REPLACE PLASTIC MATERIALS FOR FOOD PACKAGING AND WRAPPING WITH GREENER AND ECO-SUSTAINABLE ALTERNATIVES

PhD student: Emanuela Lo Faro

Tutor: Professor Patrizia Fava

PhD Coordinator: Professor Fabio Licciardello

2022/2023

Abstract

The main source of global plastic pollution comes from food and drink packaging made whit petroleum derived plastics and no-biodegradable. So, we need quickly to find a solution for the transition from the petroleum-based and no-biodegradable packaging to more sustainable alternatives.
But these alternatives need to maintain the properties of conventional plastics, such as low production costs, durability, good mechanical properties, and resistance to oil and vapor.
This PhD thesis focuses on investigating and assessing strategies for replacing common plastic materials with eco-sustainable and renewable alternatives. The aim is not only to evaluate the performance of existing alternative materials available in the market but also to develop films and coatings using eco-sustainable materials. These films and coatings are intended to enhance the performance of paper used in food wrapping. By exploring these avenues, the goal is to find viable solutions that improve the environmental impact of packaging without compromising functionality and performance.

Paper has been recognized, in recent years, as one of the most viable alternatives for replacing plastic in some fields of food packaging.
Nevertheless, paper's physical properties are not always optimal, particularly its resistance to moisture and grease. Nowadays, barrier coatings for paper are generally based on fossil oils or synthetic polymers that dominate the current market due to their low cost and easy availability. These polymers include waxes, ethylene vinyl alcohol (EVOH), polyvinylidene chloride (PVDC), poly-fluoroalkyl substances (PFASs) and polyolefins such as polyethylene (PE), low-density polyethylene (LDPE), linear low-density polyethylene (LLDPE), high-density polyethylene (HDPE), polypropylene (PP), as well as aluminum, metallized plastic layers, and other derivatives. These materials provide a significant barrier against water, grease, and oxygen permeation for food packaging materials. However, they are disadvantaged by limitations in fossil oil reserves, poor recyclability due to the chemical structure of these plastics, and lack of biodegradation, which exacerbate environmental and economic concerns, leading to increased air pollution and disposal costs. Furthermore, the use of these materials not only poses risks to the environment but also to human health. For this reason, the polymers used in this PhD thesis had the characteristic of being biodegradable and/or compostable polymers, so as to be able to improve not only the performance of paper for the food packaging function, but also to improve the end of life of these paper-based packaging. Various polymers, including PCL, PHBV, PHBH, PBS, PLA, starch, and cutin derived from tomato processing by-products, have been utilized in the study. Coated paper samples underwent a series of tests and analyses to assess the enhancement of their performance. These evaluations included determining the WVTR (Water Vapor Transmission Rate) and conducting water absorption tests. Additionally, measurements were taken to determine the contact angle with oil and water, resistance to grease using the 'Kit12' test, and characterization of the films through techniques such as SEM (Scanning Electron Microscopy) or SEM-EDX (Energy-Dispersive X-Ray Spectroscopy), FT-IR (Fourier Transform Infrared Spectroscopy), and TGA (Thermogravimetric Analysis).
The application of coatings on the base paper, achieved through the bar coating technique, resulted in substantial improvements. In certain cases, the WVTR value was enhanced by up to 82%, and the paper demonstrated the ability to withstand the most aggressive solution in the Kit12 test. Furthermore, the focus extended beyond improving these paper characteristics, as efforts were made to impart antimicrobial properties to the paper. This was accomplished by employing a complex containing zinc, a metal renowned for its antimicrobial properties. The

performance of the coated paper exhibited optimal antimicrobial functionality in this particular case as well.

To achieve the second objective, a comparative study was conducted to assess the performance and final quality of fruits when utilizing innovative, eco-friendly materials in contrast to conventional plastic materials, which are widely recognized as environmentally unfriendly. The fruit packaging process involved the use of both conventional materials and innovative alternatives, including paper trays sealed with cellulose-based film, trays made from PLA (Polylactic Acid), and various types of trays made from R-PET (Recycled Polyethylene Terephthalate).
The qualitative evaluation of the fruit samples encompassed multiple experimental analyses. These analyses included assessing weight loss, monitoring the variation of the atmosphere within the packages, measuring Brix degrees (a measure of sweetness), conducting mechanical tests on the fruits, and performing sensory and microbiological analyses.
The substitution of conventional packaging materials with alternative options proved to be a viable solution. The alternative packaging not only preserved the quality of the examined products but, in certain cases, it also better maintained their inherent characteristics compared to packaging currently available in the market. This highlights the potential of eco-friendly packaging materials to offer improved performance and contribute to the preservation of fruit quality.

Table of Contents

Acknowledgment

Prima di tutto, vorrei ringraziare il mio supervisor, Prof.ssa Patrizia Fava, per avermi guidata ed aiutata in questa esperienza di ricerca scientifica e anche nella ricerca di me stessa, in un momento in cui di Emanuela non c'era più nulla. Non è stata solo un supervisor scientifico, ma anche, e soprattutto, un faro di luce in tanti giorni di mare in tempesta, in questi 5 anni di lavoro insieme. Non potrò mai ringraziarla abbastanza per tutto il sapere di scienza e di vita che mi ha concesso. Spero un giorno di poter possedere un quarto della sua conoscenza di vita e di scienza e basterebbe anche per due persone, tanto è immensa la sua conoscenza.

Secondariamente, vorrei ringraziare la Prof.ssa Francesca Masino e il Prof. Giuseppe Montevecchi, per tutto il supporto che mi avete dato, per tutte le conoscenze che mi avete donato, per avermi fatto innamorare ancora di più di questo meraviglioso mondo, che è la ricerca scientifica e per avermi accolto nella piccola e felice famiglia del 'Tecnopolo'.

Parlando della famiglia del 'Tecnopolo', per chi ci osserva dall'esterno sembriamo dei matti, che lavorano in modo confusionario, in un posto 'sporco' e non organizzato, come se non sapessimo cosa stiamo facendo (alcune volte, è anche vero), ma questa è la mia famiglia di Reggio Emilia, questa famiglia mi ha fatto ricordare perché su un braccio mi sono tatuata un intero laboratorio, perché quando il mio mondo è crollato, quando al Mondo sono rimasta sola, il laboratorio era l'unico posto in cui mi sentivo al sicuro, l'unico posto in cui il mio cuore e la mia anima trovavano pace, l'unico posto in cui sapevo chi era Emanuela. Quindi, grazie.

Tutti gli amici di Reggio, siete così tanti, ed abbiamo passato così tante di quelle esperienze, che non basterebbe un intero capitolo per nominarvi tutti e ringraziarvi tutti, ma ognuno di voi è stato fondamentale in questo pazzo ed incredibile percorso. Vi adoro tutti!!

A 'Loro clown. Noi circo', ci sarebbero così tante cose da dire su queste ragazze, ma potrebbe esser tutto racchiuso con 'BORAHAE'.

Infine, la mia splendida, meravigliosa ed unica famiglia. Nulla di tutto ciò potrebbe esser possibile senza di voi, siete e sarete per sempre i miei pilastri, il mio esempio di vita, vi amo con tutta me stessa.

Dedico questa tesi a **Gianmaria**, **Ottavia** e **Adele**, che io possa esservi di esempio e punto di riferimento per il vostro futuro, che possa essere pieno di serenità, la zia vi ama pazzamente.

Chapter 1

Introduction

Chapter 1: Introduction

Since their invention, plastics have become integral to numerous industries and daily life, thanks to their exceptional attributes such as durability, lightweight nature, stability and cost-effectiveness. In 2022, global plastic production has soared to an astonishing 400 million tons, as reported by Plastics Europe (2023). Among this colossal quantity, approximately 359.8 million tons originated from fossil-based materials, while 32.5 million tons were derived from mechanically recycled (post-consumer) sources. Bio-based plastics accounted for 1.6 million tons, chemical recycling (post-consumer) methods contributed 0.1 million tons, and less than 0.1 million tons were generated through the innovative approach of carbon capture.

Within the confines of Europe, as show the pictures 1.1, a substantial 58.7 million tons of plastics were produced in the same year, representing a slight decrease in comparison to the preceding year's production of 60.8 million tons. Notably, the production of packaging materials sourced from fossil-based materials experienced a significant decline, marking a notable departure from the trends observed in previous years. Conversely, there was a commendable increase in the production of plastics materials derived from mechanically recycled (post-consumer) sources, with 7.6 million tons manufactured in the current year, as opposed to 5.9 million tons in the prior year. Of particular significance is the noteworthy surge in the production of plastic materials made from bio-based plastics, which escalated from 0.3 million tons in 2021 to an impressive 0.7 million tons in 2022 (Plastics Europe, 2023).

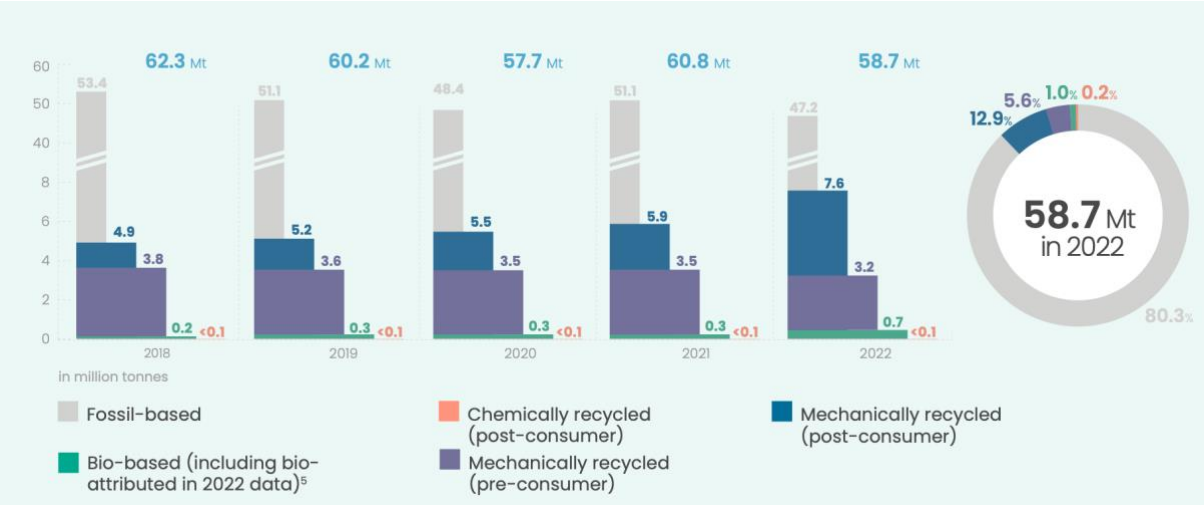

Figure 1.1 European plastics production in 2022 – Image from https://plasticseurope.org/knowledge-hub/plastics-the-fast-facts-2023/

The production of plastic for food and beverage packaging constitutes a significant portion of global plastic production, in particular, in EU is represented from the 39%. The shift from reusable containers to single-use ones has led to an increase in the manufacturing of plastic specifically designed for food purposes. Consequently, the proportion of plastics in municipal solid waste has experienced a notable surge, escalating from less than 1% in 1960 to over 10% by 2005 in middle- and high-income countries (Jambeck et al., 2015).

Currently, the world faces an overwhelming challenge in dealing with the tremendous volume of plastic waste generated. Since the emergence of mass plastic production in the 1950s, an astonishing estimate of 6,300 million metric tons of plastic waste had accumulated by 2015

(Manfra L. et al, 2021). Without substantial alterations in global plastic production and waste management practices, it is projected that an alarming 12,000 million metric tons of plastic waste could potentially end up in landfills or the environment by the year 2050 (Geyer et al., 2017).

Plastic pollution in the environment has become a prominent and widely discussed issue in recent years. The presence of plastic debris has garnered significant attention, particularly due to alarming discoveries such as the identification of plastic waste in all major ocean basins, in which plastics can easily transported because of their low-density (Barnes, 2009; Schwarz et al., 2019). A staggering estimate suggests that between 4 to 12 million metric tons of plastic waste originating from land entered the marine environment in 2010 alone (Jambeck et al., 2015). Furthermore, reports of contamination in freshwater systems and terrestrial habitats are increasingly common (Wagner, 2014; Rillig, 2012; Zubris et al., 2005), along with concerns about environmental pollution caused by synthetic fibers (Zubris et al., 2005; Dris, 2016).

The pervasiveness of plastic waste in the environment has reached such a level that it has been proposed as a potential geological indicator of the proposed Anthropocene era (Zalasiewicz et al., 2016). According to estimates, approximately 80% of marine litter is made of plastic waste. Plastic materials, unlike other substances present in aquatic environments, are unable to undergo chemical decomposition through exposure to light, as they require a dry environment for this process to occur (Crippa et al., 2019). The presence of plastic in the oceans poses a grave threat to aquatic life, leading to the deaths of numerous marine animals. While the exact number of marine animals affected by plastic pollution remains uncertain, a significant portion of these deaths goes undocumented. However, estimates suggest that over 1 million marine animals, including sea turtles, perish annually due to plastic pollution in the ocean. Seabirds are particularly affected, constituting the majority of the casualties, although it is important to note that media coverage often focuses more on mammal deaths, which account for approximately 100,000 fatalities (Plastic Pollution in The Ocean – 2023 Facts and Statistics, 2022). The scale of the issue necessitates urgent action and concerted efforts to mitigate the environmental consequences of plastic waste. By implementing effective waste management strategies, promoting sustainable practices, and raising awareness about the importance of reducing the consumption of plastic made with petroleum-fossil materials, we can strive to address this pressing environmental concern and protect our ecosystems for future generations.

Unfortunately, despite our efforts, recent studies indicate that our current measures are only capable of reducing marine plastic pollution, which is a key aspect of the plastic challenge, by a mere 7 percent (European Commission – Global Action on Plastics, 2022). To compound the issue, plastic production is projected to continue its upward trajectory, and the generation of single-use plastic waste has reached unprecedented levels.

This sobering reality highlights the need for more comprehensive and impactful actions to address the plastic crisis. Merely reducing marine plastic pollution by a small percentage is insufficient to tackle the magnitude of the problem we face. It is imperative that we reassess our approach and implement more effective strategies that target the entire lifecycle of plastic, from production to disposal. This includes reducing plastic production, promoting the use of sustainable alternatives, improving waste management practices, and fostering a shift towards a circular economy that prioritizes recycling and reuse.

Addressing the plastic challenge requires collective action from governments, industries, communities, and individuals. It demands a commitment to innovation, policy changes, and

behavioral shifts that prioritize the long-term health of our planet over short-term convenience. Through collaborative efforts and embracing a comprehensive strategy, we can achieve substantial advancements in tackling the issue of plastic pollution and ensuring the protection of our environment and the prosperity of future generations.

1.1. Strategies to solve this issue

At present, there is no internationally established instrument specifically designed to address plastic pollution across the entire lifecycle of plastics. However, various countries are implementing measures to mitigate this issue. These actions include campaigns and awareness-raising initiatives aimed at reducing plastic consumption and promoting recycling (European Commission – Global Action on Plastics, 2022). Additionally, some countries have enacted specific laws that require producers and manufacturers to minimize waste, set recycling targets, and phase out particularly problematic plastic products, such as single-use plastics.

The United Nations has played a significant role in addressing plastic pollution by employing a range of strategies, one of which is the formulation of the 'Sustainable Development Goals' (SDGs). This comprehensive global initiative aims to foster a better and more sustainable future by addressing various interconnected challenges. The SDGs consist of 17 specific goals, each targeting a different aspect of sustainable development, including poverty eradication, reducing inequality, combating climate change, addressing environmental degradation, promoting peace, and ensuring justice (United Nations - Take Action for the Sustainable Development Goals).
The SDGs recognize the intricate links between different areas of development and emphasize the need for a holistic approach. Achieving all 17 goals (Figure 1.2) by the target year of 2030 is crucial to ensure that no one is left behind in the pursuit of sustainable development. These goals are not viewed in isolation but rather as an integrated framework, acknowledging the interconnected nature of social, economic, and environmental issues (United Nations - Take Action for the Sustainable Development Goals).
Within the SDGs, several goals directly address the challenges of climate change and environmental degradation, which are closely related to plastic pollution. Goal 6, 'Clean Water and Sanitation,' aims to ensure access to clean water sources and improve sanitation facilities, which can help prevent plastic pollution in water bodies. Goal 11, 'Sustainable Cities and Communities,' focuses on creating inclusive, safe, resilient, and sustainable urban environments, including managing waste effectively to reduce plastic pollution. Goal 12, 'Ensure Sustainable Consumption and Production Patterns,' promotes responsible consumption and production practices, encouraging the reduction, reuse, and recycling of plastics. Goal 13, 'Climate Action,' aims to combat climate change and its impacts, which includes addressing the environmental consequences of plastic pollution. Finally, Goal 14, 'Life Below Water,' targets the protection and sustainable use of marine and coastal ecosystems, recognizing the urgent need to address plastic pollution in oceans and other water bodies. (United Nations - Take Action for the Sustainable Development Goals).
By integrating plastic pollution concerns into these specific goals, the United Nations and its member states are striving to create a more sustainable and resilient future for all, fostering a harmonious relationship between human development and the environment.

Figure 1.2 The 17 sustainable development goals – Image from https://sdgs.un.org/goals

Italy is actively involved in working towards the goals outlined in the '2030 Agenda' and making significant efforts to achieve them. The country has established the Italian Alliance for Sustainable Development (ASviS) with the purpose of promoting awareness about the significance of the 2030 Agenda for sustainable development (Figure 1.4). ASviS was formed in February 2016 and plays a vital role in mobilizing various sectors of Italian society, including economic and social actors as well as institutions, to actively contribute towards the attainment of the Sustainable Development Goals (SDGs). The alliance aims to galvanize collective action and foster a sense of responsibility among all stakeholders in Italy to work towards realizing the SDGs and creating a sustainable future.

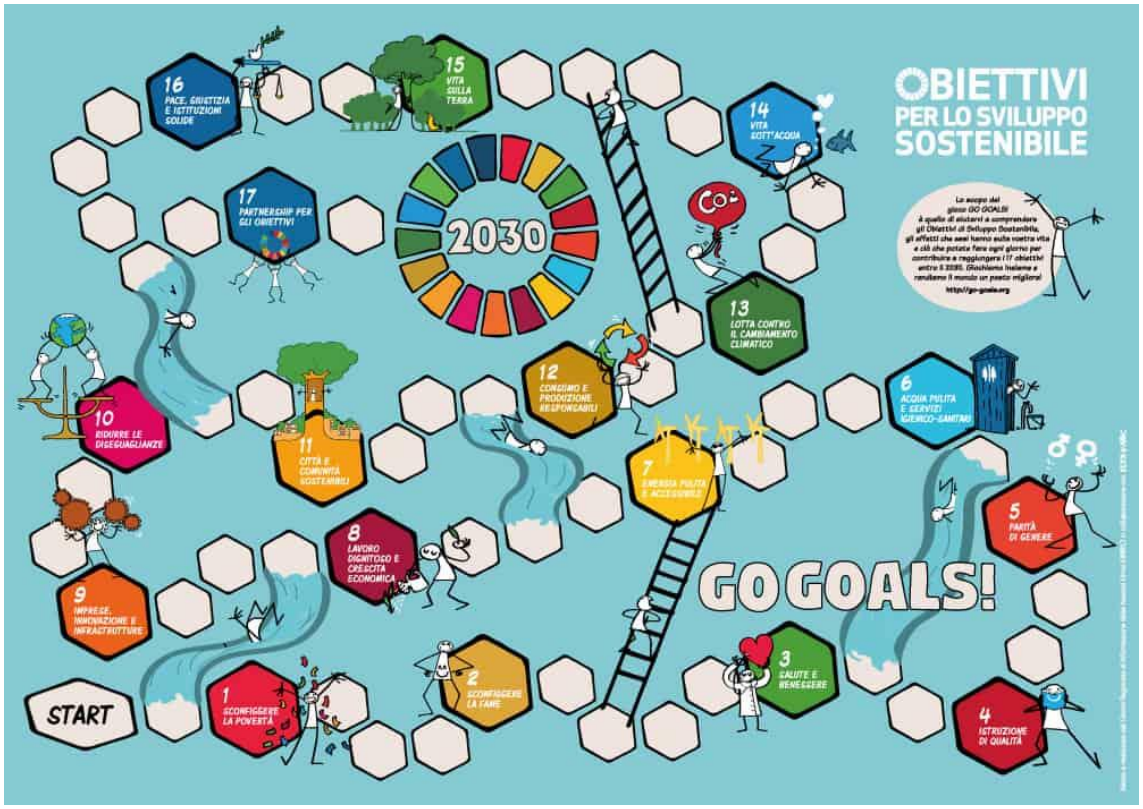

Figure 1.3. Representation of the Sustainable Development Goals - Image from https://go-goals.org/it/

The European Union (EU), including Italy, is leading the way in promoting a global agreement on plastics to support the transition to a circular economy. This objective is outlined in the Circular Economy Action Plan and is in line with the mandate given by the United Nations Environment Assembly (European Commission – Global Action on Plastics, 2022). In March 2022, negotiations were launched to develop a new legally binding international instrument on plastic pollution, expected to be finalized by the end of 2024. The aim of this instrument is to address plastic pollution across the entire lifecycle of plastics, with a focus on minimizing mismanagement and preventing plastic from entering the environment, particularly the marine environment.
However, according to the 2023 ASviS report, marine pollution, especially from plastic, remains a significant concern. It is an escalating issue, and there are uncertainties about the adequacy of the measures implemented thus far in effectively tackling the problem. For instance, in 2021, beached litter was found to comprise 273 types of objects (including single-use plastics, waste from fishing and aquaculture, plastic bags, and smoking-related waste) per hundred meters of beach.

At the national level, Italy's public policies have yet to provide comprehensive solutions that align with the commitments made at the European and international levels. These policies should address the anthropogenic structural causes contributing to biodiversity loss. For instance, Law no. 221/2015, enacted on December 28, 2015, titled "*Environmental provisions to promote green economy measures and to contain the excessive use of natural resources*," introduced certain tools to develop environmental policies based on a systemic approach. The law recognizes the importance of protecting and enhancing natural capital for social and economic prosperity. However, further efforts are needed to fully address the challenges and meet the commitments at hand (ASviS - Rapporto ASviS 2023).

According to the European Union (EU), each European citizen generates nearly 180 kilograms of plastic packaging waste annually, and this amount is steadily increasing. To address this environmentally unsustainable trend, the EU Commission has put forward a regulation on packaging designed to reduce plastic waste and improve the recycling of plastic materials in circulation. One of the proposals within this regulation is to minimize the use of disposable plastic/polystyrene packaging for unpackaged fruits and vegetables at points of sale. It should be noted that this proposal excludes pre-packaged products such as fruit salads or pre-cut vegetables.
Although only slightly over 10% of the population is aware of this proposal, a significant 80% of the population supports it. Additionally, nine out of ten individuals express their willingness to make personal sacrifices to protect the environment, emphasizing that adapting to this new rule will not be overly burdensome or "tiring."

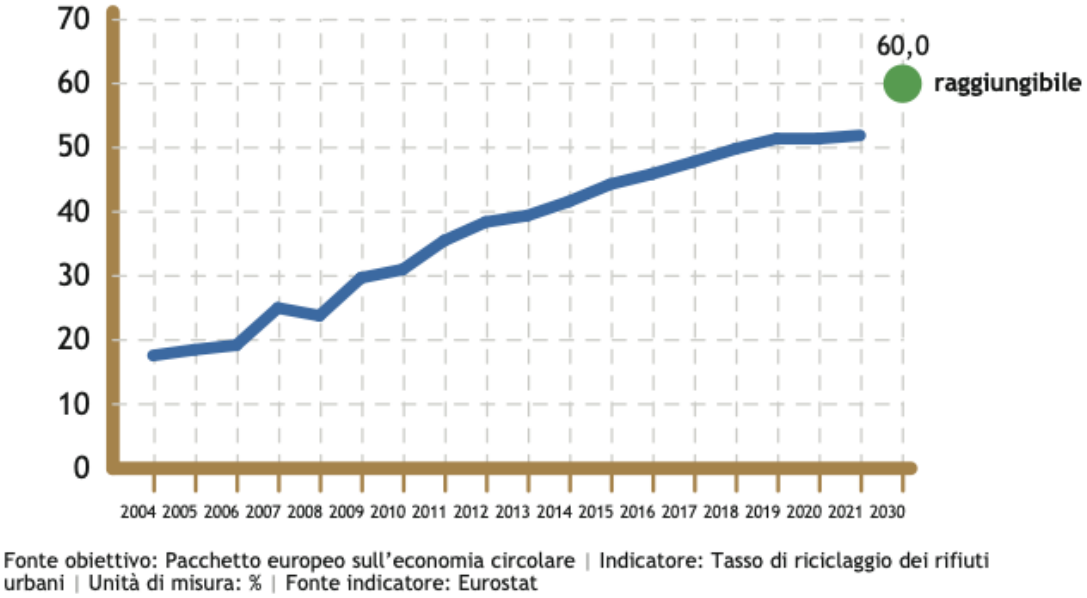

Figure 1.4 Progress in achieving the target set by the 2030 Agenda on the 60% share of the recycling rate of municipal waste in Italy - Image from asvis.it

Both the European Union (EU) and Italy have taken significant steps to address the issue of single-use plastics. One notable initiative is the **EU Directive 2019/904** (Directive (EU) 2019/904), commonly known as the SUP (Single Use Plastic) Directive, which was implemented in Italy through Legislative Decree 196/2021 in April 2021. The primary objective of this decree is to prevent and reduce the environmental impact of specific plastic products, particularly in aquatic environments, as well as protect human health.
The decree encourages the adoption of measures that promote the use of recycled plastic suitable for direct food contact in beverage bottles, as well as the utilization of innovative materials. It applies to various categories of single-use plastic products, including traceable and oxo-degradable plastics, as well as fishing gear containing plastic (Figure 1.5).

The legislation specifies certain products for which consumption reduction measures are mandated. These include cups or glasses for beverages, along with their caps and lids, as well as food containers intended for immediate consumption, such as boxes with or without lids. These containers are typically used for food that is consumed directly from the container without further preparation or cooking, including fast food containers and ready-to-eat meals. However, the decree excludes beverage containers, plates, packets, and wrappers containing food from the consumption reduction measures (Figure 1.5).
Furthermore, the decree prohibits the placement of certain products on the market, such as cotton swabs, cutlery (forks, knives, spoons, chopsticks), dishes, straws, and expanded polystyrene beverage cups or cups with their caps and lids, among others (Figure 1.5). However, this prohibition does not apply to products made of biodegradable and compostable materials, certified according to standards such as UNI EN 13432 or UNI EN 14995, provided they meet specific criteria regarding the percentage of renewable raw materials.
The implementation of this directive, including in Italy, has led to the emergence of single-use plastic food products made from alternative materials, such as bio-based and/or recyclable materials. These alternatives aim to reduce the environmental impact associated with traditional single-use plastic products and promote a more sustainable approach to packaging and food service.

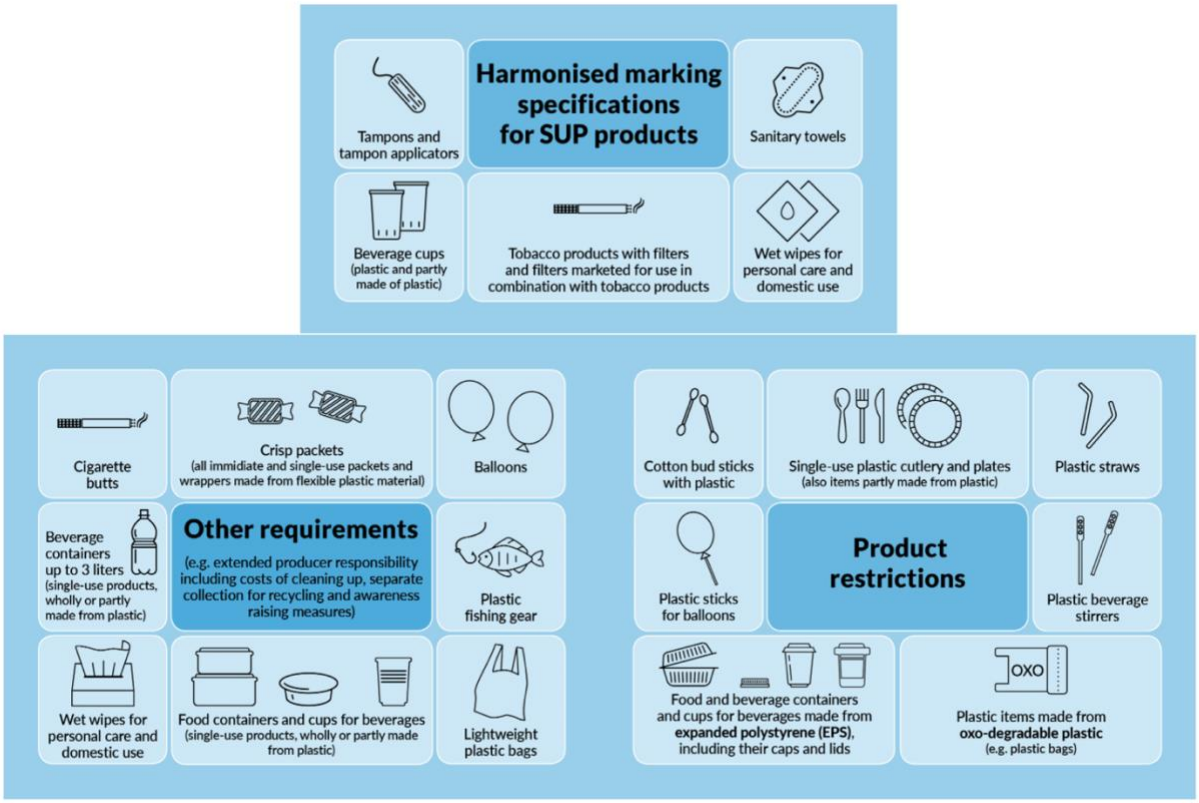

Figure 1.5 Products subject at the European Directive 2019/904 (Single Use Plastics). Image from https://www.eastcham.fi/finnishwastemanagement/municipal-solid-waste/erp/sup-directive/

In November 2022, a significant proposal was presented to the European Commission, aiming to modify Regulation (EU) 2019/1020 and Directive (EU) 2019/904, while simultaneously revoking Directive 94/62/EC. This proposal underwent a voting process by the Environment Committee of the European Parliament on October 24, 2023, and subsequently received approval from the European Parliament on November 22, 2023. As a result, formal negotiations with the European Council were initiated in order to establish a unified and mutually agreed-upon text.

The proposal revolves around the concept of enhancing the sustainability of packaging within the European Union. The EU Council, comprised of competent ministers representing the member states, expressed agreement with the initial text put forth by the European Commission, particularly regarding the recyclability of all packaging available in the market. However, it was collectively decided that packaging can only be deemed recyclable if it is specifically designed to facilitate the recycling of materials and if the ensuing packaging waste can be effectively collected, sorted, and recycled on a large scale. This requirement is set to take effect from 2035, allowing for a transition period.
Moreover, the EU Council endorsed the objectives outlined by the Commission concerning the reduction of packaging. These objectives are based on the benchmark quantities achieved in 2018 and consist of the following progressive reductions: 5% by 2030, 10% by 2035, and 15% by 2040. This commitment demonstrates the Union's dedication to minimizing the environmental impact associated with packaging materials.
In furtherance of sustainability efforts, the EU Council approved the compulsory implementation of compostable materials for tea bags and adhesive labels used on fruits and vegetables. Additionally, there was an agreement to prioritize the reduction of the volume and weight of packaging, as a means to mitigate resource consumption and waste generation.

Furthermore, the establishment of deposit and return systems for single-use plastic bottles and metal beverage containers by 2029 received endorsement. This measure aims to achieve a significant milestone of 90% separate collection for such packaging. However, it is worth noting that if collective schemes successfully attain the collection target prior to 2029, the obligation to implement deposit and return systems can be waived.
Finally, recognizing the need for adequate preparation and adjustment, the EU Council extended the timeframe for implementing the proposed regulation. The agreed-upon extension grants a period of 18 months from the regulation's date of entry into force for stakeholders to adapt and comply with the new requirements and guidelines.
Overall, this proposal demonstrates the European Union's commitment to fostering sustainability, resource efficiency, and the circular economy by promoting the recyclability of packaging, setting reduction targets, encouraging compostability, and establishing systems that facilitate the collection and recycling of certain types of packaging materials.

1.2. Paper as food packaging

According to the proposal 2022/0396(COM) submitted, in December 2022, to the European Commission, which aims to amend Regulation (EU) 2019/1020 and Directive (EU) 2019/904 while revoking Directive 94/62/EC, it is stated that a significant portion of plastic and paper used in the EU, specifically 40% of plastic and **50% of paper**, is allocated for packaging purposes.

1.2.1. Paper production

The production of paper and the annual consumption of paper for food packaging have been on a steady rise. Global statistics from 2010 to 2021, as illustrated in Figure 1.6, indicate a notable increase of 33% in the volume of paper and cardboard used for packaging. Notably, there was a 6% growth in production between 2020 and 2021. This surge can be attributed to the heightened demand for packaging, driven by increased commercial sales in the food and other sectors (Pinkas and Cheropkina, 2023; Statista Research Department, 2023).

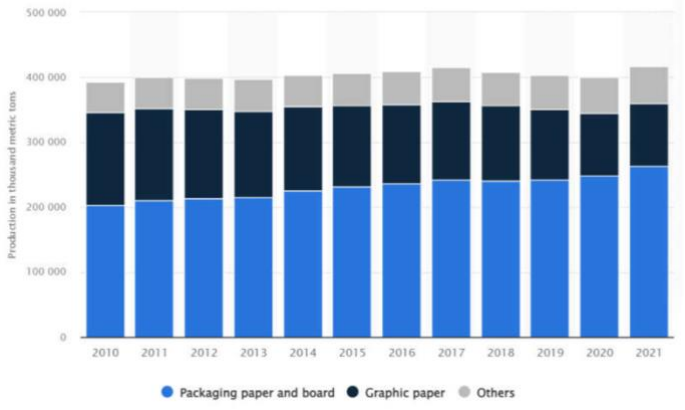

Figure 1.6 Production volume of paper and paperboard worldwide from 2010 to 2021 - Statista Research Department, 2023

The strong presence of the paper industry in Italy not only highlights its significant contribution to the country's economy but also underscores its pivotal role in various sectors. The industry's turnover of approximately 25 billion Euros serves as a testament to its economic significance.

This substantial figure demonstrates the value generated by the paper industry and its influence on Italy's overall economic landscape (Allianz Trade - The paper industry report, 2023).

With 16,600 companies operating in the sector, the paper industry provides employment opportunities for 162,700 individuals directly. These jobs contribute to the livelihoods of many families and communities across the country. The industry's ability to generate employment further emphasizes its importance as a key sector within Italy.

Italy's position as the second-largest paper industry in Europe, trailing only behind Germany, solidifies its status as a major player in the European market. Accounting for 10.7% of the total volumes, Italy's paper industry holds a considerable share of the European market. This achievement is a testament to the industry's competitiveness and its ability to meet the demands of both domestic and international markets.
Italy's prominence extends to specific segments within the paper industry. The country takes the lead in the production of paper for domestic, hygienic and sanitary use, encompassing 20% of the European volumes. This indicates Italy's expertise and specialization in manufacturing paper products that cater to everyday needs, such as tissue paper, hygiene products, and other household essentials (Allianz Trade - The paper industry report, 2023).

Furthermore, Italy holds the second position in the production **of wrapping papers, contributing 13%** to the overall production in Europe. This achievement highlights the industry's ability to meet the diverse packaging needs of various sectors, including retail, food and beverage, and e-commerce.
Italy's significance in the production of packaging paper and cardboard is evident as well. Ranking third in Europe, the country accounts for 10% and 12% of the volumes produced in packaging paper and cardboard, respectively. This demonstrates Italy's capability to provide essential packaging materials for various industries, including consumer goods, logistics, and manufacturing (Allianz Trade - The paper industry report, 2023).
In addition to these segments, Italy secures a place on the podium for several other paper-based products. This includes flexible packaging, folding cases, shopping bags, sacks, self-adhesive labels, wallpapers, and gift items. Such a diverse range of products showcases Italy's versatility and innovation in meeting the demands of different markets and consumer preferences (Allianz Trade - The paper industry report, 2023).

Overall, the strong presence of the paper industry in Italy encompasses its significant contribution to the country's economy, its role as a major player in the European market, and its ability to meet the diverse needs of various sectors. The industry's success is a result of its competitiveness, expertise, and commitment to delivering high-quality paper products to both domestic and international customers.

Italy is an excellence both in terms of recycling rate and in terms of the quality and functioning of the system. Paper, on the other hand, is the biomaterial par excellence and represents a perfect example of circular bioeconomy. On the one hand, paper is renewable, biodegradable and 100% recyclable. On the other hand, the Italian paper industry has always reused the paper and cardboard of its productions according to the principle of circular economy. The utilization rate (ratio of paper consumption to be recycled to the production of paper and cardboard), which peaked at 63.4% in 2021, reached 62% in 2022. In paper packaging, the recycling rate is now steadily over 80%. (Federazione Carta e Grafica – Confindustria e dati Assocarta, 2023).

1.2.2. Paper production: the production process

In general, the paper **supply chain can be divided into four segments: the production of new paper** carried out by paper mills**, its transformation** by the printing and paper industry, the **collection of paper waste** by waste management companies and the subsequent treatment phases aimed at **the production of end of waste (EoW) raw material.**

The paper production process begins with the acquisition of a material called "pulp," which undergoes several production steps. This pulp is a natural material consisting of cellulosic fibers that are mechanically or thermo-mechanically separated from unwanted substances, such as lignin. A crucial phase in the process is the beating phase, which aligns the cellulosic fibers and encourages the formation of hydrogen bonds between them, resulting in a more cohesive material.
Subsequently, the preparation of the paper or paperboard sheet takes place. This involves concentrating a highly diluted suspension of fibers, typically around 2%, through drainage and compression on a filter cloth. This process yields a sheet with a dry residue content of approximately 30-40%. The continuous sheet is then sent to a "drying room" where steam-heated cylinders remove moisture, reducing it to final values ranging between 4% and 10%.
Once the drying process is complete, the determination of the grammage becomes crucial in distinguishing between paper and paperboard. Grammage refers to the weight of the material per unit area and serves as a key factor in categorizing the final product.
In summary, the paper production process involves obtaining pulp from natural materials, aligning the fibers through beating, and then forming a sheet by concentrating and compressing the fiber suspension. The sheet is dried to remove moisture, and the resulting material's grammage is determined to differentiate between paper and paperboard (Robertson, G.L. (2012). Food Packaging: Principles and Practice, Third Edition (3rd ed.). CRC Press. https://doi.org/10.1201/b21347).

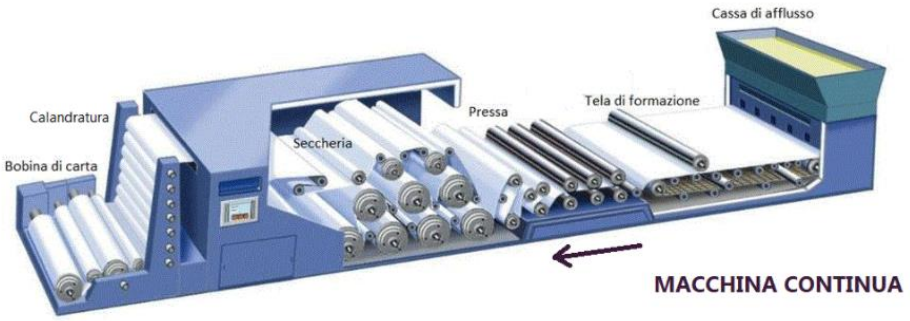

Figure 1.7 Example of a machine used for paper production – Image from https://www.tecnologiaduepuntozero.it

Over the years, the paper recycling chain is also acquiring more and more importance, in which, after a careful collection of paper and cardboard waste, these are properly washed and cleaned with the elimination of inks and other foreign substances, therefore, a pulp (recycled pulp) is obtained, which is once again part of the paper and cardboard production process.

1.2.3. Recyclability of paper: UNI 11743 and the 'Aticelca 501 Evaluation System'

In Italy, the evaluation of the recyclability and level of recyclability of predominantly cellulosic packaging is conducted using the Aticelca 501 Method, which underwent a split in 2019, leading to the development of the UNI 11743 Standard and the 'Aticelca 501 Evaluation System.'
The UNI 11743 Standard focuses on simulating the recycling steps that occur in a paper mill laboratory. This method involves evaluating various parameters to assess the recyclability of the packaging. These parameters include the quantity of coarse waste, final waste, formation of adhesive particles, formation of a sheet downstream of the production process, and its optical homogeneity (Aticelca, 2019).

The standard requires a series of laboratory tests to simulate the recycling process, which involves the following steps:

- Sample sampling and preparation: A representative amount of material is selected while preserving its essential characteristics and component proportions.
- Determination of dry matter content: The dry matter content of the sample is measured.
- Pulping and dilution of the dough: The sample is pulped in a laboratory pulper to obtain a representative dough sample for analysis. Conditions and times are set to simulate the process used in low-density industrial pulpers. The dough sample is then diluted for further testing.
- Measurement of coarse waste and preparation of the first accepted: The diluted dough undergoes mechanical separation to separate its different components. The solid fraction that does not pass through the separation cracks is considered coarse waste. The dough that passes through the perforated plates is the first accepted, which is used for subsequent tests.
- Measurement of flakes: The first accepted is further mechanically separated using plates with narrower slits compared to those used for coarse waste. The solid fraction retained by the plates represents the flakes.
- Measurement of adhesive particles (macrostickies): The first accepted undergoes mechanical separation using even finer cracks. Specimens are prepared, and an image analysis system is used to identify adhesive particles with diameters ranging from 0.1 to 2.0 mm. The total surface area covered by adhesive particles is measured.
- Preparation of second accepted dough and formation of laboratory sheets: The first accepted dough is homogenized based on adhesive particle size. Fiber consistency is determined, and test sheets are formed.
- Adhesion test: The test involves pressing the sheet between two metal plates at high temperature and checking if it adheres to the backing and covering sheets.
  Absence of adhesion is confirmed if the sheet can be fully separated from the substrate and cover without damage or breakage. Traces of paper fibers are allowed on the substrate and/or cover, but not paper fragments.
- Evaluation of optical inhomogeneities: The sheet is observed on both sides, and a judgment is made by comparing it with the references specified in the standard. The evaluation is based on a scale of 1 to 3, where level 1 indicates weak or no optical inhomogeneity (on a white or Havana basis), level 2 represents medium inhomogeneity,

and level 3 indicates high inhomogeneity. Sheets with intense, homogeneous colors fall into the second category, even if they have minimal or no optical inhomogeneity.

At the end of the test, a test report is drawn up. The results obtained are evaluated according to the parameters shown in Table 1.1, in the four levels of recyclability provided for (level A+, A, B, C), in addition to the assessment of non-recyclability with paper, i.e. impossibility of disposal within the separate collection with paper, which however does not prohibit the exploitation of the material in industrial processes or the initiation of energy recovery. The parameter with the worst value determines the class to which the sample belongs.

Aticelca 501:2019 Recyclability Assessment System	**Recyclability of paper**				**Not recyclable with paper**
	Level A+	Level A	Level B	Level C	Not recyclable with paper
Gross waste (%)	< 1.5	1.5 - 10.0	10.1 – 20.0	20.1 – 40.0	> 40.0
Adhesive particle area ø < 2000 µm. (mm2/kg)	< 2.500	2.500 – 10.000	10.001 – 20.000	20.001 – 50.000	> 50.000
Flakes (%)	< 5.0	5.0 – 15.0	15.1 – 40.0	> 40.0	-
Adhesiveness	absent	absent	absent	absent	present
Optical inhomogeneity	level 1	level 2	level 3	level 3	-

Table 1.1 Evaluation criteria for the recyclability of a predominantly cellulosic material/product.

Level A+ (Aticelca® 501): recyclable with paper in an effective and efficient way from a technological and economic point of view when used, through the currently most widespread paper production technologies, mixed with other secondary fibers obtained from the separate collection of paper. Its recycling results in a waste of less than 1.5 %;
Level A (Aticelca® 501): recyclable with paper in an effective and efficient way from a technological and economic point of view when used, through the currently most widespread paper production technologies, mixed with other secondary fibers obtained from the separate collection of paper. Its recycling results in a waste of less than 10 %;
Level B (Aticelca® 501): recyclable with paper in an effective and efficient way from a technological and economic point of view when used, through the most widespread paper production technologies, mixed with other secondary fibers obtained from the separate collection of paper. Its recycling results in a waste of less than 20 %;
Level C (Aticelca® 501): recyclable with paper when used, through the most widespread paper production technologies, mixed with other secondary fibres obtained from the separate collection of paper. Its recycling results in a waste of up to 40 % and/or a significant contribution of adhesive particles or cellulose fibre agglomerates;
Non-recyclable (Aticelca® 501): not recyclable with paper in an effective and efficient way from a technological and economic point of view when used, through the currently most widespread paper production technologies, mixed with other secondary fibers obtained from the separate collection of paper;

Figure 1.8 Levels of recyclability according to the Aticelca 501 method

The publication of version 2 of the Cepi method in July 2022 at the European level allowed for an update of the method, enabling harmonization across Europe (Cepi, 2022). The updated Cepi recyclability test method ensures that paper products can be tested for recyclability under identical conditions throughout Europe.
The Aticelca 501 Evaluation System, on the other hand, provides an overall assessment of the packaging's recyclability within the recycling process. The content of the test report in accordance with the UNI 11743 standard and the evaluation report in accordance with this Aticelca 501 system can be combined, by the qualified laboratory, in a single test and evaluation report. It determines the level of recyclability based on the worst parameter obtained during lab test described in the UNI 11743 Standard. (Aticelca, 2019).
Overall, the combination of the UNI 11743 Standard and the Aticelca 501 Evaluation System provides a comprehensive approach to evaluating and indicating the recyclability of predominantly cellulosic packaging, promoting sustainable practices and facilitating informed consumer choices (Aticelca, 2019).

1.2.4. UNI EN 643: criteria for the recyclability of paper

The compliance of recovered paper and cardboard with the UNI EN 643 standard is essential for categorizing it as recycled material rather than waste. The European standard EN 643 provides a comprehensive classification of different types of paper and cardboard for recycling, along with descriptions of the associated products under each category, commonly known as pulp. This standard acknowledges the diverse range of materials available in the market and establishes maximum acceptable tolerance levels for non-paper components. It also identifies materials that are considered undesirable or prohibited.
The maximum permitted quantity of non-paper materials allowed in most classes of pulp is set at 1.5% by weight. It is important to note that these thresholds pertain to foreign fractions, such as plastic bags or pieces of glass, and do not encompass constituents of the paper product itself, even if they are non-cellulosic in nature, such as windows, adhesive tapes, or paper clips.
The EN 643 standard defines pulping codes within five groups:
Group 1 - Ordinary Qualities: This group comprises the least valuable qualities of paper and cardboard, including unsorted mixed paper and cardboard, used corrugated containers, magazines, and descaling paper.
Group 2 - Medium Quality: It includes unsold newspapers, densely printed white trimmings, and selected office papers.
Group 3 - Superior Quality: This category consists of white and mixed printed matter trimmings, white newsprint, and white paper based on mechanical pulp containing coated paper.
Group 4 - Kraft Quality: It encompasses new corrugated cardboard trimmings, first and second grade kraft corrugated board, new kraft paper and board trimmings, and used kraft paper and board.

Group 5 - Special Qualities: This group includes codes related to mixed packaging, paper-based composites for beverages, laminates, and kraft coatings.
When assessing the suitability of recycled paper and cardboard as packaging raw materials for food contact, several aspects should be considered. These include the intended use of the final material (type of food, contact time and temperature), the likelihood of component migration during use, the quality and origin of the recycled paper, and the process technologies employed to remove undesirable substances and materials within the recycling mill. Recycling activities must employ the best available techniques to minimize or eliminate harmful ingredients from the food contact material supply chain.
Converters must evaluate the appropriateness of paper types composed of various grades of recycled paper for specific applications. This assessment should consider the intended use of the material (including the type of food, contact time, and temperature) and the potential migration of components during use.
To ensure the safety of recycled paper and cardboard intended for food contact, additional requirements outlined in documents such as CEPI Regulations, the "EN 643 standard," Recommendation BfRXXXVI (and similar), and Good Manufacturing Practices (GMP) must also be considered. These documents provide further guidance and regulations to ensure the safety and suitability of recycled materials for food packaging applications.

1.2.5. The recyclability of paper: statistics

In Italy we can boast an increasingly promising recycling chain of paper and cardboard made in Italy, according to the 2023 report of UNIRIMA (National Union of companies collection, recovery, recycling and trade of waste and other materials). Italy is in second place in Europe after Germany (followed by Spain and France) for the production of waste paper. The overall paper recycling rate in Italy rises from 72.8% to 75.9% in 2022. In the paper waste treatment sector aimed at the production of EoW raw material "waste paper", Italy can count on an "adequate plant network consolidated for decades, with an authorized capacity of paper waste treatment plants well above the quantities of paper and cardboard collected and more than sufficient even with respect to future increases". Paper and cardboard waste, coming from both municipal collection and production activities, is in fact delivered to as many as 716 paper waste treatment plants scattered throughout the country (UNIRIMA – Report 2023).

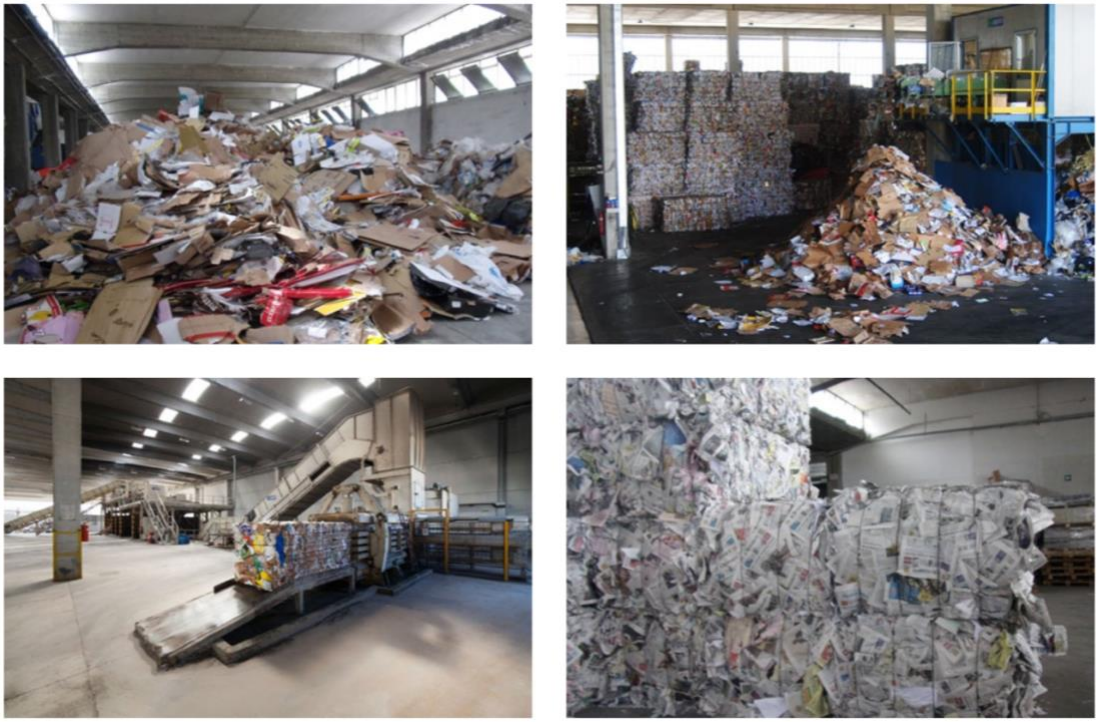

Figure 1.9. Steps in the waste paper production process. Source: UNIRIMA Companies

The increase in waste paper exports in the first half of 2023 compared to 2022 was 99.9%. Exports "continue to provide an outlet for the structural surplus of waste paper compared to the domestic needs of the Italian market". The first trading partner is India, with a share of 27.1% of the total, corresponding to over 401,000 tons. This is followed by Indonesia (18.6%), Germany (13%), Austria (12.8%) and Turkey (4.9%) (UNIRIMA – Report 2023) (Figure 1.10).

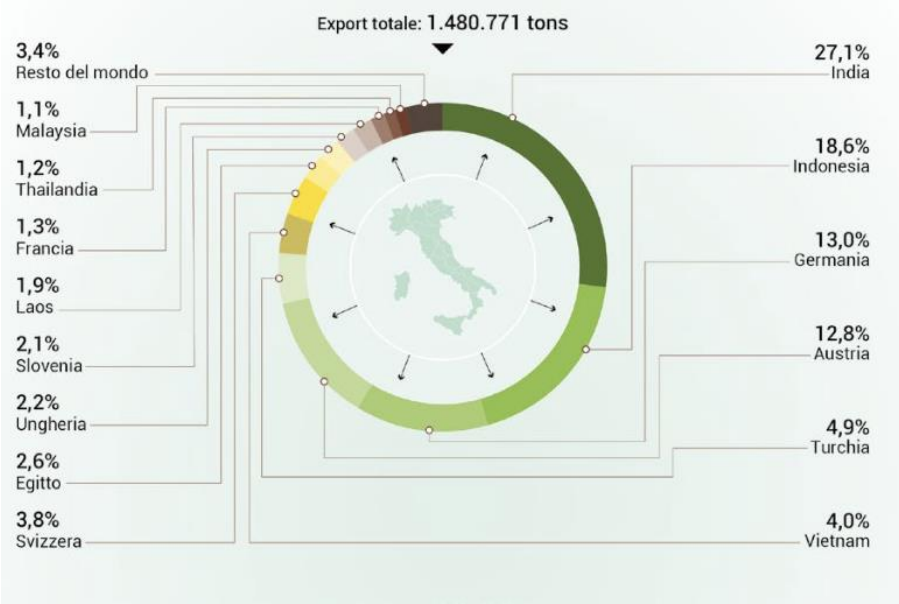

Figure 1.10. Waste paper export 2022 in Italy. Source: UNIRIMA Companies

The increasing importance of the paper recycling chain has led to significant advancements in Italy. The country has made remarkable progress in developing a robust paper and cardboard recycling system: according to the 2023 report by UNIRIMA, Italy now holds the second

position in Europe for waste paper production, closely following Germany. Spain and France rank third and fourth, respectively. This indicates Italy's commitment to sustainability and environmental consciousness.
The overall paper recycling rate in Italy has also witnessed a positive trend, rising from 72.8% in 2022 to 75.9% in 2023. This signifies the effectiveness of recycling initiatives and the growing awareness among the population regarding the importance of waste paper recovery.
Italy benefits from a well-established network of paper waste treatment plants that have been operating for several decades. These plants have obtained the necessary authorizations and have capacities that surpass the quantities of paper and cardboard collected. This ensures that the country has sufficient infrastructure and capacity to handle the current waste volume, as well as accommodate future increases in paper and cardboard recycling.
Currently, Italy boasts an impressive count of 716 paper waste treatment plants spread across the nation (Figure 1.11). These facilities play a vital role in receiving and processing paper and cardboard waste, which originates from both municipal collection systems and industrial production activities. The extensive coverage of these treatment plants ensures efficient waste management and promotes the circular economy principles.
In the first half of 2023, Italy experienced a significant surge of 99.9% in waste paper exports compared to the previous year. This indicates that Italian waste paper's surplus finds an outlet in international markets, fulfilling the demand beyond domestic requirements. Among the trading partners, India stands out as the primary recipient, accounting for a substantial 27.1% share, equivalent to over 401,000 tons. Other notable partners for waste paper exports from Italy include Indonesia (18.6%), Germany (13%), Austria (12.8%), and Turkey (4.9%).
The thriving waste paper export market demonstrates Italy's ability to contribute to global recycling efforts while stimulating economic growth through international trade. It highlights the country's role as a significant player in the waste management sector and showcases its commitment to sustainability on a global scale (UNIRIMA – Report 2023).

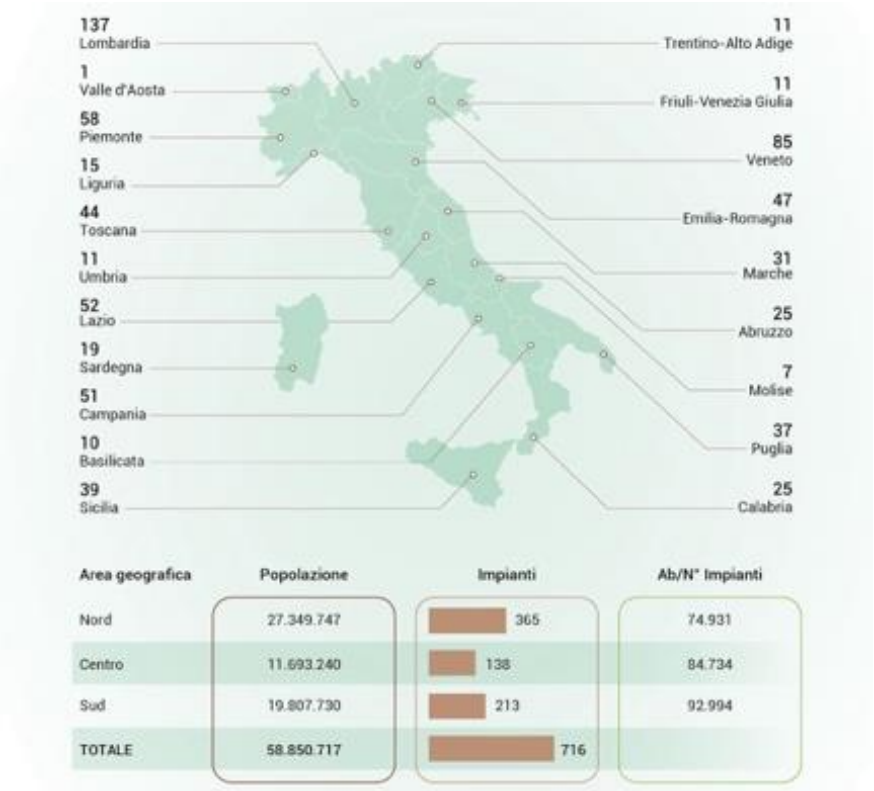

Figure 1.11 Location of the 716 paper and cardboard waste treatment plants distributed throughout Italy. Source: UNIRIMA Companies

1.2.6. The diversified CONAI Environmental Contribution (CAC)

In 2022, CONAI (National Packaging Consortium Italy) introduced new guidelines that resulted in a reduction of the annual contribution tax for users of paper and cardboard packaging. This initiative aims to promote and encourage the utilization of paper and cardboard as packaging materials.
The CONAI Environmental Contribution (CAC) was established as a financial contribution paid by producers and users to support the collection, selection, and recycling system for packaging. The CAC is determined based on the weight, quantity, and material composition of the packaging (CONAI, 2024). One of the key strategies employed by CONAI to encourage the use of more recyclable packaging is through contribution diversification.
In the paper supply chain, the diversification project initially focused on introducing an additional contribution (extra CAC) for polylaminated containers predominantly made of paper and suitable for containing liquids (CPLs). The aim was to enhance the effectiveness of the recycling process for more complex cellulose-based packaging, by strengthening collection, sorting, and recycling activities. CONAI further expanded the diversification of contributions to other types of composite packaging, specifically polylaminates with a prevalence of paper and cardboard (excluding CPLs). Through the application of an extra CAC, the contribution was aligned with the actual recyclability of these packaging types, their environmental impacts, and the emerging costs associated with their end-of-life management.
In 2021, the CONAI Board of Directors extended the contribution diversification to other paper-based composite packaging categories beyond liquid containers. Additionally, the value of the CAC for paper and cardboard packaging was decreased from €25.00/t to €10.00/t. For predominantly paper-based polylaminates designed for containing liquids (CPLs), the environmental contribution was reduced from €45.00/t to €30.00/t, while the extra CAC of €20.00/t remained unchanged. These changes took effect on January 1, 2022.
Composite packaging with a predominant paper component, excluding liquids, has been categorized into four types based on the weight of the paper component relative to the total weight of the packaging. Types A and B, with a paper component equal to or greater than 90% and 80% respectively, are currently not subject to any additional CAC.
Type C represents packaging where the paper component ranges from 60% to less than 80%. Recycling this type of packaging is complex and costly, as more than 60 kg out of 100 kg of packaging becomes non-recyclable waste using current technologies. Therefore, an extra CAC of €110/t has been applied to type C packaging since January 1, 2022.
Type D refers to composite packaging with a paper component less than 60%. This percentage significantly hampers the recyclability of the packaging, leading to adverse environmental impacts. In the recycling process, 100 kg of this packaging generates over 85 kg of dry waste and nearly 150 kg of wet waste, which must be disposed of in landfills after consuming water and electricity. Consequently, the CAC surcharge for this packaging category is €240/t. Packaging without explicit information regarding the paper component also falls into type D. (CONAI, 2022).

Table 1.2 shows the environmental contributions to be paid updated to 2024

Material/Contribution Bands		**From 1 January 2024**	**From 1 April 2024**
Paper	Level 1 (Base)	35,00 €/t	**65,00 €/t**
	Level 2 (CPL)	55,00 €/t	**85,00 €/t**
	Level 3 (Type C composites)	145,00 €/t	**175,00 €/t**
	Level 4 (Type D composites)	275,00 €/t	**305,00 €/t**

1.3. Bio-base, Biodegradable and Compostable

It is very important to clarify that the terms 'biobased' and 'biodegradable' are not synonymous; in fact, from the definition that we find in the 2017 report of the Wageningen Food & Biobased Research institute (van den Oever, 2017), they are defined:

- Bio-based: *"Bio-based is defined in European standard EN 16575 as 'derived from biomass'. Therefore, a bio-based product is a product wholly or partly derived from biomass. Biomass is material of biological origin, excluding material embedded in geological formations and/or fossilized (EN 16575, 2014). Examples are paper and wood, but also plastics such as PLA whose building blocks are produced from sugars. The bio-based carbon content in a material can be measured according to e.g. ISO 16620-4 or EN 16640. The bio-based content of a material can be determined with EN 16785-1."*

- Biodegradable: "*Biodegradable materials are materials that can be broken down by microorganisms (bacteria or fungi) into water, naturally occurring gases like carbon dioxide (CO_2) and methane (CH_4) and biomass (e.g. growth of the microorganism population). Biodegradability depends strongly on the environmental conditions: temperature, presence of microorganisms, presence of oxygen and water. So both the biodegradability and the degradation rate of a biodegradable plastic product may be different in the soil, on the soil, in humid or dry climate, in surface water, in marine water, or in human made systems like home composting, industrial composting or anaerobic digestion."*

In addition, in the same report (van den Oever, 2017), we also find the definition of 'Compostable': *"Compostable materials are materials that break down at composting conditions.*

Industrial composting *conditions require elevated temperature (55-60°C) combined with a high relative humidity and the presence of oxygen, and they are in fact the most optimal compared to other everyday biodegradation conditions: in soil, surface water and marine water. Compliance with EN 13432 is considered a good measure for industrial compostability of*

packaging materials, a.o. biodegradable plastics. According to the EN13432 standard, plastic packaging can only be called compostable if it is demonstrated that:
• The packaging material and its relevant organic components (>1 wt.%) are naturally biodegradable;
• Disintegration of the packaging material takes place in a composting process for organic waste within a certain time;
• The packaging material has no negative effect on the composting process;
• The quality of the compost is not negatively influenced by the packaging material.

*At **home composting** conditions, temperature is lower and less constant compared to industrial composting conditions due to the smaller amount of compostable material. As a result of the lower temperature, the degradation rate of a material is (much) slower compared to industrial composting, depending on the type of material. Vinçotte has its own test standard for certification of home compostable materials. An EN standard is currently being developed"*

The difference between the two terms is even more evident and clear if we look at table no. 1.3, in which polymeric materials are distinguished from those of petrochemical origin and biodegradable from non-biodegradable ones. It is clear that not all materials defined as biodegradable are in turn biobased and vice versa, i.e., there are materials of petrochemical origin that are defined as biodegradable.

Table 1.3 Table indicating positioning of bio-based versus petrochemical plastics and biodegradable versus non-biodegradable plastics.

	PETROCHEMICAL	**PARTLY BIO-BASED**	**BIO-BASED**
NO-BIODEGRADABLE	PE, PP, PET, PS, PVC	Bio-PET, PTT	Bio-PE
BIODEGRADABLE	PBAT, PBS(A), PCL	Starch blends	PLA, PHA, Cellophane

Therefore, when it is not possible to recycle the fibers contained in paper and cardboard packaging, they can be recovered together with organic waste at an industrial biological treatment plant.
At the end of the composting process, compost is obtained, a soil amendment product that is biologically stable, inert and odorless, ideal for soil nourishment and is suitable for a wide variety of agronomic uses.

The compostability of the packaging is tested in the laboratory according to the European technical standard UNI EN 13432 and was created to fill some legislative gaps left by the previous Directive 94/62/EC.

A waste, to be defined as compostable, must inevitably be biodegradable while, on the contrary, a biodegradable material is not necessarily compostable because, for example, it may not disintegrate sufficiently during a composting cycle. The main difference between the two terms

is therefore essentially in the timing of degradation. In addition, what is compostable returns to the earth as a nutrient in the form of compost, while biodegradable returns to nature in the form of mineral salts and other simple elements.

Biodegradable packaging and compostable packaging are both types of packaging that have eco-friendly characteristics but differ in how they degrade and decompose over time. To recap, in fact:

- Biodegradable packaging refers to materials that can be broken down by natural microorganisms present in the environment under proper conditions. This biodegradation process can take a varying amount of time depending on the material and environmental conditions, such as temperature, humidity, and the presence of oxygen. During biodegradation, materials decompose into simpler elements, such as water, carbon dioxide, and biomass. However, it is important to note that biodegradability does not necessarily imply that the material is completely free of environmental impacts, as residues or pollutants can be released during the process;

- Compostable packaging refers to materials that can be turned into compost through a controlled biological decomposition process, known as composting. In an industrial composting facility or suitable home environment, compostable material degrades into compost, a nutrient-rich material that can be used as a fertilizer for the soil. Compostable packaging requires specific conditions for composting, such as the presence of oxygen, humidity, and controlled temperature. It is important to follow the specific instructions and recommendations for proper disposal of compostable packaging, as landfilling or inadequate composting may not ensure complete decomposition of the material.

In summary, the main difference between biodegradable packaging and compostable packaging lies in the way they decompose. Biodegradable packaging decomposes through the action of natural microorganisms over time, while compostable packaging requires controlled composting conditions to turn into compost.

1.4. Techniques for improving the paper barrier through coating methods

Paper presents a promising alternative to conventional plastics, particularly in food packaging for fast-food, fruits and vegetables, as well as perishable items such as fish, meat, dairy products, and cured meats. It has garnered significant attention as a primary and secondary food packaging material due to its renewable and biodegradable properties (Deshwal, G.K et al., 2019; Oloyede, O.O et al., 2021). The utilization of paper and recycled paper is in line with the objectives set forth in "The UN Agenda 2030 for Sustainable Development," specifically Section 12.5, which aims to reduce waste production through prevention, reduction, recycling, and reuse (Soergel, B et al., 2021).
However, when it comes to packaging food items with a longer shelf life, uncoated paper has certain limitations. These limitations include inadequate resistance to microbial activity, low mechanical strength, and a porous microstructure that allows moisture, oils, and oxygen to penetrate through. In order to overcome these challenges, extensive research and development have been conducted on various advanced functionalization technologies, with coating being one of the prominent techniques explored in the literature.
The following are the most common coating techniques investigated:

- **Bar coating**, (Figure 1.12) also known as Mayer bar coating, is a technique used to apply a uniform layer of coating onto the surface of paper or other substrates. It involves using a metal bar, called a Mayer bar or coating rod, to spread the coating formulation onto the substrate (What is Mayer bar coating? (2022)). The coating is spread evenly across the paper, and excess coating is removed by the blade, leaving a thin, uniform layer.

  Bar coating offers several advantages:

  - Uniform Coating: The Mayer bar ensures consistent and uniform coating thickness across the substrate, resulting in a high-quality coated surface.
  - Control over Coating Thickness: The notch or groove size on the Mayer bar allows for precise control over the coating thickness. This is important for achieving the desired properties of the coated paper.
  - Versatility: Bar coating can be used with a wide range of coating formulations, including water-based and solvent-based coatings.
  - Cost-Effectiveness: Bar coating is a relatively simple and cost-effective coating method compared to some other techniques. (Solution Coating Methods: A Comparison. (n.d.))

  However, it's worth noting that bar coating may not be suitable for all coating applications. It is typically used for applying thin to moderate coating thicknesses and may not be ideal for very thick coatings or applications with highly specialized coating requirements. Additionally, the setup and cleaning process for bar coating can be time-consuming and may require careful attention to achieve consistent results.

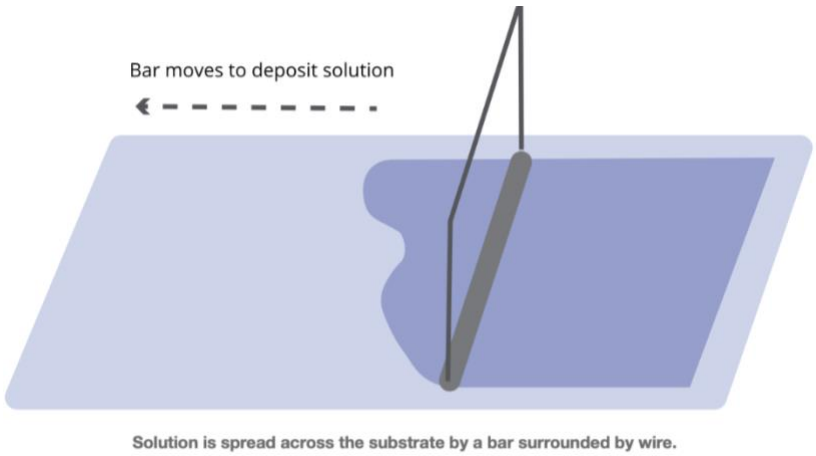

Figure 1.12 Bar coating technique

- **Extrusion Coating** (Figure 1.13) is a process where a molten polymer is extruded onto the paper surface using a metallic bar. Extrusion is widely recognized as the most reliable method for applying coatings to paper surfaces in manufacturing. This technique offers several advantages, including solvent-free applications, continuous processing, uniform coating, and reduced risks of holes and fractures. These benefits contribute to the popularity and widespread utilization of extrusion in the industry. (Basak et al., 2024). The polymer forms a continuous coating that adheres to the paper as it cools. Extrusion coating provides excellent barrier properties and is often used for packaging applications. However, extrusion coating has different limits, such as the necessity of specialized

equipment, including an extruder, die, and nip rolls, high cost manutention, the need for a large coating weight, high energy consumption and other issues that can limit coating efficiency and speed (Rastogi et al., 2015).

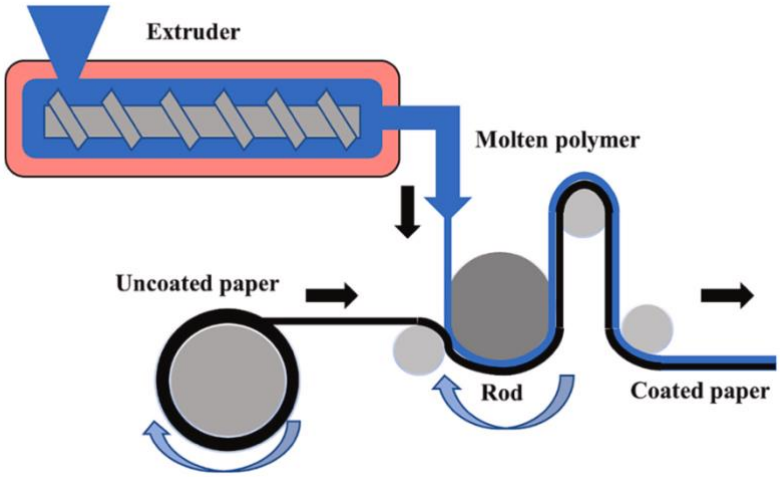

Figure 1.13 Extrusion coating technique. Image from Oil- and water-resistant paper coatings: A review (Basak et al, 2024)

- **Dip coating** (Fig. 1.4) involves immersing the substrate into a coating solution, and as it is withdrawn, a liquid layer adheres to the surface. The thickness of the coating is determined by the speed at which the substrate is withdrawn from the solution.
  Dip coating offers several advantages:
  - Simple process and setup: Minimal training is required, and specific coating thicknesses can be achieved by controlling a few parameters.
  - Suitable for flat substrates: Dip coating is well-suited for coating flat surfaces and can also be adapted for other shapes such as tubes. It coats both sides of a flat substrate simultaneously.
  - Uniform coatings: Dip coating allows for the creation of highly uniform coatings with nanometer-level surface roughness.
  - Gradient coatings: Varying the withdrawal speed during the process enables the creation of coatings with gradient properties.
  - Adaptable for different scales: Dip coating can be used in both high-precision batch processes and large-scale manufacturing.
  - Optimization with low-concentration solutions: By reducing the withdrawal speed, dip coating can be optimized for use with low-concentration coating solutions.
  - Significant drying time: Dip coating provides sufficient drying time, which is beneficial when film structure formation requires an extended period.

Overall, dip coating is a versatile method that offers simplicity, uniformity, and adaptability for various application scenarios.

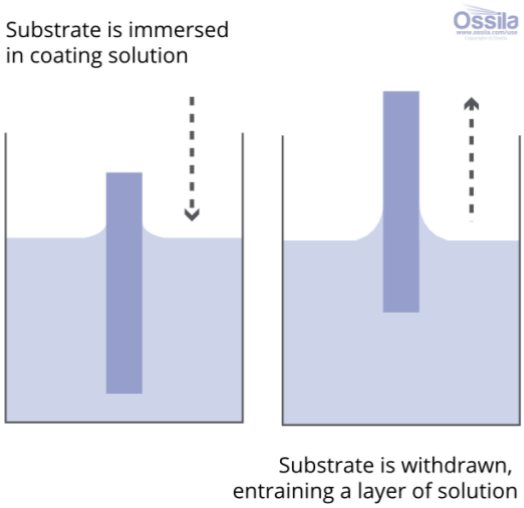

Figure 1.14 Demonstration of dip coating technique. Source: Ossila website

However, certain limitations and challenges exist when using dip coating. For instance, during the drying phase, the wet film is susceptible to environmental factors such as turbulent air flow, which can affect the coating quality. Additionally, dip coating may encounter difficulties when coating curved or flexible substrates. Moreover, depending on the coating solution used, the film may require post-deposition heat treatment, which can restrict the range of compatible substrates and increase the overall cost of the process. (Solution Coating Methods: A Comparison. (n.d.)).

- **Spray coating** involves atomizing the coating formulation into fine droplets and spraying them onto the paper surface. This method allows for precise control of coating thickness and is commonly used for applying functional coatings, such as release coatings or barrier coatings, onto paper (Basak et al., 2024).

- **Air Knife Coating** is a high-speed coating method that uses a pressurized air knife to apply a thin, uniform layer of coating onto the paper surface. The coating formulation is atomized and sprayed onto the paper, and the air knife removes excess coating, leaving behind a controlled and precise coating thickness (Basak et al., 2024).

- **Spin Coating** (Figure 1.15) is a technique used to apply a solution onto a flat substrate. In this method, the solution is dispensed onto the substrate, which is either already rotating or starts rotating afterward. The centrifugal force generated by the rotation causes the solution to spread evenly across the surface, forming a thin film. The thickness of the resulting film is determined by the shearing force, which is directly proportional to the rotation speed.

  Advantages:
  - Simple and Easy Process: Spin coating is a straightforward technique to implement, requiring minimal training.
  - Precise Coating of Small and Flat Substrates: It is well-suited for coating small and flat substrates with high precision.
  - Wide Range of Film Thickness: Spin coating allows for the deposition of films with thicknesses ranging from nanometers to microns.
  - Fast Drying Time: The thin films created by spin coating typically dry quickly, leading to short film creation times.

Spin coating has several disadvantages that restrict its applicability. Firstly, it is most effective for coating small substrates and is limited to batch processing. As a result, it is not suitable for large-scale production, making it primarily applicable to research and development settings. Another drawback is the significant amount of material wasted during the spin coating process, leading to high levels of waste generation.
Furthermore, spin coating is unsuitable for creating films on curved surfaces, limiting its utility in such cases. It also presents challenges when coating flexible surfaces, making it a less suitable method for such applications (Solution Coating Methods: A Comparison, n.d.).

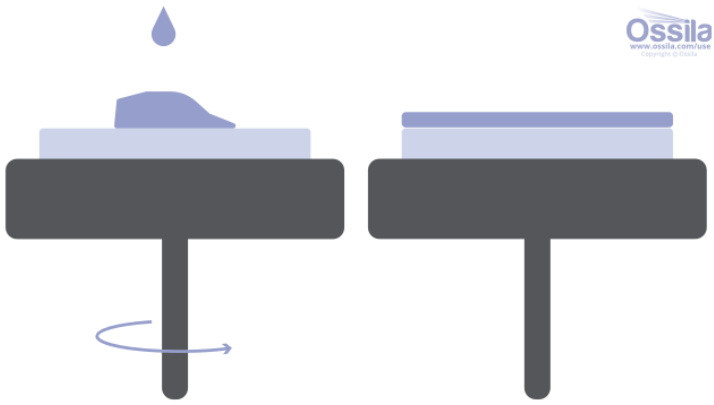

Figure 1.15 Demonstration of spin coating technique. Source: Ossila website

- **Flexographic coating** is a roll-to-roll coating method commonly used for applying functional coatings, such as barrier coatings or adhesives, onto paper. It utilizes flexible relief plates mounted on a printing press to transfer the coating formulation onto the paper surface. Flexographic coating is known for its high-speed capabilities and is widely used in packaging applications.

- **Curtain coating** involves passing the paper through a falling curtain of coating formulation. The paper is guided through the curtain, which evenly coats the surface. Excess coating is collected and recycled for reuse. Curtain coating is suitable for a wide range of coating formulations and provides excellent coating uniformity.

1.5. What materials is paper coated with to improve its properties?

The water vapor barrier and water repellency properties of paper are limited by the hydrophilic nature of cellulose, which is attributed to the presence of OH sites in the cellulose base unit and the porosity of the fiber network. In order to enhance the barrier effect, it is common practice to apply coatings of materials derived from fossil oils or synthetic polymers onto one or both sides of the paper. These materials have gained dominance in the current market due to their low cost and widespread availability.

These polymers encompass a range of materials, including waxes, ethylene vinyl alcohol (EVOH), polyvinylidene chloride (PVDC), and polyolefins such as polyethylene (PE), low-density polyethylene (LDPE), linear low-density polyethylene (LLDPE), high-density

polyethylene (HDPE), polypropylene (PP), as well as aluminum, metallized plastic layers, and other derivatives. (N Sundar et al., 2020; Schoukens et al., 2014)

In an effort to address the porosity and hygroscopicity of paper, polyolefins are often selected as coating materials. However, the addition of synthetic polymer layers compromises the biodegradability and recyclability characteristics of the resulting material (Khwaldia et al., 2010). This poses a challenge to the environmental sustainability of packaging utilizing such coatings. Furthermore, the use of these materials not only poses risks to the environment but also to human health.
Poly-fluoroalkyl substances (PFASs) represent another group of compounds employed to enhance the oil and water properties of paper. They were widely utilized in food packaging for their water and oil repellency until they were regulated in 2015 due to their harmful effects on humans, animals and the environment (Sunderland et al., 2019). The international concerns regarding potential health effects associated with PFAS exposure emerged in the early 2000s when perfluorooctanesulfonate (PFOS) was detected in the blood of polar bears in the Arctic and wildlife in other remote regions (Giesy et al., 2001). Numerous studies have since investigated the carcinogenicity of PFASs, with findings reporting prostate cancer mortality (Gilliland et al., 1993) and positive associations between Perfluorooctanoic acid (PFOA) levels and kidney and testicular cancers (Barry et al., 2013; Vieira et al., 2013).

Several studies have provided relatively consistent evidence of modest positive associations between exposure to certain synthetic polymers and lipid profiles, including total cholesterol and triglycerides. However, the magnitude of the effect on cholesterol levels appears to vary inconsistently across different levels of exposure. While there is some evidence suggesting a modest positive correlation between exposure to these synthetic polymers and metabolic diseases such as diabetes, overweight, obesity, and heart diseases, the findings in this regard are less consistent (Steenland et al., 2010; Cardenas et al., 2017; Liu et al., 2018). Additional studies have revealed further concerns related to the effects of synthetic polymer exposure. For instance, research has found a higher prevalence of high cholesterol concentration in children aged between 7 and 15 years who have been exposed to these materials (Maisonet et al., 2015). This suggests that the impact of synthetic polymers on lipid profiles may extend to younger age groups, potentially affecting their long-term health outcomes.
Moreover, exposure to synthetic polymers during pregnancy has been associated with negative effects on both the mother and child, both during gestation and later in life. These effects include an increased risk of gestational diabetes, a condition characterized by high blood sugar levels during pregnancy, in expectant mothers (Matilla-Santander et al., 2017). Such findings highlight the potential implications of synthetic polymer exposure on maternal health and the well-being of the developing fetus.

The accumulation of evidence underscores the need to further investigate and understand the potential adverse effects of synthetic polymer exposure across different age groups and stages of life. It is crucial to consider these findings when evaluating the safety and suitability of using synthetic polymers in various applications, particularly those that come into contact with food and during pregnancy. Developing alternative materials and promoting more sustainable practices can help mitigate these potential risks and safeguard the health of individuals at all stages of life.
Indeed, the increasing concerns surrounding the environmental and human health impacts associated with plastic materials and fluorinated compounds, along with their derivatives, have sparked a search for alternative solutions in the development of sustainable materials.

1.5.1. An overview of coating formulations to improve the paper characteristics

The development and implementation of eco-friendly and compostable coatings for paper packaging represent a significant step toward achieving a more sustainable solution. By addressing the limitations of paper, these coatings enhance its functionality and enable its integration into compostable supply chains.
The utilization of degradable components sourced from nature, such as biopolymers, polysaccharides, and other natural materials, is at the forefront of current research on sustainable coatings. These materials offer promising potential as coating materials due to their environmentally friendly and compostable characteristics. By leveraging these coatings, it becomes possible to improve the resistance of paper to substances like oil, water, and water vapor, effectively overcoming its inherent limitations.
Moreover, sustainable coatings can provide additional benefits to paper packaging. For instance, they can impart antimicrobial properties, helping to preserve the freshness and safety of food products. Antioxidant properties can also be incorporated, contributing to the extension of food shelf life. These functionalities are crucial for ensuring that packaged food remains safe and of high quality throughout its intended storage and consumption period.
Furthermore, by selecting coating materials derived from renewable sources, the negative environmental impact associated with traditional coatings can be minimized. Natural materials offer a sustainable alternative to petroleum-based components, reducing reliance on fossil fuels and decreasing carbon emissions. This aligns with the principles of circularity and environmental responsibility, as it promotes the use of resources that can be replenished and recycled.
It is important to note that the development of compostable coatings, that can come not only from renewable resources, is an ongoing area of research and innovation. Continued efforts in this field hold great potential for further advancements and discoveries. By combining scientific expertise, technological advancements, and a commitment to sustainability, researchers and industry professionals can collaborate to create packaging materials that fulfill both performance and sustainability requirements.

Ultimately, the successful development and widespread adoption of these coatings will contribute to a more sustainable packaging industry. It will enable the use of paper as a viable alternative to conventional materials, reducing reliance on non-renewable resources and minimizing waste generation. By embracing innovative solutions and promoting sustainable practices, the packaging industry can strive towards a more environmentally conscious future.

The subsequent paragraphs will outline scientific research conducted by scientists and industry professionals in the field of food packaging, focusing on efforts to enhance the properties of paper through the application of coatings.

The literature on this topic can be categorized into two main groups:

1. Origin of Polymers for Coating Formulation: this group focuses on the research and investigation of various polymers that are used in the formulation of coatings for paper. Scientists and researchers explore the sources, properties, and characteristics of these polymers, including their biodegradability, compostability, and compatibility with paper substrates. They examine natural polymers, such as biopolymers and polysaccharides, as well as synthetic polymers derived from renewable resources. The

aim is to identify suitable coating materials that meet environmental sustainability goals without compromising the performance of the paper.

2. Characteristics improved by the use of coating on paper: this group of studies examines the effects of applying coatings to paper and the subsequent enhancement of its properties. Researchers investigate how the coatings improve the resistance of paper to substances such as oil, water, and water vapor, as well as its mechanical strength. They explore the impact of coatings on the barrier properties of paper, its printability, and its ability to protect and preserve packaged food. The objective is to identify coating formulations and techniques that optimize the functional performance of paper as a packaging material.

Through these two groups of bibliographic works, scientists and industry experts contribute to the understanding of coating technologies for paper packaging. Their research aims to develop sustainable coating solutions that not only improve the characteristics of paper but also align with environmental considerations and support the transition towards more eco-friendly packaging materials, and above all compostable.

1.5.1.1. Origin of Polymers for Coating Formulation

In the scientific literature, numerous studies have focused on the use of natural polymers in the formulation of coatings to enhance the characteristics and properties of paper. One commonly utilized natural polymer is polyvinyl alcohol (PVOH or PVA). PVA is a non-toxic, highly crystalline polymer that is soluble in water. It is also biocompatible and biodegradable, containing a significant number of hydroxyl (OH) groups in its backbone chains, which are a source of hydrogen bonding (Kumar Panda et al., 2022).

For instance, Gu et al. (2022) developed a crosslinked polyvinyl alcohol/nanoclay (PVA/NC) hydrogel for coating the surface of paper. They prepared different solutions of **PVA** at various concentrations (2%, 5%, and 10% w/w) and mixed them with **nanoclays** in different proportions. The 10% w/w PVA solution and various PVA/NC hydrogel solutions were then applied as coatings on the paper to improve its inherent characteristics. In another study by Tarnowiecka-Kuca et al. (2023), aqueous solutions of PVA and **cellulose nanocrystals** (CNCs) were employed to coat paper samples with different grammages (40 g/m^2, 70 g/m^2, 100 g/m^2). The objective was to obtain cellulose-based packaging materials with improved barrier properties, while still maintaining recyclability. Furthermore, PVA from Kamel et al. (2004) was combined with **chitosan**, another natural polymer, to create coating solutions aimed at improving the mechanical properties of paper. Solution of PVA mixed with **starch** or starch derivatives is another of the winning combinations for obtaining coatings intended to improve the characteristics of paper, in the literature there are several authors who have obtained films and coatings from the combination of these two polymers (Alradha et al., 2023; Abedi-Firoozjah et al., 2023; Teodorescu et al., 2018; Zhu et al., 2018; Lin et al., 2017; Javed et al., 2018; Tian el al., 2017)

Indeed, **chitosan** is one of the most extensively studied natural polymers for formulating coatings for paper, as highlighted in the literature. Chitosan is a polysaccharide derived from the deacetylation of chitin, featuring β-(1-4)-linked d-glucosamine and N-acetyl-d-glucosamine units. It possesses remarkable properties that make it an attractive choice for paper coatings. Chitosan is a cationic biopolymer with hydroxyl groups capable of forming hydrogen bonds, similar to cellulose fibers. It also exhibits film-forming ability and antimicrobial

properties. Moreover, it is biodegradable, biocompatible, and non-toxic (Mitelut et al., 2015, Fithriyah et al., 2014).

In a recent study conducted by Roman et al. (2023), they explored the utilization of colloidal dispersions consisting of **xylane derivatives** (hydrophobic xylan with alkylketene-XyAKD dimers), **acetylated xylan** (XyAc), and chitosan (Ch) biopolymer as coatings for a paper substrate. These dispersions were applied in one or two successive layers using an automatic laboratory film applicator. The researchers specifically chose these two polymers because the combination of anionic xylan with cationic chitosan provides a compelling completely bio-based alternative, aligning with the scientific community's growing interest in utilizing natural materials in their research endeavors.

This study is just one example of the ongoing efforts in exploring the potential of chitosan in combination with other natural polymers as coating materials for paper. In fact, there have been several studies investigating the combination of chitosan with **antioxidants** like rosemary, astaxanthin, and genipin (Inthamat et al., 2023; Vrabič Brodnjak et al., 2020), as well as with alginate (Kopacic et al., 2018), **lipids, fatty acids, and bioresins** (Reis et al., 2011; Parvathy et al., 2021). These studies demonstrate the versatility of chitosan and its potential synergies with other natural compounds in developing innovative coatings for paper-based applications.

Another important natural polymer widely used for the formulation of paper coatings is **starch and its derivatives**. Starch is an exceptionally versatile raw material for various applications. Starch offers several advantageous properties that make it a valuable resource in the development of innovative materials with diverse applications. Firstly, as a natural polymer with a high molecular weight, starch can undergo controlled depolymerization, allowing for precise modifications. Secondly, starch is hydrophilic, which enables it to disperse in water and form hydrogen bonds with cellulose fibers and pigments, facilitating their attachment. Thirdly, the hydroxyl groups present in starch enable a wide range of substitution or oxidation reactions, allowing for adjustments to its rheological characteristics and the prevention of retrogradation. Furthermore, through graft copolymerization, starch can be utilized to produce novel materials that combine the beneficial properties of both natural and synthetic polymers. This versatility in modification and combination makes starch a valuable ingredient in the creation of innovative materials for various applications (Li et al., 2019).

Similar to chitosan, starch is frequently combined with other molecules to create paper coatings. One such combination involves the incorporation of **silver nanoparticles (AgNPs)** into starch bio-nanocomposites. Paper coated with AgNPs/starch bio-nanocomposites has demonstrated exceptional antibacterial activity, as well as enhanced barrier properties, mechanical strength, and resistance to oil. This synergistic combination of starch and AgNPs offers a multifunctional coating solution for paper, providing not only antimicrobial properties but also improved performance in terms of protection against external elements and durability. (Dang et al., 2018; Jung et al., 2018; Martins et al 2012). Starch is frequently combined with another group of nanoparticles, namely zinc oxide (ZnO) nanoparticles, in the development of bio-nanocomposite coatings for paper. The incorporation of ZnO/starch bio-nanocomposites has been shown to enhance various surface properties of paper, including brightness, whiteness, smoothness, surface strength, and printing properties. Several studies have demonstrated the positive effects of ZnO/starch coatings on paper characteristics (Chitena et al., 2023; Dehghani Firouzabadi et al., 2023; Yu et al., 2009; Ma et al., 2009; Lanje et al., 2013; Luo et al., 2018).

Furthermore, the combination of chitosan and starch blends has been found to improve the thermal stability, print quality, and oil resistance of coated paper. Studies by van den Broek et al. (2015) and Brodnjak et al. (2017) have demonstrated the beneficial effects of chitosan-starch blends on these paper properties. Additionally, various studies have explored the utilization of chitosan-starch coatings to enhance different characteristics of paper (Long et al., 2015; Reis et al., 2011; Brodnjak et al., 2017).

Polylactic acid (PLA) is another polymer that has been explored as a coating material for paper. PLA is a biodegradable and renewable polymer derived from plant-based sources, such as corn, sugarcane, or other starch-rich crops. It has gained significant attention as an environmentally friendly alternative to conventional petroleum-based plastics (Sundar et al., 2020.).

When used as a paper coating, PLA offers several advantages. It provides a protective barrier that enhances the paper's resistance to water, oil, and grease, thereby improving its durability and suitability for various applications. Additionally, PLA coatings can improve the smoothness and surface strength of the paper, resulting in enhanced tactile qualities and overall appearance.

Moreover, PLA, used to coat the paper, is still compatible with various additives and fillers, such as **nanoparticles, pigments, or other polymers** (Zang et al., 2016) allowing for further customization of the coating properties. For example, the incorporation of **nanoparticles, such as silver or zinc oxide** (Zhang et al., 2017; Bikiaris et al, 2023; Liu et al., 2024), into PLA coatings can confer antimicrobial properties to the paper.

Overall, PLA coatings offer an eco-friendly and versatile option for enhancing the performance and functionality of paper materials. Their biodegradability and renewable nature make them an attractive choice in the quest for more sustainable packaging and printing solutions (Taib et al., 2023).

Lastly, we have the family of **polyhydroxyalkanoates (PHAs),** which has gained significant interest in recent years. PHAs are renowned for their desirable properties, including biodegradability, biocompatibility, and hydrophobicity. However, it is important to note that these biopolymers also have certain drawbacks that hinder their competition with synthetic polymers. One such drawback is the cost factor. The production of PHAs involves the use of bacteria or microorganisms to ferment renewable feedstocks, which contributes to higher production costs. Additionally, PHAs exhibit inferior mechanical properties, including lower tensile strength and impact resistance, when compared to conventional plastics. Furthermore, PHAs also have a higher melting temperature than many traditional plastics, which presents challenges during processing.

To address these limitations, researchers are actively working on modifying PHAs to enhance their properties for potential applications in various fields. These modifications aim to optimize the performance of PHAs and expand their utility. By tailoring the chemical structure or incorporating additives, the properties of PHAs can be adjusted to overcome their inherent limitations and meet specific application requirements. There are many low-cost natural raw materials such as cellulose, starch, lignin, etc (Lai, et al., 2015; Mousavioun et al., 2012; Furukawa et al., 2007) that can be used in the blending of PHA.

Numerous studies have investigated the utilization of polyhydroxyalkanoates (PHAs), a family of polymers, for enhancing the characteristics of paper, particularly for packaging applications.

For instance, Salemi et al. (2007) conducted research on coated paper sheets fabricated with various blends of PHA and other biodegradable polyesters, evaluating their performance. Bourbonnais et al. (2010) compared native and artificial granules, derived from commercially available poly(3-hydroxybutyrate) (PHB) and poly(3-hydroxybutyrate-co-hydroxyvalerate) P(3HB-co-3HV), as sizing agents for paper. Sängerlaub et al. (2019) explored the application of the biopolymer poly(3-hydroxybutyrate-co-3-hydroxyvalerate) (PHBV) on a paper substrate through extrusion coating. Additionally, Lauzier et al. (1993) developed a biodegradable latex on paper by employing a PHA solution through heat press techniques.

These studies demonstrate the efficiency of using biodegradable polymers to create coating materials to improve the characteristics and performance of paper. By harnessing the unique properties of these polymers, researchers are exploring ways to improve the mechanical strength, barrier properties, and other functional aspects of paper-based packaging materials.

The improvement of paper characteristics for food packaging is not limited to natural polymers and molecules alone; it also involves the use of synthetic polymers, either alone or in combination with natural polymers and molecules. Numerous studies in the literature demonstrate how the incorporation of these polymers can enhance the intrinsic properties of paper. The key factor is not necessarily the origin of the polymers but their biodegradability/compostability.

One commonly used petrochemical-based polymer with biodegradable characteristics is poly(ε-caprolactone) (PCL). PCL is a semicrystalline aliphatic polyester known for its biodegradability and possesses high mechanical strength and ductility. For instance, Lim et al. (2013) blended PCL with poly(3-hydroxybutyrate-co-3-hydroxyhexanoate) (PHBHHx), resulting in enhanced toughness and substantial elasticity of PHBHHx. Chiono et al. (2008) developed a blend of poly(3-hydroxybutyrate-co-3-hydroxyvalerate) (PHBV) and PCL in chloroform, producing fibers with low mass and surface porosity.

Sogut and Seydim (2018) created bilayer films by combining PCL, chitosan, nanocellulose, and grape seed extract. This combination improved the suitability of chitosan films for food packaging applications while maintaining the inherent biodegradability of the paper and natural polymers used. Bota et al. (2017) employed PCL in combination with silicon and aluminum nanoparticles to coat printed cardboard samples. They prepared four different paints: pure PCL (K/P), PCL with 2% SiO_2 (K/P/2Si), PCL with 1% Al_2O_3 (K/P/1Al), and PCL with 2% SiO_2 and 0.5% Al_2O_3 (K/P/2Si/05Al). These combinations aimed to enhance the characteristics of PCL coatings while ensuring biodegradability.

It is worth mentioning that PCL can also be associated with nanoparticles such as ZnO, TiO_2, and various other compounds and polymers to further improve its coating properties while maintaining biodegradability (Cigula et al., 2021; Hudika et al., 2020; Selvaraj et al., 2023). These studies demonstrate the versatility and potential of PCL and its combinations with other substances in enhancing the properties of paper coatings while remaining biodegradable.

Poly(butylene-adipate-co-terephthalate) (PBAT) is a promising biodegradable polymer derived from petrochemicals. It is produced through polycondensation of butanediol (BDO), adipic acid (AA), and terephthalic acid (PTA). PBAT has been found to possess excellent properties and good biodegradability, making it a suitable choice for various applications (Jian et al., 2020). In a compost simulation test conducted by Witt et al. (1995), PBAT co-polyesters were shown to degrade at 60 °C, resulting in a PTA content of approximately 50 mol%. While

PBAT is commonly used in the production of envelopes and films, its application as a paper coating is a relatively new technology. However, several studies in the literature have explored the combination of PBAT with different polymers for paper coating production.

One such study investigated the use of pristine and esterified lignin as functional fillers in PBAT-based bioplastic paper coating formulations. The researchers dispersed 10-50 wt% of pristine and esterified lignin separately in a solvent, incorporated them into PBAT solutions, and applied them onto paper substrates (Shorey and Mekonnen, 2022). Another study by Lamsaf et al. (2023) introduced hemp stalk fibers, derived from the processing of Cannabis sativa, into PBAT to create coating papers. The incorporation of 2% (w/w) hemp in the PBAT matrix enhanced several properties of the coating paper.

In a different approach, Eslami and Mekonnen (2023) developed a multilayer film for paper coatings consisting of a 12 μm layer of starch and a thin layer (12 μm) of either PBAT, PLA, PHBV, or PVOH. This research aimed to explore the performance of different polymers in paper coatings.

Poly(butylene succinate) (PBS) is another aliphatic polyester produced by condensation polymerization of succinic acid and 1,4 butanediol. PBS can be derived entirely from bio-based sources, using bio-derived succinic acid and 1,4 butanediol (Liminana et al., 2018). Thunber and Curtzwiler (2020) investigated the potential of PBS as a sustainable alternative to conventional non-eco-friendly coatings for paper. PBS demonstrated resistance to oil migration at elevated temperatures and compostability properties, making it an environmentally friendly option. In one study, PBS was combined with PVOH to create coatings for Kraft paper. The biodegradation of the materials under composting conditions showed some extent of degradation with the development of the priming effect, although further studies are needed (Hamdanin et al., 2023).

The versatility of PBS was also demonstrated in the study by Petchwattana et al. (2021), where it was used to create a sachet for extending the shelf-life of white bread, with controlled release of an antimicrobial agent. The bag was composed of PVOH and PBS combined with the antimicrobial agent, providing an alternative approach to minimize food waste. Additionally, Bi et al. (2021) found that PBS was effective in improving the performance of mulch paper. Their work focused on the fabrication of multi-layer fertilizer-infused mulch papers using biodegradable poly(butylene succinate) (PBS), poly(hexamethylene succinate) (PHS), and their copolyesters through blade coating and melt compression molding techniques.

1.5.1.2. Characteristics improved by the use of coating on paper

This collection of studies delves into the application of coatings on paper and explores the subsequent improvements in its properties. Researchers aim to understand how these coatings enhance the paper's resistance to various substances, including oil, water, and water vapor, while also bolstering its mechanical strength.

By applying coatings to paper, scientists seek to create a protective barrier that shields the paper from external factors. These coatings act as a shield against oil, preventing it from seeping into the paper fibers and causing stains or damage. Similarly, the coatings enhance the paper's resistance to water, making it more resilient against moisture absorption, which can lead to

deformation or weakening of the paper structure. Moreover, the coatings play a crucial role in minimizing the permeability of water vapor through the paper, preserving its integrity and preventing warping or curling.

In addition to the barrier properties, the coatings contribute to the mechanical strength of the paper. They reinforce the paper's surface, making it more resistant to tearing, folding, or creasing.

- Improvement hydrophobic characteristics of paper by the use of coating: Several scientific studies have focused on improving the hydrophobic characteristics of paper through the application of coatings. The hydrophilic nature of cellulose, which contains OH sites and a porous fiber network, limits the water vapor barrier and water repellency properties of paper. To address this issue, researchers have explored various coating formulations. One study by Kopacic et al. (2018) involved coating paper samples with solutions of chitosan and alginate. The results showed that the introduction of chitosan alone significantly improved the paper's barrier against water vapor. The water vapor transmission rate (WVTR) decreased by 60% compared to uncoated paper, with a minimum reduction of 35%. Chitosan has been associated with improved water vapor resistance in other studies as well. Brodnjak and Tihole (2018) combined chitosan with a solution of zein-rosemary oil, resulting in a WVTR reduction from approximately 500 g/m²·24 h for uncoated paper to 254 g/m²·24 h for the coated sample containing the mixture of the three molecules. In a more recent application, Roman et al. (2023) analyzed the potential of xylan and chitosan-based coatings and achieved WVTR values of 30 g/m². Li et al. (2019) coated paper with 8.6 wt% chitosan and 2.2% PDMS, resulting in good repellent capacity with a water contact angle (WCA) of 95.2°. Nair et al. (2022) used an aqueous solution of chitosan-g-PDMS, which exhibited a WCA of 120.53 ± 0.96° when applied as a coating over a paper substrate. Over the years, various formulations based on chitosan have been tested to improve the water vapor resistance of paper. These include combinations with starch, fatty acids, and other materials (Reis et al., 2010; Inthamat et al., 2024). Tarnowiecka-Kuca et al. (2023) demonstrated that the use of polyvinyl alcohol (PVA) with cellulose in the formulation of paper coatings improved the WVTR value. Different coating techniques, such as flexographic printing, rotogravure printing, and blade printing, were evaluated, resulting in a decrease in WVTR from 5000 g/m²·day to 1000 g/m²·day. Gu et al. (2022) showed that the use of PVA/nanoclay cross-linking coating reduced the WVTR value from 1861 g/m²·day to 195 g/m²·day. In the study by Sogut and Seydim (2018), the creation of a bilayer using PCL polymer combined with chitosan and grape seed led to a reduction in both WVTR and water vapor permeability (WVP). The effectiveness of bilayer systems has been demonstrated by several authors (Khwaldia et al., 2014; Rivero et al., 2009). Shorey and Mekonnen (2022) found that adding 50 wt% esterified lignin to PBAT increased the water contact angle by 72.6% compared to PBAT alone. Wang et al. (2022) discovered that coating paper with a 1:1 mixture of carboxymethyl chitosan (CMCS) and CMC improved moisture repellency, with a coating load of 5.1 g/m² resulting in a 30° increase in WCA. These studies highlight the potential of various coating formulations to enhance the hydrophobic properties of paper, including improved water vapor resistance and water repellency. By exploring different combinations of materials and developing innovative coating techniques, researchers aim to optimize the performance of paper coatings for a wide range of applications.

- Improvement fat and oil resistance of paper by the use of coating: Oil resistance is a crucial characteristic of packaging materials used for oily and fat-containing foods. It is essential for packaging materials, especially in the food industry, to resist the permeation of oil. Oils and fats in food products can interact with the packaging material, leading to undesirable consequences such as flavor loss, compromised quality, or contamination. Therefore, developing coatings that effectively prevent oil migration through the packaging substrate is of utmost importance. Further research and development efforts are needed to investigate and optimize the performance of coatings in terms of oil resistance for food packaging. In one study by Tayeb et al. (2020), thin films (16 g/m²) made from cellulose nanofibrils (CNF) and lignin-containing cellulose nanofibrils (LCNF) were filtered and coated onto paper substrates. The inclusion of lignin enhanced the oil-proof performance, and these layered structures exhibited outstanding grease resistance with a maximum Kit value of 12. Wang et al. (2022) found that using sodium alginate treated with CMCS as a paper coating resulted in excellent oil barrier efficacy, with a Kit score of 8. Jiang et al. (2014) applied a sodium starch-alginate composite coating on transparent paper, achieving a Kit value of 12 when the coating weight reached 3.3 g/m². Zhu et al. (2023) developed a series of epoxy resin heteropolymers based on chitosan and tannin for coating cards, resulting in a Kit value of 12 compared to 0 for the uncoated paper. Li et al. (2019) used a chitosan coating to fill the holes in the paper, followed by a PDMS coating for oleophobicity, and achieved an outstanding Kit rating score of 12/12 when the paper was coated with 8.6 wt% chitosan and 2.2% PDMS. In the study by Bordenave et al. (2010), chitosan, chitosan-palmitic acid formulations, or combinations of chitosan and O,O'-dipalmitoyl chitosan were applied to paper, resulting in Kit values ranging from 6 to 8 in the oil resistance test. Chitosan appears to be a fundamental component in several studies aimed at improving the resistance of paper to fats or oils (Wang et al., 2021; Hamdani et al., 2020; Nair et al., 2022; Nair et al., 2021; Kopacic et al., 2018). Chi et al. (2020) discovered that coatings made of high molecular weight starch and starch-derived polyelectrolytes achieved significantly higher Kit scores ranging from 6 to 12. Song et al. (2020) developed an aqueous combination of hydrophilic and hydrophobic cross-linked copolymers for coating the outer layer of paper to enhance oil resistance. The majority of the combination consisted of hydroxy-terminated PDMS-tetramethoxysilane cross-linked copolymer networks treated with sodium alginate. The coated paper exhibited excellent oil resistance with a Kit value as high as 10. Gu et al. (2022) formulated paper coatings using crosslinked polyvinyl alcohol/nanoclay, resulting in a Kit value of 12 for all coated paper types. These studies demonstrate the importance of chitosan and other coating materials in improving the oil resistance of paper. By exploring different formulations and combinations, researchers aim to develop coatings with excellent oil barrier properties for various applications in food packaging.

- In addition to enhancing water and oil resistance, the use of coatings on papers offers the opportunity to impart other valuable functionalities, such as antimicrobial and antioxidant properties. These additional properties are of great importance in various applications, particularly in the context of food packaging, where ensuring food safety and extending shelf life are essential. The functionalization of papers with antimicrobial coatings is a promising area of research. Microbial contamination poses significant risks to food products, leading to spoilage and potential health hazards. By incorporating antimicrobial agents into paper coatings, it becomes possible to inhibit the growth and

proliferation of bacteria, molds, and other microorganisms that can cause product deterioration. Several studies have explored the use of different antimicrobial agents in paper coatings. For example, essential oils extracted from plants, such as oregano, thyme and rosemary, have demonstrated antimicrobial properties and have been incorporated into coatings for paper applications (Vrabič Brodnjak et al., 2020; Rodriguez et al., 2007; Battisti et al., 2017). These essential oil-based coatings have shown effectiveness against a wide range of microorganisms, including bacteria and fungi, and have the potential to enhance the shelf life of food products by reducing microbial contamination. In addition to antimicrobial properties, coatings can also provide papers with antioxidant capabilities. Antioxidants play a crucial role in preventing the oxidation of food components, which can lead to the development of off-flavors, color changes, and nutrient degradation. Incorporating antioxidant compounds into paper coatings can help protect food products from oxidative damage and extend their shelf life. Natural antioxidants such as vitamin E, ascorbic acid, and plant extracts rich in phenolic compounds have been investigated for their potential to be incorporated into paper coatings (Hassan et al., 2022 Han et al., 2020; Yasar et al.,2022). These antioxidant coatings have shown to be promising in preventing lipid oxidation and maintaining the quality of packaged food products. The functionalization of papers with antimicrobial and antioxidant coatings offers a multifaceted approach to enhancing food safety and extending the shelf life of packaged products. By integrating these properties into paper coatings, it becomes possible to provide an additional level of protection against microbial contamination and oxidative deterioration. Further research and development efforts are underway to explore new antimicrobial and antioxidant agents, optimize coating formulations, and ensure the effectiveness and safety of these functionalized papers for various applications in the food industry.

Chapter 2

Aims and objectives

Chapter 2: Aims and objectives

The primary objectives of this PhD thesis can be divided into two main areas:

- The first focused on the development of coatings and films to improve the oil and water resistance of paper intended for food applications. In addition to these characteristics, we also focused on incorporating antimicrobial properties. This goal has been pursued through the use of eco-sustainable materials, in line with environmentally friendly practices.
- The second objective aimed to evaluate and compare the performance of renewable materials already available on the market with conventional plastics in terms of their impact on the final quality of fruits. This objective sought to assess the suitability of renewable materials as alternatives to traditional plastics and determine their potential benefits in preserving fruit quality.

To fulfill the first objective concerning the improvement of paper characteristics, the thesis was divided into several chapters, each representing distinct experimental works. Each experimental work focused on improving specific characteristics of paper for food applications. These chapters provided a comprehensive overview of the step-by-step process employed to enhance different aspects of the paper. While each chapter represented a separate experimental work, they should be viewed as interconnected steps within a larger experimental framework aimed at improving multiple characteristics of paper intended for food use.

Chapter 3 is focused on improving the paper resistance against moisture and oil by coating with a combination of Poly(-3-hydroxybutyrate-co-3-hydroxyvalerate) (PHBV) and Polycaprolactone (PCL), along with varying percentages of PEG.

Chapter 4 addressed the grease resistance characteristics of the paper by creating 12 different coatings. These coatings were formulated by mixing PCL, starch, agar, and glycerol in different proportions.

Chapter 5 introduced a novel approach by utilizing cutin, extracted from a food by-product, from tomato peel and seed, as a key component in the formulation of coatings. By incorporating cutin along with biodegradable polymers such as PBS and PHBH, the resistance of the paper to oil was improved, and the WVTR (water vapor transmission rate) value was significantly reduced.

Chapter 6 focused on the creation of films intended to serve as coatings for food-grade paper. A Zn^{2+}–melamine complex was synthesized and introduced into polyvinyl alcohol (PVA) using epichlorohydrin (ECH) as an epoxide crosslinker. This complex formation endowed the film with strong antimicrobial characteristics. Once applied to the paper, it is expected to enhance the shelf life of products wrapped in these coated paper samples. The experimental work described in this chapter was carried out at the Department of Packaging & Logistics at Yonsei University, Wonju, South Korea.

Throughout all the experimental works, the coatings and films were obtained using the bar coating technique or film casting technique, and extensive determinations and characterizations of the samples were conducted. Additionally, a common feature across the works was the use of biodegradable materials, regardless of their origin. This characteristic, combined with the inherent biodegradability of paper, not only improved the paper's characteristics for food

packaging but also will improve its end-of-life disposal, allowing it to be composted as organic waste.

Chapter 7 focuses on experimental studies that aimed to evaluate the influence of bio-based and/or biodegradable packaging materials on the final quality of fruit samples when compared to commercially available packaging. The objective was to assess the impact of different packaging materials, including R-PET cups and paper trays, on various fruit samples such as grapes or fruit salad. Multiple analyses were performed to gather relevant data.
This work was conducted as part of the project, funded by Emilia Romagna region, titled "Strategies for the reduction and rationalization of the use of plastic in the fruit supply chain" (STEP). The project involved collaboration with several companies, including Apofruit for the provision of fruit samples, and ILPA and BioPAP for the supply of packaging materials.
By conducting these experimental studies and analyses, the aim was to gain insights into the potential benefits and implications of utilizing bio-based and/or biodegradable packaging materials in the fruit supply chain. The collaboration with various companies allowed for a comprehensive assessment of different packaging options and their effects on the quality of fruit products.

APOFRUIT

Apofruit Italia is an Agricultural Cooperative Society recognized by the relevant EU and national legislation as a Producer Organization (O.P.). Apofruit Italia has 3,947 producers. The company operates with its own structures from the North to the South of Italy as it presents associated growers in all Italian regions, productions of the entire range of first and fourth range fresh fruit and vegetables obtained with integrated and organic production techniques, processing centers and fruit and vegetable distribution platforms. Today Apofruit Italia means: • 12 processing plants and 6 product delivery and storage centers where over 200,000 tons of fruit and vegetables are processed; • application of procedures for the control of the production process: integrated production regulations, Globalgap, BRC, IFS, GRASP, ISO 9001, ORGANIC Reg. 2018/848, BIO SUISSE, Naturland, LEAF certifications; • direct relationship with the national and international market with a turnover of about 200 million euros; • staff of over 100 specialized technicians for agronomic technical assistance, for assistance in the post-harvest phases, for quality control and improvement and for the marketing of productions; • development and enhancement of integrated and organic quality productions under the SOLARELLI and ALMAVERDE BIO brands, which represent the leading brands in the fresh fruit and vegetable sector.

ILPA Group

The ILPA Group, made up of ILIP, MP3 and AMP, is one of the few European groups able to ensure the control of the recycled PET cycle in all the production phases required to produce a new rPET food packaging: from the selection of post-consumer material, to washing, grinding,

extrusion and thermoforming. The vertical integration of the ILPA Group allows the complete traceability of the recycled material and, thanks to the approval received from EFSA (European Food Safety Authority) for the production of Food Grade rPET for direct contact with food, we are able to produce products suitable for food contact 100% rPET.
MP3 is in fact able to process rPET flakes, obtaining semi-finished products of excellent quality and being able to reach food grade. Similarly, ILIP, the group's company specialising in the production of solutions for packaging and food preservation, is increasingly committed to expanding its range of rPET products, alongside the bioplastic range. The cycle closes with the work of AMP Recycling, able to recover and send for recycling not only traditional transparent PET bottles, but, for the first time in Italy, also trays and containers for opaque PET liquids.

BIOPAP

BIOPAP ® is an Italian company, leader in the production of patented biodegradable and compostable containers and trays, with very high performance, derived from renewable raw materials. They believe in a sustainable world and their supply chain is all European. The unique features of the BIOPAP disposable containers make them ideal for preparing, storing and consuming food today and tomorrow. They use only green electricity produced by their photovoltaic system. Very attentive to innovations, always investing in research and development to improve their products and process efficiency.

2.1. Preliminary introduction to chapter 3, chapter 4 and chapter 5

In recent times, there has been a significant research emphasis on sustainability in the field of packaging, specifically on finding new ways to enhance the eco-friendliness of packaging materials (Ruiz-Real et al., 2018; Vila-Lopez et al., 2021). One of the most widely studied materials for primary and secondary food packaging is paper, a renewable and biodegradable material mainly composed of cellulose sourced from a diverse range of natural origins (Deshwal et al., 2019; Oloyede et al., 2021). The positive aspects related to the use of paper and recycled paper are also considered by “The UN Agenda 2030 for Sustainable Development”, where in Section 12.5 it is stated, as one of the main objectives, “by 2030, substantially reduce the production of waste through prevention, reduction, recycling and reuse” (Soergel et al., 2021). In addition, CONAI (National Packaging Consortium Italy), with the guidelines of 2022, has released a new classification, decreasing the tax for the annual contribution that the users of paper and cardboard packaging must pay, encouraging their use as packaging.

Paper is a light, flexible, biodegradable, highly recyclable and compostable material, derived from renewable resources and its appreciable environmental compatibility often confirms it as the first choice by several food industries, both as primary and secondary packaging (Khwaldia et al., 2010; Deshwal et al., 2019; Nechita et al., 2020). Nevertheless, base paper, is not ideal for packaging food items with an extended shelf life due to its inherent limitations. These drawbacks include inadequate resistance to microbial activity, low mechanical strength, and a porous microstructure that hinders the prevention of moisture, oils, and oxygen from permeating through. In order to overcome these drawbacks, various advanced functionalization technologies have been extensively studied and developed. For example, paper is commonly

coated with chemicals or laminated with aluminum foil or plastic thin films to improve its barrier effect to water vapor, oxygen, mineral oils, and grease (Kopacic, et al., 2018; Nair et al., 2022). The best-performing papers' coating, having excellent barrier properties, is obtained with polyethylene, fluorinated compounds, and other petroleum-based polymers. On the other hand, when synthetic polymers are used to coat the paper, it significantly diminishes its biodegradability and recyclability. Consequently, the environmental sustainability of such packaging is adversely impacted by these coatings (Khwaldia et al., 2010). Indeed, growing concerns regarding the ecological and human health implications of plastic materials and fluorinated compounds (as well as their derivatives) have prompted a quest for alternative solutions in the pursuit of sustainable materials.

Moreover, food-grade paper contamination with food residues makes recycling often impossible. In the case of polyethylene coated papers, if the recycling of such a composite product already requires specialized facilities and systems and additional costs (the plastic layer can break down in flakes which tend to clog the fine screens, and by melting from roller heat, provoke paper breaking, meaning downtimes and production losses), further issues are encountered at the time when food solid residues could remain anchored to the packaging: food residues can bypass filtration and fiber separation systems. This means they can interfere, by contamination, with paper sheet formation, or increase the organic load that treatment systems then have to handle (mechanical, physical, biological or physicochemical wastewater treatment). That is why paper mills are unwilling to receive such contaminated products (Marinelli et al., 2020; Triantafillopoulos et al., 2020). According to CONAI (2020) (Marinelli et al., 2020), composting can be an alternative disposal for cellulosic materials contaminated with food, at least as long as the percentages entering in the organic waste stream remain at the actual level. At the same time, research on the development of bioplastics and/or biodegradable/compostable, suitable both as stand-alone film and as paper coatings, has moved forward: these materials may offer interesting functionalities contributing to the food products protection and shelf-life extension and to sustainability (Nicu et al., 2013).

Chapter 3

Improvement of Paper Resistance against Moisture and Oil by Coating with Poly(-3-hydroxybutyrate-co-3-hydroxyvalerate) (PHBV) and Polycaprolactone (PCL)

Chapter 3: Improvement of Paper Resistance against Moisture and Oil by Coating with Poly(-3-hydroxybutyrate-co-3-hydroxyvalerate) (PHBV) and Polycaprolactone (PCL)

3.1. Introduction

This work aims to develop and characterize the properties of paper coated with compostable bioplastics: in particular, poly(3-hydroxybutyrate-co-3-hydroxyvalerate) (PHBV) and polycaprolactone (PCL) have been assessed. PHBV belongs to the polyhydroxyalkanoates (PHA) category, an aliphatic biogenic polyesters family, produced by bacterial fermentation and it is an isotactic copolyester obtained by copolymerization of hydroxybutyrate and hydroxyvalerate (Bugnicourt et al., 2014). PCL is a semicrystalline biodegradable synthetic polyester obtained by a ring-opening polymerization (in presence of catalysts) of ε-caprolactone, which represents the monomeric unit (Rydz et al., 2018; McKeen, 2012). Their biodegradability has been extensively studied and many different degradation times can be found; however, biodegradability is a material property that is influenced by many factors. A recent review (Kliem et al., 2020) provides an overview of the main environmental conditions in which biodegradation occurs and then presents the degradability of numerous polymers. For example, strips of PHBV with a thickness of 1 mm showed a total mass loss of 100% after 70 days at 20–24 °C in industrial composting facilities; a complete degradation via composting can be observed for PCL within a few weeks. Figures on biodegradation of PHA and PHB can be found in another review (Meereboer et al., 2020) and the biodegradability in marine environment of PHA and PCL has been extensively discussed (Suzuki et al.; 2021).
Many studies concerning the processing of these materials and the comparison with traditional plastic materials are available, but they are mainly focused on the development and evaluation of films, while the paper coating application still remains a little-explored research field. First, structural, diffusional and surface (water and oil affinity) properties of paper samples coated with PHBV at different thicknesses (in single and double layer) were evaluated; then, the optimization of PHBV and PCL coating solutions was attempted by addition of polyethylene glycol (PEG) (at 5%, 10% and 20% on biopolymer dry weight) to improve coating uniformity and spreadability. PEG may be defined as a natural-based plasticizer, whose ability to improve the mechanical properties of different biopolymers is well known (Bugnicourt et al., 2014; Vieira et al., 2011). PEG was used in the production of film via chloroform casting of 20% PEG and 80% PHB mixtures (Gamba et al., 2017), reducing stiffness and increasing the elongation at break; PHB added with 10% of PEG (different MW) was used to produce film by compression molding (Requena et al., 2016a; Requena et al., 2016b; Requena et al., 2017); similar results have been obtained for PCL films prepared by solvent casting and added with 10% PEG 400 and PEG 1500 (Rosa et al., 2005). In this work, different concentrations of PEG have been used, considering a range already investigated by other authors for different application: production of standalone film via solvent casting (Parra et al.,2006), via extrusion (Jost et al., 2015) or for the extrusion of PHBV on paper (Sängerlaub et al., 2019).

3.2. Materials and Methods

3.2.1. Materials

In this work a calendered bleached paper (Advantage MG White High Gloss, Mondi Group, Addlestone, UK) was used as reference paper. According to technical sheet, it is obtained from a long-fiber sulphate pulp, with a grammage of 35 g/m^2, a thickness of 50 μm, a tensile strength of 3.5 and 1.5 kN/m, a tear resistance of 280 and 420 mN (respectively in machine and cross direction). Commercial polyethylene-coated paper and fluorinated paper were used as commercial references. Polyethylene coated paper (CCM Soc. Coop. Group, Modena, Italy) has a thickness of 73 μm and a grammage of 54 g/m^2, 9 g/m^2 of which represent the polymeric coating. Fluorinated paper (ACL, Azienda Cartaria Lombarda s.p.a., Malagnino, Italy) is superficially treated with fluorinated compounds, to grant an elevated grease resistance, and with epichlorohydrin, a polyamide polymer which cross-links during paper drying, partially hindering water penetration. Chloroform was used because of the good solubility of PHBV, PCL and PEG (Anbukarasu et al., 2016) in this solvent and to avoid paper modification during the coating. Only few solvents are suitable candidates for PHB, of which chloroform is one of the most compatible and most commonly used (Anbukarasu et al., 2016; Xu et al., 2017). The good solubility of PCL in chloroform has been demonstrated in previous studies (Tang et al., 2004; Zhang et al., 2019a; Zhang et al., 2019b).
Coating paper solutions were prepared dissolving in chloroform two biopolymers: poly(-3-hydroxybutyrate-co-3-hydroxyvalerate) (PHBV) and polycaprolactone (PCL). In the first case, the product used was PHI 003 (NaturePlast®, Ifs, France). It is 94% biobased according to ASTM D6866 standard and industrially compostable according to ASTM D6400 standard. The product is a powder with a melt flow rate of 15–30 g/10 min (tested at 190 °C and with 2.16 Kg). PCL (Sigma-Aldrich, Mw ~80.000) has a melt flow rate in the range from 2.01 to 4.03 (tested at 160 ◦C and with 5.00 Kg) and a water content lower than 0.5%; melting point at 60 °C and relative density of 1.145 g/mL at 25 °C. As a plasticizer, in the second phase of the study, polyethylene glycol (PEG) 200 (Mw ~190–210; Fluka Analytical) was used, the choice fell on the use of PEG 200, as it is the most suitable choice when you want to obtain more fluid solutions and thinner coatings.

3.2.2. Methods

3.2.2.1. Coating Solution Preparation

This work was organized in two sequential operational phases, starting from the preparation of the solutions. In the first set, coating solutions were prepared dissolving 5% w/v PHBV in previously heated chloroform, under continuous stirring in water bath for about 2 h at 55 °C. In the second set, in the purpose to obtain clearer solutions and a better solubilization of polymers, solvent was heated, always in water bath and under magnetic stirring, at 50 °C; then, the polymer was added (5% w/v of PHBV or PCL) and dissolved in chloroform under magnetic stirring at 60 °C for 50 min, and subsequently, at about 75 °C for 10 min. The solutions were cooled at room temperature under continuous stirring. A recovery system for the vapors condensation was used, to minimize the solvent evaporation losses. Any loss of solvent by evaporation was, however, restored to the initial volume. Solution of pure PHBV and PCL and solutions of each biopolymer added with plasticizer (PEG) at 5%, 10%, and 20% (on polymer dry weight basis) were prepared. A PEG stock solution in chloroform was previously prepared (Catoni et al., 2013), which was added in due amounts to the bioplastic solutions, followed by stirring at room temperature for 10 min.

3.2.2.2. Sheets Coating

Paper sheets (210 × 297 mm) were coated via bar coating with a Compact AB3650 (TQC Sheen) automatic film applicator, working under a fume hood. The instrument allows different coating rates, which could affect continuity and uniformity of the coatings. Once coated, sheets were partially dried under fume hood, to remove the chloroform, and then placed in an oven at 40 °C for about 20 min. The samples were kept for 24 h at room temperature before testing. If a double layer was applied, the drying phase in the oven was performed only after the deposition of the second layer. The first set of samples was realized varying coating thickness with an application rate of 80 mm/s, except one sample coated at 50 mm/s. In Table 3.1 the different coating conditions and resulting samples are listed: nominal thickness refers to the thickness of the solution (wet coating), 3 replicate coated sheets were prepared for each formulation.

Table 3.1. Coating conditions and codification of samples from the first and second set.

Sample Code	Layers	Nominal Coating Thickness (μm)	Application Speed (mm/s)	Bioplastic	PEG (% *w*/*w*)
SET 1					
80s80	1	80	80	PHBV	-
80s50	1	80	50	PHBV	-
80d	2	80 + 80	80	PHBV	-
100s	1	100	80	PHBV	-
100d	2	100 + 100	80	PHBV	-
SET 2					
PHBV	2	80 + 80	80	PHBV	-
PHBVpeg5	2	80 + 80	80	PHBV	5
PHBVpeg10	2	80 + 80	80	PHBV	10
PHBVpeg20	2	80 + 80	80	PHBV	20
PCL	2	80 + 80	80	PCL	-
PCLpeg5	2	80 + 80	80	PCL	5
PCLpeg10	2	80 + 80	80	PCL	10
PCLpeg20	2	80 + 80	80	PCL	20

The second set of coated sheets were all obtained with double layer coatings, using the 80 μm application bar at 80 mm/s but with two different biopolymers, PHBV and PCL, also considering the addition of PEG as plasticizer at different concentrations (5, 10 and 20% w/w). In Table 3.1 the different samples are listed; 2 replicate coated sheets were prepared for each formulation.

3.2.2.3. Coating Grammage Determination

The coatings grammage was obtained by mass difference of 20 cm^2—coated paper samples and uncoated paper samples of the same size.
Results reported in Table 3.2 are the mean ± standard deviation of 3 determinations.

3.2.2.4. Scanning Electron Microscopy (SEM)

The surface and structure of the samples were analyzed by scanning electron microscopy using a Nova NanoSEM 450 (FEI, Hillsboro, OR, USA) (available at CIGS, Centro Interdipartimentale Grandi Strumenti, of the University of Modena and Reggio Emilia) provided with LVD detector, under low vacuum conditions (80 KPa) and with an acceleration of 10 kV. Images were captured with different magnifications (500×–3000×) and tilts (0°–40°), thus enabling the visualization of both surface and cross section.

Table 3.2. Coating grammages.

Code	Coating Grammage (g/m^2)
SET 1	
80s80	2.82 ± 0.97
80s50	4.81 ± 1.14
80d	7.72 ± 1.31
100s	4.60 ± 0.88
100d	9.65 ± 0.82
SET 2	
PHBV	8.48 ± 1.15
PHBVpeg5	7.42 ± 1.71
PHBVpeg10	7.92 ± 1.16
PHBVpeg20	8.57 ± 1.45
PCL	8.30 ± 1.01
PCLpeg5	6.73 ± 1.32
PCLpeg10	5.42 ± 2.83
PCLpeg20	9.77 ± 0.79

3.2.2.5. Measurement of Water Vapor Transmission Rate (WVTR)

The measurement of the water vapor transmission rate (WVTR) of the different samples was performed in triplicate according to the ASTM E96 standard, with modifications. Two grams of anhydrous $CaCl_2$ were placed in 25 mL glass bottles (55 mm high, 10 mm internal diameter mouth) to achieve a 0% internal RH. They were positioned in an oven at 45 °C, to remain completely dry and to be progressively sealed with the paper samples glued on the top of the vials, with the coated part inwards to prevent water vapor tangential diffusion. The vials were weighed at zero time, then placed in a desiccator with 90% RH obtained by $BaCl_2$ saturated solution at 45 °C.

The vials were weighted daily for 4 days of storage. The WVTR value (g 24 h^{-1} m^{-2}) was calculated using the following formula:

$$WVTR = \Delta W/(\Delta t \times A) \quad (1)$$

where: "$\Delta W/\Delta t$" represents the weight gain as a function of time (g 24 h^{-1}), obtained as the slope of the linear regression of the mass gain versus time; "A" corresponds to the exposed surface of the film (7.85×10^{-5} m^2). The reported WVTR data are the average of three replicates.

3.2.2.6. Oil and Grease Resistance (ASTM F119)

Oil and grease resistance was determined according to the ASTM F119-82 standard, with modifications (ASTM F119-82, 2015). Test specimens (60 × 60 mm) were placed on ground-glass plate (50 × 50 mm). Then, a cotton flannel (20 mm in diameter) was placed on specimens with 50 g weights (20 mm in diameter at the base) on them, and the assembly was conditioned in an oven at 40 °C for 30 min. It was subsequently removed, and after removing the weights,

150 µL of sunflower oil was pipetted on the flannel piece. Then, the weights were re-assembled and conditioned again in the oven at 40 °C. At convenient time intervals, the bottom of the ground glass plate was checked with the assembly in the oven. The time at which the first trace of wetting is visible at the position of the weight was recorded. Three specimens for each sample were used.

3.2.2.7. Water and Oil Contact Angle Measurement

Contact angle values were determined by means of an OCA 15EC contact angle meter and using OCA 20 (Dataphysics) software by the sessile drop method. For each type of sample, 1 × 3 cm paper strips were positioned on a film holder. Contact angle measurements were taken depositing 3 µL of water, and 7 µL of oil on the sample surface. For the contact angle measurement of each type of paper, 9 replicates were taken for water, while 5 for oil, the average of which was considered. The contact angle was measured immediately after the drop deposition.

3.2.2.8. Statistical Analysis

Data were submitted to analysis of variance (multi-factor analysis of ANOVA) using IBM Statistics SPSS 20 software and post hoc analysis by Tukey's test.

3.3. Results and Discussion

3.3.1. SEM Surface Analysis

The surface and cross-section of the uncoated paper and PHBV-coated paper samples obtained in step 1 were analyzed by means of scanning electron microscopy (SEM). The uncoated paper sheets show a typical fiber network and a flat surface due to the calendaring treatment (Figure 3.1a); PHBV coatings (Figure 3.1a–d) determined the filling of void space of the network; however, the surface was characterized by the presence of lumps, whose dimensions and density seemed to increase both in double layer coatings and in single layer coating of 80 µm at 50 mm/s (Figure 3.1c,d).

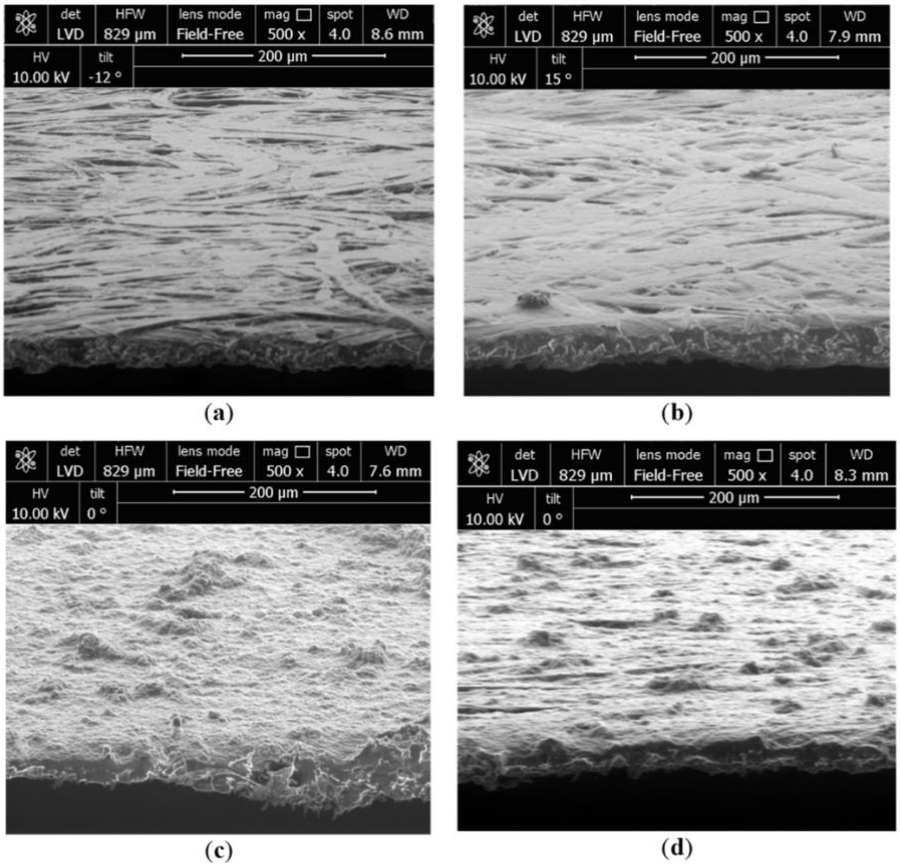

Figure 3.1. (a) Uncoated paper (calendered side) (UCP); (b) PHBV 80 µm single layer at 80 mm/s (80s80); (c) PHBV 80 µm double layer at 80 mm/s (80d); and (d) 80 µm single layer at 50 mm/s (80s50).

Other authors (Sängerlaub et al., 2019; Bedane et al., 2015) characterized PHBV paper coatings by SEM, but the different techniques, polymers and base support used do not allow a reliable comparison of results. A second set of tests was conducted by changing the coating preparation conditions, obtaining an improvement of the solubilization. The PHBV solutions appeared more homogeneous and transparent compared to the ones obtained in the first set; PCL completely solubilized in chloroform and the solutions were more transparent and homogeneous than PHBV ones.

The new coated samples obtained were also observed by SEM and a significant improvement of surface homogeneity was noticed, especially in samples with 10% and 20% PEG. The comparison of PHBV-coated paper samples obtained in the first and second step allows to assume the effectiveness of the optimized solubilization strategy and the role of PEG in improving coating distribution and spreadability (Figure 3.2a,c).

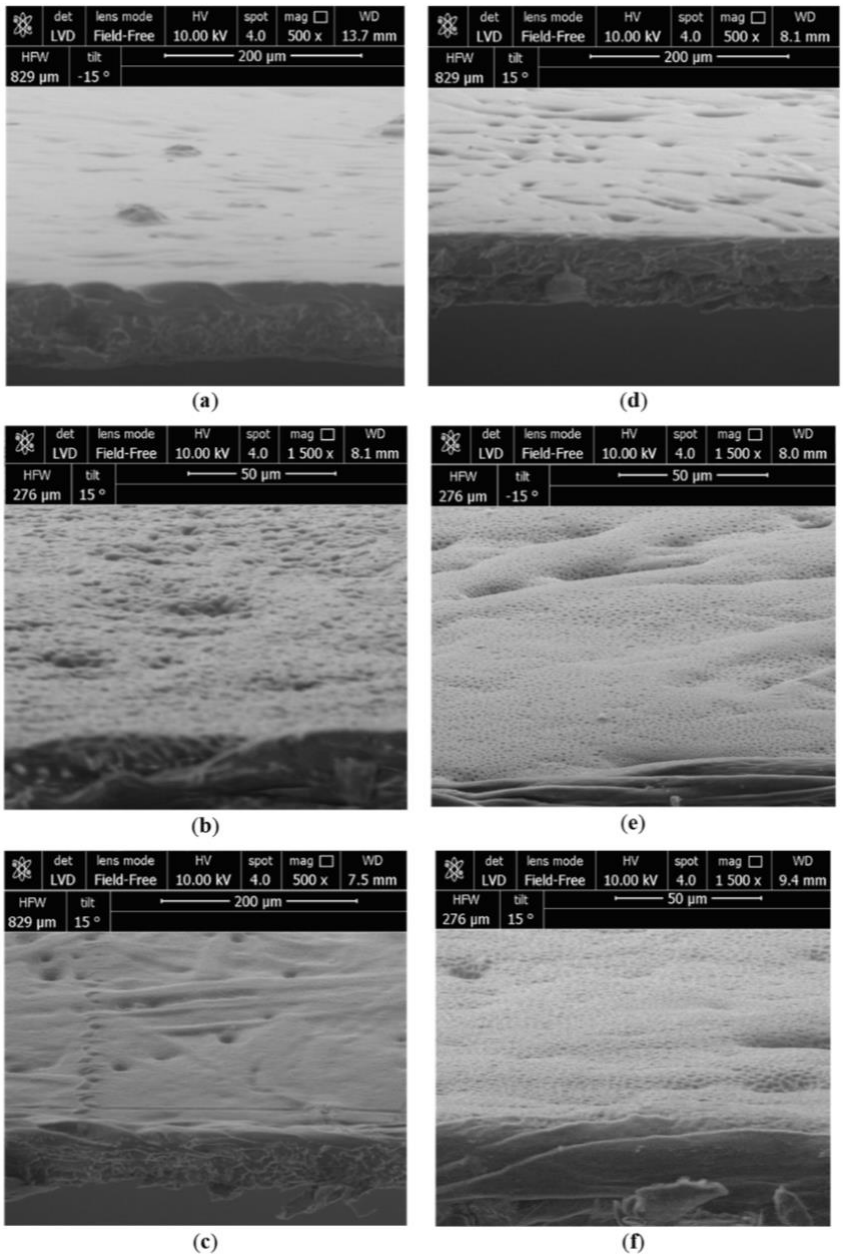

Figure 3.2. (a) PHBV without PEG; (b) PHBV with PEG 10%; (c) PHBV with PEG 20%; (d) PCL with out PEG; (e) PCL with PEG 10% ; and (f) PCL with PEG 20% .

PCL coatings show a characteristic surface, more regular and homogeneous compared to PHBV ones, although several discontinuities in the coatings were observed, but it is not clear if they are pores or simple depressions in the coating. The presence of pores in PCL coatings (of the same type used in this work, but dissolved in ethylacetate at 10%) on paperboard, was observed in a previous study too (Bota, et al., 2017) and this structural characteristic was related to a lack of interaction between coating and base support. The addition of plasticizer seemed to progressively mitigate this phenomenon (Figure 3.2d–f). In both PHBV with PEG at 10% and PCL with PEG at 10% and 20% coatings (shown at 1500× magnification for this reason), a surface presenting bubbles (PHBV) and sponge-like structure (PCL) was observed. The fast

evaporation of the solvent in combination with the plasticizer could justify this particular structure (Figure 3.2b,e).
The SEM images of the cross section in Figure 3.3, demonstrate that coating layer and base paper are not clearly distinguishable.

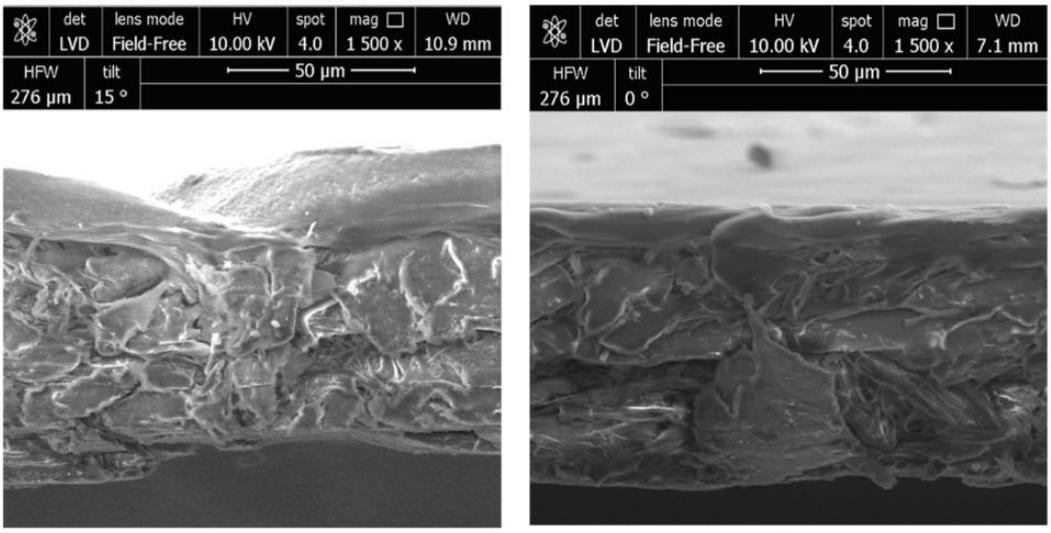

(a) **(b)**

Figure 3.3. Cross section of pure PHBV (a) and PCL (b) of the second set.

3.3.2. WVTR Measurements

Water vapor transmission rate (WVTR) is one of the main characteristics of food packaging materials, being always included in technical sheets; it may be considered as an indicator of the food packaging material sensitivity toward water vapor and low WVTR values are often requested to assure an acceptable shelf life for many food products. The diffusional performances of biopolymers, such as PHBV and PCL, have been extensively measured and considerable scientific literature can be found (Helanto et al., 2019; Reichert et al., 2020; Din et al., 2020). In a recent review (Wu et al., 2021) on the barrier performance of biodegradable polymers, PHBV and PCL, together with other biopolymers, have been classified as a function of their diffusion performances. PHBV has been considered a medium barrier grade, for both oxygen (16–160 cc·mil/m^2 day atm) and water vapor permeability (16–40 g·mil/m^2 day kPa), while PCL has been classified as a poor barrier against oxygen (>1600 cc·mil/m^2 day atm) and water vapor (>120 g·mil/m^2 day kPa). In another recent study (Jost et al., 2018), different commercial polymers, PHBV and PCL included, were transformed into films via extrusion and the permeation performances were measured. The results obtained for water vapor permeability (WVP) were the following: PCL, around 2.0 g 100 mm m^{-2} day^{-1} $mbar^{-1}$; PHBV, 0.5 g 100 mm m^{-2} day^{-1} $mbar^{-1}$, the latter being close to values of PET-BO. PHBV seems to be a good candidate for the improvement of paper performances. In a study on double-layer composites using PHB and cellulose paper, different amounts of PHB (2%, 5%, 10%, 15%) were deposited via solvent casting (using chloroform as solvent) on control paper (Cyras et al., 2007). The authors observed that the permeation decreased with the amounts of PHB due to its low permeation but only if the concentration reached the value of 10%, concluding that it is necessary for the biopolymer to form a continuous layer above the paper sheet in order to fill all of the valleys of its structure. PCL may be considered as possible coating layer; authors (Reichert et al., 2020) who evaluated the water vapor transmission of uncoated and coated

paper (via bar coating, with a wet coating thickness of 24 µm and a dry coating thickness of ~6 µm) concluded that the PCL layer determines a decrease in permeability of around 15% if compared with the control paper. In another study (Han et al., 2010) on the abilities of different coating formulations (zein, WPI, PCL and chitosan) to decrease the water vapor transmission of paperboard, PCL coating resulted to be effective at significantly ($p \leq 0.05$) reducing the WVTR of the cellulosic substrate from 513 to 320 g/m^2 24 h, i.e., a percentage decrease around 37%. Literature data for different biopolymer types coated on papers and paperboards can be found, in terms of their barrier properties, but sometimes is not easy to compare the data because of the different substrate used and coating techniques, as well as coat weight and function of coating, together with different methods of calculation and units used (Rastogi et al., 2015).
Figure 3.4 shows the WVTR values calculated in this work for coated samples (first set) and for commercial reference samples.

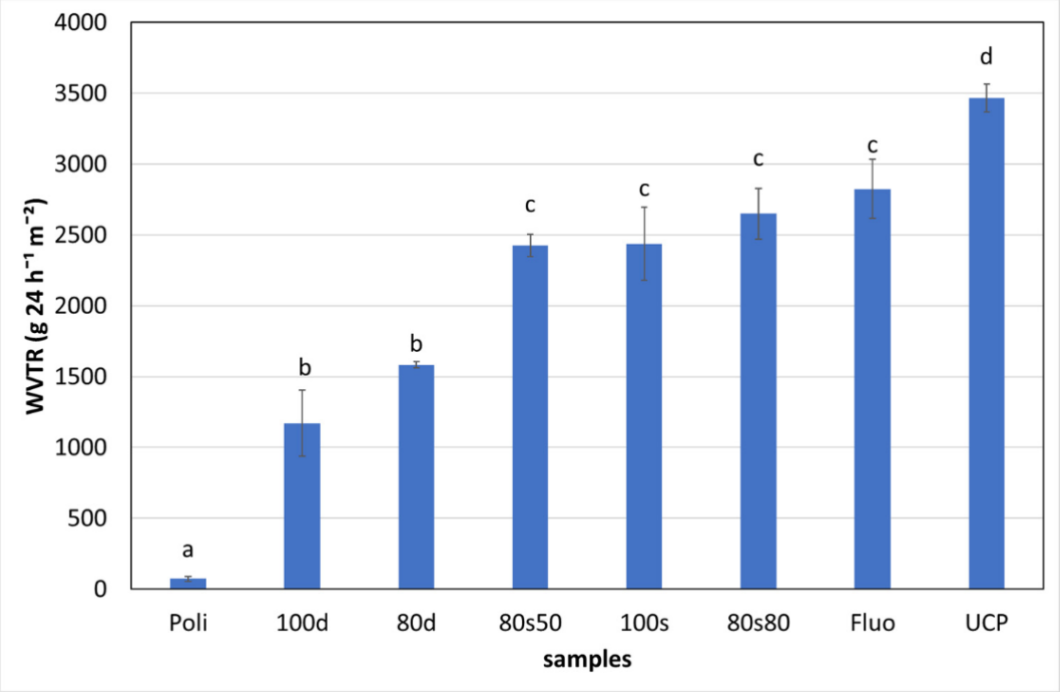

Figure 3.4. WVTR values (g 24 h $^{-1}$ m $^{-2}$) of PHBV coating at different thickness. Bars represents the average value of three determinations, error bars report standard deviation. Different letters indicate statistically significant differences (p <0.05). "UCP" refers to base paper, "Fluo" to fluorinated paper, while "Poli" to polyethylene-coated paper.

As expected, the polyethylene-coated paper (Poli) is characterized by an extremely low WVTR (average value of 71.91 g/24h*m^{-2}). Conversely, the fluorinated treatment (Fluo) slightly improved the barrier against water vapor (average value of 2825 g/24h*m^{-2}) compared to the uncoated calendered paper (sample UCP) (average value of 3468 g/24h*m^{-2}). Compared with base paper, WVTR value of PHBV coated samples significantly decreased, as a function of both coating thickness and number of layers. Single layer 100 µm (100 s) coating resulted to have a lower WVTR than single layer of 80 µm coating obtained at 80 mm/s (80s80). Comparing both single layer of 80 µm coated samples, but with different application speeds, the lower speed (50 mm/s) corresponds to a lower WVTR. This suggests a more uniform coating distribution and a higher penetration capacity in the paper support. In accordance with this assumption, grammage data (Table 3.2) show higher values at a lower coating speed.

The WVTR data for the first set samples were plotted in a graph (Figure 3.5) versus coating grammages, showing a linear inverse relationship ($R22 = -0.986$; $\alpha < 0.01$).
Significantly lower water vapor transmission rate (WVTR) values were achieved with the 80d and 100d samples compared to the single layer-coated samples (80s50, 100s, and 80s80).
In the second set, calendered paper was coated with PHBV and PCL, also considering the influence of PEG addition as plasticizer (from 0% to 20% w/w of polymer). By comparison of WVTR values of PHBV 80d sample (first set) and PHBV (second set) it could be assumed that the modification of coating solution preparation allowed a better distribution on the paper sheet, with positive effect on moisture barrier performances (Figure 3.6).

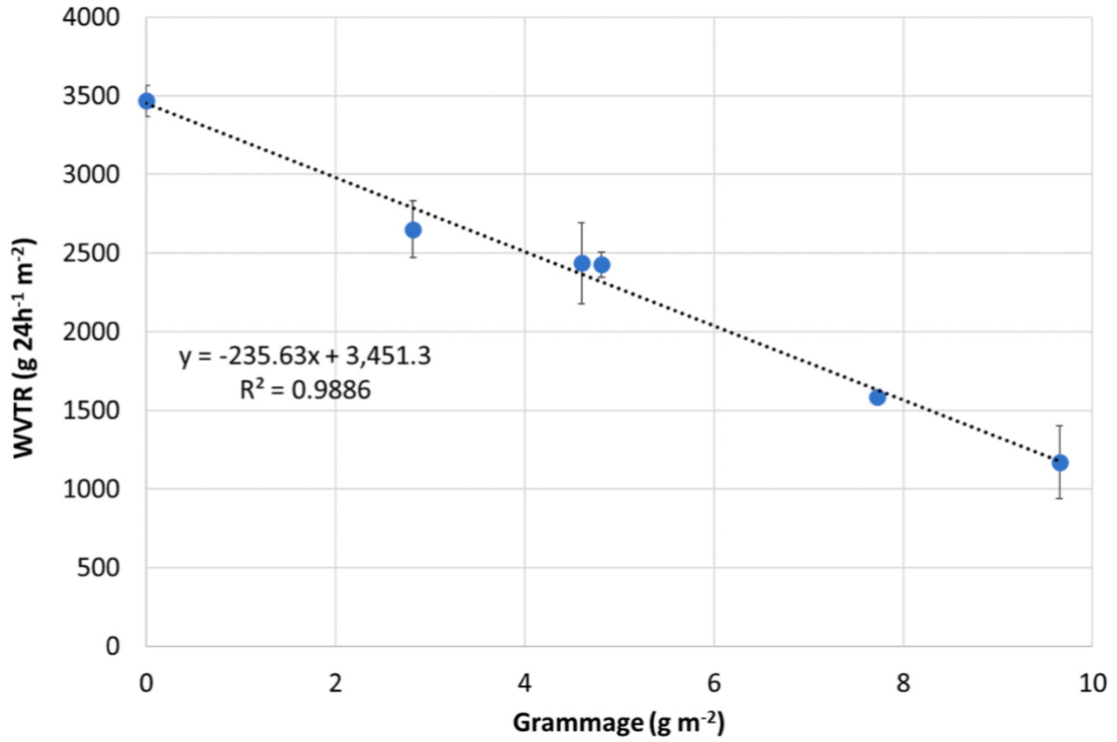

Figure 3.5. Linear correlation between coating grammage and WVTR of first set sample. Grammage equal to 0 corresponds to uncoated paper sample.

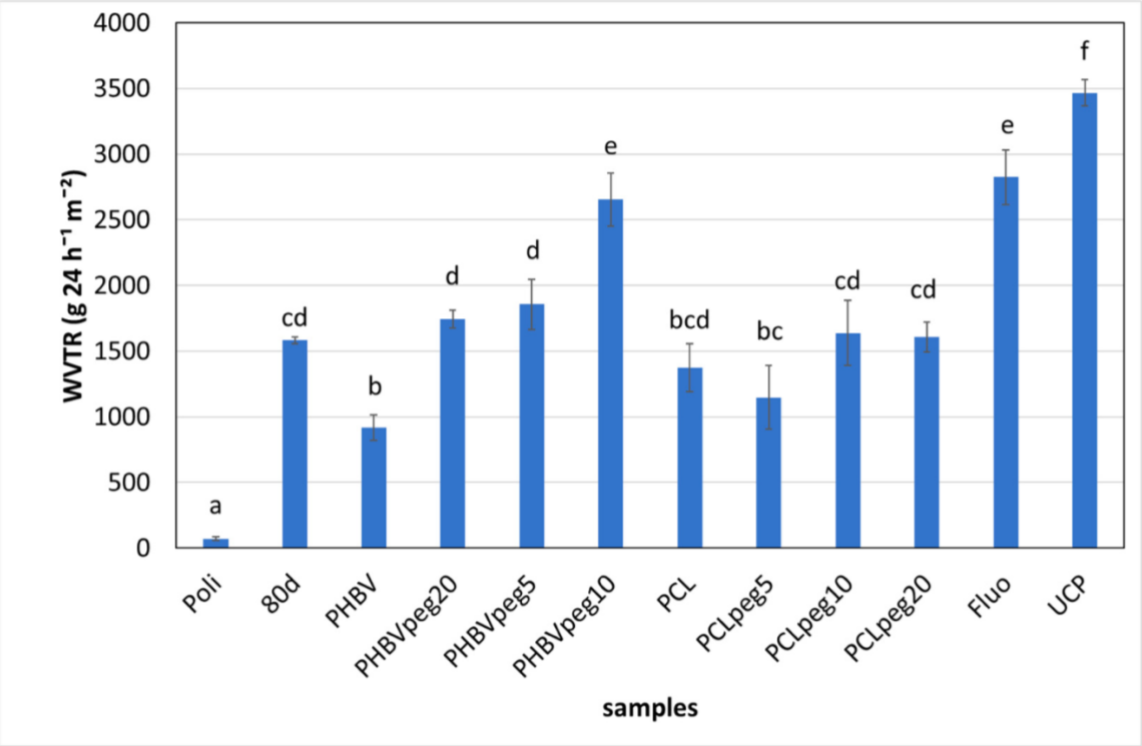

Figure 3.6. WVTR values (g 24 h^{-1} m^{-2}) of PHBV and PCL coated samples both pure and with PEG addition at different concentrations (set 2). Bars represents the average value of three determinations, error bars report standard deviation. Different letters indicate statistically significant differences ($p < 0.05$). "UCP" refers to base paper, "Fluo" to fluorinated paper, while "Poli" to polyethylene- coated paper.

Concerning the addition of PEG to PHBV, a general increase of WVTR in presence of plasticizer can be observed. These results could be explained considering the hydrophilic nature of PEG and its plasticizing action, according with previous studies that attribute this behavior to a free volume increase (which promotes molecular diffusion) and to the PEG hydrophilic nature, which tends to increase sorption capacity, solubility and water permeability of plasticized films (Requena et al., 2016a). In particular, WVTR values significantly increased in presence of plasticizer up to 10%, and then decreased at 20% PEG concentration, while maintaining a value higher than PHBV not plasticized and not significantly different compared with PHBV with 5% PEG. This trend agrees with a study about PHBV extruded films incorporated with PEG1000 at 5%, 10%, 20%. The WVTR decrease was explained in the study assuming a demixing between plasticizer and PHBV, which could, given the relatively low PHBV permeability, allow a reduction in water vapor permeability (Jost et al., 2015). This hypothesis is not necessarily in contrast with the SEM structure observed for these samples, which appeared as more uniform compared to non-plasticized films and could be explained as the result of a beginning demixing between the two materials, not always detectable by SEM images. According to Figure 3.6, pure PHBV coating showed lower, although not significantly, WVTR values compared to PCL. It is possible that discontinuities observed at SEM on PCL coatings could facilitate water vapor permeation. In accordance with a previous study (Shogren, 1997), this result could be further explained considering both that water vapor diffusion coefficient in an amorphous or semicrystalline polymer depends on molecular dynamic or amorphous regions segmental movements, and the different glass transition temperatures of the biopolymers (PCL has a lower Tg compared to PHBV), but the presence and arrangement of substituent groups (such as methyl or ethyl groups) as in PHBV case, which tend to have a minor chain flexibility on account of steric effect, and therefore, a lower WVTR, but the lack

of information does not allow to elaborate additional considerations. Compared to PHBV-based coatings, plasticizer addition did not significantly affect WVTR in PCL coatings: the ones with 10% and 20% resulted to be more permeable (though not significantly) to water vapor compared to pure PCL. In general, coated samples, in particular PCL ones, showed an improvement of barrier to vapor compared to base paper; nevertheless, barrier properties can be further improved using other application techniques: processing method plays a key role in film production and can do the same in the case of coatings. Long drying required by solvent casting process can contribute to the formation of more open microstructures and channels for easy diffusion of water vapor molecules (Fabra et al., 2016). Biopolymers hot processing may allow to achieve denser and more resistant structures.

3.3.3. Oil and Grease Resistance

The determination of oil and grease resistance of food packaging materials, cellulosic included, is important in many applications, e.g., retail packing of fresh and cured meat, cheese, fish, but also when exchange of food components with packaging materials occurs, occasionally affecting the performances of the material itself (delamination). There is a discrete number of available and known tests to assess this performance, but they (including ASTM F119 applied in this work) are largely based on subjective statements, often not allowing to obtain measurements with a statistically meaningful physical value. Especially when grease barrier properties differences are low, a more precise and reproducible measurement method will be required: for instance, mixing oils used in the tests with coloring agent and determining colorimetric coordinates using a spectrophotometer), with the aim of making results independent from individual subjectivity (Gietl et al., 2009).
Table 3.3 shows grease resistance times of all samples of this work. All the coatings improved base paper resistance (resistance ranging between 0 and 10 min), but performances were not comparable with fluorinated and polyethylene-coated papers, which did not show any failure after 72 h. Resistance times recorded for PHBV coated papers were generally lower than 20 min; only PHBVpeg5 showed resistance ranging between 40 and 60 min. The few studies available in literature report variable grease resistance data and ascribe this variability to the presence of cracks or to lack of uniformity in the material (Sängerlaub et al., 2019). PCL coated samples showed in all cases a resistance of more than 4 h, but less than 12 h, except one sample showing a higher resistance between 12 and 24 h.

Table 3.3. Grease resistance times.

Sample Code	Time (minutes)		
UCP	10	-	0
Fluo	>4320	>4320	>4320
Poli	>4320	>4320	>4320
80s80	20	20	20
80s50	10	30	20
80d	10	10	10
100s	10	10	40
100d	10	20	20
PHBV	10	20	20
PHBVpeg5	40	60	40
PHBVpeg10	20	20	20
PHBVpeg20	20	10	40
PCL	240–720	240–720	240–720
PCLpeg5	240–720	240–720	240–720
PCLpeg10	240–720	720–1440	240–720
PCLpeg20	240–720	240–720	-

3.3.4. Contact Angle Measurements

3.3.4.1. Water

As shown in Figures 3.7 and 3.8, fluorinated paper resulted far more hydrophobic than other samples, possibly because of the epichlorohydrin treatment. Contact angle values of first set samples resulted to decrease as number of layers and coating amount increase. This result could be explained by the Wenzel theory (Ryan et al., 2008), assuming the effect of the relative roughness of coatings, and in particular, assuming a raise of the measured hydrophilicity as roughness of the material increase: as noted in SEM images, double layer coating showed a higher roughness compared with single layers and resulted to be most hydrophilic.

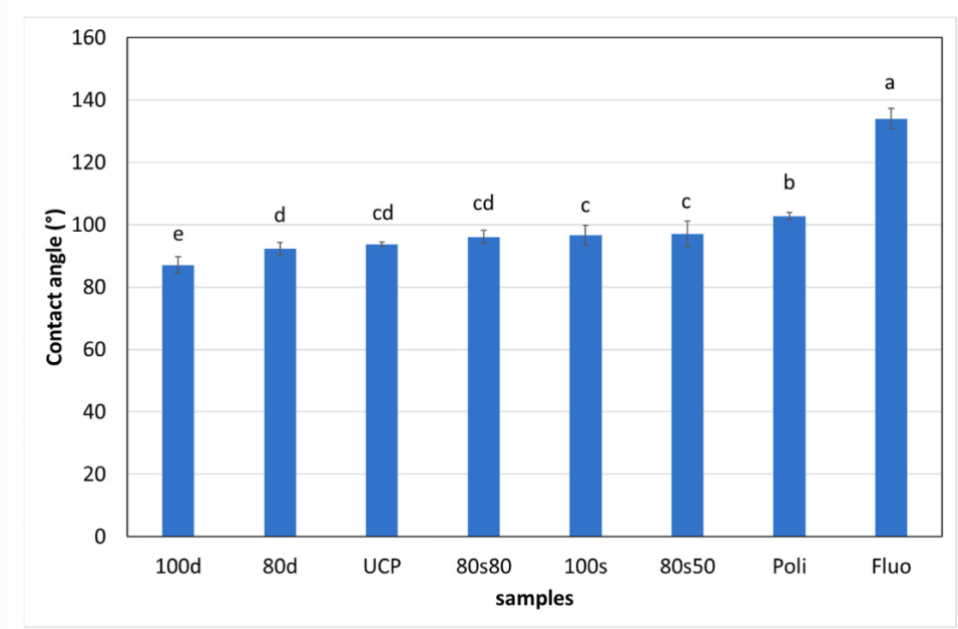

Figure 3.7. Average water contact angle values for first set samples. Error bars report standard deviation. Different letters indicate statistically significant differences ($p < 0.05$). "UCP" refers to base paper, "Fluo" to fluorinated paper, while "Poli" to polyethylene-coated paper.

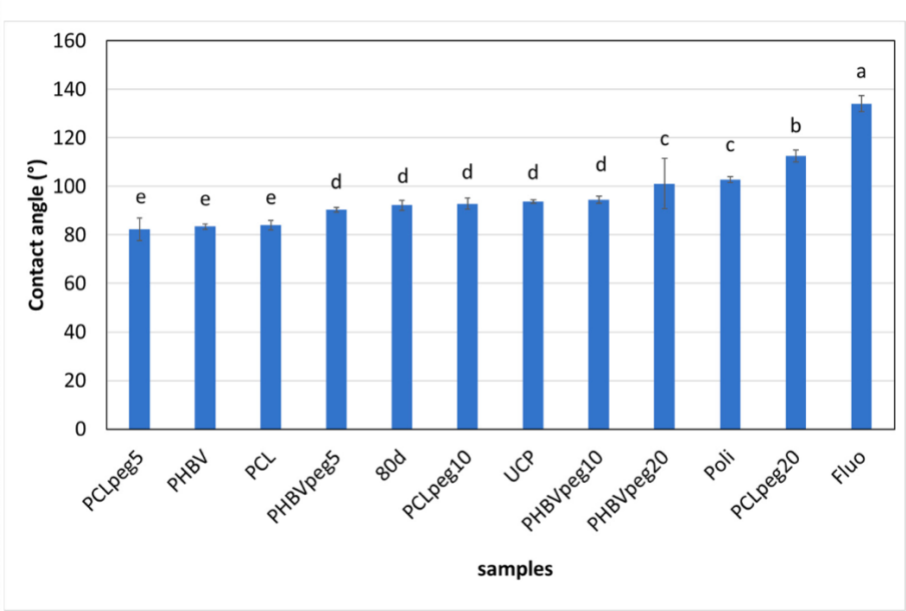

Figure 3.8. Average water contact angle values for the second set samples. Error bars report standard deviation. Different letters indicate statistically significant differences ($p < 0.05$). "UCP" refers to base to base paper, "Fluo" to fluorinated paper, while "Poli" to polyethylene-coated paper.

Calendered paper showed a good hydrophobicity. The relatively high value detected for this paper could be related to a behavior that comes closer to the Cassie-Baxter model, assuming the contribution of air bubbles entrapped between interfiber gaps, given the high porosity of this material, but it is difficult to verify such a hypothesis (Figure 3.8) (Ryan et al., 2008; Kubiak et al., 2011).

It is possible to notice a general upward trend of the contact angle (or a downward trend of wettability), by adding plasticizer. Given the relative hydrophilicity of PHBV and PEG, this result could be explained considering the Wenzel theory and the effect of surface roughness (Ryan et al., 2008). The use of plasticizer in the coating solution formulation could be associated with a better solution spreadability and a more uniform coating distribution. The SEM images seemed to support the effectiveness of PEG in this regard, as the coated surface appeared more uniform and less rough with increasing plasticizer concentrations. PCL contact angle values were higher than the ones found in literature for films based on the same PCL type used in this work (always at 5% w/v, but in trichloromethane and differently processed), equal to 64.5◦ (Barabaszová et al., 2011).

Even if the trend is not as linear as for PHBV, the Wenzel theory could explain the significantly higher contact angle values detected for PCL with PEG at 10% and 20% samples, considering the progressive increase of smoothness observed for these coatings by the SEM images. Although PCL with PEG at 5% sample showed a contact angle value lower than pure PCL, the difference was not statistically significant. PHBV and PCL both with PEG at 20% samples showed the lowest wettability (highest contact angle values) among coated samples. In particular, PCLpeg20 reached a wettability level significantly lower compared to reference polyethylene-coated paper (Figure 3.9).

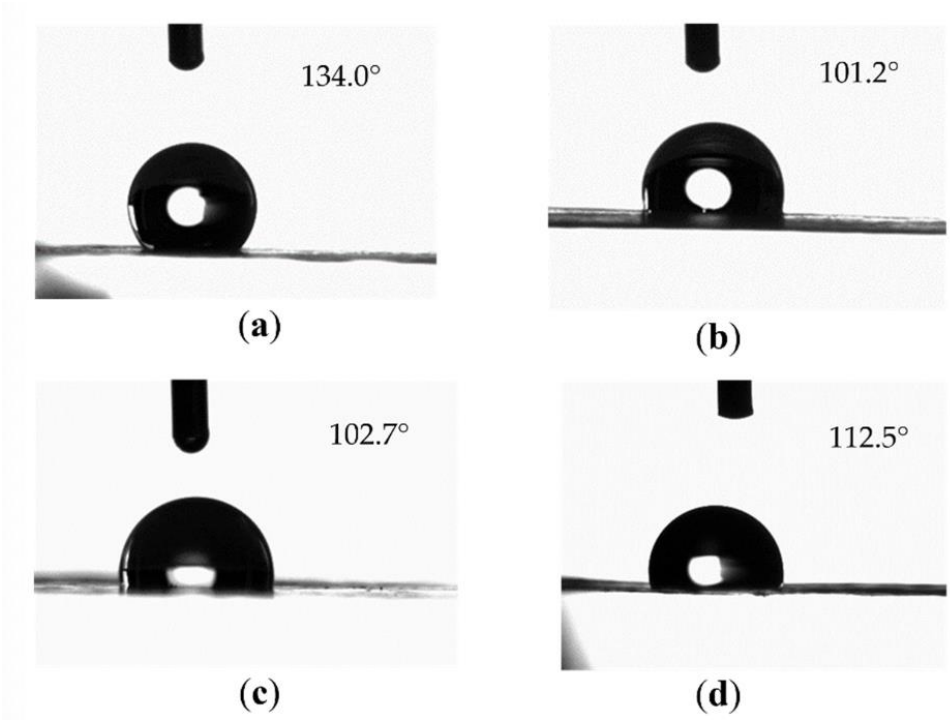

Figure 3.9. Water contact angles of (a) fluorinated paper (Fluo); (b) paper coated with PHBV with PEG 20% (PHBVpeg20); (c) polyethylene-coated paper (Poli); (d) paper coated with PCL with PEG 20% (PCLpeg20).

Furthermore, it is important to remember that unexpected results may occur, as the hydrophobic and hydrophilic surface chemistry physics is more complex than Wenzel and Cassie-Baxter models, which represent simplification of what is really going on. Rough surfaces contact angles study is still a vibrant research field (Ryan, et al., 2008).

3.3.4.2. Oil

Tables 3.4 and 3.5 show oil contact angle values of, respectively, first and second set and commercial reference samples. Oil contact angle values in both sets showed an elevated wettability (oleophilicity) of the coatings, expressed by low contact angle values (in the range from 11.3 to 37.3°), and therefore difficult to determine. As expected, given the low surface energy, fluorinated paper showed high contact angle values (average value of 101.9°) and particularly reduced wettability (high oleophobicity) (Figure 3.10).
Polyethylene-coated paper showed a low oil contact angle value (average value of 16.9°). Several coatings of the second set showed a higher oleophobicity than this commercial reference, with special regards for PCLpeg20, showing an average measured value of 37.3°.

Table 3.4. Oil contact angle values of first set samples.

Sample Code	Mean Contact Angle Value
UCP	15.1 ± 3.8^{bc}
Fluo	101.9 ± 1.5^{a}
Poli	16.9 ± 0.2^{b}
80s80	14.0 ± 1.6^{bc}
80s50	11.3 ± 0.7^{c}
80d	12.6 ± 1.8^{bc}
100s	15.5 ± 3.2^{bc}
100d	12.4 ± 1.5^{bc}

Different superscript letters indicate statistically significant differences ($p < 0.05$).

Table 3.5. Oil contact angle values of second set samples.

Sample Code	Mean Contact Angle Value
UCP	15.1 ± 3.8^{de}
Fluo	101.9 ± 1.5^{a}
Poli	16.9 ± 0.2^{d}
80d	12.6 ± 1.8^{e}
PHBV	24.7 ± 1.6^{c}
PHBVpeg5	19.3 ± 1.0^{d}
PHBVpeg10	17.2 ± 1.7^{d}
PHBVpeg20	17.6 ± 2.3^{d}
PCL	18.9 ± 1.9^{d}
PCLpeg5	16.6 ± 0.8^{de}
PCLpeg10	27.0 ± 2.3^{c}
PCLpeg20	37.3 ± 1.9^{b}

Different superscript letters indicate statistically significant differences ($p < 0.05$).

Figure 3.20. Oil contact angle of fluorinated paper (Fluo)

3.4. Conclusions

To conclude, this work, within the limits of its lab-scale, offers insights for future research lines toward the development of cellulose-based food contact materials, with special attention to a greater sustainability compared to actual commercial solutions.
The SEM analysis of the developed coated samples showed the disappearance of the typical fiber network of paper and allowed to observe a continuous layer of coating.
The smoothness of the coating surface was used as an indicator of good biopolymer solubilization. Coated samples developed in this work showed a significant improvement of water vapor barrier compared to uncoated paper and also to commercial fluorinated paper. The significant reduction of WVTR is a promising feature of the developed coated paper samples, according to the importance of this parameter for food quality preservation. Polymer-coated paper samples showed improved grease resistance, still not comparable to commercial coated samples. Among, samples, PCL-coated offered the best resistance, ranging from 4 to 12 h. PHBV and PCL coating with PEG at 20% showed good water contact angles. The measured oil contact angles were generally much lower compared to fluorinated paper, however certain coating formulations (i.e., PCLpeg20, PCLpeg10 and PHBV) showed significantly higher surface oleophobicity compared to commercial polyethylene-coated paper.
Chloroform utilized in this study is a poorly biocompatible solvent; therefore, future developments should include the evaluation of more eco-friendly solvents, when possible, or other coating techniques, such as extrusion coating. The increasing availability and commercial variety of compostable biopolymers allow a more concrete technical feasibility. The real compostability of biopolymer-coated paper should, however, be verified.

Chapter 4

Polycaprolactone/Starch/Agar Coatings for Food-Packaging Paper: Statistical Correlation of the Formulations' Effect on Diffusion, Grease Resistance, and Mechanical Properties

Chapter 4: Polycaprolactone/Starch/Agar Coatings for Food-Packaging Paper: Statistical Correlation of the Formulations' Effect on Diffusion, Grease Resistance, and Mechanical Properties

4.1. Introduction

The challenge of this thesis, as already discussed, is finding new eco-friendly and compostable alternatives with the same barrier behavior of polyethylene and fluorinated compounds. To achieve these ecological objectives, the more recent research on sustainable coating is focusing on the use of degradable components of natural origin, such as, for example, biopolymers, polysaccharides, and other materials of natural origin. Several studies have demonstrated that different biodegradable polymers, such as polylactic acid (PLA), polycaprolactone (PCL) or poly 3-hydroxybutyrate-co-3-hydroxyvalerate (PHBV), starch, chitosan and polysaccharides, can be used as barrier coatings for food-packaging paper (Khwaldia et al., 2010; Reis et al., 2011; Adibi et al., 2023). Among those, PCL has been deeply studied as it is a linear thermoplastic aliphatic polyester, partially crystalline, hydrophobic and biodegradable with good mechanical properties and high extensibility (Lo Faro et al., 2021; Sogut et al., 2018). Sundar et al. (Sundar et al., 2020) demonstrated that coatings containing PCL (5–25%) reduce the water vapor transmission rate (WVTR) of coated paper by 25% compared to uncoated ones and increase the oil/grease resistance value, reaching a 12/12 score for the TAPPI test kit. Bota et al. have demonstrated that a 10% PCL coating on paper improves the evolution of the water contact angle over time; in fact, 6 s after the deposition of the water drop on the sample, the angle still has a value greater than 15% with respect to uncoated paper (Bota et al., 2018).

Another promising candidate to develop biodegradable films and coatings is starch. Starch is characterized by a crystalline structure, presenting itself in the form of granules, and can be obtained from several natural sources, such as corn, wheat, and many others. It is soluble in water, biodegradable, and has many industrial applications, playing the role of gelling agent, stabilizer, etc. (Chi et al., 2020). Several studies have been carried out to evaluate the possibility of improving the properties of paper and cardboard with the use of starch, particularly enhancing their barrier properties against edible oils (Guo et al., 2021; Roy et al., 2020). These studies have demonstrated that the use of different starch formulations can lead to significant improvements in oil barrier properties, showing, in some cases, a 100% improvement compared to untreated paper. The studies have also shown that the effectiveness of starch coatings in preventing the passage of fat components can vary depending on the specific composition of the starch. For example, Chi et al. showed that the addition of different potato starch coatings led to varying levels of grease resistance in coated paperboard samples (Chi et al., 2020).

These findings suggest that starch coatings have the potential to significantly improve the oil barrier properties of paper and cardboard, with the specific composition of the starch playing an important role in determining their effectiveness (Ewender et al., 2013). However, starch has poor mechanical properties compared to conventional synthetic polymers, which limits its use as a packaging material. In fact, the elongation at break for coating or film with starch used for food packaging is reported in the literature to be around 10–20 MPa, in contrast with 40–70 MPa reached by the family of polyethylene polymers (Chi et al., 2020; Dobrovszky et al., 2017; Mahuwala et al., 2020). One of the most promising solutions to overcome problems such as this is to mix starch with another polymer or add functional reinforcing fillers in order to

create a composite film, such as blending starch with PCL and/or agar (Choi et al., 2017; Ortega-Toro et al., 2016; Singh et al., 2003). Researchers have explored the use of agar and starch to create binary composite films that are compatible with each other. The combination of these materials has shown promising results as their mixtures demonstrate enhanced properties when compared to their individual counterparts (Choi et al., 2017). In fact, Choi et al. (Choi et al., 2017) have developed a colorimetric pH indicator film using biodegradable materials, such as agar and potato starch. According to Guo et al., agar plays a dominant role in determining the structure and properties of starch/agar composites. The researchers discovered that the optimal properties were achieved at a specific starch/agar ratio. The addition of agar to starch resulted in notable enhancements in both tensile strength and elongation at break. However, once the agar content exceeded 50 wt.%, the improvements became insignificant (Guo et al., 2021). Finally, Mahuwala et al. have formulated a cassava starch/agar nanocomposite containing Ag and ZnO using the solution casting method and carried out an analysis of the antimicrobial properties (Mahuwala et al., 2020). These studies suggest that starch and agar are promising candidates to comply with the European objectives and standards while also accommodating consumer requests relating to the sustainability and recyclability of food packaging, as coating for paper for food packaging.

In this context, the aim of this work is to carry out a statistic-guided improvement of the physical characteristics of base paper coated with biopolymers and other compostable natural materials, with particular focus on food-wrapping papers (e.g., baking papers, wrapping papers for food delivery) while maintaining the food's adsorption of grease and water at acceptable levels during transport, storage/shelf-life, and consumption. The base paper samples were coated with water-based solutions containing PCL (5% w/v) and variable percentages of native starch (5–10% w/w PCL dry weight) and agar (0–1.5% w/w PCL dry weight). Then, to improve the uniformity and spreadability of the coating, different percentages of plasticizers were added to all formulations. In this regard, poly (ethylene glycol) (PEG) (5% w/w PCL dry weight or 15% w/w PCL dry weight) and glycerol (4% w/w PCL dry weight) were introduced to the starch–agar/PCL blend to improve coating uniformity and diffusion. As further innovation with respect to consolidated research, a design of experiments approach was implemented to obtain statistically reliable results in terms of the best coating composition, with the lowest possible number of tests due to the high number of formulation variables taken into consideration (Montgomery, 2012). Mathematical models were implemented for each measured property of the coating to quantitatively calculate how different percentages of the selected chemicals can affect the coating properties and the overall best coating composition.

4.2. Materials and Methods

4.2.1. Materials

In this work, a calendered bleached paper (Advantage MG White High Gloss, Mondi Group, Addlestone, UK) was used, with technical data shown in Table 4.1, supplied by Serchio Distribuzione (Roma, Italy). According to the technical sheet, the paper is obtained from a long-fiber sulphate pulp. Poly(hexano-6-lactone) (PCL) was purchased from Sigma Aldrich (Taufkirchen, Germany), having average Mw 80,000 g/mol, water content < 0.5%, and melt flow index (160 ◦C/5 kg) 2.01–4.03. Ethyl acetate (Ethyl acetate—ACS reagent, purity > 99.5%, Mw: 88.11 g/mol) and glycerol (1,2,3-Propanetriol, Glycerin, purity > 99.5%, Mw: 92.09 g/mol) were purchased from Sigma Aldrich (Taufkirchen, Germany). Potato starch (CAS-No 9005-84-9, analytical grade) was purchased from PanReac AppliChem ITW Reagents (Cinisello Balsamo, Milano, Italy); agar-agar was purchased from OXOID, Thermo Fisher Scientific (Rodano, Milano, Italy); polyethylene glycol (PEG) 200 (analytical grade, Density 1.124–1.126 g/cm^3, Hydroxyl value: 535–590, Mw~190–210 g/mol; Fluka Analytical, Rodano, Milano, Italy) was used as a plasticizer. Heptane (Heptane – for HPLC; ≥99%) and toluene (ACS reagent, ≥99.5%) were purchased from Sigma Aldrich (Taufkirchen, Germany). Castor oil (purity 100%) was purchased from a local pharmacy.

Table 4.1. Technical data sheet of uncoated paper.

Properties	Units	Test Method		Values
Basis Weight	g/m^2	ISO 536		40
Tensile Strength	kN/m	ISO 1924-3	MD CD	4.3 1.8
Tear Strength	mN	ISO 1974	MD CD	340 520
Burst Strength	kPa	ISO 2758		188
Air resistance (Gurley)	S	ISO 5636-5		28
Cobb-60″ MG Side	g/m^2	ISO 535		21
Gloss	%	TAPPI 480 om-99		25
Brightness	%	ISO 2470		82
Opacity	%	ISO 2471		59
Thickness	µm	ISO 534		55

4.2.2. Coating Preparations

In the coating formulation, PCL and glycerol concentration were kept constant, respectively at 5% w/v and 4% w/w PCL dry weight, whereas the amounts of agar, starch, and PEG were varied among selected ranges from previous preliminary tests (Lo Faro et al., 2021). Taking into account 3 variables in the coating formulations, a full factorial design was implemented having a total of 12 different coating formulations, each one repeated at least three times for replication. In Table 4.2, the different combinations of the 12 solutions are reported divided in 3 sets (SET 1, SET 2, and SET 3).

Table 4.2. Different combination of the 12 coating solutions divided in 3 sets, taking in account the input variables.

		Starch % (*w/w* PCL Dry Weight)	Agar % (*w/w* PCL Dry Weight)	PEG % (*w/w* PCL Dry Weight)
SET 1	S5 AG	5	1.5	0
	S10 AG	10	1.5	0
	S5	5	0	0
	S10	10	0	0
SET 2	PEG5 S5 AG	5	1.5	5
	PEG5 S10 AG	10	1.5	5
	PEG5 S5	5	0	5
	PEG5 S10	10	0	5
SET 3	PEG15 S5 AG	5	1.5	15
	PEG15 S10 AG	10	1.5	15
	PEG15 S5	5	0	15
	PEG15 S10	10	0	15

All the solutions were prepared by dissolving 5 g of PCL in 100 mL of previously heated ethyl acetate, under continuous stirring in a water bath at 60 °C for 40 min and with the use of a solvent recondensation system. After the complete cooling of the solution, PEG (5% w/w or 15% w/w PCL dry weight) was added whenever required following the experimental plan of the formulations (Table 4.2). The water solutions containing starch (5% w/w PCL or 10% w/w PCL dry weight) and agar-agar (1.5% w/w PCL dry weight) in their desired concentrations were prepared separately at room temperature. Finally, after the addition of the starch–agar solution to the one containing PCL and PEG to obtain the desirable solution from the design of experiment, 4% (w/w PCL dry weight) glycerol was added to all the samples. Paper sheets (210 × 297 mm) were coated with the different solutions, employing a bar coating with a Compact AB3650 (TQC Sheen) automatic film applicator, working under a fume hood with the layer-by-layer technique (Figure 4.1). All paper sheets were coated using the film applicator with a nominal coating thickness of 100 μm and an application speed of 50 mm/s. Once coated with the layer, the paper samples were dried under a fume hood for about 30 min in order to remove the solvent and then dried in an oven at 80 °C for 1 h. The samples were kept for 24 h at room temperature before testing.

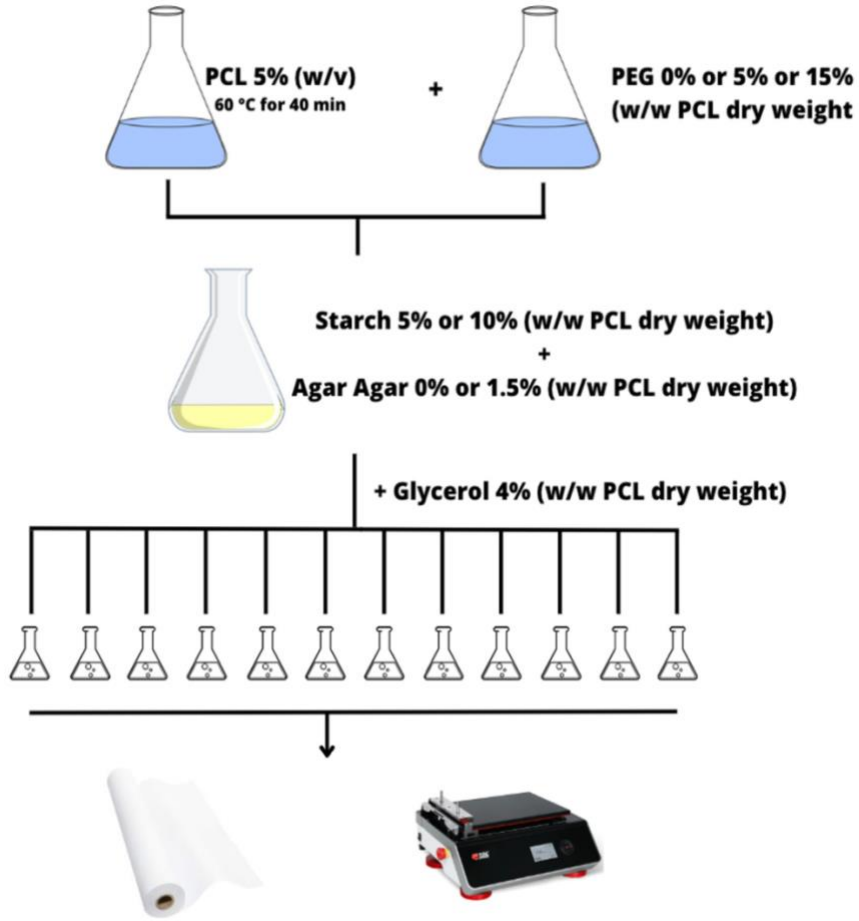

Figure 4.1. Scheme of the coatings production.

4.2.3. Characterizations

4.2.3.1. Grammage and Thickness Determination

The grammage was calculated according to the method described in par. 3.2.2.3.
A digital micrometer (Syntek, New York, NY, USA) with a sensitivity of 0.001 mm was used to measure the thickness. Three thickness measurements were carried out on both sides and in the central part of 10 rectangular specimens of 150 × 25 mm that were cut from three sheets of uncoated and coated paper (the same specimens were used for the mechanical properties determinations; see Section 4.2.3.6). A total of 30 measurements were carried out, from the mean and standard deviation values were calculated.

4.2.3.2. SEM Analysis

The surface of the paper samples was analyzed according to the method described in par.3.2.2.4, with the different that images were captured at different magnifications (500–1000×).

4.2.3.3. Contact Angle Determination

Contact angle (CA) values with water and oil were measured according to the method described in par. 3.2.2.7, with slight different: the oil used for the test was the 7 µL of castor oil; the water

CA was measured immediately after the drop deposition (t0) and after 15 s (t15) and 30 s (t30) s; oil CA was measured at different time steps with the same procedure employed for water CA.

4.2.3.4. Grease Resistance Determination (TAPPI, T 559 pm-02)

The grease resistance was tested by using the standard method, namely T 559 pm-02 (or "Kit 12" test) (TAPPI, 2002). According to this test, the 12 solutions to be analyzed were prepared by mixing castor oil, heptane, and toluene in adequate portions, thus obtaining solutions that emulate different surface tensions. Solutions with higher numbers are more aggressive, having lower surface energies (i.e., Solution 1 is the less aggressive, while Solution 12 is the most aggressive). A drop of each solution of the kit test was gently dropped onto the surface of each sample and quickly removed with a clean absorbent cloth after 15 s. The tested area was examined and evaluated, giving a specific value to each sample corresponding to the number of the kit test solution that shows the first signs of degradation. Thereafter, the higher the reported value is, higher the resistance of the sample surface to oils is.

4.2.3.5. Water Vapor Transmission Rate (WVTR) and Determination of water absorption

The WVTR value was determinate according to the method described in the par. 3.2.2.5.

The determination of the absorbed water was performed, with some modifications, according to the Cobb 60 method. The test was performed on samples with 9 cm^2 of area and on which a quantity of 1 mL of water was placed, after 60 seconds the excess water was absorbed through the use of a tissue. The samples were weighed before (G1) the deposition of the water and then at the end of the test (G2) and then the values were calculated follow the formula (2):

$$C = \frac{G2-G1}{A} \quad (2)$$

Where: C (g/m^2) is Cobb water absorption value; G1 (g) is mass of sample before water absorption; G2 (g) is mass of sample after water absorption; A (m^2) is Test area.

4.2.3.6. Mechanical Properties

4.2.3.6.1. Tensile strength measurement

The tensile strength measurements of paper samples were determined by a universal testing machine (BT1- FR1.0TH.140, Ulm, Germany) according to ASTM D882 (ASTM D882-18, 2018). For each sample, 20 specimens (dimensions of 150 × 25 mm) were taken: 10 in the machine direction (MD) and 10 in the cross-direction (XD). The dynamometer settings were initial strain 0.1 mm/mm, initial grip separation 125 mm, and speed of grip separation 12.5 mm/min. The collected data were processed by the TESTEXPERT®II (V3.31) software. The following mechanical properties have been measured: Young's modulus (E—MPa), tensile strength (σ—MPa), and elongation at break (ε—%).

4.2.3.6.2. Tear propagation measurement

The trousers tear test, conducted in accordance with the ASTM D1938-19 standard, was employed to evaluate and characterize the tear propagation behavior of a paper sample. The

test procedure involved preparing six specimens with dimensions of 7 cm x 2.5 cm. A central cut measuring 5 cm in length was made on each specimen (Figure 4.2).
To perform the test, a universal testing machine (BT1-FR1.0TH.140, Ulm, Germany) was utilized. The specimens were securely clamped in the grips of the machine, with a gripping distance of 50 mm. Prior to the test, a preloading force of a specific value (0.1 MPa) at the speed of 50mm/m were applied to the specimen. The test was then carried out at a predetermined speed of 250 mm/min.
The test continued until the tear propagation had occurred along the entire length of the specimen of 50 mm. The acquired data were subsequently analyzed using the TESTEXPERT®II software (V3.31), which facilitated the processing and interpretation of the test results.

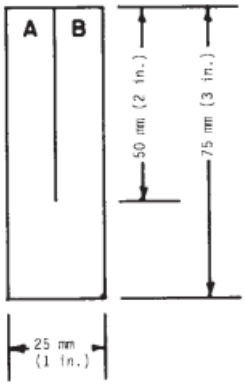

Figure 4.2. Tear Propagation Analysis Specimen Example

4.2.4. Statistical Analysis

A design of experiments (DoE) study was set up to calculate the minimum number of experiments necessary to build up mathematical model, saving time and raw materials. As stated in Section 4.2.2, three variables were considered, and thereafter a full factorial design was implemented. The other variables that occurred in the process, such as environmental humidity and temperature, were kept the same during all the tests, according to the procedure in Section 4.2.2. The Design Expert 13.0 (Stat-Ease, Minneapolis, MN, USA) code was used to set up the experimental plan and to perform the statistical analysis of the results. A total of 36 experiments were grouped in the factorial design, consisting also of repetitions for pure error estimation. The central points were included to calculate the presence of curvature in the mathematical model. All the experimental runs were performed randomly to avoid the presence of systematic errors, following the method reported in Section 4.2.2.
The data were analyzed firstly by means of PCA (principal component analysis) which made it possible to evaluate the characteristics of the paper samples in a multivariate manner. In particular, the purpose of the PCA analysis in this context was to evaluate which type of paper had overall better performance considering the characteristics evaluated: oil repellency, water repellency, and mechanical strength. Thereafter, a multivariate regression approach through analysis of variance (ANOVA) was set up to mathematically correlate and calculate each formulation effect of the specific evaluated property. The p-value (<0.05), related to the F-test, is the statistical parameter necessary to evaluate the significance of the model and each factor.

A lack-of-fit test was considered to assess a possible significant variation of the experimental points in comparison with their predicted values, R2. Adjusted-R2 and Pred-R2 were calculated to determine the mathematical model fit quality as well as its predictive power. R2 is the proportion of the variance in the dependent variables that is predictable from the independent variables, Adjusted-R2 is a corrected R2 in relation to the number of the performed runs (thereafter aiming to correct any overestimation of the R2 due to the increasing number of effects included in the model), and Pred-R2 is analogous to R2 but associated with predicted values (Montgomery, 2012).
Finally, a global desirability function was estimated to provide the most desirable combination of factors, considering all the responses analyzed simultaneously. Each response is weighed according to its specific target (Table 4.3) in terms of objectives and importance, depending on how much each response should match the purpose of the overall study, and then combined using a mean. The desirability function values can be from 0 to 1, where the lowest value (0) represents a completely undesirable combination of independent factors, and, conversely, the highest value (1) indicates a completely desirable (or ideal) combination of them (Montgomery, 2012).

Table 4.3. Output Variables investigated.

Output Variables	Goal	Importance
WVTR	to minimize	2
Grease Resistance—Kit 12	to maximize	5
Contact angle measurements oil	to maximize	4
Contact angle measurements water	to maximize	2
Thickness	to minimize	3
Grammage	to minimize	3
Mechanical properties	In range	3

4.3. Results

4.3.1. SEM Analysis

The surface of the uncoated and coated paper samples, analyzed by SEM, is reported in Figure 4.3. The uncoated paper sample showed the classic open and porous network structure with a non-uniform surface, while in all the coated samples, the typical cellulose fibers and holes of the paper are not visible. For this reason, we can assess that the coating is completely spread in all the samples in a homogeneous way, capable of covering paper fibers and closing paper holes, even if with some differences among them. In fact, the presence of agar (Figure 4.3) in the coating formulation seems to favor the spreadability of the coating, because the typical hollows of starch are less evident (Domene-López et al., 2019; Requena et al., 2016). On the contrary, these depressions are bigger and more visible in the samples without agar, especially in the samples which have 10% w/w PCL dry weight of starch in the formulation of the coating. In addition, comparing the samples with agar of SET 1 (samples without PEG in the formulation), with the ones without agar of the same set, the presence of lumps of starch, due to the hydration of starch with the water, is very clear also in the samples with agar, thus presenting a less homogeneous surface. Already confirmed by our previous studies, PEG strongly influences the spreadability and homogeneity of coatings on cellulosic materials (Sogut et al., 2018). In fact, as shown in Figure 4.3, it is possible to see a considerable improvement in the homogeneity of the surface moving from the samples with PEG 5% w/w PCL dry weight to the ones with 15% w/w PCL dry weight of PEG. It can therefore be supposed that the PEG/agar combination positively influences the achievement of a more homogeneous and smooth coating surface.

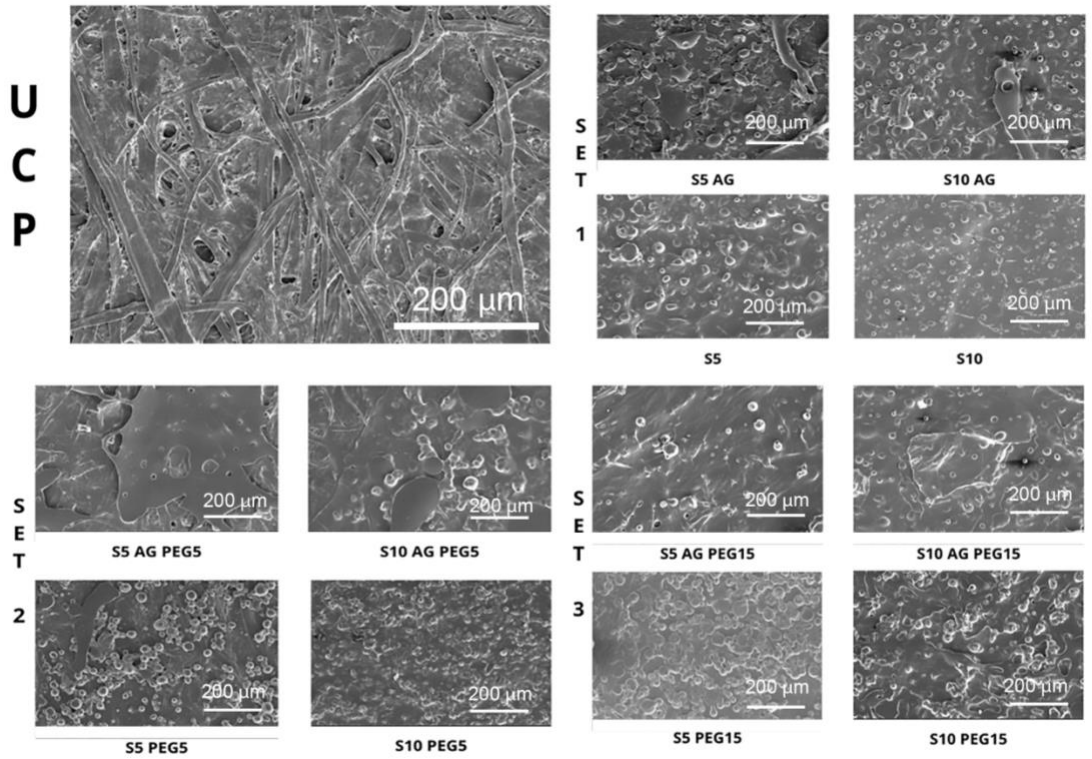

Figure 4.3. SEM micrographs representative of each investigated sample.

4.3.2. Grammage and Thickness

Grammage and thickness (the last is the thickness of the whole structure, i.e., uncoated paper and paper with coatings) increase in the coated samples with respect to the uncoated samples (see Table 4.5). Grammage values are almost the same for all the samples due to the amount of coating agents used to create the sample sets and only slight differences can be observed. On the other hand, for the thickness, the presence of agar in the coating solutions lead to significantly higher thickness of the coating layers and this behavior is common for all the three sets. In fact, for the samples coated with solution containing agar the average thickness is around 0.170 mm, while for the samples without agar it is around 0.08 mm. The gelation properties of agar, capable of forming strong gel also at low concentration, may account for an increase of the solution viscosity (Guo et al., 2021), which probably means that agar does not allow the penetration of the coating solutions into the first layers of the paper structure. It is well known that the addition of a coating generally results in an increase in both thickness and grammage compared to samples without coating, but a more specific calculation must be provided to estimate this increasing effect, both for grammage and thickness. This calculation has been made through PCA and multivariate analysis. As shown in Table 4.6, the PCA analysis suggests that the only factor that significantly affects thickness is agar. Additionally, samples that include agar in the coating solution have a higher thickness than those without agar; this is evidenced even from the multifactorial ANOVA, with $p \leq 0.001$. These observations suggest that the specific components and concentrations used in the coating formula can have a direct impact on the resulting thickness of the paper samples, especially the presence of agar. Regarding grammage, there is no statistically significant factor that influences this property.

4.3.3. Oil Contact Angle

In the measurement of the oil CA, castor oil was chosen because it is the basis of the solutions used in the test "Kit-12" (see Section 4.2.3.4), a reference method to evaluate the repellency of paper against oils and fats. Considering Table 4.6, the presence of PEG and starch in the formulation of the samples significantly influences the values of the oil CA at 0 s, with $p \leq 0.001$. Even the interaction between the factors is significant from the statistical point of view but with a restrained influence, as the p-value increases ($p \leq 0.05$). In addition, differences arise among CA measured at different times. As shown in Table 4.4, after 15 s and 30 s, the agar addition plays the key role, and, thereafter, all the variables considered for coating formulation must be carefully considered in the coating formulation to tailor this fundamental property. In particular, the oil CA after 15 s is around 38° for most of the formulations containing agar and around 32°, for the coating formulation without agar. In strong similarity, after 30 s, both CA decrease, but in the same proportion. In fact, the coatings' formulation with agar had higher CA, equal to 35°, in contrast with the CA measured in the formulation without agar, that is, 29°. In Table 4.4 of the Supplementary Materials, the data collected for each sample have been reported. Considering Table 4.4, in SET 2, sample S5 PEG5 shows the highest CA value at time zero, instead sample S10 AG PEG5 has the highest value at 15–30 s after the drop deposition. As regards the other samples of SET 2, they all have a discontinuous but, at the same time, a rather high value of CA. Samples of SET 1 instead show fairly constant values over time, in particular sample S5, which contains only 5% w/PCL of the starch component. SET 3 samples measured the highest values of all the other samples analyzed in this experiment; in fact, the values recorded at instant 0 s fell within a range between 70° and 77°. In particular, sample S5 PEG15 recorded the highest angle values at time 0. It is important to underline that

the oil CA values for all the samples (control paper included) are below 90°, indicating a relative low oleophobicity (conversely a high wettability of the surface), and only the samples of SET 3 seem to show an improvement of the oil CA if compared with the uncoated paper, demonstrating the positive effect of the starch addition to the experimental formulations. In Figure 4.5a, the response surface graph and the mathematical equation of the model have been reported, estimating quantitatively the effect of PEG and starch on the coating oil CA.

Table 4.4. Results of the Multifactorial ANOVA and Tukey's HD test regarding CA Oil. Results are reported as F-values and lowercase letters ("c" > "b" > "a"), respectively. Different letters identify significantly different samples.

	SAMPLE NAME	Time (s)		
		0 s	15 s	30 s
SET 1	S5 AG	65.77 ± 4.85^{abcd}	39.6 ± 2.74	37.10 ± 3.73
	S10 AG	56.78 ± 2.68^{de}	29.48 ± 0.36	28.22 ± 0.66
	S5	65.23 ± 4.18^{bed}	37.95 ± 0.91	37.75 ± 1.33
	S1O	53.22 ± 3.10^{e}	26.33 ± 0.62	24.07 ± 2.35
SET 2	S5 AG PEG5	58.52 ± 0.45^{de}	40.88 ± 0.16	37.07 ± 0.33
	S10 AG PEG5	57.49 ± 2.77^{de}	45.28 ± 1.31	39.93 ± 1.17
	S5 PEG5	62.22 ± 0.12^{bcde}	30.78 ± 0.31	27.90 ± 0.52
	S10 PEG5	59.03 ± 0.42^{cde}	29.15 ± 0.02	24.75 ± 0.40
SET 3	S5 AG PEG15	70.20 ± 2.61^{abc}	37.00 +1.75	34.42 ± 1.38
	S1O AG PEG15	70.90 ± 1.13^{ab}	36.25 ± 0.95	34.85 ± 1.95
	S5 PEG15	76.72 ± 3.06^{a}	32.28 ± 2.34	29.88 ± 1.70
	S10 PEG15	71.17 ± 3.45^{ab}	30.6 2± 0.50	27.87 ± 1.16
UCP		66.37 ± 3.26^{abcd}	39.33 ± 5.82	33.38 ± 2.98

Table 4.5. Mean values with standard deviation of the data collected for thickness measurement, grammage measurement, contact angle values with oil and water (1 only 0 s time), mechanical property values (Young's modulus, tensile strength, and elongation at break), Kit Test 12 values, and WVTR values. Results of multifactorial ANOVA are reported as F-values and lowercase letters ("c" > "b" > "a"), respectively. Different letters identify significantly different samples.

SET	Samples	Thickness (mm)	Grammage (g/m^2)	Oil CA [1] (Degrees)	Water CA [1] (Degrees)	Kit Test 12	WVTR ($g\ m^{-2}\ day^{-1}$) 38 °C 90% RH		Young's Modulus (MPa)	Tensile Strength (MPa)	Elongation at Break (%)
1	S5AG	$0.166^{abc} \pm 0.010$	$54.4^{ab} \pm 10.9$	$65.77^{abcd} \pm 4.85$	$54.88^{def} \pm 3.78$	$9.33^{bc} \pm 0.6$	$4943^{cdb} \pm 74$	XD	$257^{e} \pm 320$	$12.32^{ghi} \pm 0.39$	$3.43^{a} \pm 0.77$
								MD	$1790^{bcde} \pm 1362$	$27.55^{efgh} \pm 1.92$	$2.91^{a} \pm 0.29$
	S10AG	$0.227^{a} \pm 0.172$	$61.8^{a} \pm 6.9$	$56.78^{de} \pm 2.69$	$49.90^{f} \pm 5.41$	$8.33^{c} \pm 0.6$	$4987^{cbd} \pm 87$	XD	$638^{bcde} \pm 48$	$9.57^{i} \pm 0.84$	$3.41^{a} \pm 0.13$
								MD	$1951^{abcd} \pm 693$	$20.10^{fghi} \pm 1.66$	$3.59^{a} \pm 0.56$
	S5	$0.073^{f} \pm 0.004$	$52.1^{ab} \pm 6.6$	$65.23^{bcd} \pm 4.18$	$52.37^{ef} \pm 5.14$	$8.67^{bc} \pm 0.6$	$4851^{de} \pm 138$	XD	$247^{e} \pm 221$	$27.83^{efgh} \pm 1.39$	$3.42^{a} \pm 0.46$
								MD	$511^{cde} \pm 306$	$63.52^{ab} \pm 8.96$	$3.30^{a} \pm 0.65$
	S10	$0.077^{f} \pm 0.003$	$54.8^{ab} \pm 7.4$	$53.22^{e} \pm 3.10$	$57.04^{edf} \pm 3.46$	$10.33^{ab} \pm 0.6$	$4808^{de} \pm 182$	XD	$458^{de} \pm 96$	$23.25^{fghi} \pm 7.22$	$3.58^{a} \pm 1.30$
								MD	$677^{bcde} \pm 348$	$62.18^{ab} \pm 2.80$	$3.43^{a} \pm 0.25$
2	PEG5 S5 AG	$0.140^{bcdef} \pm 0.017$	$52.2^{ab} \pm 2.6$	$58.52^{de} \pm 0.45$	$80.11^{b} \pm 7.84$	$11.33^{a} \pm 0.6$	$4907^{dec} \pm 88$	XD	$477^{cde} \pm 116$	$15.06^{ghi} \pm 1.34$	$3.15^{a} \pm 0.35$
								MD	$1108^{bcde} \pm 152$	$34.88^{def} \pm 1.41$	$3.14^{a} \pm 0.25$
	PEG5 S10 AG	$0.151^{bcde} \pm 0.010$	$56.7^{ab} \pm 1.5$	$57.49^{de} \pm 2.77$	$81.99^{b} \pm 9.11$	$4.33^{d} \pm 0.6$	$4800^{de} \pm 51$	XD	$402^{de} \pm 85$	$12.51^{ghi} \pm 1.74$	$2.95^{a} \pm 0.56$
								MD	$897^{bcde} \pm 98$	$29.09^{efg} \pm 1.65$	$2.76^{a} \pm 0.23$
	PEG5 S5	$0.101^{cdef} \pm 0.005$	$55.0^{ab} \pm 4.4$	$62.22^{bcde} \pm 0.12$	$56.42^{cd} \pm 6.90$	$8.33^{c} \pm 0.6$	$4810^{de} \pm 140$	XD	$816^{bcde} \pm 86$	$23.65^{fghi} \pm 0.33$	$3.21^{a} \pm 0.16$
								MD	$1411^{bcde} \pm 244$	$51.46^{bcd} \pm 3.01$	$2.96^{a} \pm 0.25$
	PEG5 S10	$0.083^{def} \pm 0.004$	$55.7^{ab} \pm 7.7$	$59.03^{cde} \pm 0.42$	$60.48^{cd} \pm 3.65$	$10.33^{ab} \pm 0.6$	$4688^{e} \pm 110$	XD	$598^{cde} \pm 92$	$23.81^{fghi} \pm 2.99$	$3.15^{a} \pm 0.66$
								MD	$1238^{bcde} \pm 338$	$49.50^{bcd} \pm 13.42$	$2.79^{a} \pm 0.93$
3	PEG15 S5 AG	$0.155^{abcd} \pm 0.013$	$49.6^{bc} \pm 5.3$	$70.20^{abc} \pm 2.61$	$53.36^{def} \pm 4.89$	$9.33^{bc} \pm 0.6$	$5279^{a} \pm 69$	XD	$702^{bcde} \pm 200$	$12.17^{ghi} \pm 0.46$	$3.27^{a} \pm 0.48$
								MD	$1618^{bcde} \pm 108$	$24.99^{efghi} \pm 6.14$	$2.61^{a} \pm 0.92$
	PEG15 S10 AG	$0.182^{ab} \pm 0.018$	$56.0^{ab} \pm 10.4$	$70.90^{ab} \pm 1.13$	$54.64^{cdef} \pm 3.81$	$8.33^{c} \pm 0.6$	$5147^{ab} \pm 116$	XD	$572^{cde} \pm 144$	$10.73^{hi} \pm 0.60$	$3.35^{a} \pm 0.34$
								MD	$1106^{bcde} \pm 186$	$23.95^{fghi} \pm 1.58$	$3.12^{a} \pm 0.27$
	PEG15 S5	$0.079^{ef} \pm 0.004$	$58.3^{ab} \pm 8.1$	$76.72^{a} \pm 3.06$	$57.01^{cdef} \pm 4.60$	$8.67^{bc} \pm 0.6$	$5152^{ab} \pm 120$	XD	$1053^{bcde} \pm 254$	$22.13^{fghi} \pm 1.80$	$3.09^{a} \pm 0.59$
								MD	$2210^{ab} \pm 224$	$54.15^{abc} \pm 4.06$	$3.05^{a} \pm 0.25$
	PEG15 S10	$0.089^{def} \pm 0.003$	$56.1^{ab} \pm 8.1$	$71.17^{ab} \pm 3.45$	$61.91^{c} \pm 4.50$	$9.33^{bc} \pm 0.6$	$5121^{abc} \pm 176$	XD	$995^{bcde} \pm 62$	$22.62^{fghi} \pm 0.78$	$3.65^{a} \pm 0.37$
								MD	$1670^{bcde} \pm 472$	$50.92^{bcd} \pm 2.92$	$3.28^{a} \pm 0.14$
	UCP	$0.067^{f} \pm 0.001$	$41.0^{c} \pm 1.9$	$66.37^{abcd} \pm 3.26$	$129.46^{a} \pm 23.05$	$0.33^{e} \pm 0.6$	5157 ± 152	XD	$2057^{abc} \pm 1245$	$41.89^{cde} \pm 20.16$	$2.92^{a} \pm 0.32$
								MD	$3498^{a} \pm 1333$	$55.66^{abc} \pm 3.10$	$2.56^{a} \pm 0.24$

*Table 4.6.a Results of the multifactorial ANOVA and Tukey's HD test * = p ≤ 0.05; ** = p ≤ 0.01; *** = p ≤ 0.001.*

	Agar	Starch	PEG	Agar PEG	PEG Starch	Agar Starch	PEG Agar Starch
Grammage	/	*	/	/	*	/	/
Thickness	***	/	/	*	/	/	/
CA Oil 0s	/	***	***	/	*	/	/
CA Oil 15s	*	/	/	/	/	/	/
CA Oil 30s	*	/	/	/	/	/	/
Grease Resistance	***	***	/	*	***	***	***
CA Water	***	*	***	***	/	*	/
WVTR	***	*	***	/	/	/	/
Tensile Strength	/	/	***	***	*	/	/
Young's Modulus	***	**	*	***	/	/	/
Elongation	/	/	/	/	/	/	/

4.3.4. Grease Resistance

The grease resistance of the experimental samples was determined by means of the TAPPI test method procedure named "Kit test 12", one of the widely used methods to evaluate the performance of paper coatings (Long, et al., 2015; Gietl et al., 2009). In this test, 12 different grease solutions (with a surface tension ranging from 0.038 mN/m (less aggressive solution 1, pure castor oil) to 0.022 mN/m (more aggressive solution 12; a mixture of toluene/heptane: 55/45) are dropped on the coatings, observing traces of staining on the paper. When a material is rated at kit number of 8 and higher it is considered as resistant to grease penetration (Adibi et al., 2023; Yokoyama et al., 2007). The data reported in Table 4.5 show that the uncoated paper has been rated very close to 0 (no resistance against oil and grease), while all the coated samples are characterized by values ranging from 8.33 ± 0.66 to 11.33 ± 0.66. The best performance, in terms of highest resistance to grease (above 10) is recorded for samples containing 5% w/w PCL dry weight of starch when agar is present (Figure 4.5b), whereas the agar/starch combination could have a slight negative impact on the oil resistance of coated paper samples when agar is absent from the formulation (Figure 4.5c). Resistance to oil, which further improves in samples that have only the starch component in the formulation, also tends to increase as the percentage of starch increases (Figure 4.5c). Finally, it is interesting to note that oil CA measured, and results obtained from KIT 12 cannot be correlated to each other, according to their definition. In fact, for example, sample PEG5 S10 AG has a higher CA value at 15 s than the other samples (around 45◦) but a very low kit-12 value (4). Another case is sample S10, which managed to resist a greater number of kits, 10, but recorded a very low CA value (Figure 4.4). Among them, sample S5 PEG15 has high values both for the Kit 12 test and for CA measurement, and this suggests that the mere presence of starch improves the repellency to oil-based substances and, especially, coatings that do not have agar in their formulation have the best fat repellency.

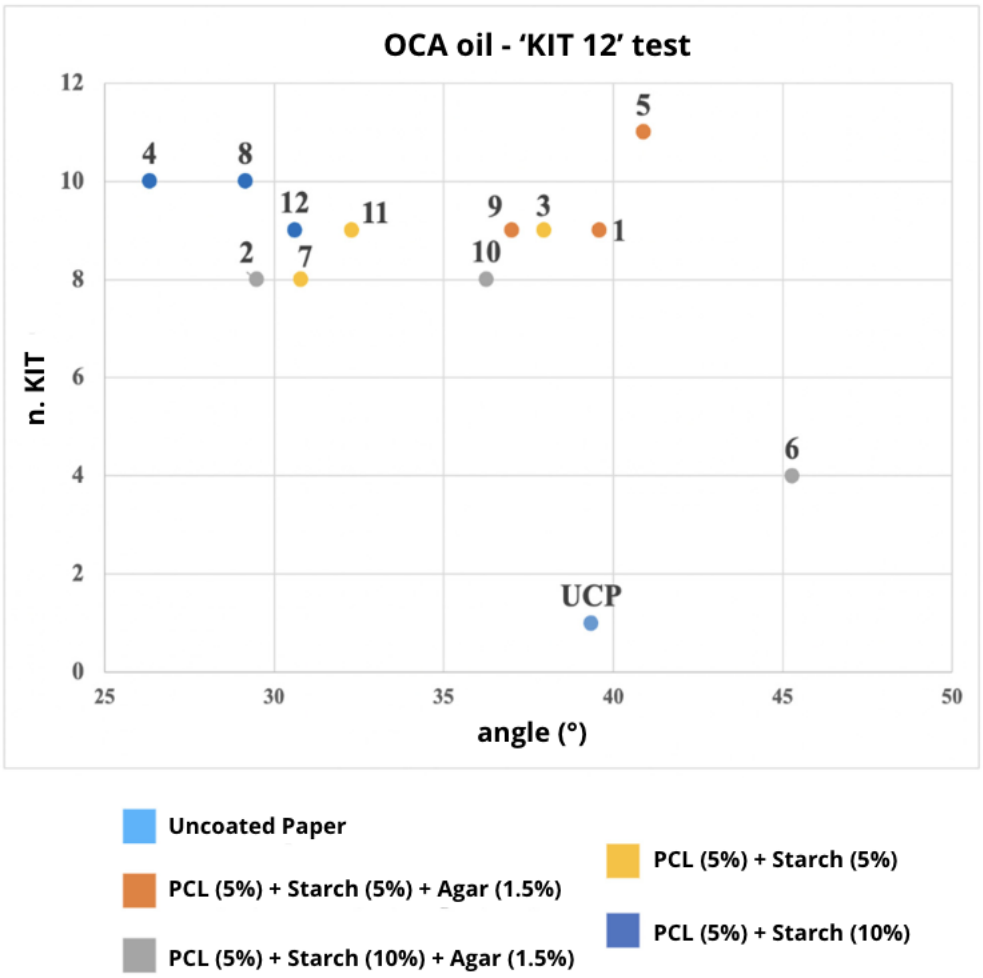

Figure 4.4. Results of the KIT 12 test.

Regarding oil resistance, together with CA, Kit 12 results should also be considered, and from this analysis we can confidently say that layering a coating on uncoated paper significantly improves its oil repellency performance. In fact, according to Table 4.6, all the variables taken in consideration in this study influence this property in single or in interaction. For example, the combination of starch and agar or even only the presence of starch have a strong effect on the performance of the paper when compared to the uncoated one ($p \leq 0.001$).

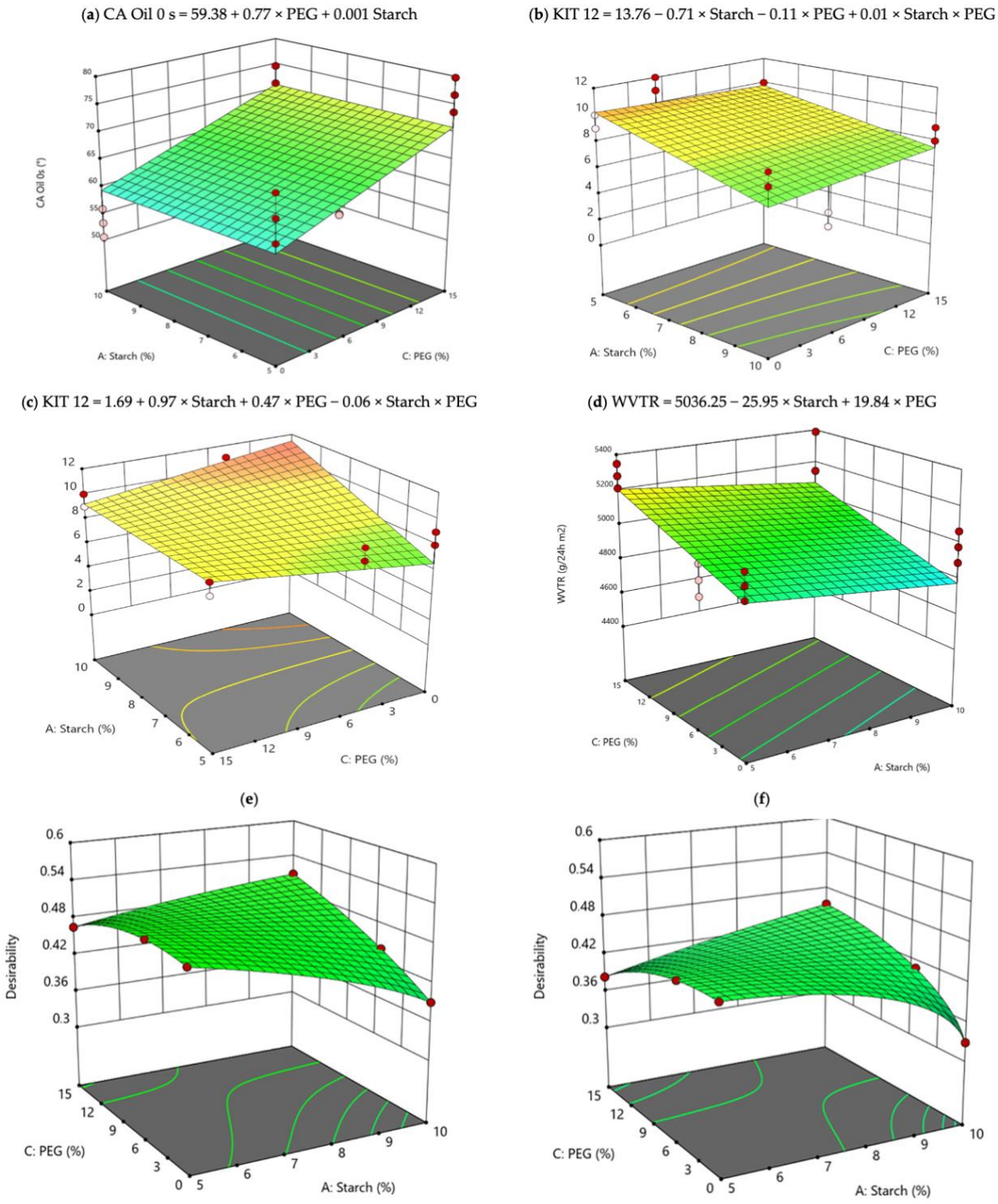

Figure 4.5. Response surface graph of the most representative mathematical models calculated: (a) CA oil 0 s; (b) KIT12 with agar; (c) KIT12 without agar; (d) WVTR with agar; (e) Desirability function with agar; (f) Desirability function without agar.

4.3.5. Behavior of Samples with Water

To complete the samples' characterization, although it was not the focus of this study, the behavior against water of the coated paper samples was also investigated. In this regard, the WVTR value of all samples was measured, and water CA analysis was performed.

4.3.5.1. WVTR

WVTR represents a measure of the interactions that the water vapor establishes with the cellulosic fibers of paper, from which low values of WVTR mean the obtainment of cellulosic materials less compatible with water and therefore less susceptible to humidity degradation. In Table 4.5, measured WVTR values for all the samples are shown. Comparing them with the control group (uncoated paper), it is clear that the lowest values were recorded by the formulations of SET2, in which 5% w/w PCL dry weight of PEG was included. The explanation for this behavior can be found precisely in the presence of PEG, which at that concentration could have favored the homogeneous dispersion of the coating on the paper surface, also promoting the penetration of the coating into the pores of the paper, thus slowing the passage of water vapor. This result is also confirmed by the SEM images shown in Figure 4.3. Furthermore, the SET 3 samples showed a higher WVTR value than the SET 2 samples. This phenomenon could be explained by the higher percentage of PEG (15% w/w PCL dry weight) present in the formulations compared to 5% w/w PCL dry weight of the SET 2 samples. In fact, as the PEG is hydrophilic at higher concentration, it could increase the permeability to water vapor, favoring the hydration of the substrate (Requena et al., 2016). In addition, interaction with the other components must be evaluated. As we can see in Table 4.6, PEG and agar seem to be the most relevant compounds in formulation from the statistical point of view also considering ANOVA. Then, if we focus our attention on the interaction between PEG and starch (Figure 4.5d), we can notice how 0% w/w PCL dry weight PEG, 10% w/w PCL dry weight starch, and 1.5% w/w PCL dry weight agar is the best combination for the WVTR performance. The presence of agar is influential on the WVTR, as we also see from the SEM analyses, because it helps with the homogeneous deposition of the coating on the paper. On the contrary, we can see that the worst coating composition is reached for 15% w/w PCL dry weight PEG combined with agar (1.5% w/w PCL dry weight), and this aspect depends on the hydrophilic nature of the PEG.

4.3.5.2. Water Contact Angle

Regarding water CA, all the experimental samples have shown a hydrophilic behavior as all the measured angles were below 90° (Table 4.6b). Among the various samples, the ones in SET 2, composed of samples containing PEG at 5% w/w PCL dry weight, recorded the highest CA values, in particular for samples that have agar in their formulation. In the other sets of samples, it is not possible to find significant differences as in the samples present in SET 2. However, we can state that the presence of PEG and agar, and even more their interaction, significantly influences the water CA; this is also confirmed by the multifactor ANOVA analysis (Table 4.6b), where the factors considered, and their interaction are shown.

Table 4.6.b Results of the Multifactorial ANOVA and Tukey's HD test regarding CA Water. Results are reported as F-values and lowercase letters ("c" > "b" > "a"), respectively. Different letters identify significantly different samples.

	SAMPLE NAME	Time (s)		
		0 s	15 s	30 s
SET 1	S5 AG	54.88 ± 3.78^{def}	51.35 ± 6.80	48.50 ± 7.77
	S10 AG	49.90 ± 5.411^{f}	47.74 ± 6.58	46.00 ± 6.67
	S5	$52.37 \pm 5.14e^{f}$	47.91 ± 8.47	44.86 ± 8.69
	S10	57.04 ± 3.46^{cdf}	50.23 ± 6.33	47.39 ± 7.81
SET 2	S5 AG PEG5	30.11 ± 7.48^{b}	78.74 ± 7.23	77.74 ± 6.41
	S10 AG PEG5	51.99 ± 9.11^{b}	80.90 ± 8.70	77.52 ± 9.19
	SS PEG5	56.42 ± 6.90^{cde}	52.28 ± 10.33	49.43 ± 8.11
	S10 PEG5	60.48 ± 3.65^{cd}	58.48 ± 5.07	56.50 ± 9.19
SET 3	S5 AG PEG15	53.36 ± 4.89^{def}	47.40 ± 8.34	44.98 ± 8.38
	S10 AG PEG15	54.69 ± 3.81^{cdef}	51.75 ± 7.12	48.95 ± 7.71
	S5 PEG15	57.01 ± 4.60^{cdef}	55.06 ± 5.73	53.65 ± 5.69
	S10 PEG15	61.94 ± 4.50^{c}	61.31 ± 4.83	59.32 ± 5.65
UCP		129.46 ± 23.05^{a}	123.69 ± 3.90	122.05 ± 6.29

Particular attention has to be focused on the water CA of the uncoated paper, whose value was around 120°, indicating a relatively high hydrophobicity of the samples. This result may be attributed to the high smoothness of the surface of the calendered paper used, a condition which seems to impact positively on wettability (it decreases). From the results of the water CA, it is evident that the presence of the coatings seems to increase the wettability of the surfaces (i.e., an increase of hydrophilicity). This is probably due to the roughness induced by the coatings themselves.

4.3.5.3. Water absorption

The water absorption test aimed to determine the amount of water, measured in grams per square meter (g/m^2), absorbed by the samples within a 60-second timeframe. The obtained data, presented in the table 4.7, were subjected to a multivariate analysis of variance (ANOVA) test. Additionally, the Tukey significance test was performed to assess the statistical significance, considering the p-values (table 4.8).

The results indicate that the presence of PEG (polyethylene glycol) has a notable impact on water absorption. Specifically, samples containing PEG15 exhibited higher water absorption values. This can be attributed to the pronounced hydrophilicity of PEG, which enables a strong affinity with water, thereby increasing its absorption by the sample.

In contrast, the interaction between PEG and starch (PEGxSTARCH) does not appear to favor water absorption by the sample, particularly when PEG5 is combined with a 10% starch content in the sample formulation. This is evident in the S10AGPEG5 and S10PEG samples, which recorded water absorption values of 39.24 g/m^2 and 41.81 g/m^2, respectively. Therefore, the interaction between 5% PEG and starch seems to be the most promising combination for mitigating water absorption by the paper samples. This finding is further supported by the measurement of the contact angle with water (Section 4.3.5.2.), where the SET2 samples (containing 5% PEG) exhibited the highest contact angle values, indicating reduced water wettability.

An interesting phenomenon observed across all the samples is that the water used in the experiment was effectively retained by the coating and did not pass through to the opposite

side of the sheet. This coating, predominantly composed of starch in the SET1 samples, was consistently present in all formulations. Starch exhibits a remarkable capacity to absorb and interact with water, even at room temperature, although the absorption process is comparatively slower than when the mixture is heated.
The fact that the water was trapped by the starch-based coating suggests its ability to create a barrier that prevents water from permeating through the sample. Starch, being hydrophilic, readily absorbs water molecules, forming a gel-like structure that hinders the passage of water.
In summary, the presence of PEG in the samples increased water absorption, with PEG15 showing the highest water absorption values. Conversely, the interaction between PEG5 and starch demonstrated potential for reducing water absorption, as suggested by the water absorption results and the contact angle measurements.

Table 4.7. Results of the Multifactorial ANOVA and Tukey's HD test regarding Water Absorption measurement. Results are reported as F-values and lowercase letters ("c" > "b" > "a"), respectively. Different letters identify significantly different samples.

Samples	Water absorbed (g/m2)	SD	Test HSD Tukey
S5 AG	44.06	±2.91	ab
S10 AG	48.19	±11.09	ab
S5	49.03	±7.81	ab
S10	42.79	±9.26	b
S5 AG PEG5	48.62	±12.81	ab
S10 AG PEG5	39.24	±11.44	b
S5 PEG5	52.97	±7.94	ab
S10 PEG5	41.81	±9.26	b
S5 AG PEG15	45.78	±7.04	ab
S10 AG PEG15	59.31	±14.5	a
S5 PEG15	48.75	±7.5	ab
S10 PEG15	53.56	±3.61	ab

Table 4.8. Results of the Multifactorial ANOVA and Tukey's HD test regarding PEG factor and interaction PEGxSTARCH. Results are reported as F-values and lowercase letters ("c" > "b" > "a"), respectively. Different letters identify significantly different samples.

	p-value	%PEG	Test HSD Tukey	PEGxSTARCH	Test HSD Tukey
PEG	2.E-02	0	a	PEG0S5	abc
Interaction (PEG x Starch)	7.E-04	5	a	PEG0S10	bc
		15	b	PEG5S5	ab
				PEG5S10	c
				PEG15S5	abc
				PEG15S10	a

4.3.6. Mechanical Properties

In general, the mechanical properties of paper were determined in two orthogonal directions: the machine direction (MD) and cross-machine direction (XD). Young's modulus (E) and tensile strength (σ) are expected to decrease from MD to XD. This is due to the fact that machine made paper has more fibers aligned along MD, therefore making it less deformable in that direction but more resistant (Requena et al., 2016). We can see from Table 4.5 that the collected data, independently of the presence of a coating or not, follows this trend, indicating a specific orientation of the papers' fiber.
In addition, strong variations are due to the application of a coating and generally a sudden lowering of the recorded value of E and σ can be appreciated with respect to the uncoated paper samples. More in detail, observing the significant values of the multi-factorial ANOVA (Table 4.6), in addition to the direction of the samples, it can be detected that PEG inclusion into the coating formula significantly influences the deformability of the samples. Indeed, PEG acts as a plasticizer, by improving the diffusion of the coating and the deformability of the sample (Rogovina et al., 2018). Thereafter, lower E values are recorded for the samples coated with PEG in their formulation (Rogovina et al., 2018). Indeed, agar plays a significant role in single or in combination with PEG (Table 4.6). In fact, along the XD, samples containing agar recorded lower σ (27 MPa) with respect to the samples which do not have agar in the coating formulation (56 MPa), regardless of the amount of starch and PEG (Figure 4.6). Finally, the elongation at break was found to not be significantly affected by the presence of the coatings and therefore was not analyzed further. In summary, the coated paper samples are much more deformable as they reach lower E and σ values, with a consequent decrease in the resistance, which, however, increases with respect to the uncoated paper, in particular for the samples containing only starch in the coating formulation.

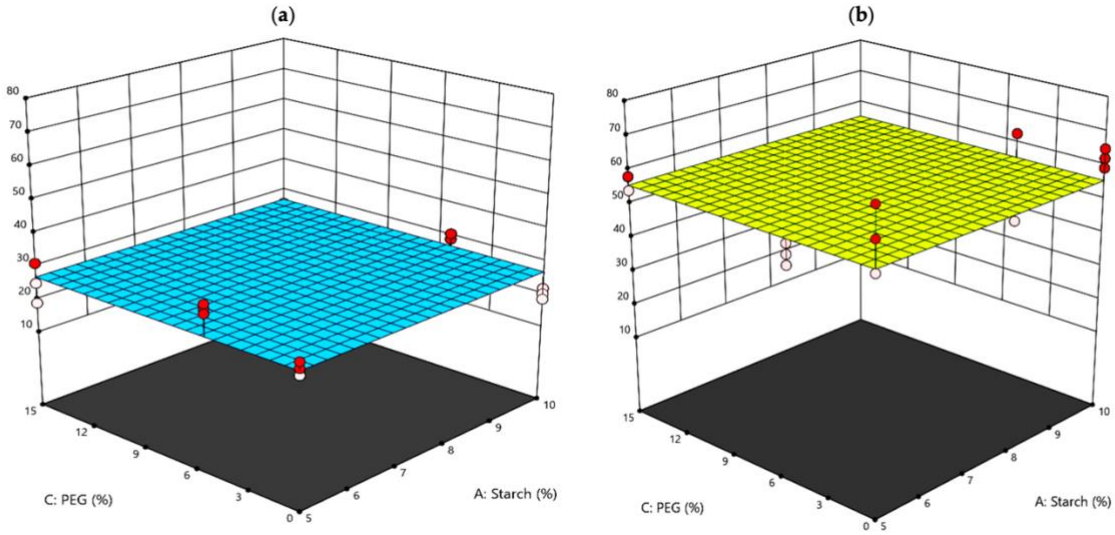

Figure 4.6. Response surface graphs of the tensile strength XD property: (a) AGAR = YES; (b) AGAR = NO.

The test of tear propagation was carried out following the indications in ASTM D1938 – 19. This method is employed to determine the force required to propagate a "tear" on plastic samples and very thin samples (1 mm thick or less) with a single tear method, so the greater the force needed, the more resistance the sample poses.
The following table (Table 4.9) shows the maximum mean values of stress required to propagate the shear in the experimental samples.
In green, the highest average "tear prop" values were highlighted, which seem to correspond to samples with coatings not containing agar: this observation is common to all three experimental SETs. In addition, the average "tear prop" value seems to be higher when PEG is present in the coating formulation for both percentages tested. For a better understanding of the data, Figure 4.7 shows the curves recorded on the universal testing machine during the shear propagation test for samples 2, 4, 8 and 12 (samples highlighted in orange in table 4.9).

Table 4.9. Mean Maximum Stress Values Required to Propagate Shear in Experimental Samples.

	N°	tear prop (Mpa)	STARCH 5%	STARCH 10%	AGAR 1.5%	GLYCEROL	PEG 5%	PEG 15%
SET 1	1	0.216	X		X	X		
	2	0.215		X	X	X		
	3	0.302	X			X		
	4	0.379		X		X		
SET 2	5	0.215	X		X	X	X	
	6	0.174		X	X	X	X	
	7	0.504	X			X	X	
	8	0.498		X		X	X	
SET 3	9	0.205	X		X	X		X
	10	0.203		X	X	X		X
	11	0.187	X			X		X
	12	0.412		X		X		X

What is observed is that sample 2 of SET 1 (example of agar coating – blue curve) actually has lower tear propagation resistance values, representative of the average values recorded for similar samples of SET 2 and SET 3. Sample 4 (red curve) is part of the same SET 1, but no

agar is present in the coating formulation; samples 8 (green curve) of SET 2 and 12 (blue curve) of SET 3 show higher maximum mean values of "tear prop" and comparable with those of sample 4, due to the absence of agar in the coating formulation.

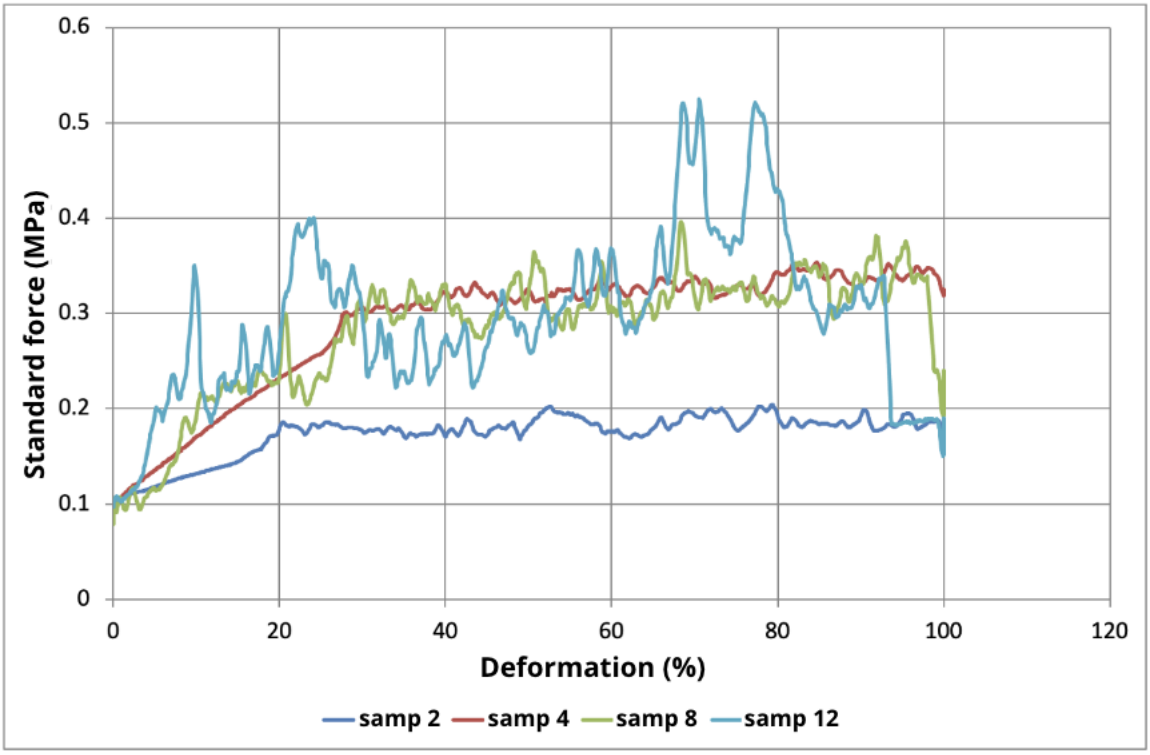

Figure 4.7. Shear propagation curves of experimental samples 2,4,8 and 12.

The curves relating to samples 2 and 4, although different for the stress values recorded, have a very similar trend to each other, with minimal variations in the values around an average value; on the contrary, the curves of samples 8 and 12 have a less regular pattern, with a greater variation around the mean value. This behavior could be explained by the presence of PEG in the coating formulation, at 5 and 15% respectively in samples 8 and 12. That is, samples with a plasticized coating appear to respond to stress by regularly alternating the rigid behavior of the carrier paper with the plastic behavior of the coating.

This last observation is confirmed by observing the final part of the tear propagation curves of the four selected samples (Figure 4.8).

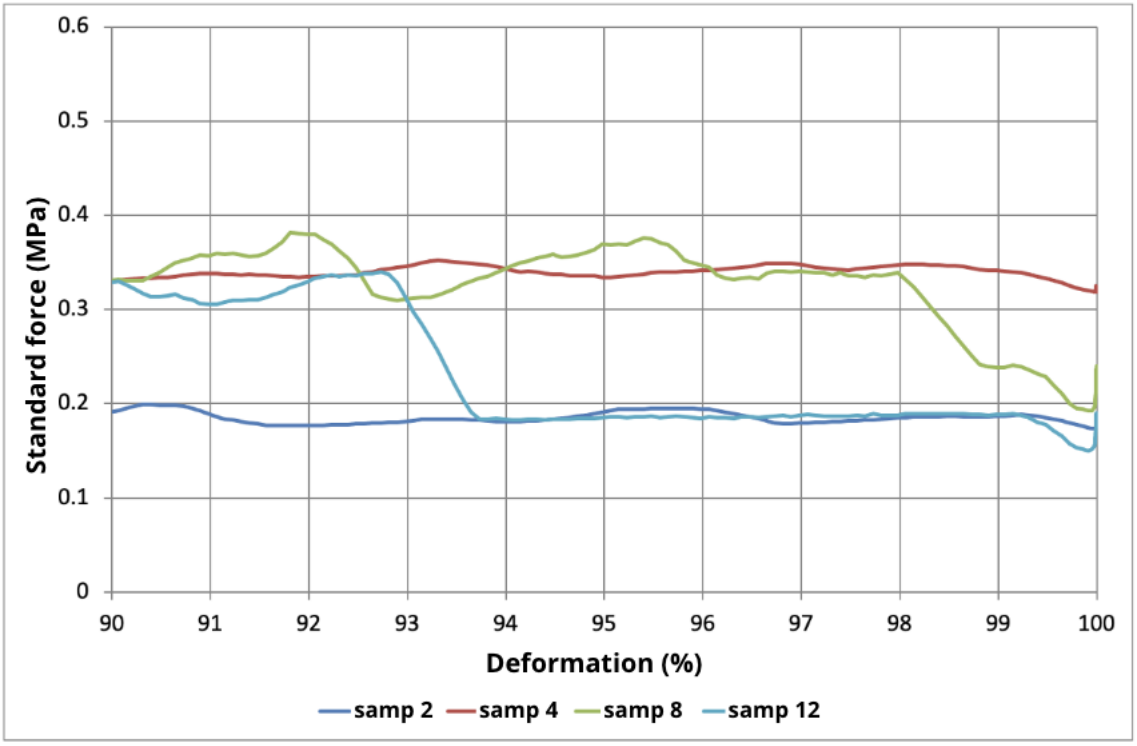

Figure 4.8. Tear propagation curves at the end of the test

While the curves of samples 2 and 4 maintain the maximum value of stress until the end of the test and stop abruptly, those of samples 8 and 12 see a decrease in effort, earlier in sample 12, characterized by the highest percentage of PEG in the coating formulation. This trend represents that of a rigid material coupled with a more flexible and plastic one: up to a certain point, the rigidity of the paper prevails, in this case, and then once the paper is broken, the effort required to lengthen the most plastic layer (coating) decreases and remains constant, but at a lower value until the material is completely broken.

4.4. Discussion

In this work, coatings to improve the properties of wrapping paper were formulated by mixing variable percentages of native starch, agar and PCL. Furthermore, in order to address the well-known issue of phase separation and weak interfacial adhesion in starch-agar/PCL blends, which is attributed to the lack of chemical affinity between these polymers, the incorporation of an interfacial agent or compatibilizer was explored. This represents a novel approach compared to previous studies in the literature (Singh et al., 2003). The coating formulations explored in this work have been evaluated for their ability to improve or modify some important characteristics of paper, such as wettability (by means the measure of oil and water CA), water vapor transmission rate, and resistance to grease. Concerning wettability, the results obtained measuring the oil and water contact angle demonstrate that the coating solutions do not decrease in a significant way the wettability of the coated paper in comparison with the values of CA measured on the control paper. In fact, regarding oil CA, the average value measured for the control paper is around 66°, in the region of high wettability, according to the "rules of 90° contact angle" (Hubbe et al., 2015) and the oil CA of all the three sets of coated samples remained below the critical value of 90°; in particular, the samples of SETs 1 and 2 registered oil CA values very close to those of the control paper, as in a previous work (Lo Faro et al., 2021). The samples of SET 3 showed an increase of the oil CA at values greater than 70°, demonstrating the beneficial effect of the simultaneous presence of starch (Ewender et al., 2013) and a high concentration of the hydrophilic plasticizers (PEG) in the formulation, able to improve the homogeneity of the coating (Singh et al., 2003). Considering the water CA, uncoated paper showed the higher values (120°) due probably to high smoothness of the calendered surface (Hubbe et al., 2015); in a previous work (Lo Faro et al., 2011), the same results have been obtained and justified by means the Cassie–Baxter model, which accounts for the contribution of the entrapping of air bubbles into the pores created by the cellulose fibers.

Instead, the relatively low water CA measured on all the coated samples can be explained by the non-homogeneous surface induced by the coatings, evident from the images in Fig. 4.3, despite their good spreadability and penetration ability. The WVTR of the coated samples decreased, but not significantly, and only for the SET 1 and SET 2 samples with respect to the average high value determined for the control paper (WVTR 5157 g m^{-2} day^{-1}, tropical conditions) despite its high-water CA. There does not seem to be a relationship between water CA and WVTR; in a previous work, for example, it was demonstrated that a commercial fluorinated paper had a very high value of WVTR (2825 g m^{-2} day^{-1}) but also a high value of water CA (around 135°), and a polyethylene coated paper had a low WVTR (72 g m^{-2} day^{-1}) and a low water CA (around 100°) (Lo Faro et al., 2011). If the grease resistance properties are concerned, the results obtained by the Kit Test demonstrated that all the coated samples reached a value higher than 8 despite their oil CA < 90°, confirming that a direct correlation between wettability and oil absorption and diffusion into the paper structure probably does not exist.

Taking into account all the previous results, a complete comparison of the obtained data has been reported through PCA and multivariate analysis in which a desirability function has been finally calculated. The optimal dimensionality of the PCA model, i.e., the number of PCs to consider, was defined using the screen plot, a graph that displays the percentage of variance explained by each PC. In this specific study, it was decided to consider two principal components, where PC1 describes 42.13% of the explained variance, while PC2 describes 25.81% of the explained variance. To fully interpret the results of the PCA model, it is necessary to combine the scores graph (Figure 4.9) with the loading graph (Figure 4.10). The scores graph allows one to evaluate the relationships between samples, while the loading graph allows for an evaluation of the relationships between output variables. In the score graph (Figure 4.9), we

can see a clear separation of two groups of samples mainly along PC2, namely, the agar-coated group in red (having PC2 positive values), the group without agar in green (with negative PC2 values), and the control samples, represented in blue, clearly separated from the other samples along PC1. It can therefore be stated that PC1 mainly distinguishes between the control samples and the coated paper samples prepared in this study, while PC2 allows for distinguishing between the samples covered with agar and the samples without agar. Comparing the graph of scores with that of loads (Figure 4.10), we can also see that the samples with agar, positioned at positive values of PC2, show high values of thickness and high levels of CA OIL (0 s, 15 s, and 30 s), as they are variables with positive loading values along PC2, indicating that agar has a more positive influence on these responses, especially in oil resistance. The addition of starch, as also demonstrated by Hormoz et al. (Hormoz et al., 2023), even at its lowest level (5% w/w PCL dry weight), is fundamental for this property as it has a relevant influence on the CA measured with oil. The improvement of the grease resistance by the introduction of starch is also demonstrated by the test kit results; all the samples recorded a kit value greater than 8. Samples with any result number higher than 8 are considered grease resistant; similar results were obtained also from Nair et al. (Nair et al.; 2022), and the introduction of starch to obtain the paper coating in their samples led to a marked improvement in oil resistance, with Kit 12 values exceeding 7.

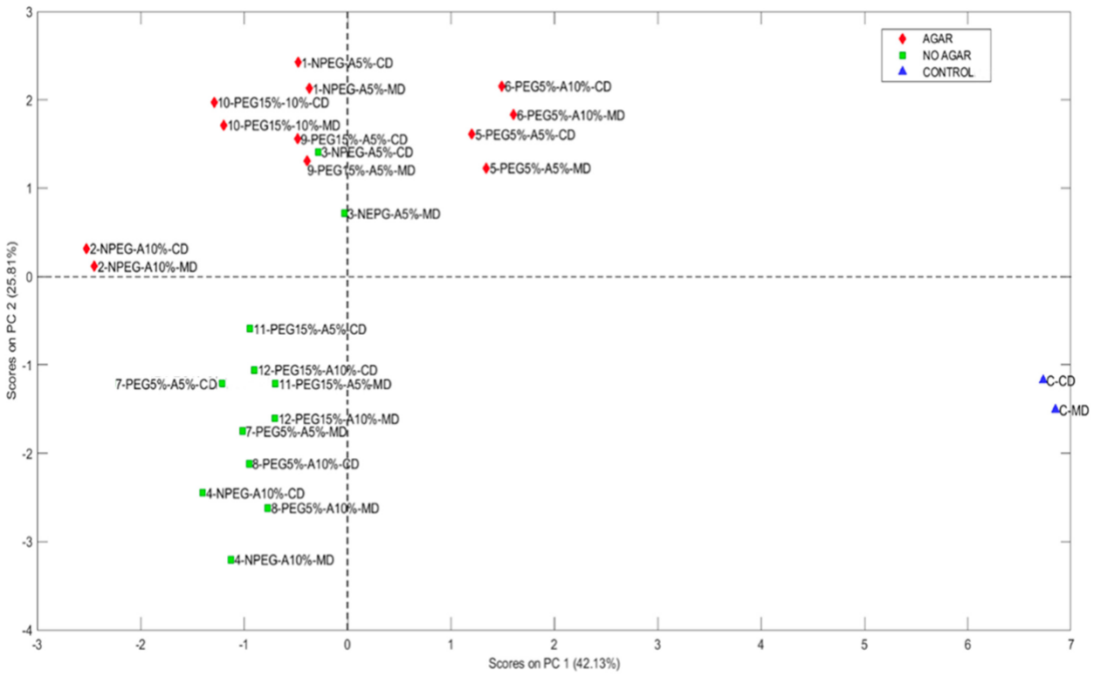

Figure 4.9. Scores of the PCA analysis.

In addition, agar presence in combination with PEG has been shown to play a beneficial key role in improving oil resistance and decreasing water vapor transmission rate. Similar results were obtained by Amariei et al. (Amariei et al., 2022), nevertheless, causing a significant detriment to the mechanical properties.

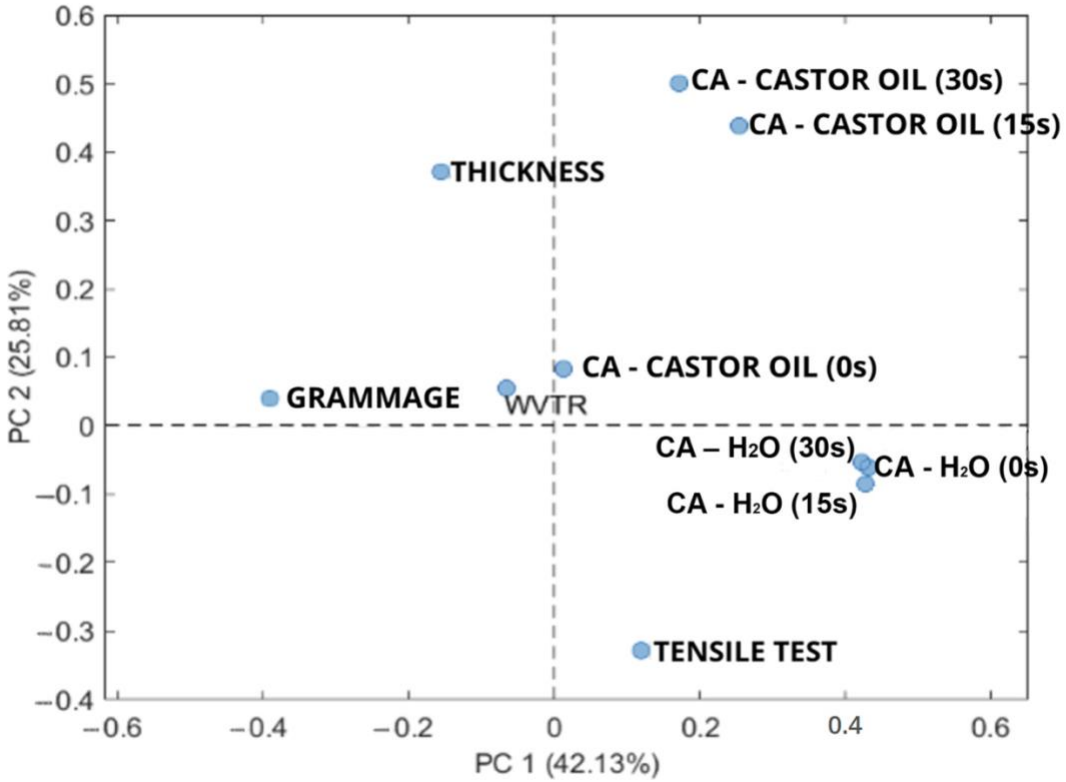

Figure 4.10. Loading plot of the PCA analysis.

Furthermore, the tensile strength and thickness variables are inversely related to each other, as we can see in the load graph PC1 and PC2. Therefore, at greater coating thickness, lower values of tensile strength are observed. Finally, grammage is inversely related to the water CA value (CA-H_2O 0 s, 15 s, 30 s), thereafter indicating that some restrictions on the coating formulation must be applied to balance these two responses. For this reason, it is necessary to calculate the best coating formulation to satisfy all the output variables through a desirability function as explained in Section 4.2.4. In fact, with the desirability function, we can take in consideration the synergic effect among variables and calculate the optimum conditions of work which in this case is the best coating formulation. The results of the calculation of this function are graphically shown in Figure 4.5, where the graphs are reported for the two conditions: with and without agar, respectively; see Figure 4.5e,f. It is possible to see the condition with the higher desirability regarding the formulations with agar (Figure 4.5e) showing desirability over 0.5. More in depth, the calculated best coating formulation is 10% w/w PCL dry weight starch, 1.5% w/w PCL dry weight agar, and 15% w/w PCL dry weight PEG, showing that all the compounds investigated in this study are relevant to produce the more promising coating for packaging paper.

4.5. Conclusions

In the present research, a quantitative calculation of the best performing paper coating for food-wrapping applications has been investigated. Given the growing interest from the food-packaging scientific community in imparting desirable barrier properties to paper (Yokoyama et al., 2007), agar, PEG and starch, in combination with PCL and glycerol dissolved in water, showed highly functional potential as a polymer matrix for film-coating formation. The application of a design of experiments approach allowed investigating the influence of environment-friendly plasticizer and cross-linking agents on the physical properties of paper coating in a systematic way by clearly identifying composition regions where the formation of a well-balanced coating is promoted and where a synergetic effect can be observed between agar, PEG, and starch. The best coating composition has been calculated, and it is 10% w/w PCL dry weight of starch, 1.5% w/w PCL dry weight of agar, and 15% w/w PCL dry weight of PEG. However, improvements should be made (in terms of new further mixture components) to overcome mechanical property depletion and to achieve a trend comparable to uncoated paper. In addition, further studies regarding degradation mechanisms related to this type of coating should be addressed to evaluate their performance over time and at the end of their life. This study confirms that a well-balanced combination of biopolymers, also from natural origins, could be used to obtain bioplastic coating suitable for the functionalization of paper for food packaging in a circular economy perspective.

Chapter 5

Improvement of paper wrapping resistance against moisture and oil by the formulation of coatings with Poly(3-hydroxybutyrate-co-3-hydroxyhexanoate) (PHBH) or Poly-Butylene Succinate (PBS) and Cutin

Chapter 5: Improvement of paper wrapping resistance against moisture and oil by the formulation of coatings with Poly(3-hydroxybutyrate-co-3-hydroxyhexanoate) (PHBH) or Poly-Butylene Succinate (PBS) and Cutin

5.1. Introduction

The primary objective of this study goes beyond enhancing the properties of paper, as previous research has already addressed that aspect. Instead, our aim is to improve its end-of-life characteristics, as not all solutions documented in the literature ensure complete biodegradability and suitable end-of-life outcomes for paper. We seek to address this gap by leveraging two topics of current interest: the utilization of by-products from the food industry and the exclusive use of polymers classified as biodegradable. Specifically, we intend to harness cutin, which can be extracted from tomato seed and peel waste. This approach is motivated by the fact that a medium-sized plant, processing 110,000 quintals of fresh tomatoes in a season, generates approximately 2,000-2,500 quintals of by-products (equivalent to 1.8-2.3% of production) in the form of skins and seeds. These by-products serve as suitable substrates for extracting cutin.

Cutin possesses several desirable properties, including excellent film-forming capabilities, and its chemical structure composed of long chains of C16 and C18 fatty acids imparts superior resistance to water vapor and other attributes (Simões et al., 2023; Hood et al., 2021; Dominguez et al., 2011).

Cutin has found various applications in the field of packaging and food packaging since its initial use as a bio-lacquer for coating metal food packaging by Cigognini et al. (2015). Subsequently, researchers have explored different approaches utilizing cutin in combination with other materials. For instance, Tedeschi et al. (2018) combined cutin with sodium alginate and beeswax to produce a self-supporting hydrophobic film. This innovative approach demonstrated the potential of cutin in creating films that repel water effectively.

Another study conducted by Manrich et al. (2017) focused on developing a water-resistant plastic casing by incorporating cutin with pectin. The resulting plastic casing exhibited enhanced resistance to water, making it suitable for packaging applications where moisture protection is crucial. Additionally, Marc et al. (2021) explored the use of cutin in fabricating hydrophobic elastomers. By incorporating cutin into the elastomer formulation, they achieved materials with excellent water repellency properties. These hydrophobic elastomers hold promise for various packaging applications where resistance to water is desired.

Collectively, these studies highlight the valuable potential of cutin in the field of packaging. The versatility of cutin, when combined with different materials, offers opportunities to develop new and improved packaging solutions with enhanced hydrophobic and water-resistant properties.

In the realm of biodegradable polymers, there are various options and numerous solutions available today, such as PHBH (Poly(3-hydroxybutyrate-co-3-hydroxyhexanoate)) or PBS (Polybutylene succinate). These polymers originate from different sources yet share the common trait of being biodegradable.

Poly(butylene succinate) (PBS) is another aliphatic polyester produced by condensation polymerization of succinic acid and 1,4 butanediol. PBS can be derived entirely from bio-based sources, using bio-derived succinic acid and 1,4 butanediol (Liminana et al., 2018). Thunber and Curtzwiler (2020) investigated the potential of PBS as a sustainable alternative to conventional non-eco-friendly coatings for paper. PBS demonstrated resistance to oil migration at elevated temperatures and compostability properties, making it an environmentally friendly option.

PHBH (polyhydroxy butyrate hexanoate) is a copolymer belonging to the family of polyhydroxyalkanoates (PHA), biodegradable polyesters synthesized in the cellular structure of various microorganisms. Thanks to their biodegradability, compostability and their origin, PHAs have gradually become a valid alternative to the common polyolefins used in the packaging industry and, in particular, among all PHAs, PHBH has emerged as one of the most versatile polymers, thanks above all to its thermal stability and good flexibility and hardness (Eraslan et al, 2022).
In this study, coatings for food grade paper were created to improve moisture and grease resistance characteristics. The formulated coatings were divided into two sets, one consisting of solutions with chloroform solubilization of PHBH and cutin, the other consisting of coatings made with ethyl-acetate solubilization of PBS polymer and cutin. Some solutions involved the addition of the plasticizer glycerol, and the addition of cutin took place in variable percentages (0 – 60 – 100 $w/w_{polymer}$). The coatings on paper were made using an automatic bar coating and with the use of a metal bar, the coatings were made in single layer or double layer.
The coated paper samples were then characterized by recording weight and thickness, the characteristics of resistance to greases and oils were evaluated using the Kit 12 test method; the WVTR and its decrease due to the presence of coatings was verified, in addition, the angle of contact with the use of water and castor oil, the latter being the basic ingredient for the formulation of the solutions used in the test kit12, was measured.

5.2. Materials and Methods

5.2.1. Materials

In this work, a calendered bleached paper (Advantage MG White High Gloss, Mondi Group, Addlestone, UK) was used, gently supplied by Serchio Distribuzione (Roma, Italy) (see Table 5.1 for technical data). According to the technical sheet, the paper is obtained from a long-fiber sulphate pulp. Polybutylene succinate (PBS) and polyhydroxybutyrate-hexanoate (PHBH) were purchased from MAIP Group (Torino, Italy) and technical data showed in Table 5.2. and Table 5.3, respectively. Cutin was supplied from TomaPaint (Borgo Girolamo Cantelli, Parma, Italy). Ethyl acetate (Ethyl acetate—ACS reagent, purity > 99.5%, Mw: 88.11 g/mol) and glycerol (1,2,3-Propanetriol, Glycerin, purity > 99.5%, Mw: 92.09 g/mol) were purchased from Sigma Aldrich (Taufkirchen, Germany). Chloroform, used as a solvent, was supplied by the Merck (Darmstadt, Germania), it occurs as a colorless, highly volatile and toxic liquid, with a purity ≥ 99.5% and a molecular weight of 119.38 g/mol.

Table 5.1. Technical data of paper used for the experimental work.

Properties		Test Method		Values
Basis Weight	g/m^2	ISO 536		35
Tensile Strength	kN/m	ISO 1924-3	MD CD	3,5 1,5
Tear Strength	mN	ISO 1974	MD CD	280 420
Burst Strength	kPa	ISO 2758		165
Air resistance (Gurley)	S	ISO 5636-5		28
Cobb-60'' MG Side	g/m^2	ISO 535		21
Gloss	%	TAPPI 480 om-99		26
Brightness	%	ISO 2470		82
Opacity	%	ISO 2471		55
Thickness	µm	ISO 534		48

Table 5.2. Technical data of polybutylene succinate (PBS)

Properties		Test Method	Unit	Values
Density		ISO 1183	g/cm^3	1.2
MFR (190°C, 2.16 kg)		ISO 1133	g/10 min	4
Melting Point		ISO 3146	°C	84
Tensile Modulus	MD	ISO 527	MPa	280
	TD			320
Yield Stress	MD	ISO 528	MPa	18
	TD			17
Stress at Break	MD	ISO 529	MPa	32
	TD			27
Strain at Break	MD	ISO 530	%	600
	TD			580
Elmendorf tear strengrh	MD	ISO 6383	N/mm	2
	TD			5
Puncture Impact		PTTMCC method	kJ/m	6

Table 5.3. Technical sheet of polyhydroxybutyrate-hexanoate (PHBH).

Properties		Test Method	Values
Density	g/cm^3	ISO 1183	1.2
Humidity Permeability	g-mm/m^2-day-atm	JIS Z0208	5
Oxygen Permeability	cm^2-mm/m^2-day-atm	JIS K7126	5
Melt Flow Index	g/10 min (at 165°C, 5kg)	ISO 113	3
Carbon Dioxide Permeability	cm^2-mm/m-day-atm	JIS K7126	19
Melting Point	°C		145
Heat Deflection Temperature	°C	ISO 75	107
Glass Transition Temperature	°C		2
Flexural Modulus	MPa	ISO 178	1650
Tensile Elongation	%	ISO 527	4
Tensile Modulus	MPa	ISO 527	1820
Tensile Strength	M/Pa	ISO 527	36
Tear Strength	N/mm	ISO 6383-2	3
Haze	%	ISO 14782	45

5.2.2. Coating Preparations

The initial preparation of the coatings, as shown in Table 5.4, involved dividing the samples into SET1 (samples with PHBH polymer in the formulation) and SET2 (samples with PBS polymer in the formulation). The polymers were solubilized in their respective solvents: chloroform for PHBH and ethyl acetate for PBS, at a concentration of 10% w/v. Only one sample containing PBS in the formulation was solubilized in chloroform, as indicated in Table

5.4. The solvents were heated to temperatures of 60 °C for chloroform and 80 °C for ethyl acetate. Then, the corresponding polymer was added to each solvent. The solutions were continuously agitated using a system equipped with a fallout chiller for solvent recovery. Once the polymers were completely solubilized, the required amounts of PEG and cutin were added to each solution according to Table 5.4.
Paper sheets measuring 210 × 297 mm were coated with the different solutions in either a single or double layer. This was achieved using a bar coating method with a Compact AB3650 (TQC Sheen) automatic film applicator, all performed under a fume hood using the layer-by-layer technique. The film applicator ensured a nominal coating thickness of 100 µm, and the application speed was set at 50 mm/s. After the application of each layer, the paper samples were dried under a fume hood for approximately 30 minutes to remove the solvent, then dried in an oven at 80°C for 1 hour. Subsequently, the samples were left at room temperature for 24 hours before testing.

Table 5.4. Coating formulations and codification of samples from the first and second set.

SET 1

Polymer	Code	Solvent	Glycerol (%w/wPHBH)	Cutin (%w/wPHBH)	Layer
PHBH	PHs	Chloroform	0	/	single
PHBH	PHGs	Chloroform	5	/	single
PHBH	PHG6s	Chloroform	5	60	single
PHBH	PHG6d	Chloroform	5	60	double
PHBH	PH1d	Chloroform	0	100	double

SET 2

Polymer	Code	Solvent	Glycerol (%w/wPBS)	Cutin (%w/wPBS)	Layer
PBS	PBs	Ethyl Acetate	0	/	single
PBS	PBGs	Ethyl Acetate	5	/	single
PBS	PBG6s	Ethyl Acetate	5	60	single
PBS	PBG6d	Ethyl Acetate	5	60	double
PBS	PB1d	Chloroform	0	100	double

5.2.3. Characterizations

5.2.3.1. Grammage and Thickness Determination

The grammage was calculated according to the method described in par. 3.2.2.3.
The thickness determination was carried out follow the method described in par. 4.2.3.1.

5.2.3.2. Water Vapor Transmission Rate (WVTR)

The WVTR value was determinate according to the method described in the par. 3.2.2.5.

5.2.3.3. Grease Resistance Determination

The grease resistance was determinate follow the procedure described in par. 4.2.3.4.

5.2.3.4. Contact Angle Determination

Contact angle (CA) values with water and oil were measured according to the method described in par. 4.2.3.3.

5.2.3.5. Statistical Analysis

For all samples, the mean and standard deviation was calculated. In addition, the data were treated with a multi-factor analysis (ANOVA) and the HSD Tukey test by the use of STATISTICA software.

5.3. Results and Discussion

5.3.1. Grammages and Thickness Determination

Referring to Table 5.5, let's analyze the weight of paper samples coated with PHBH-based coatings. It is evident that the UCP sample (uncoated paper) has a lower weight, as expected due to the absence of any coating. Now, focusing on the PHs (45.6 g/m^2), PHGs (41.0 g/m^2), and PHG6s (44.4 g/m^2) samples, we can observe that the presence of the coating increases their weight compared to uncoated paper. However, there are no significant differences between these three samples, as indicated by their similarities and confirmed by the Tukey test.
On the other hand, the PHG6d and PH1d samples show a different pattern compared to the other samples in the same set. They have weights of 52.3 g/m^2 and 66.3 g/m^2, respectively. This difference can be attributed not only to the increased percentage of cutin in the PH1d sample but also to the fact that these two samples have a double layer of coating instead of just one, like the other samples in the set.

Table 5.5. Mean values with standard deviation of the data collected for grammage measurement of samples from SET1 and SET2. Results of multifactorial ANOVA are reported as F-values and lowercase letters. Different letters identify significantly different samples.

SET 1			**SET 2**		
Sample	**average (g/m2)**	**dev.std**	**Sample**	**average (g/m2)**	**dev.std**
UCP	32.4 ±	2.95 **d**	UCP	32.4 ±	2.95 **c**
PHs	45.6 ±	2.32 **bc**	PBs	42.2 ±	2.82 **bc**
PHGs	41.0 ±	1.80 **c**	PBGs	41.9 ±	3.35 **c**
PHG6s	44.4 ±	2.55 **bd**	PBG6s	45.3 ±	3.77 **bc**
PHG6d	52.3 ±	2.12 **b**	PBG6d	55.6 ±	3.69 **ab**
PH1d	66.3 ±	5.12 **a**	PB1d	68.9 ±	3.52 **a**
pvalue			**pvalue**		
Glycerol		n.s.	Glycerol		n.s.
Cutin		2.E-02	Cutin		2.E-02
Layer		n.s.	Layer		n.s.

Based on the ANOVA statistical test, the only significant difference among the SET1 samples regarding the weight parameter appears to be the percentage of cutin. This difference is particularly pronounced in the last SET1 samples. Similarly, for the samples in SET2, the factor that significantly influences the weight difference between the samples is the cutin content. The uncoated paper in SET2 (table 5.5) has a lower weight compared to the other samples in the set, which are coated with solutions containing the PBS polymer.
The samples with a single layer of coating in SET2 exhibit similarities, as supported by Tukey's statistical test. The last two samples in SET2, which have a double coating, stand out from the rest with weights of 55.6 g/m^2 and 68.9 g/m^2, respectively. The higher weight in the latter sample can be attributed to its coating formulation containing 100% w/w PBS of cutin, compared to 60% in the other samples. Therefore, the increased weight is likely due to this factor.
In terms of evaluating the thickness of the SET1 samples, as shown in Table 5.6, we can categorize the samples into four distinct groups based on statistical differences. The group

marked with the letter "c" in the Tukey statistical test consists of samples with a single layer of coating, regardless of the formulation. On the other hand, we have separate groups with no similarity between them: the base paper sample (d), the sample with 60% cutin and a double layer (b), which is statistically different from its counterpart with a single layer, and finally, the paper samples with a double layer of coating (a), obtained from solutions containing 100% cutin and without glycerol.
In the case of the samples with a double layer and the absence of glycerol, the absence of glycerol might have influenced the spreadability and diffusion of the coating in the paper's pores, resulting in a higher presence of the solution on the surface and recording a greater average thickness. It is worth noting that this sample also had the highest weight value among all the samples (Table 5.5). In the ANOVA test for the SET1 samples, all the factors considered are significant, but the "Layer" factor carries more weight in statistically differentiating the data.

Table 5.6. Mean values with standard deviation of the data collected for thickness measurement of samples from SET1 and SET2. Results of multifactorial ANOVA are reported as F-values and lowercase letters. Different letters identify significantly different samples.

SET 1			**SET 2**		
Sample	**average (mm)**	**dev.std**	**Sample**	**average (mm)**	**dev.std**
UCP	0.040 ±	0.001 **d**	UCP	0.042 ±	0.001 **d**
PHs	0.047 ±	0.002 **c**	PBs	0.057 ±	0.006 **bc**
PHGs	0.049 ±	0.001 **c**	PBGs	0.055 ±	0.005 **c**
PHG6s	0.045 ±	0.003 **c**	PBG6s	0.067 ±	0.004 **bc**
PHG6d	0.060 ±	0.001 **b**	PBG6d	0.086 ±	0.005 **a**
PH1d	0.068 ±	0.003 **a**	PB1d	0.069 ±	0.005 **b**
pvalue			**pvalue**		
Glycerol		4.E-02	Glycerol		n.s.
Cutin		4.E-03	Cutin		n.s.
Layer		1.E-07	Layer		4.E-03

Moving on to the determination of the thickness of the SET2 samples, as shown in Table 5.6, most of the samples have thickness values consistent with expectations. All the samples exhibit greater thickness compared to the control sample, which is derived from the addition of polymers on the surface. Another noteworthy observation from Table 5.6 is that the two type of double-layer samples (PBG6d and PB1d) have the greatest thickness, as expected due to their double coating.
However, there is an unexpected reversal when comparing SET1 and SET2. In SET1, the sample with 100% cutin had the greatest thickness, but in SET2, the PBG6d sample has a thickness of 0.086 mm, while the PB1d sample has a thickness of 0.069 mm. The difference between the two series is attributed to the use of solvents, with chloroform used in PB1d and ethyl acetate used in PBG6d. The use of chloroform, which seems to be a better dispersing phase for the biopolymer and possibly cutin, resulted to improve in spreadability of the coating on paper also facilitated its penetration into the sheet's structure, leading to a seemingly lower coating thickness.

By comparing the single layer with 60% cutin (PBG6s) and the double layer (PBG6d), it is possible to calculate the difference in thickness between the two samples, which gives us the thickness of the single layer of polymer (0.017 mm). Additionally, the use of glycerol in the PBGs sample compared to the PBs sample does not appear to increase the thickness. This observation is supported by the analysis of the ANOVA, where glycerol, along with cutin, does not seem to be a significant factor influencing thickness.

5.3.2. Water vapor transmission rate (WVTR)

The WVTR is a measurement that indicates the amount of water vapor that can permeate per unit area of the packaging material (square meter), in 24 hours and under defined conditions of temperature and relative humidity – driving force (Song., et al., 2014); increasing the hydrophobic properties of cardboard packaging can improve the water vapor barrier properties (Aulin et al., 2013). This characteristic, together with other diffusional properties, is of considerable importance in the development of packaging materials. In the case of the paper samples we considered, the WVTR represents a measure of the interactions that water vapor establishes with cellulosic fibers, from which low or decreased values of WVTR mean the obtaining of cellulosic materials less similar to moisture.

Table 5.7. Mean values with standard deviation of the data collected for WVTR values of samples from SET1 and SET2 Results of multifactorial ANOVA are reported as F-values and lowercase letters. Different letters identify significantly different samples.

SET 1			SET 2		
Sample	**average (g/24h*m2)**	**dev.std**	**Sample**	**average (g/24h*m2)**	**dev.std**
UCP	3761 ± 65	**a**	UCP	3761 ± 65	**a**
PHs	3241 ± 35	**b**	PBs	3669 ± 116	**a**
PHGs	3271 ± 107	**b**	PBGs	3761 ± 93	**a**
PHG6s	2752 ± 144	**c**	PBG6s	3638 ± 140	**a**
PHG6d	1834 ± 278	**d**	PBG6d	3057 ± 215	**b**
PH1d	673 ± 93	**f**	PB1d	917 ± 70	**c**
pvalue			**pvalue**		
Glycerol	n.s.		Glycerol	n.s.	
Cutin	2.E-06		Cutin	1.E-09	
Layer	4.E-04		Layer	1.E-04	

Analyzing the data from Table 5.7 for SET1, which pertains to samples with a coating formulated using the PHBH polymer, we can observe a reduction in WVTR (water vapor transmission rate) compared to the control sample (UCP) with a value of 3761 g/24h*m². Starting from the sample identified as PHs, which contains only 10% PHBH, the WVTR value decreases to 3241 g/24h*m². Another notable observation from Table 5.7 is that the PHGs sample, composed of polymer and glycerol dissolved in chloroform, has a WVTR value statistically equal to the PHs sample, which contains only PHBH solubilized in chloroform. This suggests that the presence of glycerol does not negatively affect the WVTR value. This observation is supported by the statistical analysis of ANOVA, which indicates that glycerol is not a significant factor in WVTR value. In fact, due to its hydrophilic nature and the presence of three hydroxyl groups, glycerol could facilitate the diffusion of water vapor through the paper's cellulose cavities.
However, a significant decrease in WVTR value is observed in samples containing cutin. This is evident in the PHG6s sample, which has a WVTR value of 2752 g/24h*m² and consists of a

single layer with 60% cutin and the addition of glycerol. The WVTR value decreases further in samples coded as PHG6d, which have a double layer of coating. The presence of the second layer appears to improve the closure of the paper's pores, resulting in a further reduction in WVTR value. This reduction is even more drastic in the PH1d sample, which has a WVTR value of 673 g/24h*m². This sample does not contain glycerol in the formulation and consists of 10% PHBH, 100% cutin (based on the weight of PHBH), and a double-coated structure.
Thus, considering the overall values and the statistical differences highlighted by the Tukey test, it is evident that the presence of PHBH alone leads to a decrease in WVTR value, which is not influenced by the presence of glycerol (PHGs). The value decreases further with the addition of cutin (PHG6s) and the application of a double layer of coating on the paper (PHG6d), the lowering of water vapor permeation due to the presence of cutin has also been verified by Schreiber and Schonher (2009), showing that the low water permeance value shown by cutin is comparable with that of conventional plastics and cellulose derivatives. The best result is achieved with the formulation containing 10% PHBH mixed with 100% cutin based on the weight of PHBH, and a double-coated structure, resulting in an 82% reduction in WVTR value compared to the base paper, as shown in Figure 5.1.

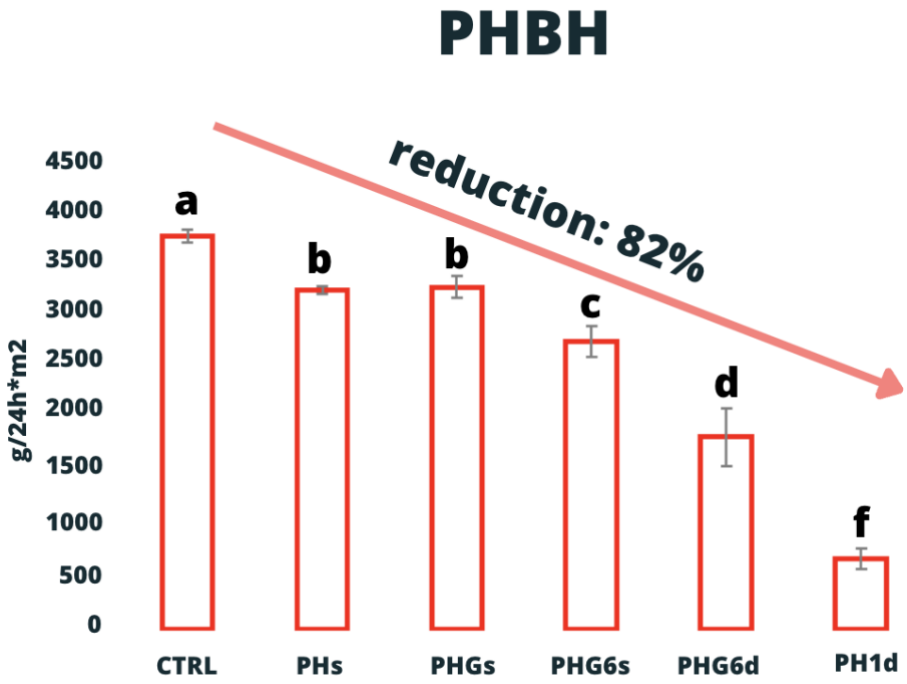

Figure 5.1. WVTR values of samples with PHBH in the coating formulation and % of reduction of water vapor transmission rate value.

Examining Figure 5.2, which presents the paper samples coated with PBS formulations, the situation differs from SET1 samples. The statistical evaluation of the Tukey test (Table 5.7) reveals that the first three coated paper samples (PBs, PBGs, and PBG6s) do not exhibit significant differences between them. The significant differences compared to the control sample occur with the PBG6d sample, which has a double coating and a WVTR value of 3057 g/24h*m², compared to the control's value of 3761 g/24h*m². The presence of the double-layer polymer explains this behavior, leading to a decrease in water vapor transmission.
Finally, the PB1d sample shows a drastic decrease in WVTR value, reaching 917 g/24h*m². This phenomenon can be attributed to the change in solvent used for solubilizing PBS. As explained earlier in section 5.3.1, the use of chloroform as a dispersing phase for the biopolymer and possibly cutin results in decreased viscosity of the final solution. This

improvement in spreadability of the coating on paper facilitates its penetration into the sheet's structure, likely leading to better closure of the paper's pores and achieving a 76% reduction in WVTR value compared to the control.

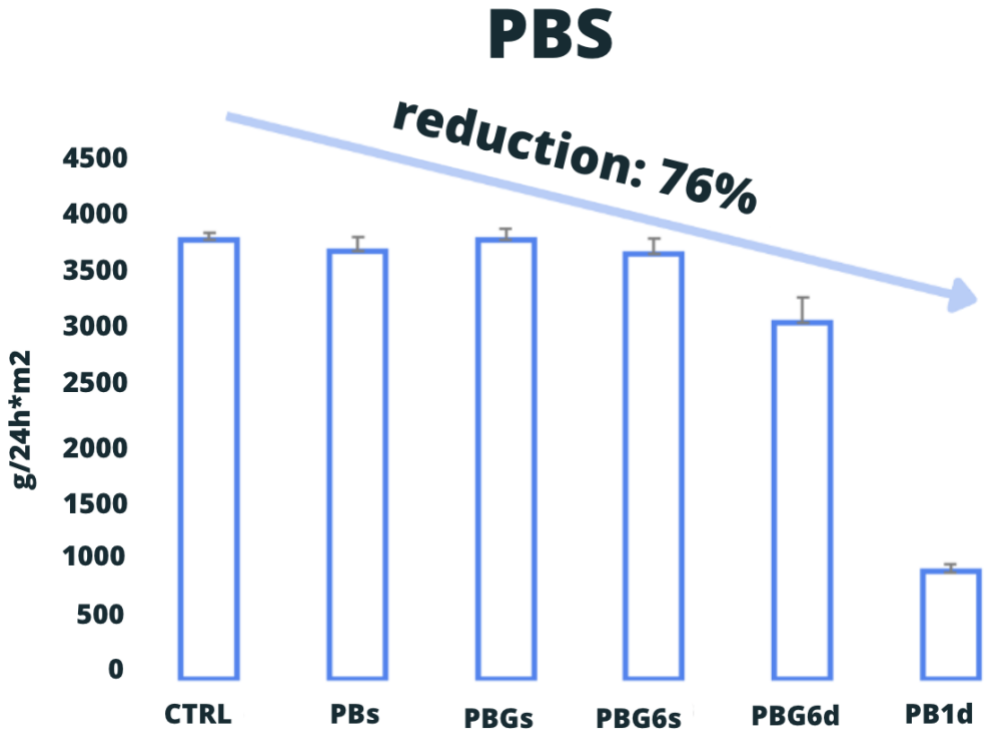

Figure 5.2. WVTR values of samples with PBS in the coating formulation and % of reduction of water vapor transmission rate value.

5.3.3. Grease resistance value

The 'Kit 12' test is used to assess the grease resistance of paper samples. Samples achieving a value of at least 8 are considered oil-resistant. Examining Figure 5.3, we observe an increase in grease resistance starting from the PHs sample. However, it is with the PHG6s sample, the first sample containing cutin in its coating formulation, that the cci value approaches the number of kits required for oil resistance. Although statistically similar to the PHs sample according to the Tukey test, which consists only of PHBH and chloroform, the PHG6s sample shows the initial improvement in the barrier against oils and fats.
The subsequent samples, PHG6d and PH1d, demonstrate a significant enhancement in grease resistance. This improvement is primarily attributed to the presence of a bilayer of cutin, which is statistically significant according to the ANOVA test (Table 5.8) for enhancing this property. In the PH1d sample, which has a double layer of coating with 100% cutin based on the polymer's weight, the grease resistance surpasses the threshold value of 8. Remarkably, the

PH1d sample achieves the maximum value among the tested solutions of the kit, indicating its ability to withstand all 12 solutions of the test.

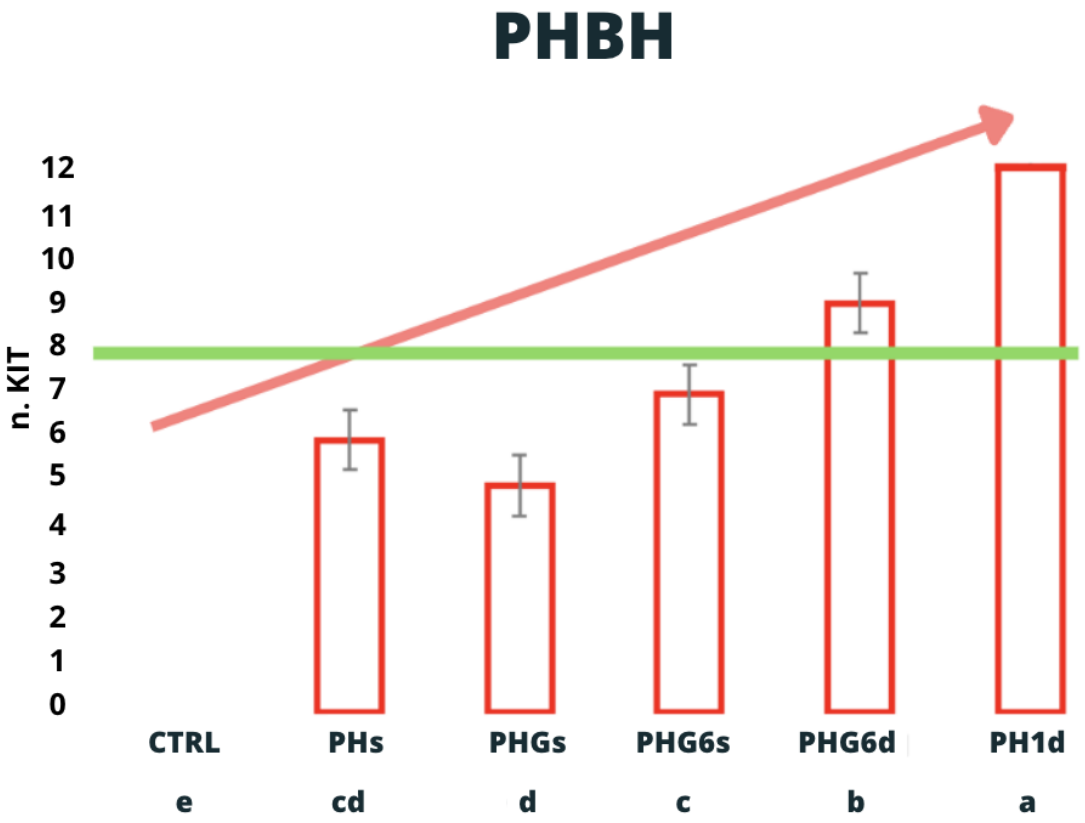

Figure 5.3. Value of Kit 12 test of samples with PHBH in the coating formulation.

Table 5.8. Results of multifactorial ANOVA are reported as F-values and lowercase letters. Different letters identify significantly different samples.

SET 1	
pvalue	
Glycerol	n.s.
Cutin	5.E-02
Layer	n.s.

Turning to Figure 5.4, which presents data on grease resistance of paper samples formulated with PBS coatings, we observe that the control sample (UCP) obtains a value of 0, indicating immediate failure as the recognition halo forms with solution number 1, similar to SET2 samples. The other samples in SET2, solubilized in Ethyl Acetate, obtain very low values below the threshold of 8. This is likely because the solvent used for solubilizing PBS and cutin does not adequately penetrate the paper's pores. However, the situation changes with the PB1d sample, which achieves the maximum value (PB1d = 12), indicating optimal grease repellency well above the value of 8. The use of chloroform as a solvent for polymer solubilization in the PB1d sample allows for optimal distribution of the coating solution within the paper's pores,

effectively occluding them and making oil absorption and diffusion through the cellulose material highly challenging or non-existent. In addition, the presence of cutin and the double layer of coating were fundamental for the improvement of the oil resistance characteristic, as also evidenced by the ANOVA test (Table 5.9.), in which the presence of the cutin and the number of layers were found to be statistically significant.

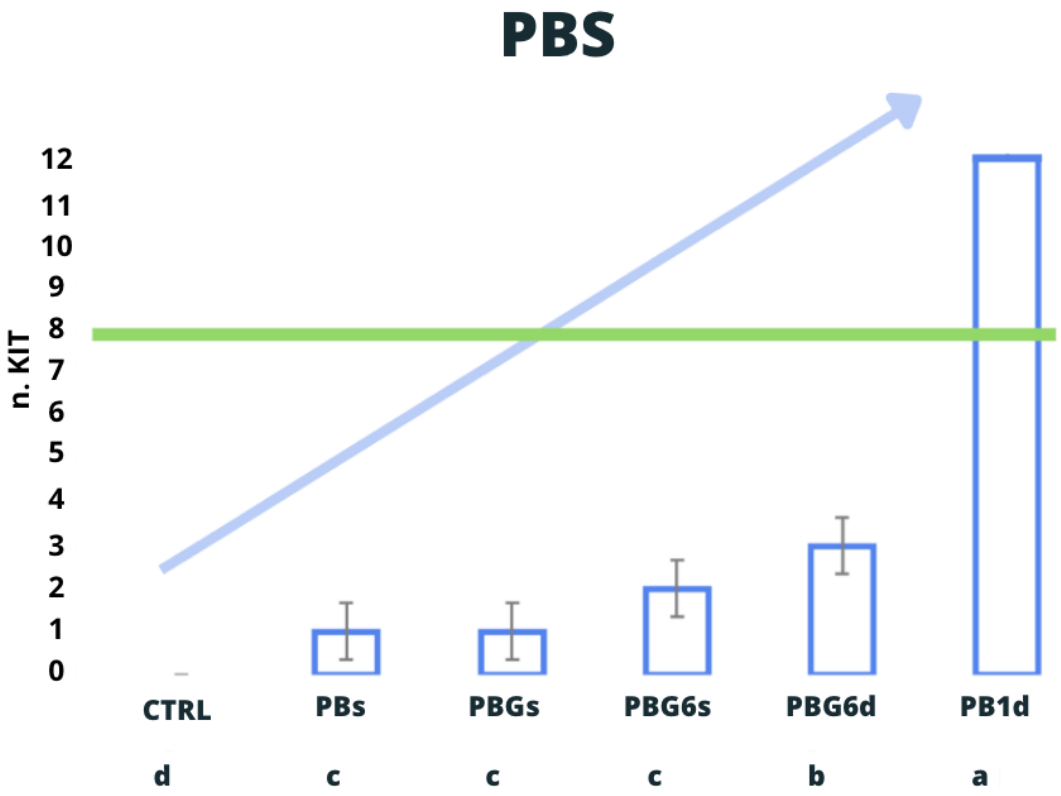

Figure 5.4. Value of Kit 12 test of samples with PHBH in the coating formulation.

Table 5.9. Results of multifactorial ANOVA are reported as F-values and lowercase letters. Different letters identify significantly different samples.

SET 2	
pvalue	
Glycerol	n.s.
Cutin	1.E-09
Layer	2.E-02

5.3.4. Contact angle measurement

The contact angle is a measure of the ratio between the liquid/gas interface and the solid surface. Generally, a surface is considered hydrophobic or oleophobic when the liquid droplet forms an angle greater than 90°, while it is considered hydrophilic or oleophilic if the angle formed is less than 90°.

Examining the water/paper contact angle values of the SET1 samples in Table 5.10, we observe that values close to or greater than 90° were obtained with the base paper samples (90.26 ± 5.8) and the samples coded as PHG6s (92.75 ± 2.7), PHG6d (87.53 ± 3.5), and PH1d (94.37 ± 3.8), all of which contain cutin (60% or 100%). The ANOVA test (Table 5.10) confirms that factors such as cutin and layer are statistically significant in determining the water contact angle, in fact the absence of glycerol and the presence of cutin improves the value of the contact angle, also reported by Heredia-Guerrero et al. (2009) and Manrich et al. (2017), cutin shows a low interaction with water molecules. The only sample that significantly differs from the others, including the control, is the PHs sample. In this case, the base paper is coated with a solution containing only the solubilized polymer, which is insufficient to improve the hydrophilicity of the base paper.

For the measurement of the contact angle with oil, castor oil was used, as it serves as the basis for the solutions used in the kit 12 test, which evaluates the oil repellency of paper and cardboard samples.
It is evident from Table 5.10 that all the SET1 samples, including the base paper, recorded contact angles below 90°, indicating very low oleo-repellency. However, the situation improves when glycerol (10%) is introduced into the PHBH formulation. Glycerol, being highly hydrophilic, contributes to enhancing the oleo-repellent characteristics of the coating layer while still maintaining contact angles below 90°. This phenomenon is also supported by the ANOVA analysis (Table 5.10), which identifies glycerol as a significant factor in improving the contact angle measurement with castor oil.
The situation undergoes further changes when cutin is added to the PHBH coatings, with or without glycerol. Cutin, composed of long chains of fatty acids, can interact with the fat component, negatively impacting the contact angle measurement with oil. Consequently, the contact angles obtained with these samples closely resemble those of the control paper.

Table 5.10. Mean values with standard deviation of the data collected for CA values with water or oil of samples from SET1. Results of multifactorial ANOVA are reported as F-values and lowercase letters. Different letters identify significantly different samples.

SET 1

	CA - water		**CA - oil**	
Sample	**CA (°)**	**dev.std**	**CA (°)**	**dev.std**
UCP	90.26 ±	5.73 **ab**	47.2 ±	6.21 **bc**
PHs	84.23 ±	9.07 **c**	51.05 ±	5.09 **bc**
PHGs	87.71 ±	4.78 **bc**	59.25 ±	9.38 **a**
PHG6s	92.75 ±	2.64 **a**	46.65 ±	4.27 **bc**
PHG6d	87.53 ±	3.52 **bc**	45.56 ±	3.75 **c**
PH1d	94.37 ±	3.82 **a**	52.64 ±	4.04 **bc**

pvalue - water		**pvalue - oil**	
Glycerol	n.s.	Glycerol	4.E-05
Cutin	3.E-06	Cutin	1.E-06
Layer	4.E-03	Layer	n.s.

Upon examining the water contact angle values for the SET2 samples (Table 5.11), it is evident that all experimental samples exhibit values close to or exceeding 90°C. The base paper (UCP)

has a contact angle of 90.26°, while PBs, PBGs, PBG6s, PBG6d, and PB1d samples have contact angles of 108.24°, 90.11°, 126.3°, 120.51°, and 88.82°, respectively. These values indicate a high hydrophobicity of the surface. Among the samples, PBG6s demonstrates the highest contact angle value (126.3°). This can be attributed to the presence of cutin (60%), a highly hydrophobic lipid substance dissolved in ethyl acetate, which, in synergy with glycerol (5%), enhances the repellent properties of the sample. A similar observation applies to the PBG6d sample, which also exhibits an excellent contact angle value (120.51°). The only difference is that the PBG6d sample has a double coating. The Tukey test confirms the similarity between the two samples, as they are both marked with the letter 'a'. The ANOVA test further supports the synergistic effect of the glycerol/cutin mixture, assigning high statistical significance to cutin and lower but still significant significance to glycerol.
However, the situation is different for the PB1d sample. Despite having a higher concentration of cutin (100% compared to 60%) and the absence of glycerol (a hydrophilic plasticizer), it exhibits the lowest contact angle value among all observed samples. This is because chloroform, instead of ethyl acetate, was used as a solvent in the production of the PB1d sample. Chloroform has a stronger diluting power and allows the solution to penetrate deeper into the paper, causing a loss of surface hydrophobicity.

Turning to the oil contact angle values in Table 5.11, it can be observed that PBS used individually as a coating (PBs) and with the addition of 5% glycerol (PBGs) have no positive effect on oil repellency. The values remain almost identical to that of the control (UCP). This is because PBs and glycerol do not possess lipid-repellent properties. However, when they come into contact with cutin, as seen in the PBG6s sample, there is an improvement in repellent properties resulting from the combined and synergistic action of the various components. The PBG6s sample achieves the best contact angle value (62.26° ± 12.08°) due to the synergy between PBS, glycerol, and cutin. As for the PB1d sample, the measured value is similar to that of the initial samples (44.95°). This is likely due to the PB1d sample being solubilized in chloroform, which allows for better penetration of the solution into the paper's pores but leads to a loss of surface properties.

Table 5.11. Mean values with standard deviation of the data collected for CA values with water or oil of samples from SET2. Results of multifactorial ANOVA are reported as F-values and lowercase letters. Different letters identify significantly different samples.

SET 2

	CA - water		CA - oil	
Sample	**CA (°)**	**dev.std**	**CA (°)**	**dev.std**
UCP	90.26 ±	5.73 **c**	47.2 ±	6.21 **b**
PBs	108.24 ±	17.07 **b**	47.32 ±	9.00 **b**
PBGs	90.11 ±	8.28 **c**	44.63 ±	6.41 **b**
PBG6s	126.30 ±	7.72 **a**	62.26 ±	12.08 **a**
PBG6d	120.51 ±	5.08 **a**	65.91 ±	2.76 **a**
PB1d	88.82 ±	3.54 **c**	44.95 ±	4.20 **b**
pvalue - water		**pvalue - oil**		
Glycerol	1.E-03	Glycerol	n.s.	
Cutin	1.E-09	Cutin	1.E-09	
Layer	n.s.	Layer	n.s.	

5.4. Conclusions

The objective of this work was to enhance the hydrophobic and oil-repellent properties of food papers commonly used in retail settings, with the goal of replacing traditional plastic polymers like HDPE, PP, and PE. To achieve this, formulations consisting of biodegradable polymers, PHBH or PBS, and cutin were employed to create coatings that could improve the characteristics of the base paper. The coatings were applied using the bar coating technique, and the resulting samples underwent various analyses.

Regarding the SET1 samples, which involved the formulation of coatings based on PHBH, the focus was on reducing the water vapor diffusion capacity of the experimental samples through the application of the coating. This was achieved by incorporating cutin, which resulted in an 82% reduction in the water vapor transmission rate (WVTR) compared to the base paper. Additionally, the double-layer configuration proved to be the most significant factor in improving the water vapor barrier property. This decrease in WVTR aligns with the findings of Song et al. (2014), which highlight that increasing the hydrophobic portion of the coating leads to optimal moisture barrier values. The recorded thickness values, as measured by a micrometer, are consistent with this work, as greater thicknesses correlate with improved water barrier properties. This observation is supported by both this experimental study and the research of Song et al. (2014).

Concerning the measurement of the contact angle with water, the best results were consistently obtained with samples coated with formulations containing cutin. It is important to note that the contact angle values indicate good water repellency, as they are equal to or greater than 90°. In terms of oil repellency tests, coatings containing cutin exhibited excellent resistance to oils and greases. This can be inferred from the results of Kit 12, where the samples with cutin demonstrated the highest oleoresistance values, reaching a maximum value of 12. However, when it comes to the contact angle measurement with castor oil, the results did not indicate good oil repellency for the samples with cutin. Regarding the SET2 samples, which involved the formulation of coatings based on PBS, most of the formulations were prepared by dissolving ethyl acetate polymers. However, one sample containing PBS with 100% weight/weight (w/w) cutin was solubilized in chloroform. This was done to assess how different solvents could impact the performance of the coatings obtained.

In terms of WVTR evaluation, it was observed that the coating made with PBS and 100% w/w cutin resulted in a significant reduction in water vapor transmission compared to untreated paper. The average value decreased from 3671 g/24h*m² to 917 g/24h*m², respectively. This outcome can be attributed to the fact that this particular sample (PB1d) had a double coating, consisting exclusively of PBS and cutin solubilized in chloroform. The use of chloroform as a solvent facilitated better penetration of the solution into the paper's pores, effectively sealing them and slowing down the passage of water vapor. Consequently, differences were also observed in the thickness and weight values of the samples. The sample solubilized in chloroform (PB1d) exhibited lower thickness and greater weight compared to the samples solubilized in ethyl acetate. This was due to the enhanced spreadability and penetration of the solution on the paper's surface.

Regarding the measurement of contact angle, there was an improvement in the hydrophobic properties, particularly in the single and double coated films with 60% cutin (PBG6s) and (PBG6d). The presence of cutin and its interaction with glycerol and PBS contributed to this enhancement. However, the contact angle and kit 12 tests did not yield the expected results in terms of oil repellency. Only two types of samples (PBG6s and PBG6d) exhibited acceptable contact angle values, which resulted from the synergy between the various components (cutin, PBS, and glycerol). The kit 12 tests produced different outcomes, with only the PB1d sample

demonstrating adequate oleo-repellency, recording a value of 12. This once again emphasizes how the choice of solvent influences the coating's performance.

In conclusion, this work demonstrates the valuable potential of cutin in the field of packaging. The versatility of cutin, when combined with different materials, provides the opportunity to develop new and improved food packaging solutions with improved hydrophobic and water-resistant properties.

Chapter 6

Introduction of the Zn^{2+}-MA complex to polyvinyl alcohol (PVA) as an antimicrobial packaging film for coating

Chapter 6: Introduction of the Zn^{2+}-MA complex to polyvinyl alcohol (PVA) as an antimicrobial packaging film for coating

6.1. Introduction

In past years, there has been extensive research on metal-ligand complexes and their potential applications in various fields. These applications include drug delivery (Renfrew, 2014; Lainé et al., 2012), sensory systems (Wang et al., 1997), stabilizers (Smirnov et al. 1970), semiconductors (Ehrend et al., 1974), and self-healing polymeric hydrogels (Hui et al., 2013). Metal-ligand interactions provide materials with unique functions associated with the metal ions. As a result, the interest in using metal-ligand complexes for antimicrobial applications has been steadily increasing.

Metal-ligand complexes can serve as complex antimicrobial systems, exhibiting three-dimensional morphologies that enhance their antimicrobial efficacy against microbes. The diverse geometries of these complexes help prevent microbial resistance to biocidal agents (Hosny et al., 2013; Santos et al., 2014). This diversification of antimicrobial potency against microbes is attributed to the 3D morphology of the metal-ligand complex, which contributes to its effectiveness.

By utilizing metal-ligand interactions, materials can acquire special functions associated with the metal ion, which is why the use of metal-ligand complexes for antimicrobial applications has gained significant attention. These complexes offer a variety of geometries, which helps counteract microbial resistance to biocidal agents. The exploration of metal-ligand complexes as antimicrobial systems is driven by the goal of diversifying antimicrobial potency and overcoming microbial resistance.

Anti-microbial packaging is the packaging system that can kill or inhibit spoilage and pathogenic microorganisms that are contaminating foods (Higazy et al., 2010; Joerger, 2007). Various antimicrobial systems are used in packaging to achieve this goal. For example, UV irradiation has been employed (Paik et al., 1998; Cohen et al. 1995; Tyuftin et al., 2020), as well as the direct incorporation of antimicrobial agents into polymeric materials (Khaneghah et al., 2018). Antimicrobial agents such as chitosan (Don et al., 2005; Sarasam et al., 2006; Zhang et al. 2020; Panda et al., 2022), organosulfur compounds from plants, essential oils, and synthetic molecules with antimicrobial activity have also been utilized.

The scientific community has shown increasing interest in antimicrobial packaging due to its ability to slow down the deterioration of food, extend shelf-life, and ensure the desired quality for a longer period (Tyuftin et al., 2020). This type of packaging falls under the category of active packaging, which aims to enhance the properties of existing polymers and introduce essential characteristics, such as the ability to kill or inhibit pathogenic microorganisms.

The motivation behind the growing interest in antimicrobial packaging technologies is the need to bring improved packaging systems to the market. These systems enhance the properties of existing polymers and provide fundamental characteristics required in the packaging industry, such as the ability to combat foodborne pathogens. By addressing these needs, antimicrobial packaging contributes to the preservation of food quality and safety, meeting the expectations of consumers.

Metal complexes of synthetic and natural polymers have been extensively studied by researchers, particularly in the clinical development of treatments for cancer, malaria, and neurodegenerative diseases (Hojo et al., 1974). However, their potential application as antimicrobial agents have received relatively little attention, despite ample evidence supporting their effectiveness (Frei et al., 2020). Moreover, metal ions' interaction with organic ligands has been shown to exhibit superior antimicrobial activity compared to the free, uncoordinated ligands (Santos et al., 2014). This is attributed to the three-dimensional morphology of the

metal-ligand complex, which can adopt a variety of geometries, in contrast to the one-dimensional or two-dimensional structures of conventional antimicrobial agents (Gianferrara et al., 2009).

In this study, a zinc-melamine complex (Zn^{2+}–melamine complex) was incorporated into polyvinyl alcohol (PVA) using epichlorohydrin (ECH) as an epoxide crosslinker. The introduction of the metal-ligand complex led to the functionalization of PVA, imparting it with potent antimicrobial properties. PVA, a hydrophilic and cost-effective polymer, is an excellent candidate as a solid support material. It can be transformed into a hydrogel through appropriate physical or chemical crosslinking. Numerous studies in the literature have demonstrated the successful binding of ECH to PVA, resulting in a support structure capable of accommodating metal complexes (Wan et al. 2004; Gauthier et al., 2004). PVA is widely used for the creation of complex and metal complexes due to its non-toxic nature, high crystallinity, water solubility, biocompatibility, and biodegradability (Hosny et al., 2013; Hojo et al., 1974; Hui et al., 2016). It possesses a significant number of hydroxyl (OH) groups in its backbone chains, which facilitate hydrogen bonding (Panda et al., 2022). The abundance of hydrogen bonding sites in PVA allows it to form strong interactions with molecules acting as crosslinkers, thereby serving as a bridge between PVA as the supporting structure and the metal-ligand complex.

In this study, melamine was chosen as the ligand. Melamine is a triazine heterocyclic compound that contains multiple nitrogen atoms in its structure. These nitrogen atoms play a crucial role in constructing organic metal structures. The aromatic ring of melamine, along with its coordination sites and amine groups, facilitates hydrogen bonding with metal ions, thereby strengthening the three-dimensional structure of the complex.

The presence of melamine in the PVA complex has additional benefits. It can enhance the thermal stability of PVA and, when combined with ECH, improve the mechanical properties of the material. For example, it can reduce the Young's modulus of PVA filaments, imparting greater elasticity and reducing brittleness (Song et al.; Ricciotti et al., 2013; Gauthier et al., 2004). Melamine has been extensively studied for its ability to bind transition metals. Several articles demonstrate how melamine readily coordinates with metal ions to form complexes that have been used for various purposes. For instance, melamine complexes have been utilized in the manufacturing of sponges with high oil absorption capacity and for oil/water separation. In these applications, the presence of the complex renders the sponge surface hydrophobic, enabling effective separation between oil and water (Gao et al., 2018). Additionally, melamine can act as a tridentate ligand towards silver ions, forming a material suitable for the selective removal of anionic contaminants from wastewater (Baraka et al., 2019).

In this scientific work the Zn^{2+}–melamine complex was introduced to polyvinyl alcohol (PVA) using epichlorohydrin (ECH) as an epoxide crosslinker. Accordingly, the PVA was first modified using ECH, followed by the interactions between PVA-ECH and melamine (MA). Subsequently, zinc ions were introduced to the PVA-ECH-MA to develop the metal-ligand complex in the PVA matrix. Films whit various contents of melamine were fabricated whit the film casting technic; the chemistry and structural properties of the metal-ligand complex film was assessed using FTIR and SEM-EDX, the thermal properties of the samples were verified by TGA, WVTR values were recorded, and mechanical properties checked; and finally, the antimicrobial properties of the metal-ligand complex film were evaluated against Staphylococcus aureus (*S. aureus*) and Escherichia coli (*E. coli*).

6.2. Materials and Methods

6.2.1. Materials

For the formulation of the metal-ligand complex films the following materials were used: commercial grade (F-17A) poly (vinyl alcohol) (PVA) with a degree of hydrolysis of 98.0–99.5 % and a molecular weight of 74,800 g/mol was purchased from OCI Co., Ltd. (Incheon, Korea); (±)-Epichlorohydrin, Zinc nitrate hexahydrate and melamine were purchased from Sigma-Aldrich (MO, USA); sodium hydroxide was obtained from Daejung. Escherichia coli (E. coli, DH5α) and Staphylococcus aureus (S. aureus, ATCC29213) were procured from the Korea Culture Center of Microorganisms (Seoul, South Korea). Deionized water (DI) was used throughout the experiments.

6.2.2. Preparation of metal-ligand complex films

To prepare the PVA-ECH solution, PVA (9%w/v) and Epichlorohydrin (ECH) (20%w/w_{PVA}) were mixed together in an alkaline environment using a stirrer. The alkaline ambient was created by adding NaOH (0.5 M) to the mixture. The stirring process took place at 90 °C and lasted for 24 hours.
After the 24-hour period, when the solution reached room temperature, the PVA-ECH solution was precipitated using acetone (v/v%). The precipitate was then collected and dried overnight at 60 °C to ensure complete dehydration.
Once the precipitate was completely dry, it was gently ground using a mortar and pestle, then it was mixed with an aqueous solution of melamine in varying percentages (2.5 – 5 – 10% w/w_{PVA}). The mixture was stirred for 24 hours at 90 °C.
Finally, Zn^{2+} (15% w/$w_{Melamine}$) was added to the mixture and stirred for 1 hour at room temperature.
Control solutions were also prepared for the experiment. The control solution included the following formulations:

- PVA (9% w/v) solution: A solution of polyvinyl alcohol (PVA) with a concentration of 9% by weight/volume.
- PVA (9% w/v) with Epichlorohydrin (20% w/wPVA): PVA solution containing Epichlorohydrin at a concentration of 20% by weight relative to PVA.
- PVA (9% w/v) with Epichlorohydrin (ECH) (20% w/wPVA) and Melamine (10% w/wPVA): PVA solution with Epichlorohydrin at a concentration of 20% by weight relative to PVA, along with the addition of Melamine at a concentration of 10% by weight relative to PVA.

For the microbiological tests, a specific sample, also, was formulated, which incorporated only zinc and not melamine into the formulation. This was achieved by adding a certain amount of zinc to the solution that was used in the PVA9E20MA10Zn15 sample. The different solutions (Table 6.1) were used to create the films by the use of an automatic film-coater (KIPAE E&T Co., Ltd., Hwasung, Korea) at the speed of 50mm/min and thickness set at 100 μm.

*Table 6.1. Codification of samples. *In the CTRL3 sample, the % of zinc added corresponds to the amount calculated on 10%w/wPVA of melamine.*

Code of Samples	*PVA (%w/v)*	*ECH (%w/wPVA)*	*MELAMINE (%w/wPVA)*	*ZINC (%w/wMelamine)*
PVA 9%	9		/	/
CTRL1 (PVA9ECH20)	9	20	/	/
CTRL2 (PVA9ECH20MA10)	9	20	10	/
CTRL3 (PVA9ECH20Zn15)	9	20	/	15*
PVA9E20MA2.5Zn15	9	20	2.5	15
PVA9E20MA5Zn15	9	20	5	15
PVA9E20MA10Zn15	9	20	10	15

6.2.3. Characterization

6.2.3.1. SEM-EDX

The surface morphologies of the composites were observed using field-emission scanning electron microscopy (SEM) (FESEM, JEOL-7800F, JEOL Ltd., Japan) at an acceleration voltage of 10 kV and a working distance of 10 mm. For the fractographic analysis of composites, all samples were cryo-fractured in the liquid nitrogen. Prior to the SEM analysis, all samples were coated with a thin layer of platinum. Energy dispersive X-ray spectroscopy (EDX) mapping (X-max N80 form Oxford instruments, UK) was used to further evaluate the microstructure of the composites using a distribution of elements.

6.2.3.2. ATR-FTIR analysis

The chemical structures of the samples were examined using a Fourier-transform infrared (FTIR) spectrometer from PerkinElmer, located in Waltham, MA, USA. The analysis was performed in the attenuated total reflection (ATR) mode.
To obtain the FTIR spectra, the samples were analyzed in the transmission mode (T) over a wavenumber range of 4000–400 cm^−1. During data collection, 32 scans were accumulated to enhance the signal-to-noise ratio and improve the accuracy of the results.
In order to establish a reference, air was used during the analysis. This reference allowed for the comparison and identification of specific functional groups and chemical bonds present in the samples.

The FTIR analysis provided valuable information about the chemical composition and molecular structures of the samples, enabling a detailed characterization of their chemical properties.

6.2.3.3. Thermogravimetric Analysis (TGA)

Thermogravimetric analysis (TGA) was employed to evaluate the thermal properties of the samples. The TGA measurements were conducted using a TGA 4000 instrument from PerkinElmer Inc., located in Waltham, MA, USA.
To investigate the thermal stability of the samples, approximately 10-11 mg of each sample was used. The analysis involved heating the samples from 30 °C to 800 °C at a constant rate of 10 °C per minute. Throughout the analysis, a continuous flow of nitrogen gas was supplied at a rate of 20 mL per minute to ensure purging.
The weight percentage of the samples was recorded as a function of temperature, and the data was used to generate graphs illustrating the TGA results. These graphs provided insights into the thermal behavior and stability of the samples as they underwent heating.

6.2.4. Mechanical Properties Tests

The mechanical performance of the films was evaluated using a universal testing machine (QM100T_C, Qmesys Co., Uiwang, South Korea) and according to ASTM D882 (ASTM D882-18, 2018). For each sample, 10 specimens (dimensions of 150 × 25 mm) were analyzed.

6.2.5. Antimicrobial Activity: Clear Zone Inhibition Test

The antibacterial activity of the film samples was assessed using the Kirby-Bauer test, also known as the disc diffusion method. The test involved determining the inhibition zone around the film samples when tested against *E. coli* and *S. aureus*.
To prepare for the test, a single colony of each microorganism was transferred to nutrient and tryptic soy broths and incubated at 37 °C for 24 hours. A portion of the microbial suspension was then evenly spread on nutrient agar using a cotton swab.
Next, the film samples were prepared by cutting them into 5 mm x 5 mm dimensions. Each sample was placed on the surface of the microbial culture, ensuring that the corresponding bacteria were previously spread in that area. The plates were then incubated at 37 °C for 24 hours.
The antimicrobial potency of the film samples was determined by measuring the diameter of the inhibition zone around each sample. This measurement represented the extent to which the film inhibited the growth of the bacteria and was reported in millimeters (mm). Additionally, a streptomycin disc (10 mg) was used as a positive control (PC) to compare the efficacy of the film samples against a known antimicrobial agent.

6.3. Results and Discussion

6.3.1. Scanning Electron Microscope (SEM) and Energy Dispersive Spectrometry (EDX)

The microstructural morphology of the films was examined using scanning electron microscopy (SEM) to observe the top surface. Additionally, elemental analysis of the top of the samples was conducted using energy-dispersive X-ray spectroscopy (EDS) mapping.
As depicted in Figure 6.1, the samples a1, b1, c1, and d exhibited distinct surface morphologies. Notably, sample a1 displayed a completely different structure compared to the other samples. In samples b1, c1, and d, which contained zinc-melamine, a significant change in morphology was observed, characterized by the formation of a pronounced three-dimensional structure.
This three-dimensional structure confirms the formation of a complex resulting from the interaction between melamine, which is connected to the PVA-ECH structure, and zinc. The formation of this complex is particularly evident in samples b1 and c1, highlighting the successful formation of the three-dimensional structure between the elements.
In sample D, which contained a higher concentration of melamine in the formulation, a greater abundance of complexes was observed. These complexes covered the surface and exhibited a prismatic shape with parallelogram bases, a characteristic structure previously described by Salah et al. (2023).

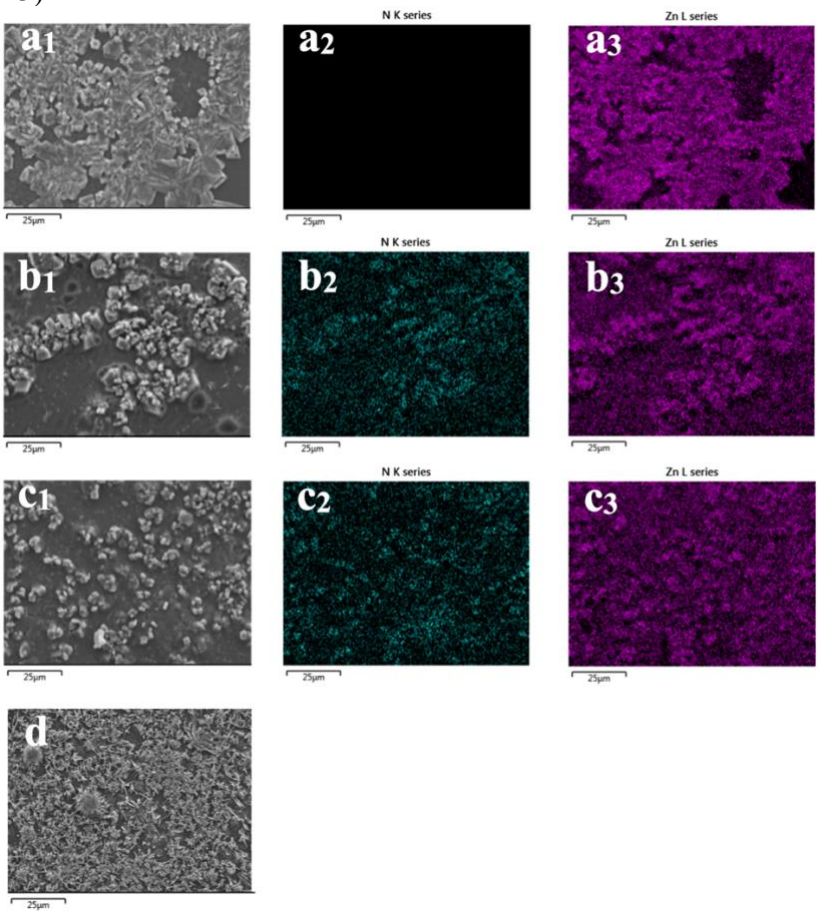

Figure 6.3. SEM micrographs illustrating the morphology of ***a₁*** *PVA9ECH20Zn15,* ***b₁*** *PVA9ECH20MA2.5Zn15,* ***c₁*** *PVA9ECH20MA5Zn15 and* ***d*** *PVA9ECH20MA10Zn15. EDS elemental analysis results showing the distribution of N (****a₂*** *PVA9ECH20Zn15,* ***b₂*** *PVA9ECH20MA2.5Zn15 and* ***c₂*** *PVA9ECH20MA5Zn15) and Zn (****a₃*** *PVA9ECH20Zn15,* ***b₃*** *PVA9ECH20MA2.5Zn15 and* ***c₃*** *PVA9ECH20MA5Zn15).*

Figure 6.1 presents the mapping images of all the samples, corresponding to their upper surfaces, obtained through EDX mapping analysis. The distribution models of nitrogen (N) and zinc (Zn) elements provide additional insights into the microstructural morphology of the samples.
In particular, sample a_2, which did not have melamine added to the initial solution, served as a control to evaluate the morphology and distribution of zinc in the absence of the melamine-zinc complex formation. Looking at Figure a_3, the pink color indicates the non-uniform distribution of zinc on the surface of the film. The black areas represent the absence of zinc and the lack of formation of the three-dimensional complex structure. This confirms the importance of melamine in the formation of the complex.
The situation changes when melamine is present in the samples. In the images of samples b_2 and c_2 (shown in green), the presence of melamine is evident, evenly distributed across the entire surface, forming protrusions that indicate the formation of the complex and its interaction with the PVA-ECH structure.
Furthermore, in Figures b_3 and c_3, the pink color represents the distribution of zinc, which covers the entire surface of the sample, similar to the distribution of melamine. This strongly suggests that zinc directly binds to melamine, completely covering the surface. This phenomenon was not observed in samples where melamine was absent, as depicted in Figure a_3.
The distribution of zinc over the entire surface of the film, forming a complex with melamine, is crucial for its antimicrobial action, as further explained in section 6.3.5.

To summarize:

- Melamine binds to the PVA-ECH structure and distributes itself evenly across the film's surface.
- In the absence of melamine, zinc is not uniformly distributed over the surface, and the three-dimensional structure is not as evident.
- In the presence of melamine, zinc binds to it and covers the entire film surface, which is essential for exerting its antimicrobial action.

These observations highlight the significance of the melamine-zinc complex formation and its distribution on the film's surface for achieving antimicrobial properties.

6.3.2. Fourier Transform Infrared (FT-IR)

In the figure 6.2.a, the neat PVA exhibits specific vibrational bands associated with its molecular structure (Gopinatha et al., 2023; Park et al, 2022; Kim at al., 2019). These vibrational bands and their corresponding wavenumbers are as follows in the figure 6.2.a, one of the prominent vibrational bands of PVA is the stretching vibration of the O-H bond, which occurs within the range of 3000–3750 cm^{-1}, this band signifies the presence of hydroxyl groups within the PVA molecule.
Additionally, PVA exhibits both asymmetric and symmetric stretching vibrations of the $-CH_2$ bond. The asymmetric stretching vibration occurs at a wavenumber of 2938 cm^{-1}, while the symmetric stretching vibration occurs at 2907 cm^{-1}. Another significant vibrational band is the symmetric stretching vibration of the C-O-C bond, observed at a wavenumber of 1653 cm^{-1}. Furthermore, PVA demonstrates a wagging vibration of a single -CH group, which can be detected at a wavenumber of 1430 cm^{-1}. Lastly, the stretching vibration of the C-OH bond occurs at a wavenumber of 1086 cm^{-1}.

The FTIR spectrum of melamine, as presented in Figure 6.2.b and discussed by Zhao et al. (2005) and Jawaid et al. (2013), provides valuable insights into the molecular structure and functional groups of this compound.
First all, in the spectrum is evident the band spanning from 3000 to 3650 cm^-1, which is attributed to the N-H stretching vibration modes. Then, a band is observed in the range of 1100 to 1650 cm^-1. This band corresponds to the stretching vibrations associated with the C-N bonds and is typically related to the skeletal stretching vibrations of the aromatic rings present in melamine. At 810 cm^-1, an absorption peak is observed, which characterizes the out-of-plane bending modes of the triazine ring in melamine. This specific absorption provides insights into the structural conformation and geometry of the triazine ring. Furthermore, the band ranging from 460 to 850 cm^-1 is linked to the C-NH_2 group and the ring breadth or bending vibration modes.

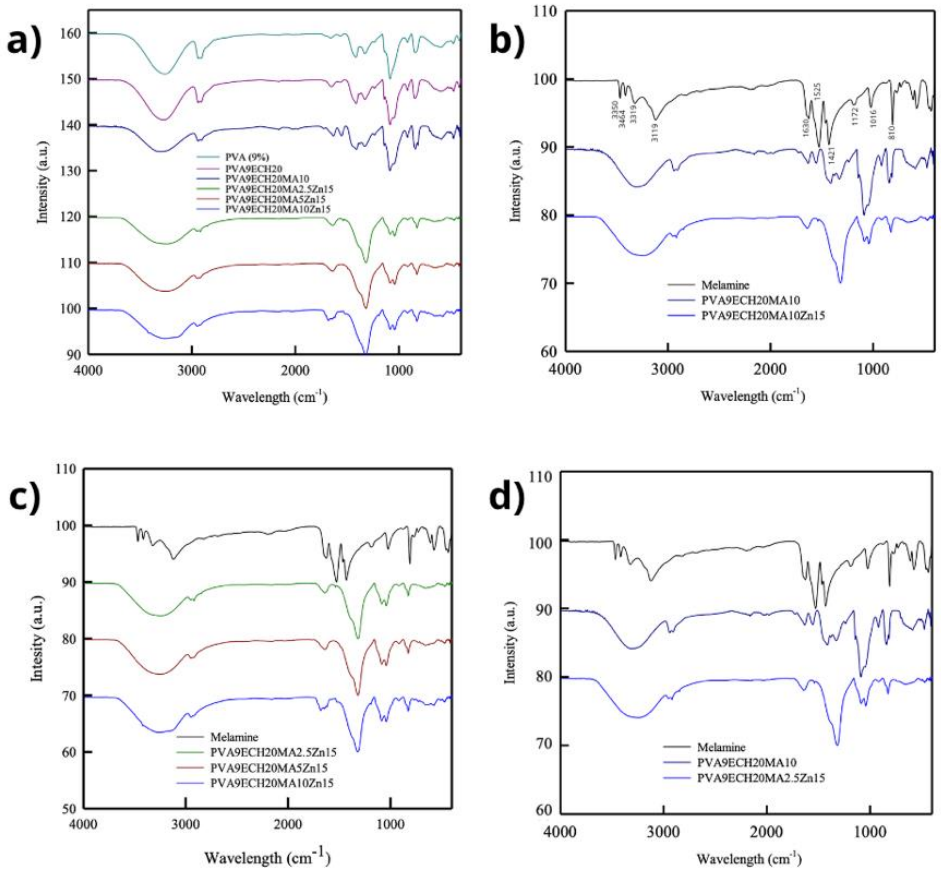

*Figure 6.4. FTIR spectra of **a** (all samples), **b** (Melamine, PVA9ECH20MA10, PVA9ECH20MA10Zn15), **c** (Melamine, PVA9ECH20MA2.5Zn15, PVA9ECH20MA5Zn1, PVA9ECH20MA10Zn15) and **d** (Melamine, PVA9ECH20MA10, PVA9ECH20MA2.5Zn15)*

The FTIR spectrometric analysis, depicted in Figure 6.2a, provides insights into the chemical changes occurring in PVA throughout the reaction steps. The absorption band in the range of 3000–3750 cm^-1, corresponding to the stretching vibration of the O-H bond, gradually decreases its absorption intensity. This decrease suggests the involvement of the O-H bond in the formation of the new chemical structure of the complex. Similarly, the peaks at wavenumbers of 2938 cm^-1 and 2907 cm^-1 also exhibit a decrease in absorption intensity, indicating further structural modifications of PVA following the ECH modification and binding to melamine. Additionally, the appearance of new peaks within the range of 1450 cm^-1 and

800 cm^-1 may be attributed to the interactions between zinc and melamine. These observations suggest the successful incorporation of Zn into the PVA-MA complex, as previously reported by Reddy et al. in 2019. Furthermore, the structural evaluation of the complex regarding the increase in melamine content is depicted in Figure 6.2.c. Interestingly, the absorption curves do not exhibit any noticeable changes as the percentage of melamine increases. This implies that from a structural perspective, the characteristics of the final complex remain unaffected by the quantity of melamine present, but it just impact by the presence of melamine.
In conclusion, the spectrometric analysis of the various samples confirms the formation of the complex, involving the binding of Zn and the establishment of a structure that imparts strong antimicrobial properties to the films, as discussed in paragraph 6.3.5.

6.3.3. Thermogravimetric analysis (TGA)

TGA was performed to identify the thermal stability of the film samples and the Fig. 6.3 shows the thermal decomposition. Thermal degradation of pure PVA generally occurs in three stages, as reported by Liu et al. (2018). In this case, the first step, which takes place in the range between 69 and 150 °C, for the removal of physically and chemically bonded water, is not very evident, this is probably due to the fact that the samples have been subjected to a strong drying cycle before analysis. The second stage occurred at around 230-400 °C due to side chain degradation, while the third step occurred at roughly 410-468 °C due to PVA polymer backbone breakage, steps two and three are prominently present.

The other samples can be divided into two groups with regard to their thermal stability:

- The samples that do not have zinc in the formulation (PVA9ECH20 and PVA9ECH20MA10), in these samples we observe a thermal degradation that occurs in several steps, after the first thermal decay around 230 °C up to 290 °C and the second up to about 400 °C, due to the decomposition of the PVA and melamine side chains, leading to a weight loss of 60% and 58% respectively. Finally, we observe the last step of thermal decomposition in the range between 410 and 500 °C, due to the decomposition of the main chains of PVA and melamine, as also observed by Bhat et al. (2020).

- Samples that have zinc in the formulation, these samples (PVA9ECH20MA2.5Zn15, PVA9ECH20MA5Zn15 and PVA9ECH20MA10Zn15) after an initial weight loss and then degradation in the temperature range ranging from 180 °C to 410 °C, undergo a slowdown until they reach a plateau, leading to an overall weight loss of around 60%, as also observed by Bharati et al. (2020).

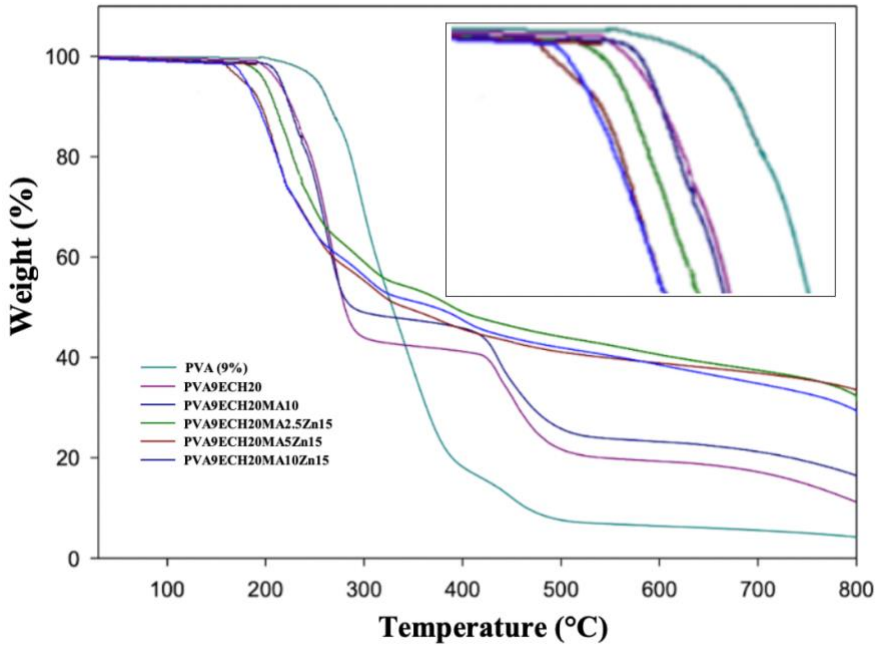

Figure 6.3. TGA spectra of film samples.

6.3.4. Mechanical Test

The mechanical properties of the samples were evaluated to understand how the modification of PVA with the introduction of the Zn-MA complex could affect its mechanical behavior. The results presented in Table 6.2 provide clear evidence of the significant impact of incorporating the crosslinker ECH on the mechanical characteristics of PVA, particularly the Young's modulus and elongation at break. Previous studies (Bai et al., 2010 and Gautam et al., 2022) have documented that the addition of ECH to PVA leads to the formation of a hydrogel, enhancing its deformability and elastic behavior.
Moreover, the presence of melamine in combination with ECH further enhances the mechanical properties of PVA. Specifically, it decreases the Young's modulus, making the PVA filaments more elastic and reducing their brittleness, as reported in studies by Song et al. (2013), Ricciotti et al. (2013), and Gauthier et al. (2004).
Furthermore, the introduction of zinc into the formulation and the subsequent formation of the complex result in a noticeable decrease in tensile strength and Young's modulus, accompanied by a significant increase in elongation at break. This behavior indicates a material that exhibits characteristics opposite to those of the initial PVA. Consequently, the material becomes less brittle and highly elastic.
Overall, the incorporation of the Zn-MA complex into PVA leads to a substantial improvement in the mechanical properties of the material, making it more flexible, elastic, and resistant to breaking.

Table 6.2. Mean values with standard deviation of the data collected for mechanical property values (tensile strength, elongation at break and Young's modulus).

Samples	*Tensile strength* (N/mm^2)	*Elongation at break* (%)	*Young's Modulus* (N/mm^2)
PVA (9%)	37.65±2.64	89.29±6.63	740.40±195.15
PVA9ECH20	26.97±6.28	195.43±16.04	86.00±9.41
PVA9ECH20MA10	26.41±1.54	183.55±14.90	12.00±0.37
PVA6E20MA2.5Zn15	8.63±0.88	303.72±26.76	2.58±0.76
PVA6E20MA5Zn15	6.78±0.87	289.53±2.29	2.29±0.11
PVA6E20MA10Zn15	7.49±2.34	338.67±14.54	2.51±0.26

6. 3.5. Antimicrobial Activity: Clear Zone Inhibition Test

The results of the antimicrobial activity of the samples are presented in Table 6.3. As expected, the pure PVA sample and all zinc-free film samples do not exhibit any antibacterial activity against the tested microorganisms, *E. coli* and *S. aureus*.

However, the situation changes when zinc is present in the film formulations. The antibacterial properties of zinc have been widely recognized by many researchers, although the exact mechanism of action is not fully understood. Various mechanisms have been proposed and summarized by Lallo da Silva et al. (2019), including the production of reactive oxygen species (ROS), disruption of cellular integrity through contact between Zn particles and the cell wall, release of Zn^{2+} ions, and internalization of Zn particles.

In the context of this study, the most plausible mechanism appears to be the disruption of cellular integrity through contact between Zn particles and the cell wall. Additionally, Stanković et al. (2013) demonstrated that the shape of zinc particles can influence their antibacterial activity. The particles synthesized with polyvinyl alcohol (PVA), which had a larger surface area, exhibited improved antibacterial activity, as like in this study. This characteristic resulted in significant antibacterial effects against both *S. aureus* and *E. coli*. Notably, the antimicrobial activity was more pronounced against *E. coli* due to its elongated cell shape, which allowed for greater contact with zinc particles. Table 6.3 clearly shows that all formulations have a higher antimicrobial activity against *E. coli*, with inhibition zone values greater than even the positive control (7.5±0.5 mm).

Table 6.3. Antibacterial performance of film samples against E. Coli and S. Aureus.

Code of Samples	*E. Coli*	*Staphylococcus Aureus*
PVA 9%	0	0
CTRL1 (PVA9ECH20)	0	0
CTRL2 (PVA9ECH20MA10)	0	0
CTRL3 (PVA9ECH20Zn15)	10±0.5	4.0±1
PVA9E20MA2.5Zn15	13.0±1	5.0±1
PVA9E20MA5Zn15	14.0±1	4.0±1
PVA9E20MA10Zn15	13.0±1	5.0±1
POSITIVE CONTROL	7.5±0.5	6.0±1

Another important observation is the enhanced antimicrobial activity against E. coli with the addition of melamine and the subsequent formation of the Zn-MA complex. In the presence of zinc alone, there is an inhibition zone of 10±0.5 mm. However, when the complex is formed, there is a noticeable increase in antimicrobial efficacy against *E. coli*, with inhibition zones reaching around 13/14±0.5 mm. The antimicrobial activity against *S. aureus*, although less pronounced, is still evident and depicted in Figure 6.4, approaching the performance of the positive control.

Overall, the findings demonstrate that the introduction of zinc and the formation of the Zn-MA complex with the 3-D structure in the film samples confer antimicrobial properties, particularly against *E. coli*. This highlights the potential of these modified PVA films for applications requiring antibacterial activity.

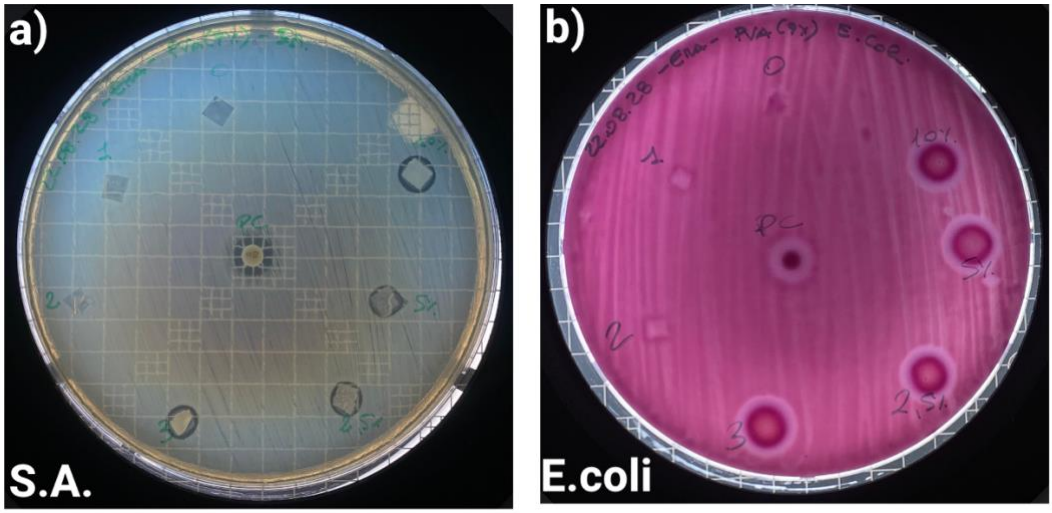

Figure 6.4. The inhibition zone around film samples against E. coli and S. aureus.

6.4 Conclusion

In this experimental study, the objective was to incorporate a Zn^{2+}-melamine complex into polyvinyl alcohol (PVA) using epichlorohydrin (ECH) as a crosslinker. The aim was to create PVA films that would possess a chemical structure capable of binding a three-dimensional metal complex containing zinc, known for its strong antimicrobial characteristics.
To verify the successful formation of the complex and the bonding between different molecules, FTIR analysis was conducted. The characteristic peaks of PVA and melamine were observed, and with the addition of zinc, these peaks changed, indicating the formation of a new chemical structure.
SEM images revealed that the three-dimensional structure was more pronounced in samples containing the zinc-melamine complex compared to those without melamine. Additionally, EDX images demonstrated that the presence of melamine was crucial for the uniform distribution of zinc across the surface, as areas without any zinc binding were evident in samples lacking melamine.
Thermogravimetric analysis indicated that the thermal resistance of the samples changed at each reaction step. Samples containing zinc exhibited a decrease in overall weight loss, around at 58-60%, which could be attributed to the presence of inorganic material, such as zinc.
The mechanical properties of the samples underwent significant improvements. PVA, on its own, displayed rigidity, brittleness, and lack of elasticity. However, the incorporation of the Zn-MA complex led to substantial enhancements in the mechanical properties of the material, resulting in increased flexibility, elasticity, and resistance to breakage.
Finally, antimicrobial tests conducted on the samples and control films against microorganisms such as E. coli and S. aureus demonstrated the successful achievement of the study's primary goal. The films exhibited strong antimicrobial activity, particularly against E. coli, with an inhibition area of approximately 13-14 mm, surpassing the positive control (7.5±0.5 mm). It was evident that zinc possessed antimicrobial properties, which were significantly enhanced by the formation of the complex with melamine.
Overall, the experimental work successfully achieved its objectives, yielding PVA films with a Zn-MA complex that displayed remarkable antimicrobial efficacy, particularly against *E. coli*.

Chapter 7

Comparison of the performance of packaging for fruits made from environmentally sustainable and renewable materials with non-biodegradable petroleum-based packaging

Chapter 7: Comparison of the performance of packaging for fruits made from environmentally sustainable and renewable materials with non-biodegradable petroleum-based packaging.

7.1. Introduction

In recent years, consumers have become increasingly conscious and mindful about the food they consume and the packaging it comes in. Two key aspects that garner attention are the origin and end-of-life of these containers. These topics have not only captured the interest of the scientific community (D. K. A. Barnes, 2009; Schwarz et al., 2019; Plastic Pollution in The Ocean – 2023 Facts and Statistics, 2022), but also the general public. The issue of plastic pollution has gained widespread coverage in various media platforms, including television, news outlets, and documentaries such as David Attenborough's "Blue Planet II." This documentary showcased the alarming presence of plastic littering beaches and the ocean floor, leaving viewers outraged (The Guardian, 2019).
In 2022, global plastic production has reached a staggering 400 million tons, with approximately 359.8 million tons originating from fossil-based materials, as reported by Plastics Europe (2023). A significant portion of plastic production is dedicated to food and beverage packaging, representing 39% in the EU. The shift from reusable containers to single-use ones has contributed to the surge in plastic production specifically designed for food packaging. Consequently, the proportion of plastics in municipal solid waste has increased substantially, rising from less than 1% in 1960 to over 10% by 2005 in middle- and high-income countries (Jambeck et al., 2015). Without significant changes in global plastic production and waste management practices, it is projected that a staggering 12 billion metric tons of plastic waste could end up in landfills or the environment by 2050 (Geyer et al., 2017).
The use of plastic in preserving fruits and vegetables, which have a short shelf life, is a major concern. The supply chain for these perishable food items, from farm to fork, is typically brief, lasting around ten days under optimal conditions. Moreover, studies by Stea et al. (2020) indicate a rising consumption of fruits and vegetables among highly educated women in Europe. The data from the Apofruit company aligns with the increasing market demand for fruits and vegetables. In 2022 alone, the company handled a significant quantity of produce, with a total of 161498.048 kilograms passing through their facilities before being brought to market.
This highlights the rapid and significant accumulation of plastic waste resulting from the short shelf life and the high demand for these food products.
The data provided by the Apofruit company in 2022 reveals the substantial amount of packaging materials used for fruits and vegetables. In just one year, a total of 7,235,268 tons of paper, conventional plastic, and biodegradable/compostable plastic were utilized for packaging purposes. Specifically, 5835.812 tons of paper, 1366.195 tons of conventional plastic, and 33.261 tons of biodegradable/compostable plastic were used. These figures emphasize the significant quantities of packaging materials required to meet the packaging needs of the fruit and vegetable industry.
According to Mangaraj et al. (2009), the most commonly employed materials for fruit and vegetable packaging in recent years are polyvinyl chloride (PVC), polyethylene terephthalate (PET), polypropylene (PP), and polyethylene (PE). However, these materials, as extensively discussed in this thesis, suffer from various drawbacks such as reliance on finite fossil oil reserves, limited recyclability due to their chemical composition, and lack of biodegradability. Consequently, these factors contribute to environmental and economic concerns, including increased air pollution and disposal costs.

In light of these issues, the aim of our experimental study was to explore the feasibility of replacing traditional fruit packaging, which is non-eco-sustainable, with more environmentally friendly alternatives. By doing so, we sought to examine the potential qualitative impact of such a substitution.

To conduct the study, we packaged samples of white grapes, blueberries, blackberries, and fruit salad in both conventional commercial materials and alternative packaging options. For the commercial reference materials, we used R-PET trays with lids for fruit salad, blueberries, and blackberries, and R-PET cups with perforated interlocking lids for white grapes.
Similarly, we packaged the same fruits in trays made of alternative materials, including trays composed of a layer of pure bleached virgin cellulose (ECF) fiber cardboard with a suitable barrier coating for direct food contact, closed with a cellulose-based film. We also used PLA (polylactic acid) trays with interlocking lids, R-PET trays hermetically sealed with interlocking PET film, and hermetically sealed R-PET trays with laser-perforated PET top film (average hole diameter of 30 μm).
After packaging the fruits in both conventional and alternative materials, we placed them in a refrigerated environment. At specific time intervals, we conducted various analytical assessments on the fruits. These assessments included measuring weight loss for all samples, determining oxygen and carbon dioxide concentrations for hermetically sealed packages, measuring Brix degrees for grapes, blueberries, and blackberries, conducting mechanical shear tests on grape samples, performing mechanical compression tests on blueberries, conducting sensory analysis using sensory tests administered to a panel of evaluators, and performing microbiological analyses to determine bacterial load, mold, and yeast counts for white grapes, blackberries, and fruit salad samples.
The results obtained indicated that the utilization of these alternative materials could serve as a viable compromise between adopting more environmentally friendly packaging materials and maintaining the quality and shelf life of the fruit samples.

7.2. Materials and Methods

7.2.1. Materials

White grape cv. *Melanie* was supplied from Apofruit Italia (Metaponto, Italy), blueberries cv. *Blue Ribbon*, blackberries cv. *Rubus Nessensis Hall* and fruits salad were supplied from Apofruit Italia (Cesena, Italy). R-PET tray closed with lid (fruits salad, blueberries and blackberries) and R-PET cup closed with perforated interlocking lid (white grape) were supplied by Apofruit Italia (Cesena, Italy). Tray consisting of a layer of pure bleached virgin cellulose (ECF) fiber cardboard and a barrier coating suitable for direct food contact, close with cellulose-based film supplied by BIOPAP (Settimo Milanese, Milan, Italy). PLA (polylactic acid) tray closed with interlocking lid, R-PET tray hermetically sealed with interlocking PET film and hermetically sealed and R-PET tray with laser-perforated PET top film (with average hole diameter 30 μm) were supplied from ILPA (Valsamogia, Bologna; Italy). Plate Count Agar and Rose bengal agar base (RSBA) were supplied from Merck KGaA (Darmstadt, Germany).

7.2.2. Methods

7.2.2.1. Sample Preparation

The preparation of the samples involved receiving the fruit and packaging them in commercial reference containers and experimental packages.
Specifically, in Table 7.1. It can see the packaging used for each type of fruit in the trial and the coding of the samples.

Table 7.1a. Code of samples and description of the packages used for each type of fruit.

Code	Fruit	Packaging
A	White grape	R-PET cup closed with perforated interlocking lid
B	White grape	Virgin cellulose tray close with cellulose-based film
C	White grape	PLA tray closed with interlocking lid
D	White grape	R-PET tray hermetically sealed with interlocking PET film and hermetically sealed
E	White grape	R-PET tray with laser-perforated PET top film (with average hole diameter 30 μm)
A	Bluberries	R-PET tray closed with interlocking lid
B	Bluberries	PLA tray closed with interlocking lid
C	Bluberries	Virgin cellulose tray close with cellulose-based film
A	Blackberries	R-PET tray closed with inerlocking lid
B	Blackberries	PLA tray closed with interlocking lid
C	Blackberries	Virgin cellulose tray close with cellulose-based film
A	Fruit salad	R-PET tray sealed with interlocking PET film and hermetically sealed
B	Fruit salad	PLA tray closed with interlocking lid
C	Fruit salad	Virgin cellulose tray close with cellulose-based film

Table 7.1b. Hermetically sealed materials data sheet

Material	Thickness (μm)	OTR (cm^2 m^{-2} $24h^{-1}$ bar^{-1}) 23°C – 0% RH	CO_2TR (cm^2 m^{-2} $24h^{-1}$ bar^{-1}) 23°C – 0% RH	WVTR (g m^{-2} $24h^{-1}$) 38°C – 90% RH
PET	25	55	400	20
PET laser perforated (30 mm hole diameter- 132 microholes/m^2)	25	20000	18000	30
cellulose-based film	55	100	/	20

The 'A' package of each experimental set represents the commercial packaging in which the products are sold, therefore, it is the control package.
The samples, after being packaged, with not a tightly sealed for samples A and C of white grape samples, were placed in a conditioned environment at a temperature of 4±1 °C (Figure 7.1) and on the day of the experimental control only the packages to be analyzed were taken.

Figure 7.1. Disposizione dei campioni in ambiente controllato alla temperatura di 4±1 °C

7.2.2.2. Atmosphere Analysis

Concentrations of oxygen (O_2) and carbon dioxide (CO_2) in the headspace of the packaged samples were monitored using a portable gas analyzer, CheckPoint II (Dansensor). The instrument is equipped with a needle that is inserted inside the packages through a rubber septum, placed above the lid of the packages. The packages analyzed were only those that had an airtight seal and the control intervals varied according to the type of fruit, in fact, for grapes the controls were carried out at 0, 3, 6 and 8 days from packaging; for blueberries at 1, 2, 3, 4, 6, 7, 8, 9 and 10 days from packaging; for fruit salad, 1, 2 and 3 days after packaging; for blackberries at 1, 2, 3 and 6 days from packaging.

7.2.2.3. Weight Loss

The weight loss was determined by weighing the packages at defined time intervals, using an analytical scale. Weight loss was performed for grapes at 0, 2, 3, 6, 7, 8, 9, 10 and 13 days after packaging; for fruit salad at 0, 1, 2 and 3 days after packaging; for blueberries 0, 1, 2, 3, 4, 6, 7, 8, 9 and 10 days after packaging; for blackberries at 0, 1, 2, 3, and 6 days after packaging.

7.2.2.4. Brix Degrees Determination

The total soluble solids content determines the sugar content in fruits, in particular, these soluble deniers are, mainly, represented by sugars, such as: glucose and fructose, are expressed as °Brix. This measurement was carried out using a Hanna HI 96814 portable digital refractometer. A drop of the juice was placed on the lens of the instrument and the measurement was made in degrees Brix (°Bx). Brix degrees are equivalent to the % of soluble solids content (% SSC) in the fruit (Colelli and Inglese, 2020; Siddiqui, 2015). Calibration was carried out with deionized water and the lens was thoroughly rinsed between samples. Brix degrees were measured for grapes at 0, 3, 6, 8 days after packaging; for blueberries at 0, 2, 4, 6, 8 and 10 days after packaging; for blackberries 0, 2, 3 and 6 days after packaging.

7.2.2.5. Mechanical tests

Mechanical tests were carried out only for the samples of grapes and blueberries and with different methods for the two types of fruit.

The mechanical tests performed on the grape samples involved the execution of a shear test on a single fruit, with the use of a Zwick/Roell dynamometer model Z1.0 (Ulm, Germany) and equipped with a 1 kN load cell. The grapes under analysis were placed on the lower shelf, the analysis was performed with the use of a dovetail blade, a preload of 0.5 N, a test speed of 150 mm/min and a descent of the blade of 15 mm after reaching the preload. The data was processed using the testXpert II software. The test was performed at 0, 3, 6, and 8 days after packaging.

The mechanical tests performed on the blueberry samples involved the execution of a compression test on a certain quantity of fruit. In fact, 41 g of blueberries were placed inside a beaker. The test was carried out using a 10 mm flat cylinder, test speed of 50 mm/min and cylinder descent of 30 mm. The stress data expressed in Newtons were performed using the statistical software testXpert II. The test was performed at 0, 2, 6, 8 and 10 days after packaging.

7.2.2.6. Sensory analysis

Sensory analyses involved the administration of a sensory card. The card provided a hedonistic scale from 0 to 5 for each factor considered.
In the sensory analysis of the grape, blackberry and blueberry samples, seven parameters were evaluated: color acceptability, presence of wilting, presence of rot, crispness of the grape, pulp texture, sweetness and acidity. Analyses were performed for grapes at 0, 2, 6 and 8 days after packaging; for blueberries at 0, 2, 4, 6, 8, and 10 days after packaging; for blackberries at 0, 2, 3, and 6 days after packaging.
The sensory analysis for the fruit salad was carried out with a slightly different sensory card and modality: the panel was asked to taste and evaluate the individual fruits present in the fruit salad following the sensory card (figure 7.2.). The test was performed at 0, 2 and 3 days after packaging.

Overall visual acceptability 1: not acceptable 5: acceptable		1	2	3	4	5
Acceptability of fruit color 1: not acceptable 5: acceptable	ANANAS	1	2	3	4	5
	KIWI	1	2	3	4	5
	APPLE	1	2	3	4	5
Development of abnormal odors	1: no abnormal odor 3: some 5: many	1	2	3	4	5
Acceptability of fruit texture 1: not acceptable 5: acceptable	ANANAS	1	2	3	4	5
	KIWI	1	2	3	4	5
	APPLE	1	2	3	4	5
Acceptability of fruit 1: not acceptable 5: acceptable	ANANAS	1	2	3	4	5
	KIWI	1	2	3	4	5
	APPLE	1	2	3	4	5
development of anomalous flavors	1: no abnormal odor 3: some 5:many	1	2	3	4	5
Overall acceptability	1: not acceptable 5: acceptable	1	2	3	4	5

Figure 7.2 Sensory card for acceptability testing of fruit salad samples.

7.2.2.7. Microbiological analysis

The microbiological analysis of the fruit samples involved the determination of the mesophilic, yeasts and mold load at different times. After weighing and chopping, the samples were subjected to a serial dilution with saline, of each dilution 1 mL of solution was placed in the plates with the growth medium, using the embedding technique. The plates were incubated for 48h at 30°C for bacteria, for 72h at 30°C.
Microbiological tests were performed for the grapes at 0, 3, 6 and 9 days after packaging; for blackberries at 0, 2, 3 and 6 days after packaging; for fruit salad at 0, 2 and 3 days after packaging.

7.3. Results and Discussion

7.3.1. Atmosphere Analysis

The analysis of the headspace atmosphere in the packages containing white grapes was conducted specifically for packages B, D, and E, as packages A and C were not tightly sealed. In Figure 7.3, the concentration trends of O_2 and CO_2 over time can be observed for packages B, D, and F.

In package B, which consists of a virgin cellulose tray sealed with a cellulose-based film, there is a slight decrease in the percentage of O_2 as the storage time increases. This decrease is attributed to the fruit's respiration, which consumes O_2 and releases CO_2 into the package's headspace. However, due to the poor barrier properties of the paper tray, the respiratory effect is undetectable.

Moving on to package D, there is a notable decrease in the oxygen concentration from 20% at the time of packaging to 11% after 8 days of storage. On the other hand, the concentration of CO_2 exhibits an opposite behavior. Initially absent, it gradually increases and reaches around 30% after 8 days of storage. This phenomenon can be attributed to the package's airtightness and the permeability characteristics of the PET material. PET is known for its barrier capacity, which allows the accumulation of CO_2 and the reduction of O_2.

Package E exhibits a different behavior compared to packages B and D. It shows an initial increase in CO_2 concentration and a decrease in O_2 concentration, which continues until the sixth day of storage. However, on the eighth day of storage, there is a sudden change in the concentration curves. This change suggests that the fruit reached its peak respiration around the sixth day of storage. The increase in CO_2 concentration is associated with grape ripening, as described by Piazzolla et al. (2016). After reaching this stage, the respiratory activity slows down, which could possibly be linked to the aging process of the fruit itself.

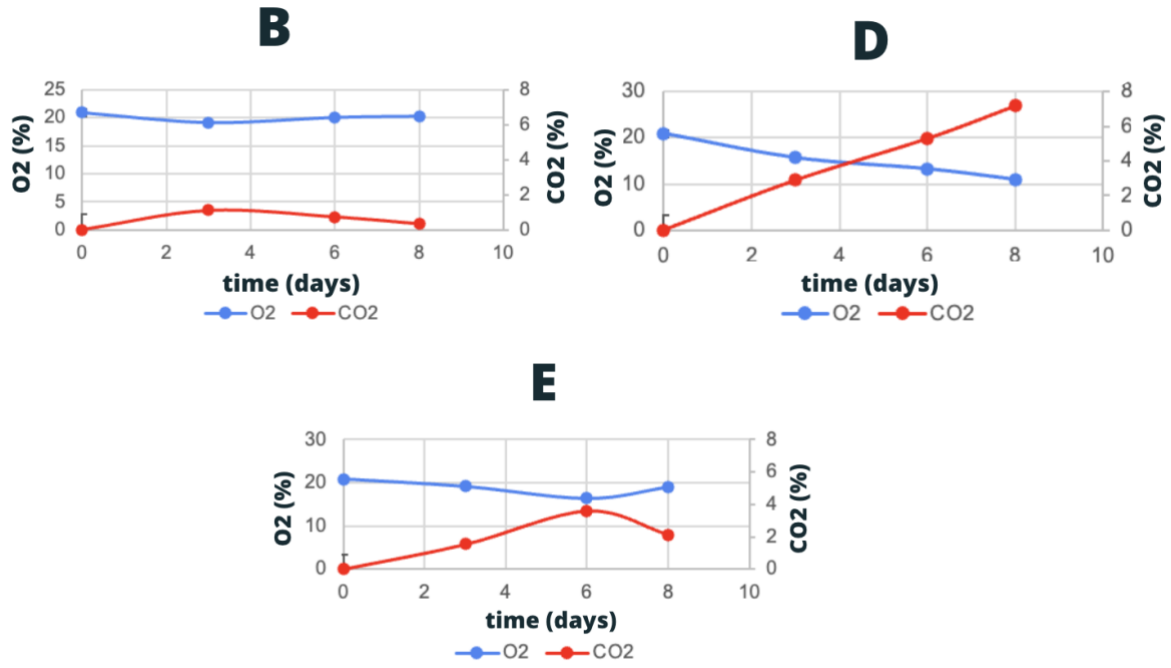

Figure 7.3. Trend of O2 and CO2 concentrations in grape packages.

Figure 7.4. The curves of the oxygen and carbon dioxide concentration trends inside the B (PLA tray closed with interlocking lid) and C (Virgin cellulose tray close with cellulose-based film) packages in which the blueberries were packaged are shown. We can immediately see

how the behavior of both packages is very similar; in fact, there is a concentration of the O_2 content that is around 20%, which is represented by atmospheric oxygen and a slight increase in the value of CO_2, which is always in the range of 1.5% and 2.7% for both packages. From these data, it is easy to deduce the fact that both packages are easily allowed to pass through the air and allow exchange with the outside, despite the presence of the hermetic seal.

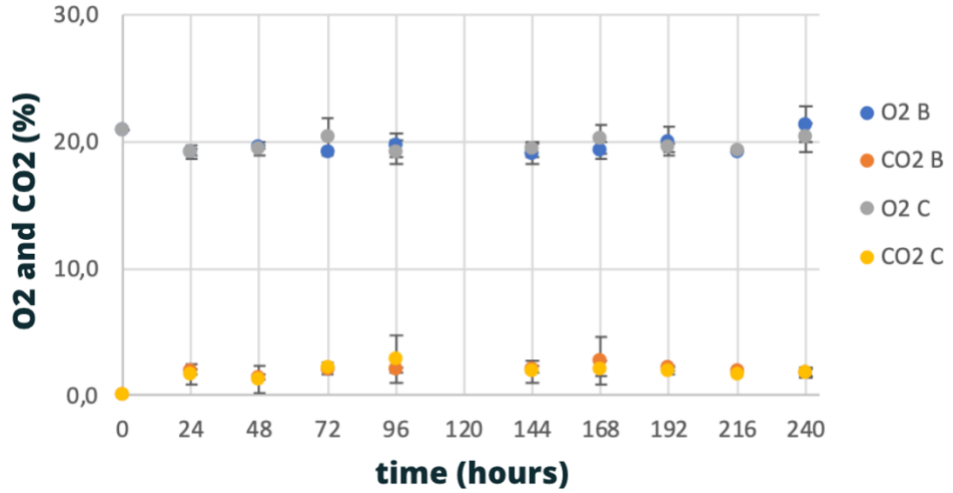

Figure 7.4.Trend of O_2 and CO_2 concentrations in blueberries packages.

In Fig. 7.5. there are trends of O_2 and CO_2 concentrations in blackberries packages, an increase in CO_2 and a decrease in O_2 in B packaging can be seen due to the respiration of the blackberries and the gas-holding capacity, even if low, of the PLA tray; a different trend is recorded in package C, the paper one, in which the trend of the concentration of oxygen and carbon dioxide does not seem to vary over time, so the release of CO_2 of the fruit due to its respiration is not evident, since it comes out almost completely from the paper package and the lid, which are highly permeable.

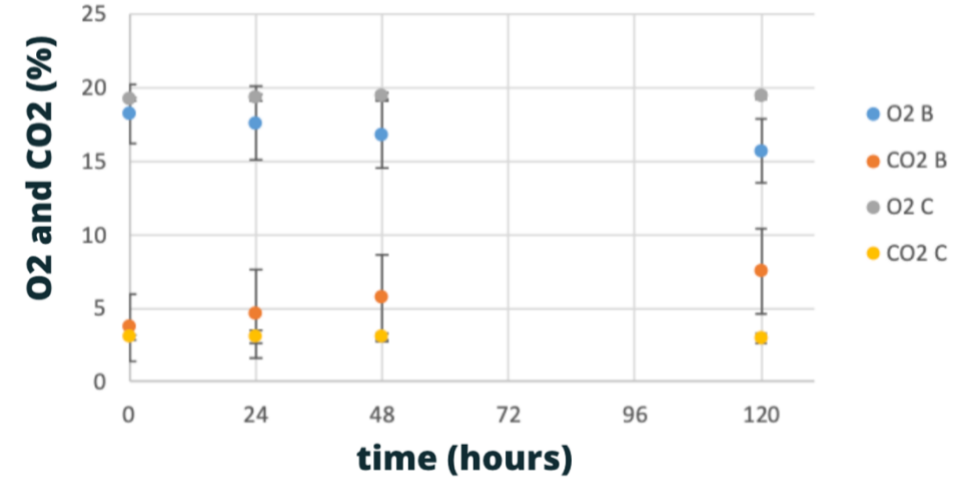

Figure 7.5. Trend of O_2 and CO_2 concentrations in blackberries packages.

Checks over time of the headspace of the packages in which the fruit salad was contained (Fig. 7.6) showed a slight decrease in the oxygen content and a slight increase in the % of carbon dioxide compared to the beginning of the test, the values subsequently remained almost constant during the refrigerated storage period, regardless of the type of material used for packaging, demonstrating a low barrier to gases of all the packaging used, innovative and not.

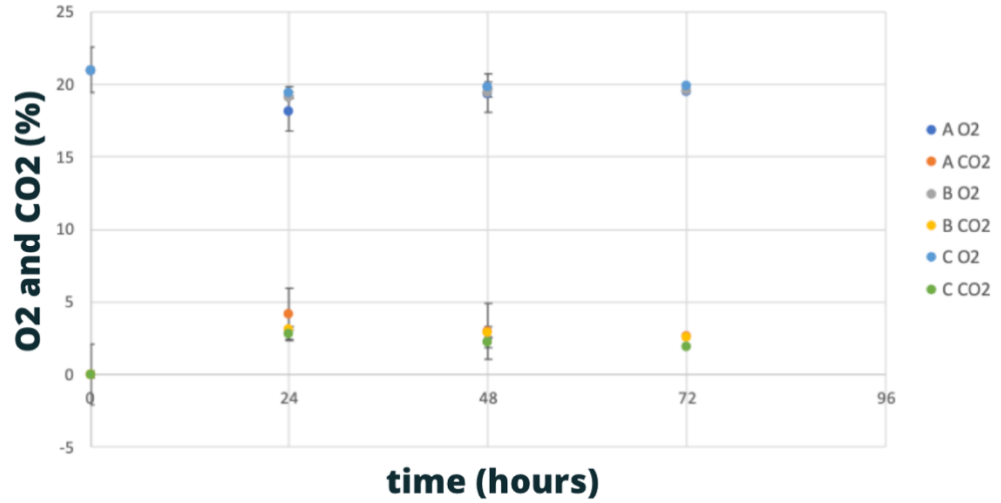

Figure 7.6. Trend of O_2 and CO_2 concentrations in fruits salad packages.

In conclusion, R-PET packaging and in some cases PLA packaging were solutions that allowed less CO_2 to escape, which was produced during the respiration of the fruit. The accumulation of CO_2 concentration inside the packaging played a positive role in the microbial load (see par. 7.3.6).

7.3.2. Weight Loss

Table 7.3 displays the daily weight losses in grams for different samples of bank grapes, blueberries, blackberries, and fruit salad. Additionally, the table includes estimates for the weekly weight loss of these samples. These estimates were made to facilitate a fair comparison between the various fruit samples, which were packaged in different types of packages and underwent weight control at different time intervals.
Upon examining the table, it becomes evident that, with the exception of fruit salad, package A consistently resulted in the highest weight loss for all types of fruits on a weekly basis. Specifically, blueberries exhibited a weekly loss of 2.80 g, blackberries lost 2.60 g, and grapes decreased by 2.45 g, for this last sample, grapes, this drop in weight was to be expected, given the non-airtight nature of the container and the presence of holes in the upper and lower part of the package. In contrast, the situation differed for paper packages (package B for grape samples and package C for all other fruits). It appears that the grape-containing packages experienced the greatest weight loss, with 0.84 g per week, followed by blueberries at 0.42 g. However, the paper packaging demonstrated a distinct behavior for blackberries and fruit salad. By referring to figures 7.7 and 7.8, one can observe the weight loss trend of the paper packages containing blackberries and blueberries represented in gray. Notably, the weight loss in these packages did not follow a linear pattern. Instead, at certain points, the product appeared to gain weight rather than lose it.
This phenomenon could be attributed to the characteristics of the packaging, which is composed of cellulose and possesses hydrophilic properties. As a result, the packaging likely retains both the water released by the fruits and the ambient humidity. The weight gain is likely due to the packaging absorbing moisture rather than the product itself increasing in weight.
The two R-PET packages (packages D and E) that contained white table grapes exhibited the best performance, with a weekly weight gain of 0.04 g in both cases. Lastly, the PLA packages demonstrated intermediate performance between the control packages and the R-PET packages.

Although they still exhibited low weekly weight loss values, similar to blueberries and fruit salad, with 0.28 g and 0.21 g respectively.

Table 7.3. Daily weight loss and after 7 days, expressed in grams, for samples of white grapes, blueberries, blackberries and fruit salad, pack in control packs (A) and alternative packs.

sample	weight loss (g/day)	after 7 days (g)
white grape		
A	0.35	2.45
B	0.12	0.84
C	0.06	0.42
D	0.006	0.04
E	0.006	0.04
bluberries		
A	0.40	2.80
B	0.04	0.28
C	0.06	0.42
blackberries		
A	0.37	2.6
B	0.07	0.5
C	/	/
fruits salad		
A	0.033	0.23
B	0.03	0.21
C	0.18	1.24

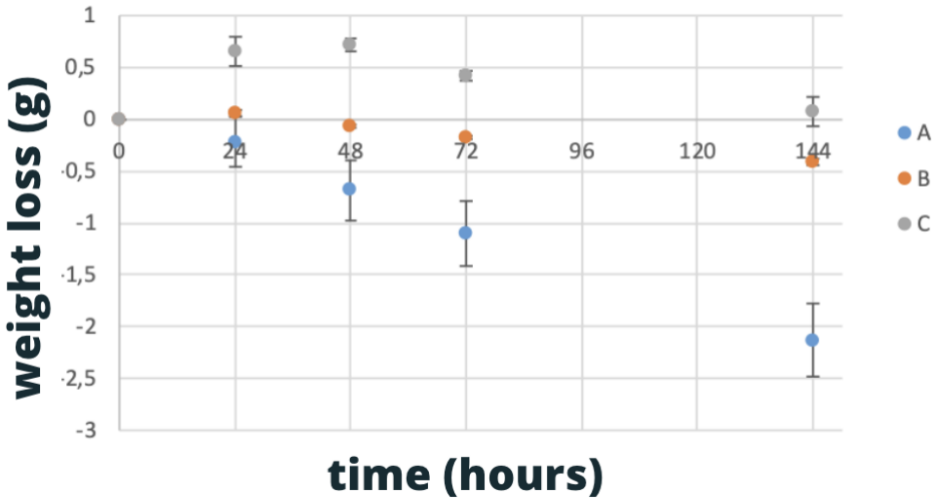

Figure 7.7. Trend of weight loss of blackberry packs.

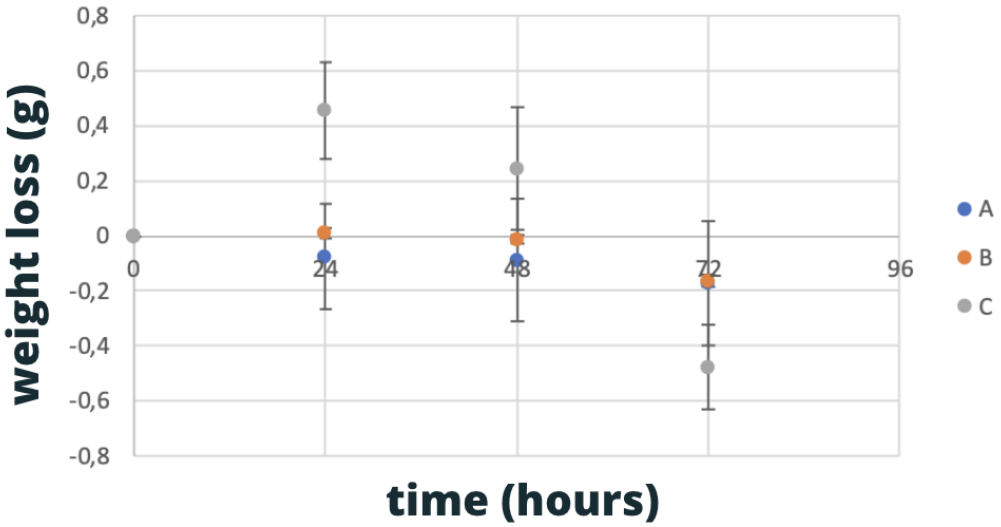

Figure 7.8. Trend of weight loss of fruits salad packs.

7.3.3. Brix Degrees Determination

In general, when measuring Brix degrees, lower values are typically recorded for fruits that are not fully ripe and have not yet released their simple sugars completely. This phenomenon has been observed and reported by various authors (Colelli and Inglese, 2020), and it is also partly evident in the experimental samples of this study. By examining Figure 7.9, which illustrates the trend of Brix degrees for grape samples, we can observe the described pattern. After reaching a peak at 144 hours, most of the samples exhibit a decrease in Brix degrees. This decline can be attributed to the fruit reaching its maximum ripeness after harvest and subsequently entering the stage of senescence, leading to over-ripeness. During this period, there is a significant decrease in the content of soluble solids in the fruit (Rooban et al., 2016; Sampaio et al., 2007).

Additionally, there are no noticeable differences in the variation of Brix degrees based on the type of packaging used, except for packages A and D, where the decrease in Brix degrees over time appears to be slower.

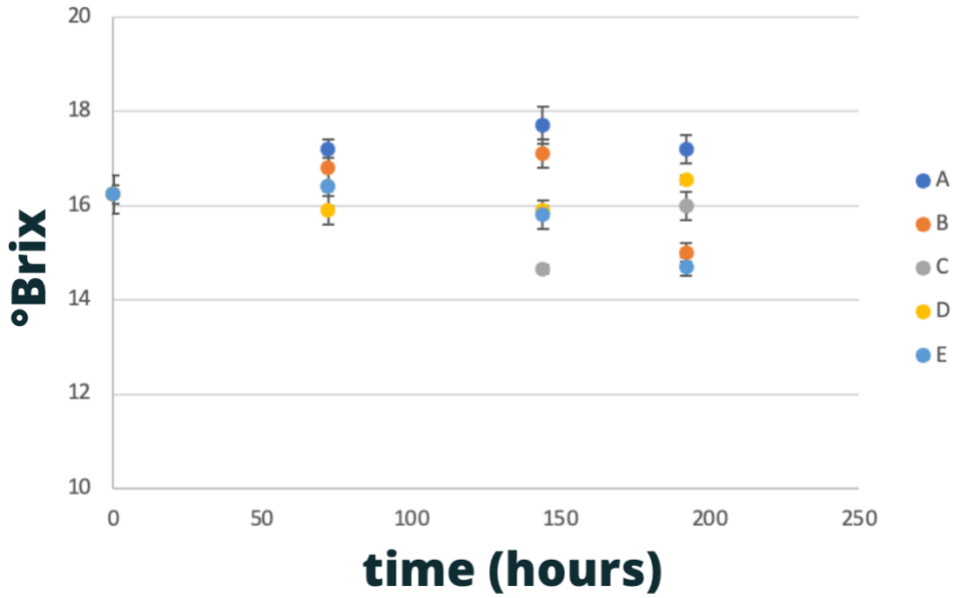

Figure 7.9. Trend over time of the brix degrees (°) for the white grape samples in the different packages.

Figure 7.10 illustrates the total soluble solids content of blueberries, irrespective of the tray type, showing a slight increasing trend in the first few days followed by a decrease. In the case of package A, the content returns to a slightly higher value than the initial measurement, while packages B and C have a lower value of total soluble solids after 10 days of storage compared to the initial measurement. This difference is likely due to the greater weight loss experienced by samples packaged in R-PET, which leads to a higher concentration of sugars in the product. The collected data demonstrate a non-constant trend over time, with values varying within a narrow range. This variation is likely attributed to the natural variability of the product and the measurement uncertainty of the instrument used. Regarding the concentration of sugars during storage, there are no significant differences between the samples.

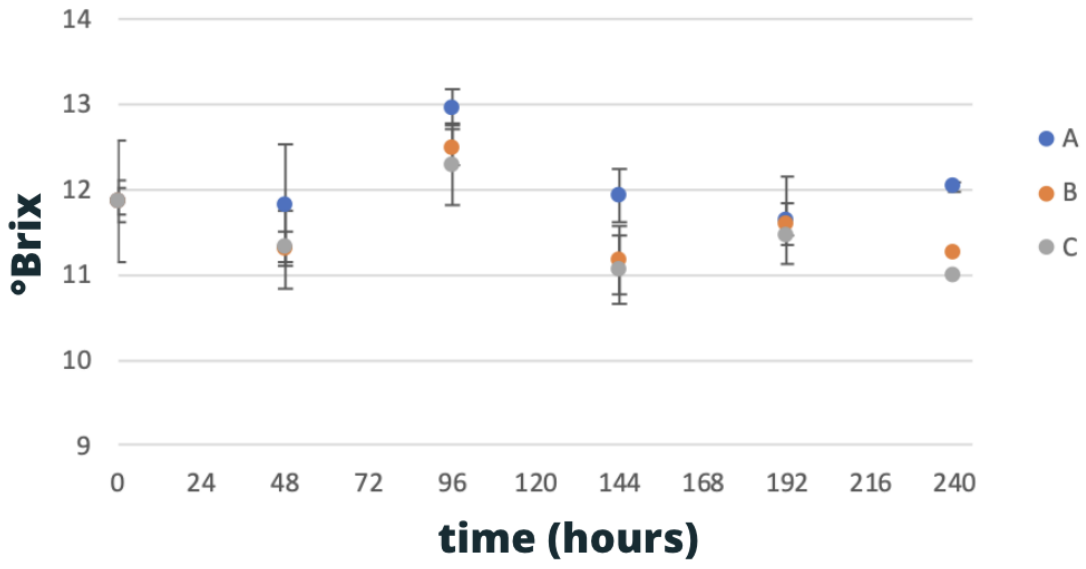

Figure 7.10. Trend over time of the brix degrees (°) for the blueberries samples in the different packages.

For blackberries packaged in the three different types of packages (Figure 7.11), the Brix degrees exhibit distinct behaviors over time. The samples in the reference packaging (A) consistently decrease over time. The samples stored in PLA and paper packaging demonstrate fluctuating behavior, but they do not deviate significantly from the control sample. Similar to blueberries, there are no significant differences between the samples in this case.

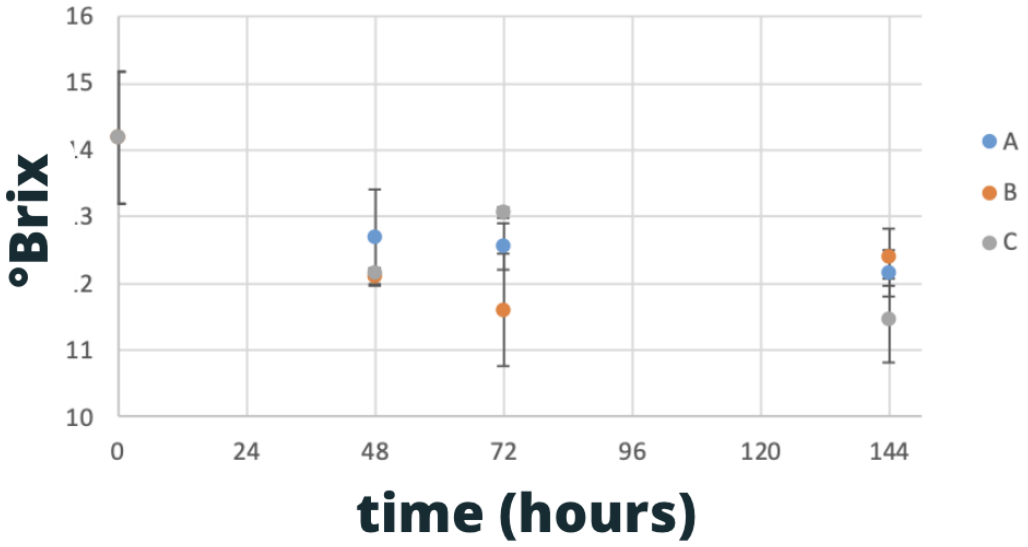

Figure 7.11. Trend over time of the brix degrees (°) for the blackberries samples in the different packages.

7.3.4. Mechanical tests

During the storage and ripening process, fruits undergo various biochemical, physiological, and structural changes that influence their appeal to consumers (Nambi et al., 2016). Among these changes, texture alterations occur, primarily associated with fruit softening caused by the activity of degradative enzymes that affect the structure and composition of the cell wall. These enzymes lead to the partial or complete solubilization and depolymerization of cell wall polysaccharides like pectins and celluloses.

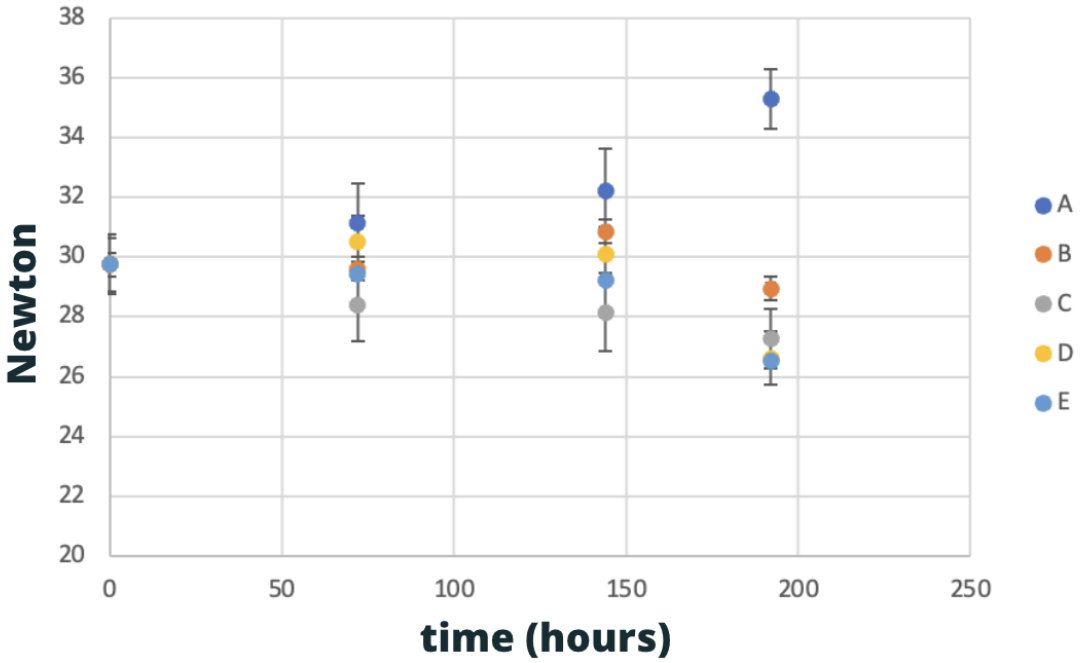

Figure 7.12. Trend of the force, expressed in Newtons, deriving from the shear test of white grape samples packaged in different packages

To assess the texture changes in grape samples, a shear test was conducted (refer to Figure 7.13), where each grape was cut using a dovetail blade to evaluate the structural modifications of the fruit over time. Figure 7.12 depicts that the samples packaged in the tray A exhibit a different trend compared to those in the experimental trays. It appears that the structure of these samples is more turgid, resulting in higher Newton values over time. However, this effect is primarily due to dehydration, as indicated by the data in section 7.3.2. The dehydration causes the blade to drag the skins during the experimental test (Figure 7.13), leading to artificially higher force values. Furthermore, the force values of the samples packed in the experimental trays decrease over time, indicating that the texture of the grapes does not change significantly and there is no shriveling of the product.

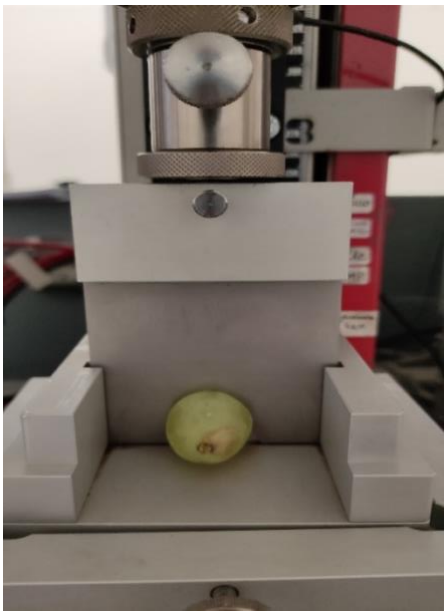

Figure 7.13. Cutting of a grape using a dynamometer to which a swallow-shaped plate is attached.

In the case of blueberries, a mechanical control has been carried out that simulates chewing and allows us to understand the degree of consistency of the fruit. Fig. 7.14 shows the force in Newton (N) in relation to time in hours.
As far as the test of the compressive force (expressed in Newtons) of the fruits contained in thesis A is concerned, a force at time zero (first day of control) equal to 20.6N was found, after two days it increased to 22.5 N and then progressively decreased and increased on the tenth day until it reached a value equal to 23.9. Considering also the standard deviation value of the replicates, the value for the whole test does not seem to be far from the initial value, thus confirming the maintenance of quality from the mechanical point of view of the product. For the blueberries contained in the PLA tray, a decreasing trend in strength was found as the days increased. For those stored in paper packaging, on the other hand, the strength increased slightly over time and then returned, on the tenth day, to about the same value found immediately after packaging (day 0).
However, this very variable trend over time falls within a very low deviation range and therefore it can be said that no major differences have been found between the packages used over time.

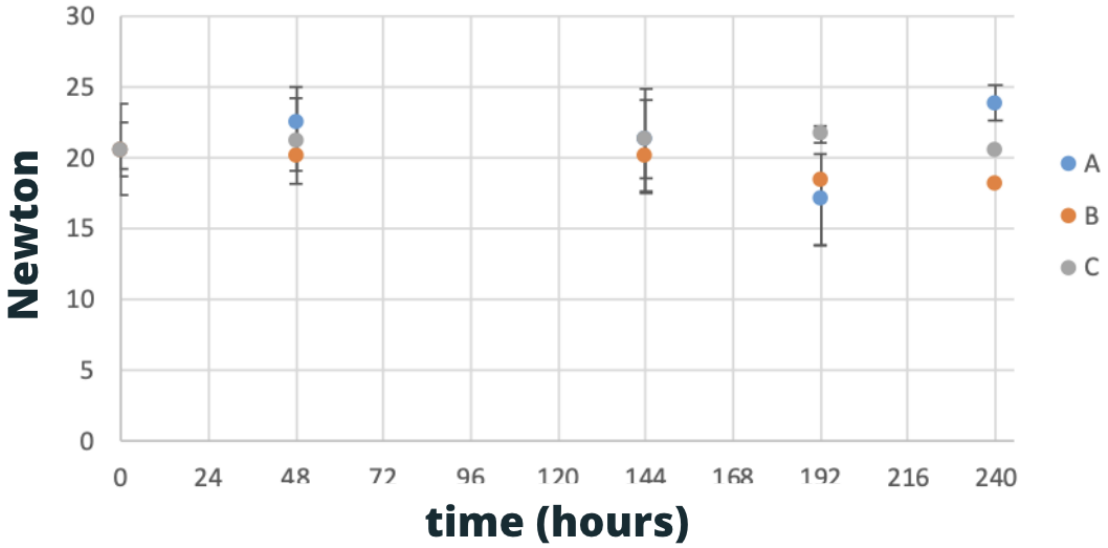

Figure 7.14. Trend of the force, expressed in Newtons, deriving from the compression test of blueberry samples packaged in different packages.

7.3.5. Sensory analysis

A sensory test was conducted on all fruit samples used in this experiment to evaluate how the chemical and physical changes identified through analysis were perceived by consumers.

Figure 7.15 displays radar graphs representing the sensory tests conducted over time on grape samples packaged in different containers.
In Package A samples, parameters such as the presence of rot and wilting remained consistently low across all sensory analysis sessions. The acceptability of color appeared to be highest in the initial two evaluations, gradually decreasing in the last two sessions but still remaining

acceptable. Sweetness and acidity showed an increase after 48 hours and then decreased over time. Other factors examined exhibited a steady decrease over time, albeit not excessively. No significant variations in the presence of rot and wilting were detected. Crispness appeared to decrease over time, transitioning from a value close to 5 to a value of 3.

Similarly, samples in Tray B exhibited variable color acceptability, and parameters such as crunchiness, pulp texture, sweetness, and acidity showed a decreasing trend over time, followed by a slight increase in the final evaluation. However, these variations were subtle. The presence of rot and wilting was not perceived. Crispness demonstrated a decline over time, shifting from a value close to 5 to a value of 3.

Samples C, D, and E displayed a decrease over time in all parameters assessed, without exhibiting any notable differences among the containers used in the experiment.

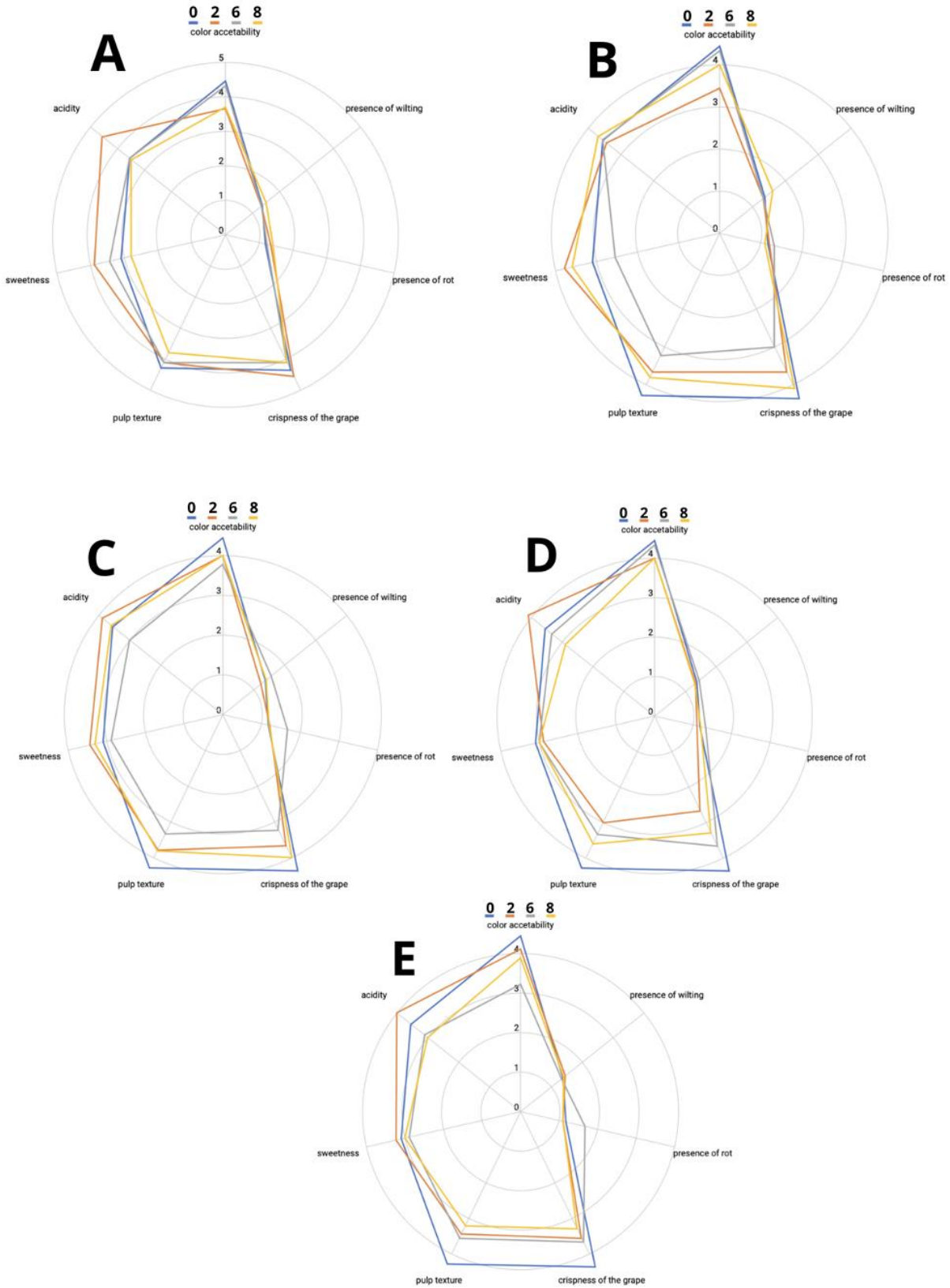

Figure 7.15. Radar graphs of the sensory tests carried out over time of the grape samples contained in the different packaging

Figure 7.16 displays radar graphs illustrating the sensory tests conducted over time on blueberry samples packaged in different containers. From a visual standpoint, the color of the product remained highly acceptable throughout the duration of the experiment, regardless of the packaging type. The absence of rot was consistently maintained across all three test conditions, and no abnormal flavors were detected in any of the three scenarios.
The most significant variation was observed in the presence of wilting, which increased in all cases but not in a linear manner over the shelf life. Additionally, it can be noted that the presence of shriveling at the end of storage was slightly more pronounced in Thesis A.

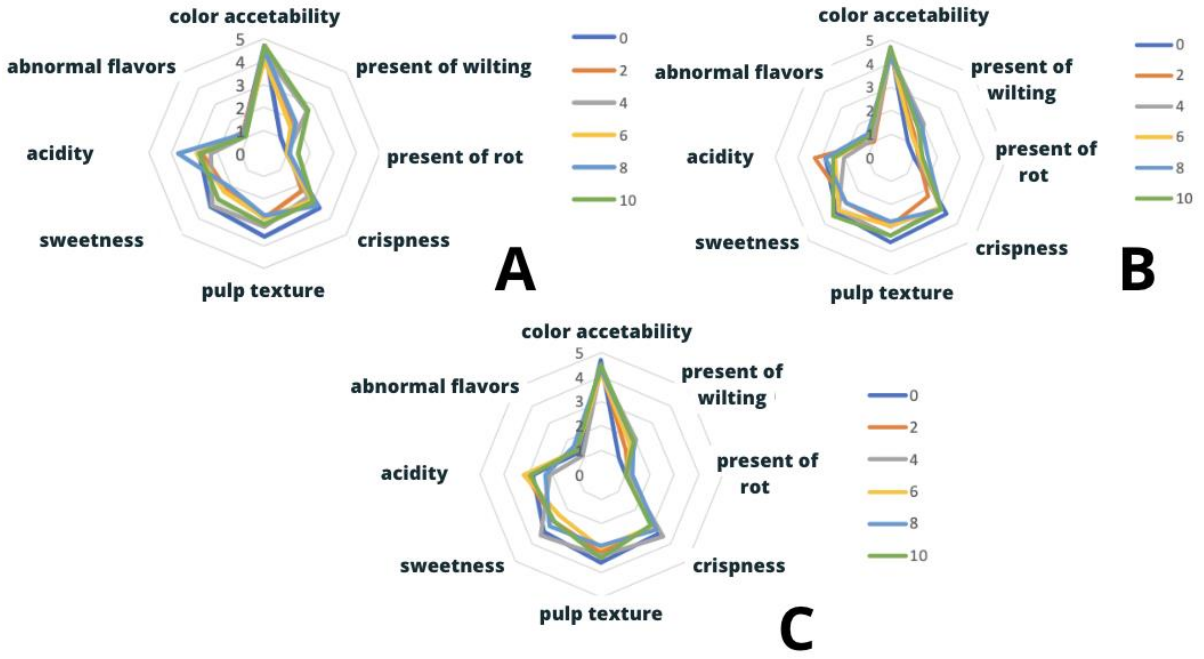

Figure 7.16. . Radar graphs of the sensory tests carried out over time of the blueberries samples contained in the different packaging.

As can be seen from fig. 7.17, in which the sensory evaluations of blackberry samples are present, the acceptability of the color of the product has maintained high values over time, regardless of the type of packaging used; the presence of wilting was high only in the last control for blackberries packaged in the R-PET (A) tray; The product within the three theses has always reported the absence of rot and the development of abnormal flavors.

In the first check, the turgidity was high and then decreased, while maintaining similar values between the three theses; the greatest variation, increasing, was found in the perception of sweetness for the fruit in the PLA tray (B), paper (C) allowed intermediate values to be kept constant, thesis A found evaluations similar to thesis B but with a narrower range; the acidic sensation during the experiment was found to decrease with increasing time and not in a linear fashion for thesis B and C.

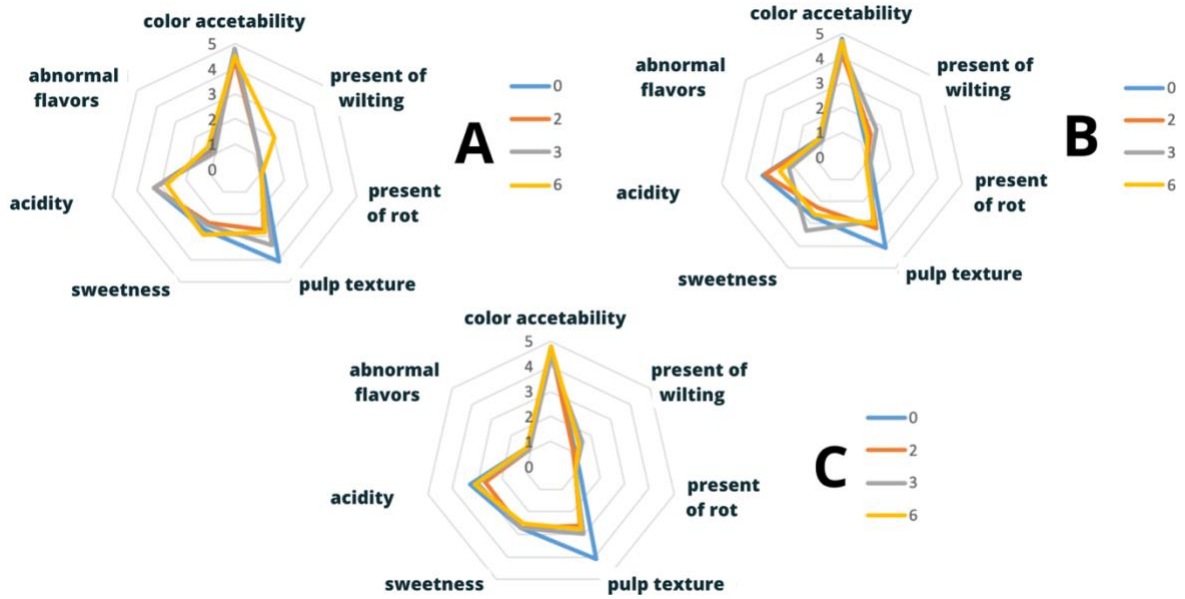

Figure 7.17. Radar graphs of the sensory tests carried out over time of the blackberries samples contained in the different packaging

Regarding individual fruit salad components, they were evaluated separately due to their distinct qualitative characteristics that cannot be compared directly. Figure 7.18 displays radar graphs illustrating the sensory tests conducted over time on fruit salad samples packaged in different containers.

Color variations in pineapple were similar across all packaging types, with the color becoming less acceptable as time progressed. The consistency of pineapple remained relatively constant at intermediate values for Thesis A, while it exhibited a non-linear decrease over time for Thesis B and C. Gustatory acceptability of pineapple in Thesis A showed similarities in the first two days, followed by a decrease. In Thesis C and B, the acceptability decreased in the initial two days and remained similar between the second and third day. Similar trends were observed for kiwi descriptors.

Visual acceptability, texture, and gustatory acceptability of apple did not significantly vary over time or between theses, except for minor differences.

Abnormal odors in the fruit salad packaged in PET (A) and PLA (B) containers remained consistently low over time, while those in Thesis C (paper tray) increased on the third day of storage but remained acceptable. Abnormal flavors increased over time for the product in all three trays.

The overall acceptability of the fruit salad decreased over time, regardless of the packaging material used. The assigned values by the tasters decreased by 0.5 for Thesis B and C and by 0.4 for Thesis A. However, the decrease was not significant in terms of time or differences between the three trays, and the product was still considered acceptable even after three days of refrigerated storage.

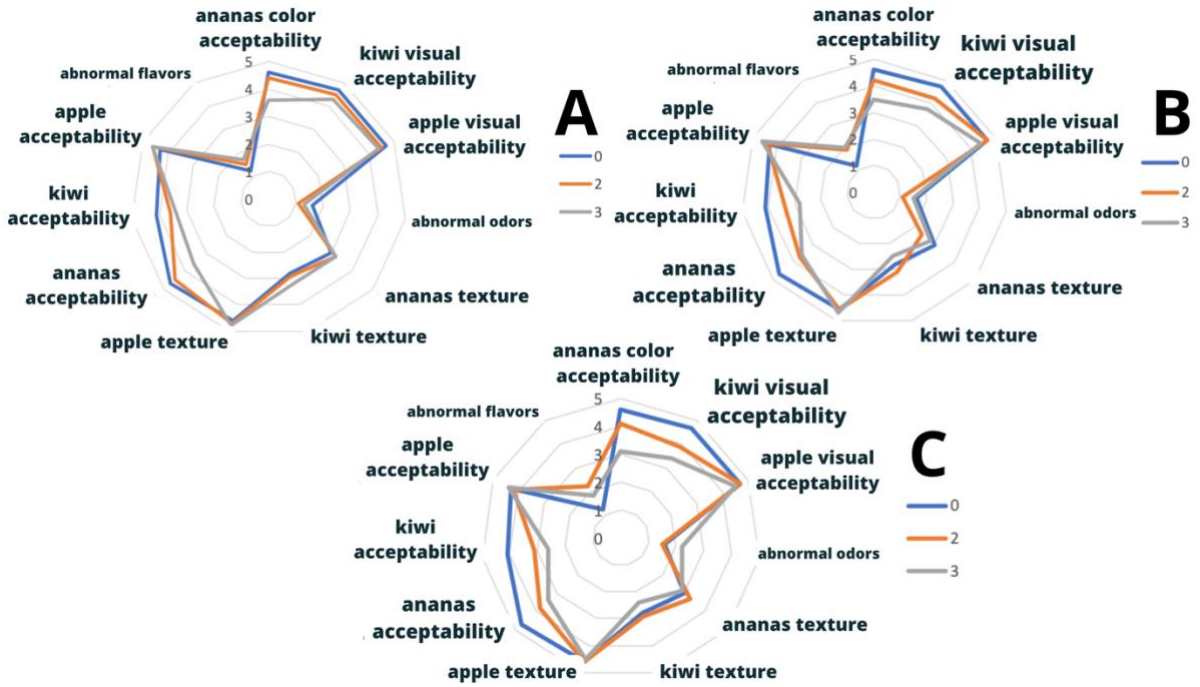

Figure 7.18. Radar graphs of the sensory tests carried out over time of the fruit salad samples contained in the different packaging.

7.3.6. Microbiological analysis

Microbiological tests were conducted to determine the levels of bacteria, molds, and yeasts in the fruit samples contained in different packages over time. The aim was to assess the microbiological acceptability of the product, considering that a product should not exceed 10^{-7} CFU/g (colony-forming units per gram) for bacteria e 10^{-6} CFU/g for yeasts and mold to be suitable for the market.

Examining Figure 7.19, in which showed the bacterial growth for the heads of grapes over time, it is evident that the bacterial load consistently increased over time for the samples in package A (control). Conversely, when analyzing the trend of bacterial load for the alternative packages (B, C, D, E), it can be observed that package B showed a slower increase over time compared to package A. The same trend applies to the samples in packages D and E, where an initial decrease in bacterial load was followed by a subsequent, albeit less significant, increase. Only the samples in package C exhibited a decrease in bacterial load over time. Overall, it can be concluded that the use of packages D and E helped slow down the logarithmic growth of bacterial load. This effect is likely due to reduced gas exchange and higher concentration of CO_2 in the headspace of the packages, which possesses antibacterial properties supported by scientific literature (Devlieghere and Debevere, 2000; Lee and Baek, 2008; Bae et al., 2011; Yildirim et al., 2018). CO_2 dissolved in the package headspace inhibits microbial growth by influencing the lag phase, maximum growth rate, and maximum population densities, as described by Devlieghere and Debevere (2000).

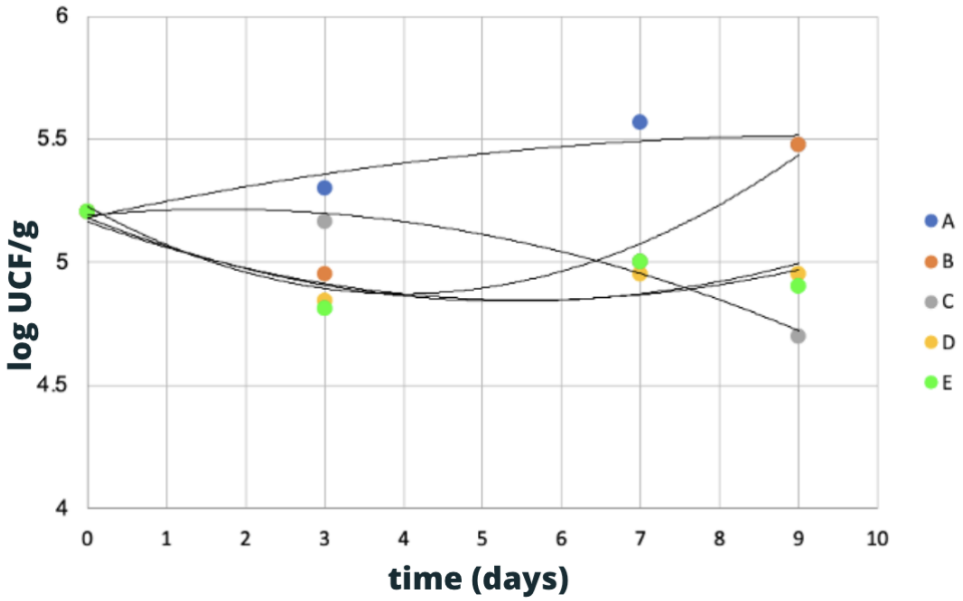

Figure 7.19 Microbial growth over time of grape samples packaged in different packages.

Looking at Figure 7.20, it can be observed that between the first and second checks, the growth of yeasts and molds appeared similar across the various packages, except for the samples in package D, which displayed a decrease in yeast and mold growth. However, this decrease was not observed in the final control, where the yeast and mold content values were similar among all the packages, including package D. Although all packages allowed for a slow growth of yeast and mold content, they ensured microbiological safety throughout the product's shelf life.

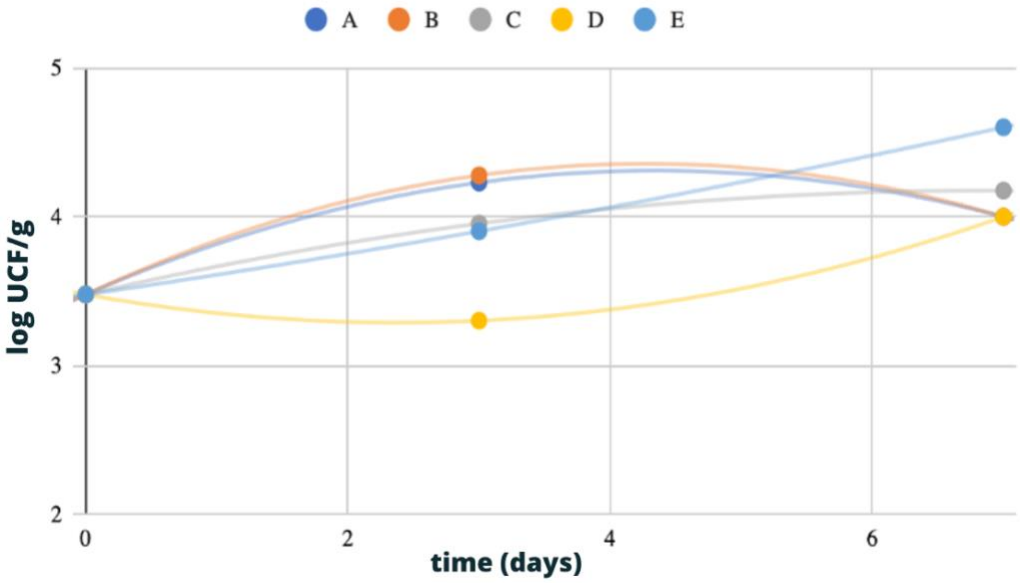

Figure 7.20 Growth of yeasts and molds over time of the grape samples packaged in the different packages.

In Figure 7.21, the graph illustrates the bacterial growth over time in blackberry samples packaged in different packages. The microbial load inside the packages shows variation, with two samples for each package type. The blackberry samples in Package A1 exhibited a decrease in CFU/g as time progressed. In contrast, the samples in Package A2 initially showed an increase in values for the first three days and then a decrease on the sixth day (after 144 hours).

The samples in Thesis B and C demonstrated fluctuating trends over time for both B1 and B2 samples, with a similar trend observed in the samples in Package C1. However, the samples in Thesis C2 displayed a different growth pattern, with an increase in load as the storage duration increased from the second day (after 48 hours), followed by a rapid decrease during the final check.

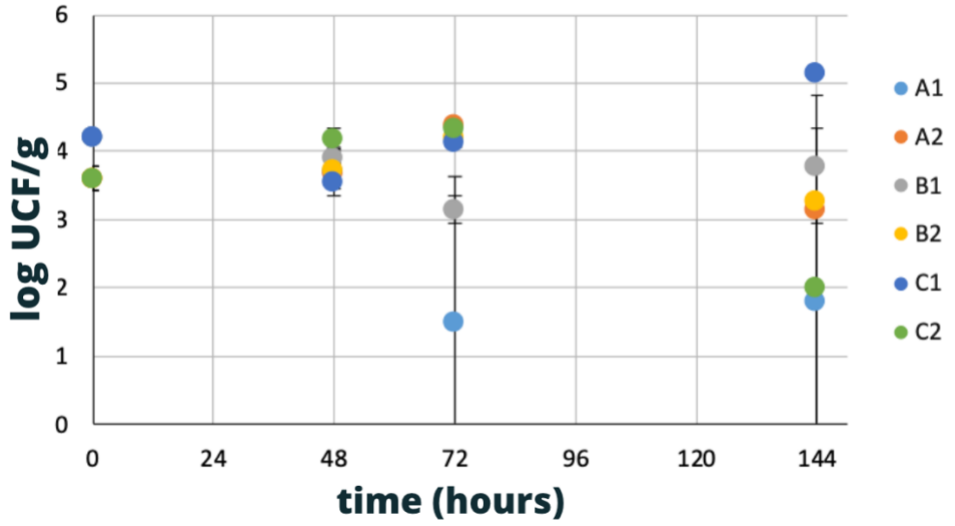

Figure 7.21 Microbial growth over time of blackberries samples packaged in different packages.

In Figure 7.22, the graph depicts the growth trends of yeasts and molds over time in blackberry samples stored in the reference package (A) and the experimental packages (B and C). Regardless of the packaging used, the growth of yeasts and molds exhibited fluctuating trends over time. The values for all three theses were similar in the initial days of storage but diverged after 72 hours and even more so after 144 hours. The growth patterns varied among the different replicas but remained within the regulatory limits.

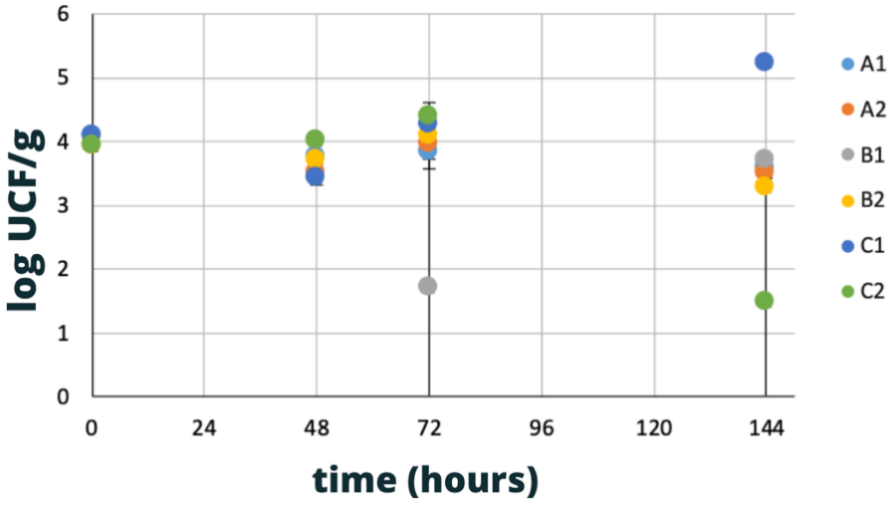

Figure 7.22 Growth of yeasts and molds over time of the blackberries samples packaged in the different packages.

Since fruit salad is a fresh-cut product that undergoes mechanical processing, resulting in increased surface area for microbial growth and greater handling, it was important to assess the trends of mesophilic aerobic load, yeasts, and molds during the shelf-life. Observing Figure

7.23, bacterial growth in all samples remained constant and similar over time, except for the samples in Package C2. These samples initially experienced a decrease in bacterial load at 48 hours of storage but reached the same bacterial load as other packages at 72 hours. Overall, bacterial growth remained low in all samples throughout the 72-hour storage period, regardless of the package used, ensuring microbiological safety.

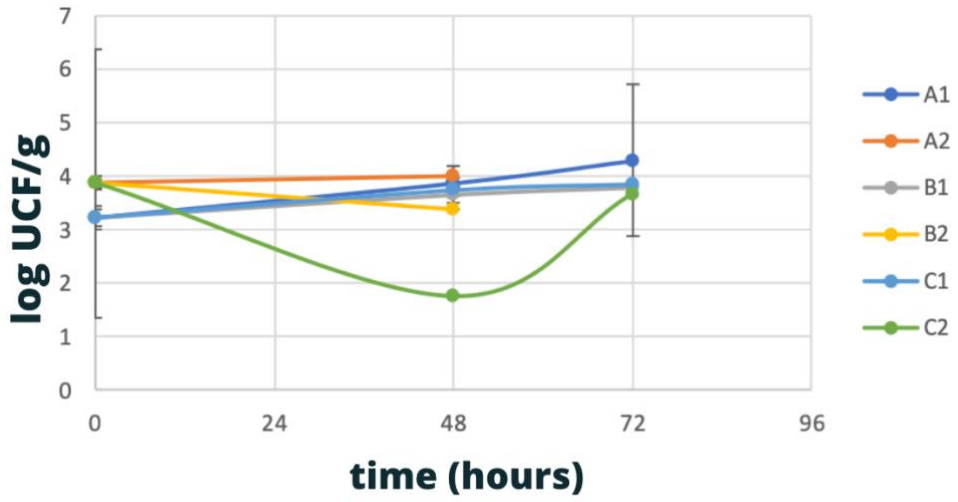

Figure 7.23 Microbial growth over time of fruit salad samples packaged in different packages.

Finally, Figure 7.24 demonstrates the growth trend of yeasts and molds in fruit salad samples, which closely paralleled the bacterial growth in the same samples, except for the samples in Package B1 (PLA tray). These samples exhibited a decreasing trend over time, particularly noticeable after 72 hours of storage.

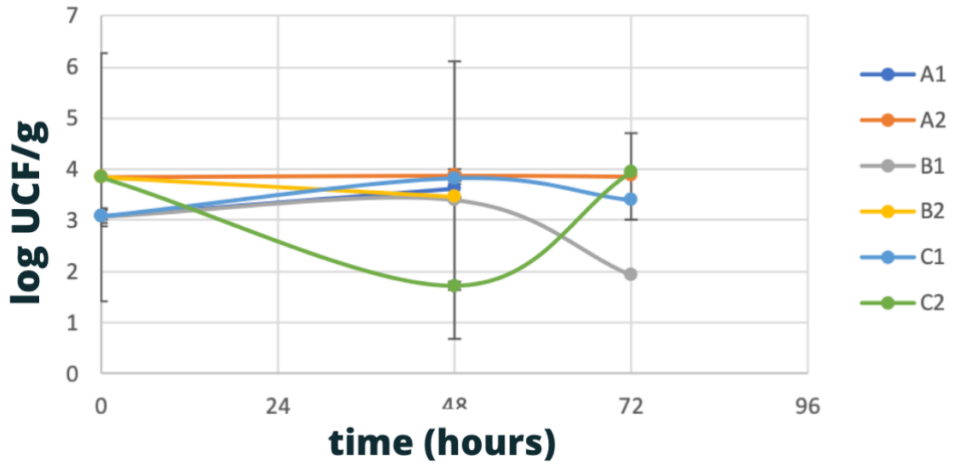

Figure 7.24 Growth of yeasts and molds over time of the fruit salad samples packaged in the different packages.

In conclusion, according to the "Guidelines for risk analysis in the field of food microbiology (Annex B)," the limit for aerobic mesophilic microorganisms in the category of vegetables and fruits is 10^{-7}, while for yeasts and molds, it is 10^{-6}. Considering these limits, all the samples analyzed in this experiment showed a decreasing microbial load over time, indicating that they are consistently suitable and safe for consumption from a microbiological perspective.

7.4. Conclusions

The objective of this experimental study was to assess and compare the efficacy of various alternative packaging solutions, in preserving fruit quality and prolonging shelf life. The fruit samples were placed in different designated packages and then subjected to periodic evaluations, including measurements of weight loss, assessment of atmospheric modifications (only for hermetically sealed samples), determination of total microbial load and yeast/mold counts, mechanical tests (for grapes and blueberries), and sensory analysis.

It is important to note that the purpose of this experiment was not to establish the superiority of alternative packaging over the already established commercial packaging options. Rather, the aim was to investigate the feasibility of replacing traditional containers with greener and more sustainable alternatives, thereby reducing the reliance on plastics in the fruit and vegetable industry. Based on the comprehensive analysis of all the obtained data, it can be concluded that such substitutions are indeed viable. The alternative packaging options not only maintained the quality of the examined products but, in certain cases, also better preserved their inherent characteristics compared to the currently available market packaging. This demonstrates the potential for embracing greener and more sustainable choices in the industry without compromising product quality.

Chapter 8

General conclusions and future perspectives

Chapter 8: General conclusions and future perspectives

My research doctorate was focused in two mains objectives, i.e., the first objective involved the creation of coatings and films intended to coat food paper to improve its water and oil barrier properties and functionalize it with antimicrobial properties, through the use of polymers with biodegradability/compostability characteristics and which in some cases derive from by-products of the food chain; as for the second objective, I conducted a comparative study to evaluate the performance and final quality of fruits when utilizing innovative, eco-friendly materials versus conventional plastic materials, which are widely acknowledged as non-eco-friendly.

The achievements of the first topic have been very encouraging. In fact, through the use of polymers such as PCL, PHBV, PHBH, PBS, PLA, starch and cutin derived from by-products of tomato processing, it has been possible to create coatings that would significantly improve the grease and water vapor barrier characteristics of food paper, a packaging material recognized for its poor barrier properties, due to the presence of pores deriving from the arrangement of cellulose fibers. The most encouraging results demonstrated an impressive 82% reduction in the WVTR (Water Vapor Transmission Rate) value compared to the control, as well as achieving resistance to solution number 12 in the 'kit 12' test for grease resistance. Additionally, by introducing a metal complex into PVA-based films, these films have been successfully functionalized with antimicrobial properties, making them ideal coatings for food paper.

Based on a comprehensive analysis of the data obtained, it can be concluded that the objectives of the second topic have been successfully achieved. The substitution of conventional packaging materials with alternative options has proven to be a viable solution. The alternative packaging not only preserved the quality of the products under examination but, in certain instances, also better maintained their inherent characteristics compared to the packaging currently available in the market.
It is essential to clarify that the purpose of this experiment was not to establish the superiority of alternative packaging over commercial options. Rather, the aim was to demonstrate the feasibility and potential benefits of utilizing alternative packaging materials.

In terms of future objectives regarding the formulation of coatings on food paper, the next crucial step is industrial scaling up. It is imperative to evaluate whether the procedures and practices developed at the laboratory scale can effectively meet the demands and challenges of the industrial reality, which significantly differs from the controlled environment of a research laboratory.

Another important objective will be to assess the end-of-life characteristics of these coated materials, specifically their actual recyclability and/or compostability. The evaluation will follow the 'Aticelca 501 Evaluation System,' which is employed in Italy to assess the recyclability and level of recyclability of predominantly cellulosic packaging. This evaluation method involves analyzing various parameters and conducting laboratory tests to simulate the recycling process. Parameters examined include the quantity of coarse waste, final waste, formation of adhesive particles, formation of a sheet downstream of the production process, and optical homogeneity. The test results assign a letter grade (from A+ to C) indicating the level of recyclability of the cellulose-based packaging. It is crucial to determine the recyclability level of the laboratory-created materials to gain a realistic perspective on their end-of-life possibilities and environmental sustainability.

Furthermore, an essential aspect related to the disposal and end-of-life management of these paper materials is evaluating their potential inclusion in the organic waste supply chain. It is important to test their compostability in small-scale industrial settings and/or domestic environments using domestic composters. The ability to dispose of these materials in the composting chain would enable complete and environmentally sustainable disposal. In addition, it could allow the use of compost in different agronomic contexts, creating a cycle in which materials, often coated with polymers from by-products of the agri-food industry, give rise to compost, used, in turn, in the cultivation of agri-food products.

In summary, future objectives involve industrial scaling up to assess feasibility, as well as evaluating the recyclability and compostability of the coated materials according to established standards. Additionally, exploring their integration into the organic waste supply chain and testing their compostability will be integral to achieving a comprehensive perspective on their end-of-life management.

References chapter 1

- Abedi-Firoozjah, R., Chabook, N., Rostami, O., Heydari, M., Kolahdouz-Nasiri, A., Javanmardi, F., Khaneghah, A. M. "PVA/starch films: An updated review of their preparation, characterization, and diverse applications in the food industry." *Polymer testing*, **2023,** 118: 107903.
- Alradha, Rusul M., Jawad Hanaa, and Ali A. Al-Zubiedy. "Preparation and characterization of Polyvinyl Alcohol/Starch/Bio Oil Extraction Blends Coating for Food Packaging Using Electrospinning Technique." *Egyptian Journal of Chemistry* **2023**, 66.2: 141-149.
- Barnes, D. K., Galgani, F., Thompson, R. C., & Barlaz, M. Accumulation and fragmentation of plastic debris in global environments. *Philosophical transactions of the royal society B: biological sciences*, **2009**: *364*(1526), 1985-1998.
- Barry, Vaughn, Andrea Winquist, and Kyle Steenland. Perfluorooctanoic acid (PFOA) exposures and incident cancers among adults living near a chemical plant. *Environmental health perspectives*, **2013**, 121.11-12: 1313-1318.
- Basak, Sumanta, Milind Shrinivas Dangate, and Shanmugha Samy. "Oil-and water-resistant paper coatings: A review." *Progress in Organic Coatings*, **2024**, 186:107938.
- Battisti, R., Fronza, N., Júnior, Á. V., da Silveira, S. M., Damas, M. S. P., & Quadri, M. G. N. Gelatin-coated paper with antimicrobial and antioxidant effect for beef packaging. *Food Packaging and Shelf Life*, **2017**, 11:115-124.
- Bi, S., Pan, H., Barinelli, V., Eriksen, B., Ruiz, S., Sobkowicz, M. J. Biodegradable polyester coated mulch paper for controlled release of fertilizer. *Journal of Cleaner Production* **2021**, 294: 126348.
- Bikiaris, N.D.; Koumentakou, I.; Samiotaki, C.; Meimaroglou, D.; Varytimidou, D.; Karatza, A.; Kalantzis, Z.; Roussou, M.; Bikiaris, R.D.; Papageorgiou, G.Z. Recent Advances in the Investigation of Poly(lactic acid) (PLA) Nanocomposites: Incorporation of Various Nanofillers and their Properties and Applications. *Polymers* **2023**, *15:*1196.
- Bordenave, Nicolas, Stephane Grelier, and Veronique Coma. Hydrophobization and antimicrobial activity of chitosan and paper-based packaging material. *Biomacromolecules.* **2010**, 11.1: 88-96
- Bota, J., Vukoje, M., Brozović, M., & Hrnjak-Murgić, Z. "Reduced water permeability of biodegradable PCL nanocomposite coated paperboard packaging." *Chemical and Biochemical Engineering Quarterly*, **2017**. 31.4: 417-424.
- Brodnjak, U. Vrabič, and D. Muck. "Printing quality of chitosan-rice starch coated packaging paper." *Bulgarian Chemical Communications* **2017**, 49: 85-91.
- Brodnjak, U. Vrabič, and D. Muck. "Printing quality of chitosan-rice starch coated packaging paper." *Bulgarian Chemical Communications* **2017**, 49: 85-91.
- Cardenas, A., Gold, D. R., Hauser, R., Kleinman, K. P., Hivert, M. F., Calafat, A. M., Oken, E. Plasma concentrations of per-and polyfluoroalkyl substances at baseline and associations with glycemic indicators and diabetes incidence among high-risk adults in the diabetes prevention program trial. *Environmental health perspectives*, **2017**, *125*:10, 107001.
- Chi, Kai, Hui Wang, and Jeffrey M. Catchmark. Sustainable starch-based barrier coatings for packaging applications. *Food Hydrocolloids*. **2020**, 103: 105696.
- Chiono, V., Ciardelli, G., Vozzi, G., Sotgiu, M. G., Vinci, B., Domenici, C., & Giusti, P. "Poly (3-hydroxybutyrate-co-3-hydroxyvalerate)/poly (ϵ-caprolactone) blends for tissue engineering applications in the form of hollow fibers." *Journal of Biomedical*

Materials Research Part A: An Official Journal of The Society for Biomaterials, The Japanese Society for Biomaterials, and The Australian Society for Biomaterials and the Korean Society for Biomaterials. **2008**, 85.4: 938-953.

- Chitena, Lorraine, Cosmas Muiva, and Lemme P. Kebaabetswe. "Application of in-situ casted ZnO-starch nanocomposite for packaging of strawberries (Fragaria x ananassa)." *Heliyon*, **2023**, 9.11
- Cigula, Tomislav, Tomislav Hudika, and Tamara Tomasegovic. "Lightfastness, surface and interfacial properties of colour-printed paper substrates coated with PCL/ZnO and PCL/TiO2 nanocomposites." *Surfaces and Interfaces*. **2021**, 27:101522.
- Crippa, M., De Wilde, B., Koopmans, R., Leyssens, J., Muncke, J., Ritschkoff, A. C., Wagner, M. *A circular economy for plastics: Insights from research and innovation to inform policy and funding decisions*. **2019**
- Dang, C., Yin, Y., Xu, M., & Pu, J. (2018). Hydrophobic noncrystalline porous starch (NCPS): dispersed silver nanoparticle suspension as an antibacterial coating for packaging paper. *BioResources*, **2018,** 13.1, 192-207.
- Dehghani Firouzabadi, Mohammadreza, and Meysam Aliabadi. "The comparison of coated paper properties with cellulose nanofiber-zinc nanooxide and strach-zinc nanooxide." *Forest and Wood Products* **2023**, 75.4: 377-386.
- Deshwal, G.K.; Panjagari, N.R.; Alam, T. An Overview of Paper and Paper Based Food Packaging Materials: Health Safety and Environmental Concerns. J. Food Sci. Technol. **2019**, 56, 4391–4403.
- Dris, R., Gasperi, J., Mirande, C., Mandin, C., Guerrouache, M., Langlois, V., & Tassin, B. A first overview of textile fibers, including microplastics, in indoor and outdoor environments. *Environmental pollution*, **2017**, *221*, 453-458.
- Fithriyah, Nurul Hidayati, and Erdawati. "Mechanical properties of paper sheets coated with chitosan nanoparticle." *AIP Conference Proceedings*. **2014** Vol. 1589. No. 1. American Institute of Physics.
- Furukawa, Tsuyoshi, et al. "Comparison of miscibility and structure of poly (3-hydroxybutyrate-co-3-hydroxyhexanoate)/poly (l-lactic acid) blends with those of poly (3-hydroxybutyrate)/poly (l-lactic acid) blends studied by wide angle X-ray diffraction, differential scanning calorimetry, and FTIR microspectroscopy." *Polymer,* **2007,** 48.6: 1749-1755.
- Geyer, Roland, Jenna R. Jambeck, and Kara Lavender Law. "Production, use, and fate of all plastics ever made." *Science advances,* **2017**, 3.7: e1700782.
- Giesy, John P., and Kurunthachalam Kannan. "Global distribution of perfluorooctane sulfonate in wildlife." *Environmental science & technology*, **2001**, 35.7: 1339-1342.
- Gilliland, Frank D., and Jack S. Mandel. "Mortality among employees of a perfluorooctanoic acid production plant." *Journal of Occupational Medicine*, **1993**: 950-954.
- Gu, F.; Yang, W.; Song, J.; Xiao, H.; Wang, W.; Cai, Z. Crosslinked PVA/Nanoclay Hydrogel Coating for Improving Water Vapor Barrier of Cellulose-Based Packaging at High Temperature and Humidity. *Coatings* **2022**, 12.10:1562.
- Hamdani S.S., Li Z., Rabnawaz M., Kamdem D.P, Khan B.A., Chitosan -graft-poly (dimethylsiloxane)/zein coatings for the fabrication of environmentally friendly oil- and water-resistant paper, *ACS Sustain Chem Eng*. **2020**, 8:5147–5155.
- Hamdani, S. S., Emch, H., Isherwood, J., Khan, A., Kumar, V., Alford, A., Rabnawaz, M. "Waterborne Poly (butylene succinate)-Coated Paper for Sustainable Packaging Applications." *ACS Applied Polymer Materials*, **2023**, 5.10: 7705-7717.

- Han, Hee-Seon, and Kyung Bin Song. Antioxidant activities of mandarin (Citrus unshiu) peel pectin films containing sage (Salvia officinalis) leaf extract. *International Journal of Food Science & Technology* **2020**, 55.9:3173-3181.
- Hassan, E., Fadel, S., Abou-Elseoud, W., Mahmoud, M., Hassan, M., Cellulose nanofibers/pectin/pomegranate extract nanocomposite as antibacterial and antioxidant films and coating for paper, *Polymers*, **2022**, 14.21: 4605.
- Hudika, T., Cigula, T., Žličarić, M., & Strižić Jakovljević, M. "PCL-TiO 2 nanocomposite to improve ageing of offset prints." *Proceedings of the 10th International Symposium GRID*. **2020**.
- Jambeck, J. R., Geyer, R., Wilcox, C., Siegler, T. R., Perryman, M., Andrady, A.,Law, K. L. Plastic waste inputs from land into the ocean. *Science*, **2015**, 347.6223: 768-771.
- Javed, A., Rättö, P., Järnström, L., Ullsten, H. "Crack analysis of barrier coatings based on starch and starch-PVOH with and without plasticizer." *Nordic Pulp & Paper Research Journal*, **2018**, 33.2, 336-347.
- Jian, J., Xiangbin, Z., & Xianbo, H. "An overview on synthesis, properties and applications of poly (butylene-adipate-co-terephthalate)–PBAT." *Advanced Industrial and Engineering Polymer Research*. **2020**. 3.1:19-26.
- Jiang, Xuan, Gang Chen, and Zhi Qiang Fang. "The application of starch-sodium alginate composite coating on transparent paper for food packaging." *Advanced Materials Research*. **2014**, 893: 472-477.
- Jung, J., Raghavendra, G. M., Kim, D., & Seo, J. One-step synthesis of starch-silver nanoparticle solution and its application to antibacterial paper coating. *International journal of biological macromolecules*, **2018**, 107:2285-2290.
- Jung, Jeyoung, Gopinath Kasi, and Jongchul Seo. "Development of functional antimicrobial papers using chitosan/starch-silver nanoparticles." *International journal of biological macromolecules,* **2018***,* 112: 530-536.
- Kamel, S., M. El-Sakhawy, and A. M. A. Nada. "Mechanical properties of the paper sheets treated with different polymers." *Thermochimica acta,* **2004**, 421.1-2: 81-85.
- Khwaldia, K., Basta, A. H., Aloui, H., El-Saied, H. Chitosan–caseinate bilayer coatings for paper packaging materials. *Carbohydrate polymers*. **2014**, 99: 508-516.
- Khwaldia, K.; Arab-Tehrany, E.; Desobry, S. Biopolymer Coatings on Paper Packaging Materials. *Compr. Rev. Food Sci. Food Saf.* **2010**, 9.1: 82–91.
- Kopacic, S.; Walzl, A.; Zankel, A.; Leitner, E.; Bauer, W. Alginate and Chitosan as a Functional Barrier for Paper-Based Packaging Materials. *Coatings* **2018**, *8*, 235.
- Lai, Sun-Mou, Wei-Wei Sun, and Trong-Ming Don. "Preparation and characterization of biodegradable polymer blends from poly (3-hydroxybutyrate)/poly (vinyl acetate)-modified corn starch." *Polymer Engineering & Science.* **2015**, 55.6: 1321-1329.
- Lamsaf, H.; Singh, S.; Pereira, J.; Poças, F. Multifunctional Properties of PBAT with Hemp (*Cannabis sativa*) Micronised Fibres for Food Packaging: Cast Films and Coated Paper. *Coatings* **2023**, *13*, 1195.
- Lauzier, Christian A., et al. "Film formation and paper coating with poly ([beta]-hydroxyalkanoate), a biodegradable latex." *Tappi Journal;(United States)* **1993**, 76.5.
- Li, H., Qi, Y., Zhao, Y., Chi, J., & Cheng, S. Starch and its derivatives for paper coatings: A review. *Progress in Organic Coatings*, **2019,** 135:213-227.
- Li, Zhao, and Muhammad Rabnawaz, Oil- and water-resistant coatings for porous cellulosic substrates, *ACS Appl Polym Mater*. **2019**, 1:103–111,
- Lim, Jing, Chong, M. S. K., Teo, E. Y., Chen, G. Q., Chan, J. K., & Teoh, S. H.. "Biocompatibility studies and characterization of poly (3-hydroxybutyrate-co-3-

hydroxyhexanoate)/polycaprolactone blends." *Journal of Biomedical Materials Research Part B: Applied Biomaterials.* **2013**, 101.5:752-761.

- Liminana, P., Garcia-Sanoguera, D., Quiles-Carrillo, L., Balart, R., and Montanes, N. Development and Characterization of Environmentally Friendly Composites from Poly(butylene Succinate) (PBS) and Almond Shell Flour with Different Compatibilizers. *Compos. Part B Eng*. **2018**, 144, 153-162.
- Lin, D., Kuang, Y., Chen, G., Kuang, Q., Wang, C., Zhu, P., Fang, Z. "Enhancing moisture resistance of starch-coated paper by improving the film forming capability of starch film." *Industrial Crops and Products* **2017**, 100, 12-18.
- Liu, G., Dhana, K., Furtado, J. D., Rood, J., Zong, G., Liang, L., ... & Sun, Q. Perfluoroalkyl substances and changes in body weight and resting metabolic rate in response to weight-loss diets: a prospective study. *PLoS medicine*, **2018**, *15*.2: e1002502.
- Liu, Y., Wang, L., Wang, F., & Ma, S. "Water-resistant, antibacterial, PDA@ ZnO/PLA cellulose composite paper with thermoformability." *Materials Letters.* **2024** 354: 135339.
- Long, Zhu, et al. "Preparation and oil-resistant mechanism of chitosan/cationic starch oil-proof paper." *BioResources* **2015**, 10.4: 7907-7920.
- Maisonet, M., Näyhä, S., Lawlor, D. A., & Marcus, M. Prenatal exposures to perfluoroalkyl acids and serum lipids at ages 7 and 15 in females. *Environment international*, **2015**:*82*, 49-60.
- Manfra, L., Marengo, V., Libralato, G., Costantini, M., De Falco, F., & Cocca, M. Biodegradable polymers: A real opportunity to solve marine plastic pollution?. *Journal of Hazardous Materials*, **2021**, 416: 125763.
- Martins, N. C., Freire, C. S., Pinto, R. J., Fernandes, S. C., Pascoal Neto, C., Silvestre, A. J.,Trindade, T. (2012). Electrostatic assembly of Ag nanoparticles onto nanofibrillated cellulose for antibacterial paper products. *Cellulose*, **2012**, 19:1425-1436.
- Matilla-Santander, N., Valvi, D., Lopez-Espinosa, M. J., Manzano-Salgado, C. B., Ballester, F., Ibarluzea, J., Vrijheid, M. Exposure to perfluoroalkyl substances and metabolic outcomes in pregnant women: evidence from the Spanish INMA birth cohorts. *Environmental Health Perspectives*, **2017**:*125*.11, 117004.
- Mitelut, A.C.; Tanase, E.E.; Popa, V.I.; Popa, M.E. Sustainable alternative for food packaging: Chitosan biopolymer—A review. *AgroLife Sci. J.* **2015**, *4*, 2286.
- Mousavioun, Payam, Graeme A. George, and William OS Doherty. "Environmental degradation of lignin/poly (hydroxybutyrate) blends." *Polymer degradation and stability*. **2012** 97.7: 1114-1122.
- Nair A.,. Kansal D, Khan A., Rabnawaz M., Oil- and water-resistant paper substrate using blends of chitosan-graft-polydimethylsiloxane and poly(vinyl alcohol), *J. Appl. Polym. Sci*. **2021**, 138.21: 50494.
- Nair, Aditya, Kansal, D., Khan, A., Rabnawaz, M. New alternatives to single-use plastics: Starch and chitosan-graft-polydimethylsiloxane-coated paper for water-and oil-resistant applications. *Nano Select*, **2022**, 3.2: 459-470.
- Oloyede, O.O.; Lignou, S. Sustainable Paper-Based Packaging: A Consumer's Perspective. Foods **2021**, 10, 1035.
- Panda, Pradeep Kumar, Kambiz Sadeghi, and Jongchul Seo. "Recent advances in poly (vinyl alcohol)/natural polymer based films for food packaging applications: A review." *Food Packaging and Shelf Life*, **2022**, 33: 100904.

- Parvathy, P. A., and Sushanta K. Sahoo. "Hydrophobic, moisture resistant and biorenewable paper coating derived from castor oil based epoxy methyl ricinoleate with repulpable potential." *Progress in Organic Coatings* **2021**, 158: 106347.
- Petchwattana, N., Naknaen, P., Cha-Aim, K., Suksri, C., Sanetuntikul, J. "Controlled release antimicrobial sachet prepared from poly (butylene succinate)/geraniol and ethylene vinyl alcohol coated paper for bread shelf-life extension application." *International Journal of Biological Macromolecules,* **2021**, 189: 251-261.
- Rastogi, Vibhore Kumar, and Pieter Samyn. "Bio-based coatings for paper applications." *Coatings*, **2015**, 5.4: 887-930.
- Reis, A. B., Yoshida, C. M., Reis, A. P. C., & Franco, T. T."Application of chitosan emulsion as a coating on Kraft paper." *Polymer International* **2011**, 60.6, 963-969.
- Rillig, Matthias C. "Microplastic in terrestrial ecosystems and the soil?." **2012**: 6453-6454.
- Rivero, S., García, M. A., Pinotti, A. Composite and bi-layer films based on gelatin and chitosan. Journal of Food Engineering. **2009**, 90:531–539.
- Roman, M.; Nechita, P.; Vasile, M.-A.; Cantaragiu Ceoromila, A.-M. Barrier and Antimicrobial Properties of Coatings Based on Xylan Derivatives and Chitosan for Food Packaging Papers. *Coatings* **2023**,13,1761.
- Salemi, F., Lamagna, G., Coco, V., & Barone, L. G. "Preparation and characterization of biodegradable paper coated with blends based on PHA." *International Symposium on High Technology for Greenhouse System Management: Greensys.* **2007** 801. 2007.
- Sängerlaub, S.; Brüggemann, M.; Rodler, N.; Jost, V.; Bauer, K.D. Extrusion Coating of Paper with Poly(3-hydroxybutyrate-co-3-hydroxyvalerate) (PHBV)—Packaging Related Functional Properties. *Coatings* **2019**, *9*, 457.
- Schwarz, A. E., Ligthart, T. N., Boukris, E., & Van Harmelen, T. Sources, transport, and accumulation of different types of plastic litter in aquatic environments: a review study. *Marine pollution bulletin*, **2019**: *143*, 92-100.
- Selvaraj, V., Karthika, T. S., Mansiya, C., & Alagar, M. "ZnO nano grafted chitin–chitosan based hybrid composite coated super hydrophobic filter paper for water flow cleaning and oil–water separation applications." *New Journal of Chemistry*. **2023**, 47.28:13397-13408.
- Shorey, Rohan, and Tizazu H. Mekonnen. "Sustainable paper coating with enhanced barrier properties based on esterified lignin and PBAT blend." *International Journal of Biological Macromolecules*, **2022**, 209: 472-484.
- Soergel, B.; Kriegler, E.; Weindl, I.; Rauner, S.; Dirnaichner, A.; Ruhe, C.; Hofmann, M.; Bauer, N.; Bertram, C.; Bodirsky, B.L.; et al. A Sustainable Development Pathway for Climate Action within the UN 2030 Agenda. Nat. Clim. Chang. **2021**, 11, 656–664.
- Sogut, Ece, and Atif Can Seydim. "Development of Chitosan and Polycaprolactone based active bilayer films enhanced with nanocellulose and grape seed extract." *Carbohydrate Polymers*, **2018**. 195: 180-188.
- Song, Z., Tang, J., Wang, H., Guan, F., Wu, Y., & Liu, W Water and oil resistance improvement of paper coated with aqueous mixture of hydrophilic and hydrophobic cross-linked copolymers. *BioResources*. **2020**, 15.2:3147-3160.
- Steenland, Kyle, Tony Fletcher, and David A. Savitz. "Epidemiologic evidence on the health effects of perfluorooctanoic acid (PFOA)." *Environmental health perspectives,* **2010***,* 118.8: 1100-1108.
- Sundar, N., Kumar, A., Pavithra, A., Ghosh, S. "Studies on semi-crystalline poly lactic acid (PLA) as a hydrophobic coating material on kraft paper for imparting barrier

properties in coated abrasive applications." *Progress in Organic Coatings* **2020** 145: 105682.

- Sunderland, E. M., Hu, X. C., Dassuncao, C., Tokranov, A. K., Wagner, C. C., & Allen, J. G. A review of the pathways of human exposure to poly-and perfluoroalkyl substances (PFASs) and present understanding of health effects. *Journal of exposure science & environmental epidemiology*, **2019**, *29*(2), 131-147.
- Taib, N. A. A. B., Rahman, M. R., Huda, D., Kuok, K. K., Hamdan, S., Bakri, M. K. B., Khan, A."A review on poly lactic acid (PLA) as a biodegradable polymer." *Polymer Bulletin* **2023**, 80.2: 1179-1213.
- Tarnowiecka-Kuca, A.; Peeters,R.;Bamps,B.;Stobin´ska,M.; Kamola, P.; Wierzchowski, A.; Bartkowiak,A.;Mizielin´ska,M. Paper Coatings Based on Polyvinyl Alcohol and Cellulose Nanocrystals Using Various Coating Techniques and Determination of Their Barrier Properties. *Coatings* **2023**, 13, 11:1975.
- Tayeb A.H.,. Tajvidi M, Bousfield D., Paper-based oil barrier packaging using lignin-containing cellulose nanofibrils, Molecules. **2020,** 25.6: 1344.
- Teodorescu, Mirela, Maria Bercea, and Simona Morariu. "Biomaterials of poly (vinyl alcohol) and natural polymers." *Polymer Reviews***, 2018***,* 58.2: 247-287.
- Thurber, H., and Curtzwiler, G. W. Suitability of Poly(butylene Succinate) as a Coating for Paperboard Convenience Food Packaging. *Int. J. Biobased Plastics 2*, **2020**, 1–12. doi:10.1080/24759651.2020.1785094
- Tian, H., Yan, J., Rajulu, A. V., Xiang, A., & Luo, X. "Fabrication and properties of polyvinyl alcohol/starch blend films: Effect of composition and humidity." *International Journal of Biological Macromolecules*, **2017**, 96: 518-523.
- van den Broek, Lambertus AM, et al. "Chitosan films and blends for packaging material." *Carbohydrate polymers* **2015**, 116: 237-242.
- Vieira, V. M., Hoffman, K., Shin, H. M., Weinberg, J. M., Webster, T. F., & Fletcher, T. Perfluorooctanoic acid exposure and cancer outcomes in a contaminated community: a geographic analysis. *Environmental health perspectives*, **2013**, 121.3: 318-323.
- Vrabič Brodnjak, U.; Tihole, K. Chitosan Solution Containing Zein and Essential Oil as Bio Based Coating on Packaging Paper. *Coatings* **2020**, *10*, 497.
- Wagner, M., Scherer, C., Alvarez-Muñoz, D., Brennholt, N., Bourrain, X., Buchinger, S., Reifferscheid, G. Microplastics in freshwater ecosystems: what we know and what we need to know. *Environmental Sciences Europe*, **2014**, 26.1: 1-9.
- Wang, F. J., Wang, L. Q., Zhang, X. C., Ma, S. F., Zhao, Z. C. "Enhancement of oil resistance of cellulose packaging paper for food application by coating with materials derived from natural polymers." *Journal of Food Engineering.* **2022**, 332: 111039.
- Wang, Kaipeng, Lihong Zhao, and Beihai He. Chitosan/montmorillonite coatings for the fabrication of food-safe greaseproof paper. *Polymers*. **2021**, 13.10: 1607.
- Witt, U., R. J. Muller, and W. D. Deckwer. "Biodegradable Polyester Copolymers with Adaptable Application Properties Based on Mass Chemical-Products." *Chemie Ingenieur Technik.* **1995**, 67.7:904-907.
- Yasar, S., Nizamlıoğlu, N. M., Gücüş, M. O., Bildik Dal, A. E., & Akgül, K. Origanum majorana L. essential oil-coated paper acts as an antimicrobial and antioxidant agent against meat spoilage. *ACS omega*, **2022**, *7*.10, 9033-9043.
- Zalasiewicz, J., Waters, C. N., Do Sul, J. A. I., Corcoran, P. L., Barnosky, A. D., Cearreta, A., Yonan, Y. The geological cycle of plastics and their use as a stratigraphic indicator of the Anthropocene. *Anthropocene*, **2016**: *13*, 4-17.

- Zhang, C., Sundaram, R., Maisog, J., Calafat, A. M., Barr, D. B., & Louis, G. M. B. A prospective study of prepregnancy serum concentrations of perfluorochemicals and the risk of gestational diabetes. *Fertility and sterility*, **2015**, *103*.1, 184-189.
- Zhang, H., Bussini, D., Hortal, M., Elegir, G., Mendes, J., & Beneyto, M. J. "ZnO-PLA nanocomposite coated paper for antimicrobial packaging application." *Lwt*. **2017**, 78: 250-257.
- Zhang, Hai, et al. "PLA coated paper containing active inorganic nanoparticles: material characterization and fate of nanoparticles in the paper recycling process." *Waste management*. **2016** 52: 339-345.
- Zhu, P., Kuang, Y., Chen, G., Liu, Y., Peng, C., Hu, W., Fang, Z. "Starch/polyvinyl alcohol (PVA)-coated painting paper with exceptional organic solvent barrier properties for art preservation purposes." *Journal of materials science* **2018**, 53, 5450-5457.
- Zhu, Q., Tan, J., Li, D., Zhang, T., Liu, Z., Cao, Y. Cross-linked chitosan/tannin extract as a biodegradable and repulpable coating for paper with excellent oil-resistance, gas barrier and UV-shielding. *Progress in Organic Coatings*. **2023**, 176: 107399.
- Zubris, Kimberly Ann V., and Brian K. Richards. "Synthetic fibers as an indicator of land application of sludge." *Environmental pollution,* **2005**, 138.2: 201-211.

Web sites

(https://plasticseurope.org/knowledge-hub/plastics-the-fast-facts-2023/)

- Alleanza Italiana per lo Sviluppo Sostenibile - Rapporto ASviS 2023 – L'Italia e gli obiettivi di sviluppo sostenibile. (2023). Available at link: https://asvis.it/rapporto-2023/
- Aticelca. Sistema di valutazione 501:2019 valutazione del livello di riciclabilità di materiali e prodotti a prevalenza cellulosica sulla base della norma UNI 11743:2019. **2019**. Available at link: https://www.aticelca.it/1/wp-content/uploads/2019/08/sistema_di_valutazione_501_2019.pdf
- Cepi. Harmonized European laboratory test method to generate parameters enabling the assessment of the recyclability of paper and board products in standard paper and board recycling mills. **2022.** Available at link: https://www.cepi.org/cepi-recyclability-test-method-version-2/
- CONAI. Contributo ambientale. **2022**. Available at link: https://www.conai.org/imprese/contributo-ambientale/contributo-diversificato-carta/
- CONAI. Contributo ambientale. **2024**. Available at link: https://www.conai.org/imprese/contributo-ambientale/
- Directive 2019/904. *Directive (EU) 2019/904 of the European Parliament and of the Council of 5 June 2019 on the reduction of the impact of certain plastic products on the environment*. Available at link: http://data.europa.eu/eli/dir/2019/904/oj
- European Commission – Global Action on Plastics, **2022.** Available at link: https://environment.ec.europa.eu/topics/plastics/global-action-plastics_en
- Facts and Statistics 2023 - Plastic Pollution in The Ocean , **2022**. Available at link: https://www.rts.com/blog/plastic-pollution-in-the-ocean-2023-facts-and-statistics/
- Federazione Carta e Grafica – Confindustria e dati Assocarta - Relazione del presidente - Carta: la buona fibra per la transizione. **2023**. Available at link:

https://www.assocarta.it/it/documenti/category/2-chi-siamo.html?download=430:relazione-presidente-2023

- Gifasp - linee guida: per la conformità di materiali e oggetti di carta e cartone destinati al contatto con gli alimenti https://gifasp.it/wp-content/uploads/sites/4/2021/10/Food-Contact-Industry-Guidelines_2019_final_IT.pdf
- Legislative Decree 196/2021, April **2021**. Available at link: https://www.gazzettaufficiale.it/eli/id/2021/11/30/21G00210/sg
- Pinkas, Mariia Vasylivna, and Romaniia Ivanivna Cheropkina. Tendencies of manufacture of packing materials from cardboard. **2023** Available at link: http://www.konferenciaonline.org.ua/ua/article/id-954/
- Plastics Europe (2023) Plastics—the fast Facts 2023.
- Solution Coating Methods: A Comparison. (n.d.). Available at link: https://www.ossila.com/pages/solution-processing-techniques-comparison#BarCoating
- Statista Research Department, 2023. Global production volume of paper and paperboard 2010-2021, by type. Available at link: https://www.statista.com/statistics/270317/production-volume-of-paper-by-type/#statisticContainer
- UNIRIMA 2023 Report: the production of raw materials – end of waste from the separate collection of paper and cardboard, **2023**. Available at link: https://www.unirima.it/2023/10/30/rapporto-unirima-2023/
- United Nations - Take Action for the Sustainable Development Goals. Available at link: https://www.un.org/sustainabledevelopment/sustainable-development-goals/
- What is Mayer bar coating? **2022**. Available at link: https://en.huayang-ppm.com/article/what-is-mayer-bar-coating.html

Books

- Robertson, G.L. Food Packaging: Principles and Practice, Third Edition (3rd ed.). CRC Press. **2012** https://doi.org/10.1201/b21347
- Van den Oever, M., Molenveld, K., van der Zee, M., & Bos, H. Bio-based and biodegradable plastics: facts and figures: focus on food packaging in the Netherlands (No. 1722). Wageningen Food & Biobased Research. **2017**

References chapter 2

- Deshwal, G.K.; Panjagari, N.R.; Alam, T. An Overview of Paper and Paper Based Food Packaging Materials: Health Safety and Environmental Concerns. *J. Food Sci. Technol*. **2019**, 56, 4391–4403.
- Deshwal, G.K.; Panjagari, N.R.; Alam, T. An Overview of Paper and Paper Based Food Packaging Materials: Health Safety and Environmental Concerns. *J. Food Sci. Technol.* **2019**, 56, 4391–4403.
- Khwaldia, K.; Arab-Tehrany, E.; Desobry, S. Biopolymer Coatings on Paper Packaging Materials. *Compr. Rev. Food Sci. Food Saf.* **2010**, 9, 82–91.
- Kopacic, S.; Walzl, A.; Zankel, A.; Leitner, E.; Bauer, W. Alginate and Chitosan as a Functional Barrier for Paper-Based Packaging Materials. *Coatings* **2018**, 8, 235.
- Marinelli, A.; Santi, R.; Del Curto, B. Guidelines for Facilitating the Recycling of Packaging Made Predominantly from Paper, CONAI. **2020.** Available online: http://www.progettarericiclo.com/en/docs/guidelines-facilitating-recycling-packaging-made- predominantly-paper.
- Nair, A.; Kansal, D.; Khan, A.; Rabnawaz, M. New Alternatives to Single-use Plastics: Starch and Chitosan- Graft -polydimethylsiloxane-coated Paper for Water- and Oil-resistant *Applications. Nano Select*. **2022**, 3, 459–470.
- Nechita, P.; Roman (Iana-Roman), M. Review on Polysaccharides Used in Coatings for Food Packaging Papers. *Coatings* **2020**, 10, 566.
- Nicu, R.; Lupei, M.; Balan, T.; Bobu, E. Alkyl-Chitosan as Paper Coating to Improve Water Barrier Properties. *Cellul. Chem. Technol*. **2013**, 47, 623–630.
- Oloyede, O.O.; Lignou, S. Sustainable Paper-Based Packaging: A Consumer's Perspective. *Foods* **2021**, 10, 1035.
- Ruiz-Real, J.L.; Uribe-Toril, J.; Valenciano, J.D.P.; Gázquez-Abad, J.C. Worldwide Research on Circular Economy and Environment: A Bibliometric Analysis. *Int. J. Environ. Res. Public Health* **2018**, 15, 2699.
- Soergel, B.; Kriegler, E.; Weindl, I.; Rauner, S.; Dirnaichner, A.; Ruhe, C.; Hofmann, M.; Bauer, N.; Bertram, C.; Bodirsky, B.L.; et al. A Sustainable Development Pathway for Climate Action within the UN 2030 Agenda. *Nat. Clim. Chang*. **2021**, 11
- Triantafillopoulos, N.; Koukoulas, A.A. The Future of Single-Use Paper Coffee Cups: Current Progress and Outlook. *BioResources* **2020**, 15, 7260–7287.
- Vila-Lopez, N.; Küster-Boluda, I. A Bibliometric Analysis on Packaging Research: Towards Sustainable and Healthy Packages. *Br. Food J*. **2021**, 123, 684–701

References chapter 3

- Anbukarasu, P.; Sauvageau, D.; Elias, A. Tuning the Properties of Polyhydroxybutyrate Films Using Acetic Acid via Solvent Casting. *Sci. Rep.* **2016**, 5, 17884.
- ASTM F119-82. Standard Test Method for Rate of Grease Penetration of Flexible Barrier Materials (Rapid Method); ASTM International:West Conshohocken, PA, USA, **2015**.
- Barabaszová, K. C.; Holešová, S.; Hundáková, M.; Mohyla, V. Vermiculite in Polycaprolactone Films Prepared with the Used of Ultrasound. *Mater. Today Proc.* **2021**, 37, 13–20.
- Bedane, A.H.; Xiao, H.; Eic´, M.; Farmahini-Farahani, M. Structural and Thermodynamic Characterization of Modified Cellulose Fiber-Based Materials and Related Interactions with Water Vapor. *Appl. Surf. Sci.* **2015**, 351, 725–737.
- Bota, J.; Vukoje, M.; Brozovic´, M.; Hrnjak-Murgic´, Z. Reduced Water Permeability of Biodegradable PCL Nanocomposite Coated Paperboard Packaging. *Chem. Biochem. Eng. Q.* **2017**, 31, 417–424.
- Bugnicourt, E.; Cinelli, P.; Lazzeri, A.; Alvarez, V. Polyhydroxyalkanoate (PHA): Review of Synthesis, Characteristics, Processing and Potential Applications in Packaging. *Express Polym. Lett.* **2014**, 8, 791–808.
- Catoni, S.E.M.; Trindade, K.N.; Gomes, C.A.T.; Schneider, A.L.S.; Pezzin, A.P.T.; Soldi, V. Influence of Poly(Ethylene Grycol)—PEG) on the Properties of Influence of Poly(3-Hydroxybutyrate-CO-3-Hydroxyvalerate)—PHBV. *Polímeros* **2013**, 23, 320–325.
- Cyras, V.P.; Commisso, M.S.; Mauri, A.N.; Vázquez, A. Biodegradable Double-Layer Films Based on Biological Resources: Polyhydroxybutyrate and Cellulose. *J. Appl. Polym. Sci.* **2007**, 106, 749–756.
- Din, M.I.; Ghaffar, T.; Najeeb, J.; Hussain, Z.; Khalid, R.; Zahid, H. Potential Perspectives of Biodegradable Plastics for Food Packaging Application-Review of Properties and Recent Developments. *Food Addit. Contam.* Part A **2020,** 37, 665–680.
- Fabra, M.J.; López-Rubio, A.; Cabedo, L.; Lagaron, J.M. Tailoring Barrier Properties of Thermoplastic Corn Starch-Based Films (TPCS) by Means of a Multilayer Design. *J. Colloid Interface Sci.* **2016**, 483, 84–92.
- Gamba, A.M.; Fonseca, J.S.; Méndez, D.A.; Viloria, A.C.; Fajardo, D.; Moreno, N.C.; Rojas, I.C. Assessment of Different Plasticizer Polyhydroxyalkanoate Mixtures to Obtain Biodegradable Polimeric Films. *Chem. Eng. Trans.* **2017**, 57, 1363–1368.
- Gietl, M.L.; Schmidt, H.-W.; Giesa, R.; Terrenoire, A.; Balk, R. Semiquantitative Method for the Evaluation of Grease Barrier Coatings. *Prog. Org. Coat.* **2009**, 66, 107–112.
- Han, J.; Salmieri, S.; Le Tien, C.; Lacroix, M. Improvement of Water Barrier Property of Paperboard by Coating Application with Biodegradable Polymers. *J. Agric. Food Chem*. **2010**, 58, 3125–3131.
- Helanto, K.; Matikainen, L.; Talja, R.; Rojas, O.J. Bio-Based Polymers for Sustainable Packaging and Biobarriers: A Critical Review. *BioResources* **2019**, 14, 4902–4951.
- Jost, V. Packaging Related Properties of Commercially Available Biopolymers—An Overview of the Status Quo. *Express Polym. Lett.* **2018**, 12, 429–435.
- Jost, V.; Langowski, H.-C. Effect of Different Plasticisers on the Mechanical and Barrier Properties of Extruded Cast PHBV Films. *Eur. Polym. J.* **2015**, 68, 302–312.
- Kliem, S.; Kreutzbruck, M.; Bonten, C. Review on the Biological Degradation of Polymers in Various Environments. *Materials* **2020**, 13, 4586.

- Kubiak, K.J.; Wilson, M.C.T.; Mathia, T.G.; Carval, P. Wettability versus Roughness of Engineering Surfaces. *Wear* **2011**, 271,523–528.
- McKeen, L.W. Environmentally friendly polymers. In Permeability Properties of Plastics and Elastomers, 3rd ed.; William Andrew Publishing: Norwich, NY, USA, **2012**; pp. 287–304. ISBN 978-1-4377-3469-0.
- Meereboer, K.W.; Misra, M.; Mohanty, A.K. Review of Recent Advances in the Biodegradability of Polyhydroxyalkanoate (PHA) Bioplastics and Their Composites. *Green Chem.* **2020,** 22, 5519–5558.
- Parra, D.F.; Fusaro, J.; Gaboardi, F.; Rosa, D.S. Influence of Poly (Ethylene Glycol) on the Thermal, Mechanical, Morphological, Physical–Chemical and Biodegradation Properties of Poly (3-Hydroxybutyrate). *Polym. Degrad. Stab.* **2006,** 91, 1954–1959.
- Rastogi, V.; Samyn, P. Bio-Based Coatings for Paper Applications. *Coatings* **2015**, 5, 887–930.
- Reichert, C.L.; Bugnicourt, E.; Coltelli, M.-B.; Cinelli, P.; Lazzeri, A.; Canesi, I.; Braca, F.; Martínez, B.M.; Alonso, R.; Agostinis, L.; et al. Bio-Based Packaging: Materials, Modifications, Industrial Applications and Sustainability. *Polymers* **2020**, 12, 1558.
- Requena, R.; Jiménez, A.; Vargas, M.; Chiralt, A. Effect of Plasticizers on Thermal and Physical Properties of Compression- Moulded Poly[(3-Hydroxybutyrate)-Co-(3-Hydroxyvalerate)] Films. *Polym. Test.* **2016a**, 56, 45–53.
- Requena, R.; Jiménez, A.; Vargas, M.; Chiralt, A. Poly[(3-Hydroxybutyrate)-Co-(3-Hydroxyvalerate)] Active Bilayer Films Obtained by Compression Moulding and Applying Essential Oils at the Interface: Antimicrobial PHBV Active Bilayer Films Obtained by Compression Moulding. *Polym. Int.* **2016b**, 65, 883–891.
- Requena, R.; Vargas, M.; Chiralt, A. Release Kinetics of Carvacrol and Eugenol from Poly(Hydroxybutyrate-Co-Hydroxyvalerate) (PHBV) Films for Food Packaging Applications. Eur. *Polym. J.* **2017**, 92, 185–193.
- Rosa, D.S.; Guedes, C.G.F.; Casarin, F.; Bragança, F.C. The Effect of the Mw of PEG in PCL/CA Blends. *Polym. Test.* **2005**, 24, 542–548.
- Ryan, B.J.; Poduska, K.M. Roughness Effects on Contact Angle Measurements. *Am. J. Phys.* **2008**, 76, 1074–1077.
- Rydz, J.; Musioł, M.; Zawidlak-We ̨grzyn ́ska, B.; Sikorska, W. Present and future of biodegradable polymers for food packaging applications. In Handbook of Food Bioengineering, Biopolym.Food Design; Alexandru, M.G., Alina, M.H., Eds.; Academic Press: Cambridge, MA, USA, **2018**; Volume 20, pp. 431–467. ISBN 978-0-12-811449-0.
- Sängerlaub, S.; Brüggemann, M.; Rodler, N.; Jost, V.; Bauer, K.D. Extrusion Coating of Paper with Poly(3-Hydroxybutyrate-Co-3- Hydroxyvalerate) (PHBV)—Packaging Related Functional Properties. *Coatings* **2019**, 9, 457.
- Shogren, R. Water Vapor Permeability of Biodegradable Polymers. *J. Environ. Polym. Degrad.* **1997**, 5, 91–95.
- Suzuki, M.; Tachibana, Y.; Kasuya, K. Biodegradability of Poly(3-Hydroxyalkanoate) and Poly(ε-Caprolactone) via Biological Carbon Cycles in Marine Environments. *Polym. J.* **2021**, 53, 47–66.
- Tang, Z.G.; Black, R.A.; Curran, J.M.; Hunt, J.A.; Rhodes, N.P.; Williams, D.F. Surface Properties and Biocompatibility of Solvent-Cast Poly[ε-Caprolactone] Films. *Biomaterials* **2004**, 25, 4741–4748.
- Vieira, M.G.A.; da Silva, M.A.; dos Santos, L.O.; Beppu, M.M. Natural-Based Plasticizers and Biopolymer Films: A Review. *Eur. Polym. J.* **2011**, 47, 254–263.

- Wu, F.; Misra, M.; Mohanty, A.K. Challenges and New Opportunities on Barrier Performance of Biodegradable Polymers for Sustainable Packaging. *Prog. Polym. Sci*. **2021**, 117, 101395.
- Xu, Y.; Zou, L.; Lu, H.; Kang, T. Effect of Different Solvent Systems on PHBV/PEO Electrospun Fibers. RSC Adv. **2017**, 7, 4000–4010. *Appl. Sci.* **2021**, 11, 8058 17 of 17
- Zhang, S.; Campagne, C.; Salaün, F. Influence of Solvent Selection in the Electrospraying Process of Polycaprolactone. *Appl. Sci.* **2019a**, 9, 402.
- Zhang, S.; Campagne, C.; Salaün, F. Preparation of Electrosprayed Poly(Caprolactone) Microparticles Based on Green Solvents and Related Investigations on the Effects of Solution Properties as Well as Operating Parameters. *Coatings* **2019b**, 9, 84.

References chapter 4

- Adibi, A.; Trinh, B.M.; Mekonnen, T.H. Recent progress in sustainable barrier paper coating for food packaging applications. *Prog. Org. Coat.* **2023,** 181, 107566.
- Amariei, S.; Ursachi, F.; Petraru, A. Development of New Biodegradable Agar-Alginate Membranes for Food Packaging. *Membranes* **2022**, 12, 576.
- ASTM D1938-19. Standard Test Method for Tear-Propagation Resistance (Trouser Tear) of Plastic Film and Thin Sheeting by a Single-Tear Method. **2019**
- ASTM D882-18; Standard Test Method for Tensile Properties of Thin Plastic Sheeting. ASTM International: West Conshohocken, PA, USA, **2018**.
- Aulin, C.; Ström, G. Multilayered Alkyd Resin/Nanocellulose Coatings for Use in Renewable Packaging Solutions with a High Level of Moisture Resistance. *Ind. Eng. Chem. Res.* **2013**, 52, 2582–2589.
- Bota, J.; Vukoje, M.; Brozovic, M.; Hrnjak-Murgic, Z. Reduced Water Permeability of Biodegradable PCL Nanocomposite Coated Paperboard Packaging. *Chem. Biochem. Eng. Q.* **2018**, 31, 417–424.
- Chi, K.; Wang, H.; Catchmark, J.M. Sustainable Starch-Based Barrier Coatings for Packaging Applications. *Food Hydrocoll*. **2020**,103, 105696.
- Choi, I.; Lee, J.Y.; Lacroix, M.; Han, J. Intelligent PH Indicator Film Composed of Agar/Potato Starch and Anthocyanin Extracts from Purple Sweet Potato. *Food Chem*. **2017**, 218, 122–128.
- Dobrovszky, K.; Ronkay, F. Effects of Phase Inversion on Molding Shrinkage, Mechanical and Burning Properties of Injection Molded PET/HDPE and PS/HDPE Polymer Blends. *Polym. Plast. Technol. Eng*. **2017**, 56, 1147–1157.
- Domene-López, D.; García-Quesada, J.C.; Martin-Gullon, I.; Montalbán, M.G. Influence of Starch Composition and Molecular Weight on Physicochemical Properties of Biodegradable Films. *Polymers* **2019**, 11, 1084.
- Ewender, J.; Franz, R.; Welle, F. Permeation of Mineral Oil Components from Cardboard Packaging Materials through Polymer Films. *Packag. Technol. Sci*. **2013**, 26, 423–434.
- Gietl, M.L.; Schmidt, H.-W.; Giesa, R.; Terrenoire, A.; Balk, R. Semiquantitative method for the evaluation of grease barrier coatings. *Progr. Org. Coat*. **2009**, 66, 107–112.
- Guo, Y.; Zhang, B.; Zhao, S.; Qiao, D.; Xie, F. Plasticized Starch/Agar Composite Films: Processing, Morphology, Structure, Mechanical Properties and Surface Hydrophilicity. *Coatings* **2021**, 11, 311.
- Hormoz, E.; Tizazu, H. Mekonnen, Flexible and green multilayer paper coating for barrier enhancement of paper packaging. *Sust. Mat. Technol*. **2023**, 37, e00694.
- Hubbe, M.A.; Gardner, D.J.; Shen, W. Contact angles and wettability of cellulosic surfaces: A review of proposed mechanisms and test strategies. *BioResources* **2015**, 10, 8657.
- Lo Faro, E.; Menozzi, C.; Licciardello, F.; Fava, P. Improvement of Paper Resistance against Moisture and Oil by Means Coatings with Poly(-3-Hydroxybutyrate-Co-3-Hydroxyvalerate) (Phbv) and Polycaprolactone (Pcl). *Appl. Sci*. **2021**, 11, 8058.
- Long, Z.; Wu, M.; Peng, H.; Dai, L.; Zhang, D.; Wang, J. Preparation and oil-resistant mechanism of chitosan/cationic starch oil-proof paper. *BioResources* **2015**, 10, 7907–7920.

- Mahuwala, A.A.; Hemant, V.; Meharwade, S.D.; Deb, A.; Chakravorty, A.; Grace, A.N.; Raghavan, V. Synthesis and Char- acterisation of Starch/Agar Nanocomposite Films for Food Packaging Application. IET *Nanobiotechnol*. **2020**, 14, 809–814.
- Montgomery, D.C. Design and Analysis of Experiments, 8th ed.; John Wiley & Sons: Hoboken, NJ, USA, **2012**; Volume 2, ISBN 9781118146927.
- Ortega-Toro, R.; Muñoz, A.; Talens, P.; Chiralt, A. Improvement of Properties of Glycerol Plasticized Starch Films by Blending with a Low Ratio of Polycaprolactone and/or Polyethylene Glycol. *Food Hydrocoll*. **2016,** 56, 9–19.
- Reis, A.B.; Yoshida, C.M.P.; Reis, A.P.C.; Franco, T.T. Application of Chitosan Emulsion as a Coating on Kraft Paper. *Polym. Int.* **2011**, 60, 963–969.
- Requena, R.; Jiménez, A.; Vargas, M.; Chiralt, A. Effect of Plasticizers on Thermal and Physical Properties of Compression- Moulded Poly[(3-Hydroxybutyrate)-Co-(3-Hydroxyvalerate)] *Films. Polym. Test*. **2016**, 56, 45–53.
- Rogovina, S.Z.; Aleksanyan, K.V.; Loginova, A.A.; Ivanushkina, N.E.; Vladimirov, L.V.; Prut, E.V.; Berlin, A.A. Influence of PEG on Mechanical Properties and Biodegradability of Composites Based on PLA and Starch. *Starch/Staerke* **2018**, 70, 1700268.
- Roy, S.; Rhim, J.W. Starch/Agar-Based Functional Films Integrated with Enoki Mushroom-Mediated Silver Nanoparticles for Active Packaging Applications. *Food Biosci.* **2022**, 49, 101867.
- Singh, R.P.; Pandey, J.K.; Rutot, D.; Degée, P.; Dubois, P. Biodegradation of Poly(ε-Caprolactone)/Starch Blends and Composites in Composting and Culture Environments: The Effect of Compatibilization on the Inherent Biodegradability of the Host Polymer. *Carbohydr. Res*. **2003**, 338, 1759–1769.
- Sogut, E.; Seydim, A.C. Development of Chitosan and Polycaprolactone Based Active Bilayer Films Enhanced with Nanocellulose and Grape Seed Extract. *Carbohydr. Polym*. **2018**, 195, 180–188.
- Song, Z.; Xiao, H.; Zhao, Y. Hydrophobic-Modified Nano-Cellulose Fiber/PLA Biodegradable Composites for Lowering Water Vapor Transmission Rate (WVTR) of Paper. *Carbohydr. Polym*. **2014**, 111, 442–448.
- Sundar, N.; Keerthana, P.; Kumar, S.A.; Kumar, G.A.; Ghosh, S. Dual Purpose, Bio-Based Polylactic Acid (PLA)-Polycaprolactone (PCL) Blends for Coated Abrasive and Packaging Industrial Coating Applications. *J. Polym. Res*. **2020**, 27, 386.
- TAPPI Test Method T 559 cm-02; Grease Resistance Test for Paper and Paperboard. Tappi Press: Atlanta, GA, USA, **2002**.
- Yokoyama, T.; Nakai, K. Evaluation of In-Plane Orthotropic Elastic Constants of Paper and Paperboard. *Dimensions* **2007**, 60, 50.

References chapter 5

- Aulin, C., & Ström, G. Multilayered alkyd resin/nanocellulose coatings for use in renewable packaging solutions with a high level of moisture resistance. *Industrial and Engineering Chemistry Research*, **2013**, 52(7), 2582–2589
- Cigognini,I.; Montanari,A.; Dela Torre Carreras,R.; Cardoso,G. Extraction Method of a Polyester Polymeror Cutinfrom the Wasted Tomato Peels and Polyester Polimer so Extracted. WO Patent WO2015028299, 3 May **2015**.
- Dominguez, E., Heredia-Guerrero, J.A., and Heredia, A. The bio- physical design of plant cuticles: an overview. *New Phytologist* **2011**
- Eraslan, K., Aversa, C., Nofar, M., Barletta, M., Gisario, A., Salehiyan, R., & Goksu, Y. A. Poly (3-hydroxybutyrate-co-3-hydroxyhexanoate)(PHBH): Synthesis, properties, and applications-A Review. *European Polymer Journal*, **2022**, 167, 111044.
- Heredia-Guerrero, Jose A., et al. "Synthesis and characterization of a plant cutin mimetic polymer." *Polymer* , **2009**, 50.24: 5633-5637
- Hood, C.; Laredo, T.; Marangoni, A.G.; Pensini, E. Water-repellent films from corn protein and tomato cutin. *J. Appl. Polym. Sci.* **2021**, *138*, 50831.
- Liminana, P., Garcia-sanoguera, D., Quiles-Carrillo, L., Balart, R., and Montanes, N. Development and Characterization of Environmentally Friendly Composites from Poly(butylene Succinate) (PBS) and Almond Shell Flour with Different Compatibilizers. *Compos. Part B Eng.* **2018**, 144, 153-162.
- Lo Faro, E.; Menozzi, C.; Licciardello, F.; Fava, P. Improvement of Paper Resistance against Moisture and Oil by Coating with Poly(-3-hydroxybutyrate-co-3-hydroxyvalerate) (PHBV) and Polycaprolactone (PCL). *Appl. Sci.* **2021**, 11, 8058.
- Manrich, A.; Moreira, F.K.; Otoni, C.G.; Lorevice, M.V.; Martins, M.A.; Mattoso, L.H. Hydrophobic edible films made up of tomato cutin and pectin. *Carbohydr.Polym.* **2017**, *164*, 83–91.
- Marc, Mathilde, et al. "Bioinspired co-polyesters of hydroxy-fatty acids extracted from tomato peel agro-wastes and glycerol with tunable mechanical, thermal and barrier properties." *Industrial Crops and Products,* **2021**, 170: 113718.
- Rastogi, Vibhore Kumar, and Pieter Samyn. "Bio-based coatings for paper applications." *Coatings* **2015**, 5.4: 887-930.
- Schreiber, Lukas, and Jorg Schonherr. *Water and solute permeability of plant cuticles*. Berlin: Springer, **2009**.
- Simões A., Coelhoso I.M., Alves V.D., Brazinha C. Recovery and Purification of Cutin from Tomato By-Products for Application in Hydrophobic Films. *Membranes.* **2023**; 13(3):261.
- Song, Z., Xiao, H., & Zhao, Y. Hydrophobic-modified nano-cellulose fiber/PLA biodegradable composites for lowering water vapor transmission rate (WVTR) of paper. *Carbohydrate Polymers*, **2014**, 111, 442–448.
- Tedeschi,G.; Benitez,J.J.; Ceseracciu,L.; Dastmalchi,K.; Itin,B.; Stark,R.E.; Heredia,A.; Athanassiou,A.; Heredia-Guerrero,J.A. Sustainable Fabrication of Plant Cuticle-Like Packaging Films from Tomato Pomace Agro-Waste, Beeswax, and Alginate. *ACS Sustain. Chem. Eng.* **2018**, *6*, 14955–14966.
- Thurber, H., & Curtzwiler, G. W. Suitability of poly (butylene succinate) as a coating for paperboard convenience food packaging. *International Journal of Biobased Plastics*, **2020**, 2(1), 1-12.

References chapter 6

- ASTM D882-18; Standard Test Method for Tensile Properties of Thin Plastic Sheeting. ASTM International: West Conshohocken, PA, USA, **2018**.
- Bai, Xue, et al. "Macroporous poly (vinyl alcohol) foam crosslinked with epichlorohydrin for microorganism immobilization." *Journal of applied polymer science*, **2010**, 117.5: 2732-2739.
- Baraka, A., Hatem, H., El-Geundi, M. S., Tantawy, H., Karaghiosoff, K., Gobara, M., Kotb, M. M. A new cationic silver (I)/melamine coordination polymer,[Ag2 (melamine)] n2n+: Synthesis, characterization and potential use for aqueous contaminant anion exchange. *Journal of Solid State Chemistry*, **2019**, 274, 168-175.
- Bharati, Ashok Kumar, Prem Lama, and Kafeel Ahmad Siddiqui. "A novel mixed ligand Zn-coordination polymer: Synthesis, crystal structure, thermogravimetric analysis and photoluminescent properties." *Inorganica Chimica Acta*, **2020**, 500: 119219.
- Bhat, S. A., Zafar, F., Mondal, A. H., Mirza, A. U., Haq, Q. M. R., & Nishat, N. Efficient removal of Congo red dye from aqueous solution by adsorbent films of polyvinyl alcohol/melamine-formaldehyde composite and bactericidal effects. *Journal of Cleaner Production*, **2020**, *255*, 120062.
- Cohen, J. D., Erkenbrecher Jr, C. W., Haynie, S., Kelley, M. J., Kobsa, H., Roe, A. N., & Scholla, M. H. **1995**. U.S. Patent No. 5,428,078. Washington, DC: U.S. Patent and Trademark Office.
- Don, T. M., Chen, C. C., Lee, C. K., Cheng, W. Y. and Cheng, L. P. Preparation and antibacterial test of chitosan/PAA/PEGDA bi-layer composite membranes. Journal of Biomaterials Science, *Polymer Edition*, **2005**, 16(12), 1503-1519.
- Ehrend, E., Morche, K., Kempermann, Th. and Redetzky, W. Plasticizer for natural and or synthetic rubber. *c.f. chem. Abs* **1974** 80(6):28149S.
- Frei, A., Zuegg, J., Elliott, A. G., Baker, M., Braese, S., Brown, C. and Blaskovich, M. A. Metal complexes as a promising source for new antibiotics. *Chemical science*, **2020**, 11(10), 2627-2639.
- Gao, H., Sun, P., Zhang, Y., Zeng, X., Wang, D., Zhang, Y., Wu, J. A two-step hydrophobic fabrication of melamine sponge for oil absorption and oil/water separation. *Surface and Coatings Technology*, **2018**, 339, 147-154.
- Gautam, L., Warkar, S. G., Ahmad, S. I., Kant, R., & Jain, M. A review on carboxylic acid cross-linked polyvinyl alcohol: Properties and applications. *Polymer Engineering & Science*, **2022**, *62*(2), 225-246.
- Gauthier, M. A., Luo, J., Calvet, D., Ni, C., Zhu, X. X., Garon, M., & Buschmann, M. D. Degree of crosslinking and mechanical properties of crosslinked poly (vinyl alcohol) beads for use in solid-phase organic synthesis. *Polymer*, **2004**, 45(24), 8201-8210.
- Gauthier, M. A., Luo, J., Calvet, D., Ni, C., Zhu, X. X., Garon, M., & Buschmann, M. D. Degree of crosslinking and mechanical properties of crosslinked poly (vinyl alcohol) beads for use in solid-phase organic synthesis. *Polymer*, **2004**, 45(24), 8201-8210.
- Gianferrara, T., Bratsos, I., & Alessio, E. A categorization of metal anticancer compounds based on their mode of action. Dalton Transactions, **2009**, 37, 7588-7598.
- Gopinatha, P., P. Suresh, and V. Jeevanantham. "Mechanical, structural and optical properties of pristine and PVA capped zinc oxide nanocomposites." *Journal of Ovonic Research,* **2013** 19.1.
- Higazy, A., Hashem, M., ElShafei, A., Shaker, N., & Hady, M. A. Development of anti-microbial jute fabrics via in situ formation of cellulose–tannic acid–metal ion complex. *Carbohydrate Polymers*, **2010** 79(4), 890-897.

- Hojo, Nobumasa, Hirofusa Shirai, and Sadao Hayashi. "Complex formation between poly (vinyl alcohol) and metallic ions in aqueous solution." *Journal of Polymer Science: Polymer Symposia,* **1974***,* Vol. 47. No. 1. New York: Wiley Subscription Services, Inc., A Wiley Company.
- Hosny, Wafaa M., and Perihan A. Khalaf-Alaa. "Potentiometric Study and Biological Activity of Some Metal Ion Complexes of Polyvinyl Alcohol (PVA)." *International Journal of Electrochemical Science,* **2013**, 8.1: 1520-1533.
- Hui, Y., Wen, Z. B., Pilate, F., Xie, H., Fan, C. J., Du, L. and Wang, Y. Z. A facile strategy to fabricate highly-stretchable self-healing poly (vinyl alcohol) hybrid hydrogels based on metal–ligand interactions and hydrogen bonding. *Polymer Chemistry*, **2016**, 7(47), 7269-7277.
- Jawaid, S., Talpur, F. N., Sherazi, S. T. H., Nizamani, S. M., & Khaskheli, A. A. Rapid detection of melamine adulteration in dairy milk by SB-ATR–Fourier transform infrared spectroscopy. Food chemistry, **2013**, 141(3), 3066-3071.
- Joerger, R. D. Antimicrobial films for food applications: a quantitative analysis of their effectiveness. Packaging Technology and Science: *An International Journal*, **2007**, 20(4), 231-273.
- Khaneghah, A. M., Hashemi, S. M. B., & Limbo, S. Antimicrobial agents and packaging systems in antimicrobial active food packaging: An overview of approaches and interactions. *Food and Bioproducts Processing*, **2018**, 111, 1-19.
- Kim, I., Viswanathan, K., Kasi, G., Sadeghi, K., Thanakkasaranee, S., & Seo, J. Poly (lactic acid)/ZnO bionanocomposite films with positively charged ZnO as potential antimicrobial food packaging materials. *Polymers*, **2019**, 11(9), 1427.
- Lainé, Anne-Laure, and Catherine Passirani. "Novel metal-based anticancer drugs: a new challenge in drug delivery." *Current opinion in pharmacology*, **2012**, 12.4: 420-426.
- Lallo da Silva, B., Abuçafy, M. P., Berbel Manaia, E., Oshiro Junior, J. A., Chiari-Andréo, B. G., Pietro, R. C. R., & Chiavacci, L. A. Relationship between structure and antimicrobial activity of zinc oxide nanoparticles: An overview. *International journal of nanomedicine*, **2019**, 9395-9410.
- Liu, Yaowen, Shuyao Wang, and Wenting Lan. "Fabrication of antibacterial chitosan-PVA blended film using electrospray technique for food packaging applications." *International journal of biological macromolecules*, **2018** ,107: 848-854.
- Paik, J. S., Dhanasekharan, M., & Kelly, M. J. Antimicrobial activity of UV-irradiated nylon film for packaging applications. Packaging Technology and Science: *An International Journal*, **1998**, 11(4), 179-187.
- Panda, P. K., Sadeghi, K., & Seo, J. Recent advances in poly (vinyl alcohol)/natural polymer based films for food packaging applications: A review. *Food Packaging and Shelf Life*, **2022** 33, 100904.
- Park, K., Oh, Y., Panda, P. K., & Seo, J. Effects of an acidic catalyst on the barrier and water resistance properties of crosslinked poly (vinyl alcohol) and boric acid films. *Progress in Organic Coatings*, **2022**, *173*, 107186.
- Reddy, P. L., Deshmukh, K., Chidambaram, K., Ali, M. M. N., Sadasivuni, K. K., Kumar, Y. R., ... & Pasha, S. K. Dielectric properties of polyvinyl alcohol (PVA) nanocomposites filled with green synthesized zinc sulphide (ZnS) nanoparticles. *Journal of Materials Science: Materials in Electronics*, **2019**, *30*, 4676-4687.

- Renfrew, Anna K. "Transition metal complexes with bioactive ligands: mechanisms for selective ligand release and applications for drug delivery." Metallomics **2014**, 6.8: 1324-1335.
- Ricciotti, L., Roviello, G., Tarallo, O., Borbone, F., Ferone, C., Colangelo, F., Cioffi, R. Synthesis and characterizations of melamine-based epoxy resins. *International Journal of Molecular Sciences*, **2013**, 14(9), 18200-18214.
- Salah, T., Mhadhbi, N., Ben Ahmed, A., Hamdi, B., Krayem, N., Loukil, M., ... & Costantino, F. Physico-Chemical Characterization, DFT Modeling and Biological Activities of a New Zn (II) Complex Containing Melamine as a Template. *Crystals*, **2023**, *13*(5), 746.
- Santos, A. F., Brotto, D. F., Favarin, L. R., Cabeza, N. A., Andrade, G. R., Batistote, M. and Anjos, A. D."Study of the antimicrobial activity of metal complexes and their ligands through bioassays applied to plant extracts." *Revista Brasileira de Farmacognosia*, **2014**, 24: 309-315.
- Sarasam, A. R., Krishnaswamy, R. K., & Madihally, S. V. Blending chitosan with polycaprolactone: effects on physicochemical and antibacterial properties. *Biomacromolecules*, **2006**, 7(4), 1131-1138.
- Smirnov, L.V., Kharitonov, V.M., Klyuev, V.N., Synegirev, M.P., Kravchenko, M.P. and Uzina, R.V. Stabilization of polycaprolactam, (USSR). *c.f.chem.Abs*., **1970**, 73(8):36156b.
- Song, P. A., Xu, Z., & Guo, Q. Bioinspired strategy to reinforce PVA with improved toughness and thermal properties via hydrogen-bond self-assembly. *ACS Macro Letters*, **2013**, 2(12), 1100-1104.
- Stanković A, Dimitrijević S, Uskoković D. Influence of size scale and morphology on antibacterial properties of ZnO powders hydrothemally synthesized using different surface stabilizing agents. *Colloids Surf B*. **2013**, 102:21–28.
- Tyuftin, A. A., & Kerry, J. P. Review of surface treatment methods for polyamide films for potential application as smart packaging materials: Surface structure, antimicrobial and spectral properties. *Food Packaging and Shelf Life*, **2020**, 24, 100475.
- Wan, Y., Huang, W., Wang, Z., & Zhu, X. X. Preparation and characterization of high loading porous crosslinked poly (vinyl alcohol) resins. *Polymer*, **2004**, 45(1), 71-77. Ying Wan, Wenqiang Huang, Zheng Wang,X.X. Zhu.
- Wang, Bing, and Michael R. Wasielewski. "Design and synthesis of metal ion-recognition-induced conjugated polymers: an approach to metal ion sensory materials." *Journal of the American Chemical Society*, **1997**, 119.1: 12-21.
- Zhang, X., Liu, J., Yong, H., Qin, Y., Liu, J., & Jin, C. Development of antioxidant and antimicrobial packaging films based on chitosan and mangosteen (Garcinia mangostana L.) rind powder. *International journal of biological macromolecules*, **2020**, 145, 1129-1139.
- Zhao, Y. C., et al. "Turbostratic carbon nitride prepared by pyrolysis of melamine." Journal of materials science, **2005**, 40.9-10: 2645-2647.

References chapter 7

- Bae, Y. M., Choi, N. Y., Heu, S., Kang, D. H., & Lee, S. Y. Inhibitory effects of organic acids combined with modified atmosphere packaging on foodborne pathogens on cabbage. *Journal of the Korean Society for Applied Biological Chemistry*, **2011**, *54*, 993-997.
- Colelli, G., Inglese, P., **2020**. Gestione della qualità e conservazione dei prodotti ortofrutticoli. Edagricole-New Business Media.
- D. K. A. Barnes, F. Galgani, R. C. Thompson, M. Barlaz, Accumulation and fragmentation of plastic debris in global environments. Philos. Trans. R. Soc. **2009** B364, 1985–1998.
- Devlieghere, Frank, and Johan Debevere. "Influence of dissolved carbon dioxide on the growth of spoilage bacteria." *LWT-Food Science and Technology*, **2000**, 33.8: 531-537.
- Geyer, Roland, Jenna R. Jambeck, and Kara Lavender Law. "Production, use, and fate of all plastics ever made." *Science advances*, **2017**, 3.7: e1700782.
- Jambeck, J. R., Geyer, R., Wilcox, C., Siegler, T. R., Perryman, M., Andrady, A., Law, K. L. Plastic waste inputs from land into the ocean. *Science*, **2015**, *347*(6223), 768-771.
- Lee, Sun-Young, and Seung-Youb Baek. "Effect of chemical sanitizer combined with modified atmosphere packaging on inhibiting Escherichia coli O157: H7 in commercial spinach." *Food Microbiology* , **2008**, 25.4: 582-587.
- Mangaraj, S., T. K. Goswami, and P. V. Mahajan. "Applications of plastic films for modified atmosphere packaging of fruits and vegetables: a review." *Food Engineering Reviews*, **2009**, 1: 133-158.
- Nambi, V. E., Thangavel, K., Rajeswari, K. A., Manickavasagan, A., & Geetha, V. Texture and rheological changes of Indian mango cultivars during ripening. *Postharvest Biology and Technology*, **2016**, *117*, 152-160.
- Piazzolla, Francesca, Pati, S., Amodio, M. L., & Colelli, G."Effect of harvest time on table grape quality during on-vine storage." Journal of the Science of Food and Agriculture, **2016**, 96.1: 131-139.
- Rooban, R., Shanmugam, M., Venkatesan, T., & Tamilmani, C. Physiochemical changes during different stages of fruit ripening of climacteric fruit of mango (Mangifera indica L.) and non-climacteric of fruit cashew apple (Anacardium occidentale L.). *J. Appl. Adv. Res*, **2016**, *1*(2), 53-58.
- Sampaio, S. A., Bora, P. S., Holschuh, H. J., & Silva, S. D. M. Postharvest respiratory activity and changes in some chemical constituents during maturation of yellow mombin (Spondias mombin) fruit. *Food Science and Technology*, **2007**, *27*, 511-515.
- Schwarz, A.E., Ligthart, T.N., Boukris, E., Van Harmelen, T.,. Sources, transport, and accumulation of different types of plastic litter in aquaticenvironments: a review study. *Mar. Pollut. Bull.* **2019**, 143, 92–100.
- Siddiqui, Mohammed Wasim, ed. Postharvest biology and technology of horticultural crops: principles and practices for quality maintenance. CRC Press, **2015**.
- Yildirim, S., Röcker, B., Pettersen, M. K., Nilsen-Nygaard, J., Ayhan, Z., Rutkaite, R., Coma, V. (2018). Active packaging applications for food. *Comprehensive Reviews in food science and food safety*, **2018**, *17*:1, 165-199.

Web sites

- Plastic Pollution in The Ocean – **2023** Facts and Statistics, 2022 https://www.rts.com/blog/plastic-pollution-in-the-ocean-2023-facts-and-statistics/
- Plastics Europe (**2023**) Plastics—the fast Facts 2023. https://plasticseurope.org/knowledge-hub/plastics-the-fast-facts-2023/
- The Guardian (**2019**) *The Blue Planet effect: the plastics revolution is just the start.* By Fiona Gell, 25 March 2019. Available at: https://www.theguardian.com/commentisfree/2019/mar/25/plastics-revolution-marine-life (accessed 23 January 2024).

List of Figure

List of Table